# Contribution of hippocampal diaschisis to the memory deficits associated with focal cerebral ischemia in the rat : converging behavioral, electrophysiological and functional evidence

Gratianne Rabiller

**THESE**

**UNIVERSITE DE BORDEAUX**

ECOLE DOCTORALE des Sciences du Vivant, et de la Santé

**Gratianne RABILLER**

Pour l'obtention du grade de

**DOCTEUR**

Spécialité : Neurosciences

# Contribution of hippocampal diaschisis to the memory deficits associated with focal cerebral ischemia in the rat: converging behavioral, electrophysiological and functional evidence

Sous la direction de Bruno BONTEMPI

Soutenue le 21 décembre 2015

Composition du jury :

| | |
|---|---|
| Mme JAY Thérèse, Directeur de recherche INSERM, Paris | Rapporteur |
| Mr SAVE Etienne, Directeur de recherche CNRS, Marseille | Rapporteur |
| Mr MICHEAU Jacques, Professeur à l'Université de Bordeaux | Président |
| Mr BONTEMPI Bruno, Directeur de recherche CNRS | Directeur de thèse |

Gracias

**Acknowledgments // Remerciements**

Dans un premier temps, je voudrais remercier le Dr. Erwan BEZARD de m'avoir accueillie au sein de son laboratoire, l'Institut des Maladies Neurodégénératives. Merci au Dr. Bruno BONTEMPI, mon directeur de thèse, pour m'avoir fait confiance et guidée tout au long de ce doctorat. Je voudrais également remercier Mme JAY Thérèse, Mr SAVE Etienne et Mr MICHEAU Jacques pour leurs critiques constructives afin d'améliorer ce travail.

Thanks to Dr. Jialing LIU for her warm welcoming and making me feel comfortable in a new environment in San Francisco. Her support was very precious for me. Of course, I would like to thank her all team, Jiwei, Yasuo, Yao-suan, Jack and Jason. You guys rock! Merci également à la french team pour l'american bashing du midi, Alex et Carine.

Un grand merci à l'équipe de Bruno, votre aide m'a été précieuse entre les travaux, la paperasse administrative et les bières au bar du coin. Merci Olivier, Ben, Anais, Alice, Jean-Luc, Xavier, Anne, Nathalie N et Nathalie B, ainsi que toutes les personnes que j'ai pu croiser tout au long de cette thèse.

As colleagues but also as friends, I would like to say a huge THANK YOU to Voja and Senka to host me, feed me and to share so many drinks together. Without you this PhD would not be the same. Enfin, une immense accolade à tous mes amis avec qui j'ai partagé mes joies et mes frustrations. MERCI Lionel, Melody, Marcelo, Daniela, Constanze, Ondrej, Editha, Eleonora et Dany. Désolé si j'en ai oublié, je vous payerai un verre plus tard !

Pour finir, je voudrai remercier du plus profond de mon cœur ma famille qui a su supporter mes plaintes et mes sauts d'humeur. Merci surtout aux parents qui ont su m'épauler durant cette étape. Les sœurs, le frère, mes hommages !

**Contribution of hippocampal diaschisis to the memory deficits associated with focal cerebral ischemia in the rat: converging behavioral, electrophysiological and functional evidence.**

**Summary**

The cognitive consequences and the underlying mechanisms leading to cognitive impairments after cerebrovascular occlusive diseases are still unclear. In addition to the infarct zone that suffer the deadly consequence of ischemic stroke, the penumbra surrounding the lesion site and some brain regions more remote to the ischemic areas can be functionally affected by the insult. This phenomenon is referred to as diaschisis. In light of the importance of interactions between hippocampus and cortex during memory processing, we hypothesized that the cognitive impairments observed following focal ischemia could occur in the absence of direct hippocampal insult, possibly via impaired connectivity within cortico-hippocampal networks leading to diaschisis-induced hypofunctioning in specific hippocampal subregions. To examine this possibility, we used the distal middle cerebral artery occlusion (dMCAO) ischemic model in rats which induces restricted cortical infarct in the somatosensory (SS) cortex in the absence of direct hippocampal injury. dMCAO rats exhibited reduced expression of the activity-dependent gene c-fos in the hippocampus when exploring a novel environment, indicating neuronal hypoactivation. Ischemic rats also showed impaired associative olfactory and spatial memory when tested in the social transmission of food preference (STFP) task and the Barnes maze test, respectively. To confirm that the ischemic-induced hippocampal hypofunctioning resulted from reduced afferent inputs (i.e. deactivation) originating in the damaged cortex, we performed region-specific pharmacological inactivation of SS and/or HPC using lidocaine or CNQX. Fos imaging revealed that these treatments induced hippocampal hypoactivation and impaired memory performance as measured in the STFP task. We additionally performed electrophysiological recordings of hippocampal activity in anesthetized rats during acute stroke and two weeks later or after SS cortex inactivation. We found an alteration in the occurrence of sharp-wave ripples associated with instability of theta frequency during reperfusion after stroke and SS cortex inactivation, suggesting an alteration in the dynamics of hippocampal-cortical interactions. Taken collectively, these findings identify hippocampal diaschisis as a crucial mechanism for mediating stroke-induced hippocampal hypofunction and associated memory deficits.

Key words: spatial memory, associative memory, ischemic stroke, hippocampal oscillations, c-fos, rat

**Contribution du phénomène de diaschisis hippocampique aux déficits mnésiques associés à l'ischémie cérébrale focale chez le rat: convergences comportementale, électrophysiologique et fonctionnelle**.

**Résumé**

Les mécanismes impliqués dans les troubles cognitifs induits à la suite d'une ischémie cérébrale (IC) demeurent mal compris. En plus du cœur ischémique nécrosé et de la zone de pénombre entourant cette lésion, certaines régions éloignées de la zone ischémique peuvent être fonctionnellement affectées, un phénomène connu sous le nom de « diaschisis ». Sachant qu'il existe de fortes interactions fonctionnelles entre l'hippocampe (HPC) et le cortex lors des processus mnésiques, nous avons émis la possibilité que les troubles mnésiques survenant après une IC focale qui préserve l'intégrité de l'HPC, auraient pour origine une perturbation de la connectivité cortico-hippocampique conduisant à un hypofonctionnement hippocampique induit par le phénomène de diaschisis. Afin d'éprouver cette hypothèse, nous avons utilisé le modèle d'occlusion permanente de l'artère cérébrale moyenne chez le rat (OPACM) qui reproduit l'ischémie cérébrale focale humaine. Dans ce modèle, le cortex somato-sensoriel (SS) est endommagé unilatéralement alors que l'intégrité de l'HPC est préservé. Les rats OPACM ont montré une diminution de l'expression du gène c-fos dans l'HPC lors de l'exploration d'un nouvel environnement, indiquant une hypoactivation neuronale. Les rats OPACM ont également présenté une perturbation des mémoires olfactive associative et spatiale lors des tests de transmission sociale de préférence alimentaire (TSPA) et du Barnes maze, respectivement. Afin de confirmer que l'hypofonctionnement hippocampique induit par l'IC résultait d'une réduction des afférences corticales (« déactivation ») provenant du cortex endommagé, nous avons réalisé des inactivations pharmacologiques spécifiques du cortex SS et ou de l'HPC par injection de lidocaïne ou de CNQX. Ces injections ont induit une hypoactivation hippocampique (réduction du nombre de noyaux Fos-positifs) associée à une perturbation mnésique dans le test de TSPA. L'activité hippocampique chez des rats anesthésiés pendant l'IC ou deux semaines après, ainsi que lors de l'inactivation pharmacologique du cortex SS, a également été examinée par une approche électrophysiologique. Les résultats ont montré une altération de la fréquence d'apparition des « sharp-wave ripples » hippocampiques et révélé une instabilité de la fréquence thêta hippocampique lors de la reperfusion ou deux semaines après IC, ainsi que lors de l'inactivation corticale, suggérant une altération de la dynamique d'interaction entre l'HPC et le cortex. Pris dans leur ensemble, ces résultats identifient le phénomène de diaschisis hippocampique comme un mécanisme crucial impliqué dans l'hypofonctionnement hippocampique et les déficits mnésiques observés après une IC.

Mots clés : mémoire spatiale, mémoire associative, ischémie cérébrale focale, oscillations hippocampiques, c-fos, rat

PUBLICATIONS AND COMMUNICATIONS

**Publications:**

- **G. Rabiller,** JW. He, Y. Nishijima, A. Wong, J. Liu. Perturbation of Brain Oscillations after Ischemic Stroke: A Potential Biomarker for Post Stroke Function and Therapy. Int J Mol Sci. 2015 Oct 26 ;16 (10) :25605-40.

.

- **G. Rabiller,** Y Wang, X. Leinekugel, D. Hu, Z. Liu, P. R. Weinstein, J. Zhao, G. M. Abrams, J Liu, B. Bontempi. Involvement of hippocampal diaschisis in mediating stroke-induced hippocampal hypofunction and memory deficits. In preparation.

- O. Schmitt, S. Badurek, W. Liu, Y Wang, **G. Rabiller,** J. He, P. Eipert, J. Liu. Connectome changes following MCA occlusion in the rat are correlated with behavior and c-Fos expression patterns. In preparation.

**Communications:**

- **G. Rabiller,** T. Maviel, J. Liu, B. Bontempi. Involvement of hippocampal diaschisis in mediating stroke-induced hippocampal hypofunction and memory deficits. 13th Scientific Day of the Graduate School of Life Sciences and Health of Bordeaux, Arcachon, France. April 10, 2013. Poster p-32.

- **G. Rabiller,** J. Liu, B. Bontempi. Hippocampal diaschisis in mediating stroke-induced hippocampal hypofunction and memory deficits. Meeting in Frank laboratory, UCSF, San Francisco, CA, USA . November 4, 2014.

- JW He, Y. Nishijima, Y. Akamatsu, **G. Rabiller,** J. Liu. Alteration in hippocampal oscillations after stroke: a candidate biomarker for stroke-induced cognitive impairment. International Stroke Conference/American Heart Association, Nashville, TN, USA. February 10-12 2015.

- **G. Rabiller,** J. Liu, B. Bontempi. Hippocampal diaschisis in mediating stroke-induced hippocampal hypofunction and memory deficits. Meeting in Brain and Spinal Injury center (BASIC) and the Cerebrovascular Research Program, UCSF, San Francisco, CA, USA . May 14, 2015.

- **G. Rabiller,** Y. Nishijima, J. He, X. Leinekugel, V. Andelkovic, A. Hambucken, B. Bontempi, J. Liu. Involvement of hippocampal diaschisis in mediating stroke-induced hippocampal hypofunction and memory deficits. Society for Neuroscience, Chicago, IL, USA. October 17-21, 2015.

LIST OF ABBREVIATIONS

**aCSF**: artificial cerebrospinal fluid
**AMPA:** α-amino-3-hydroxy-5-methyl-4-isoxazolepropionic acid
**AP:** action potential
**ATP:** adenosine triphosphate
**BDA:** biotinylated dextranamine
**BDNF:** brain-derived neurotrophic factor
**BSI:** brain symmetry index
**CA:** Cornu Ammonis
**CBF:** cerebral blood flow
**CCA:** common carotid arteries
**CNQX:** 6-cyano-7-nitroquinoxaline-2,3-dione
**DAB:** 3,3'-diaminobenzine-tetrachlorid solution
**DG:** dentate gyrus
**dMCAO:** distal middle cerebral artery occlusion
**EC:** entorhinal cortex
**EEG:** electroencephalography
**EPSC:** excitatory postsynaptic current
**EPSP:** excitatory postsynaptic potential
**Et-1:** endothelin-1
**fEPSP:** field excitatory postsynaptic potential
**FP:** "food preference" control
**GABA:** gamma-aminobutyric acid
**H2O2:** hydrogen peroxide
**HFO:** high-frequency oscillations
**I.P:** intraperitoneal
**IPSC:** inhibitory postsynaptic current
**IPSP:** inhibitory postsynaptic potential
**lEC:** lateral entorhinal cortex.
**LFP:** local field potentials"
**lm:** lacunosum-moleculare layer
**LTD:** long-term depression
**LTP:** long-term potentiation
**MAP:** mitogen-activated protein
**MCA:** middle cerebral artery
**MCAO:** middle cerebral artery occlusion
**MCI:** mild cognitive impairments
**mEC:** medial entorhinal cortex
**MRI:** magnetic resonance imaging
**NMDA:** N-methyl-D-aspartate
**nNOS:** nitric oxide synthase
**NO:** nitric oxide
**O2- :** superoxide anion
**OH-:** hydroxyl radical
**ONOO-:** peroxynitrite
**PBS:** phosphate buffer solution
**pdBSI:** global pairwise derived brain symmetry index
**PFA:** paraformaldehyde
**PKA:** protein kinase A
**PKC:** protein kinase C
**pMCAO:** permanent middle cerebral artery occlusion

**RAS:** reticular activating system
**REM:** rapid eye movement
**ROS:** reactive oxygen species
**SS1:** primary somatosensory cortex
**SS2:** secondary somatosensory cortex
**STFP:** social transmission of food preference
**SWRs:** sharp-waves ripples
**T/D ratio:** theta-to-delta ratio
**TIA:** transient ischemic attack
**tMCAO:** transient MCAO
**VaD:** vascular dementia

LIST OF FIGURES

## General introduction



## General Materials & Methods

## Results

## General Discussion

# Table of Contents

# General introduction

# Part I: Ischemic stroke

## 1. Types of stroke

In industrialized countries, strokes, also referred to as cerebrovascular accidents, are the 2nd cause of mortality and the first cause of handicap (Donnan et al., 2008). Stroke is a brain lesion of vascular origin leading to neurological deficits. Two main categories of stroke can be distinguished, that is intracerebral hemorrhagic stroke, a form of focal bleeding, which affects 15 % of patients and results from a vessel wall rupture that has been weakened primarily from chronic arterial hypertension and ischemic stroke which afflicts 85 % of patients. This form of stroke corresponds to a permanent or transient diminution or interruption of cerebral blood flow (CBF) either in the entire brain (cerebral hypoperfusion due to cardiac arrest) or in a more localized (focal) brain area. Focal ischemic stroke mainly observed in atherosclerosis patients is triggered by blood clots which are responsible for embolism or thrombosis of a blood vessel (Pelisek et al., 2012). An embolic stroke occurs when a blood clot (embolus) lodges in a blood vessel and blocks the blood flow after breaking loose in a remote vessel or artery and traveling through the bloodstream to the brain, whereas a thrombotic stroke occurs when cerebral blood flow is impaired by a blood clot (thrombus) forming locally in a given blood vessel (**Fig. 1**).

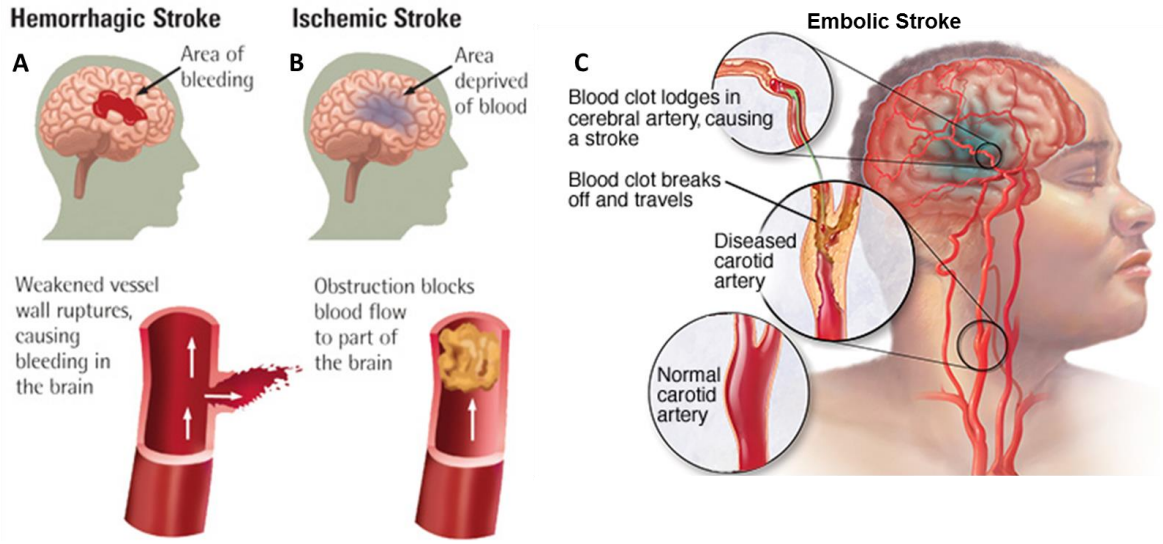


***Figure 1. The hemorrhagic or ischemic origin of stroke****. (A) Schematic illustration of hemorrhagic stroke: following vessel wall ruptures, blood spreads into a focal brain area. (B) Ischemic stroke is caused by a blood clot blocking a blood vessel and leading to blood deprivation in a focal brain area. (C) Embolic stroke, a subcategory of ischemic stroke, is caused by a blood clot lodging in a blood vessel and originating from a remote artery, and disturbing or blocking the blood flow (from Mayo Foundation www.mayoclinic.org, and Floyd Memorial Hospital http://floydmemorial.com/.).*

The location of the cerebral vessel or artery occlusion and the time that has elapsed

before reperfusion of the occluded territory leads to various sizes of the ischemic infarcts. Because energetics supply necessary for brain functioning is exclusively provided by oxidation of glucose (20 % of O2 and glucose consumption of the whole body), CBF disruption quickly leads to significant brain O2 and glucose supply reductions and disturb the energetic balance (Qutub and Hunt, 2005; Hossmann, 2006; Simpson et al., 2007). In addition to the well described severe stroke, transient ischemic attack (TIA) and silent stroke are less deleterious compared to the others kinds of stroke. Indeed, the transient ischemic attack was defined in 2002 as "a brief episode of neurological dysfunction caused by focal brain or retinal ischemia, with clinical symptoms typically lasting less than one hour, and without evidence of acute infarction." (Easton et al., 2009). This ischemic event is followed by a complete recovery during the 24 hour post-stroke period and is not associated with permanent cerebral infarction (Lewandowski et al., 2008). Risk of TIA and major stroke can be increased by silent stroke (Miwa et al., 2010; Kovacs et al., 2013). Such events are not associated with any clinical symptom but detectable by brain imaging using magnetic resonance imaging (MRI) because of the presence of focal lesions. Silent strokes are common in healthy population since 5.5 to 48.6 % of healthy elderly people are affected whereas specific population suffering from hypertension, diabetes, chronic renal failure or atrial fibrillation are affected with a higher prevalence of 11.1 to 61.2 % (Vermeer et al., 2007; Kovacs et al., 2013).

Several diseases, mostly of vascular origin, such as atherosclerosis (30 % of stroke patients) or cardiopathy inducing embolic blood nucleus (20 % of stroke patients) can cause brain ischemia. Risk factors are multiple and depend of the gender, the age or the genetics of the patients. They increase with hypertension, hypercholesterolemia, diabetes, alcohol consumption, smoking and lack of exercise (Leys et al., 2002; Mozaffarian et al., 2015). For example, 75% of stroke patients are older than 65 years and 25 % are males. Moreover, Black and Asian populations have a risk of stroke increased by twice compared to the rest of the population (Ovbiagele and Nguyen-Huynh, 2011).

## 2. Blood circulation in the brain

The origin of stroke can be related to thrombus formation in the vertebral artery or in the carotid which leads to middle cerebral artery (MCA) occlusion in majority. These two pairs of arteries (carotid and vertebral) meet in a particular location in the brain to create a circulatory anastomosis system called the circle of Willis. This system adapts the cerebral

blood flow depending of the energetic brain need or the potential artery impairment. The internal carotid arteries supply the anterior brain areas whereas the vertebral arteries (which join to a common artery "basilar artery") supply the posterior areas of the brain (**Fig. 2**) (Hartkamp et al., 1999; Liebeskind, 2003).

The MCA supplies the somatosensory cortex, the motor cortex, a part of the frontal cortex including the Broca's area (language expression), a part of the temporal lobe including the auditory cortex and the Wernicke's area (language comprehension). For these reasons, MCA occlusions which are the most common human stroke observed in the clinic could lead to motor impairment or hemiplegia, impairment of body representation, neglect symptom, aphasia and cognitive impairment (Cordonnier and Leys, 2008; Gonzalez Delgado and Bogousslavsky, 2012).

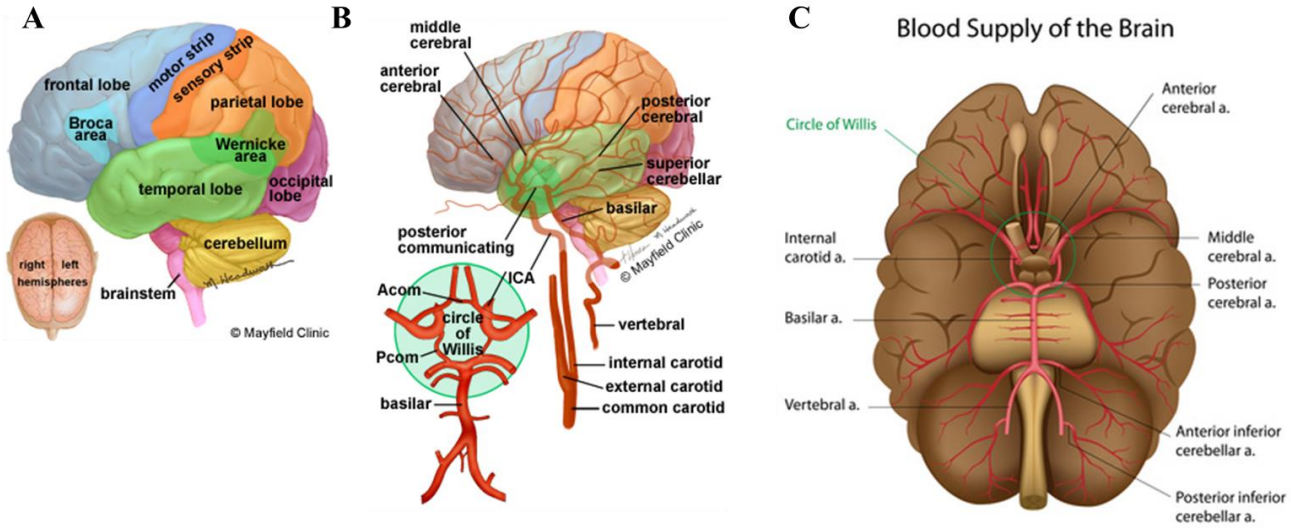


***Figure 2. Circulatory blood system and anatomy of the brain.*** ***(A)*** *The brain is divided into 3 parts: the brainstem, the cerebellum and the cerebrum. This last part is also divided in frontal, parietal, temporal and occipital lobes.* ***(B)*** *The vertebral arteries joining to form the basilar artery and the carotid arteries communicate via the circle of Willis. Each lobe is supplied by different types of arteries. The middle cerebral arteries supply the motor cortex, the somatosensory cortex, a part of the parietal lobe, the frontal lobe including the Broca's area and the temporal lobe including the Wernicke's area. Acom: anterior communicating artery, Pcom: posterior communicating artery, ICA: internal carotid artery* ***(C)*** *The circle of Willis formed an arterial polygon and is located around the optic chiasm on the base of the brain (from Mayfield Clinic www.mayfieldclinic.com).*

## 3. Core and penumbra in ischemic stroke

Because energetic supply are provided to the brain through CBF, the brain electrical activity appears to correlate with CBF (Astrup et al., 1981; Jordan, 2004; Foreman and

Claassen, 2012; O'Gorman et al., 2013), oxygen and glucose level (Lennox et al., 1938; Faught, 1993). In physiological conditions, normal range of CBF is between 35 and 75 mL/100g/min corresponding to 15% of cardiac blood flow and an oxygen consumption of 3.5 mL/100g/min (Astrup et al., 1981; Baron, 2001). In the adult, neurons start to be damaged when CBF is below 25-30 mL/100g/min for more than 2 minutes (Hossmann, 1994). When CBF falls below 18 mL/100 g/min, it crosses the ischemic threshold and induces neuronal death while when reaching 12 mL/100 g/min or below, infarction becomes evident because of the progressive loss of transmembrane potential gradients of neurons. Protein synthesis is inhibited when CBF decreases at 20 %; glutamate and lactate which are neurotoxic start to accumulate with a CBF reduction of 50 % following by a water movement causing an edema and finally, 80% of CBF reduction caused neuronal death because of ion gradient loss (Hossmann, 2006). If the CBF is below the ischemic threshold but maintained above the infarction threshold, the effect on metabolism or cell survival is still reversible. When the CBF falls below the threshold of infarction for a substantial amount of time, typically more than 45 min at 14 mL/100 g/min or less, the spontaneous neuronal activity never returns even after reperfusion, and damage is irreversible (Sharbrough et al., 1973; Gloor, 1985; Hossmann, 1994; Jordan, 2004).

The ischemic territory is not homogenous in many aspects due to the variation of the hemodynamics. Two parts can be distinguished: the core of the ischemia insult and the penumbra area. In the core of the infarct, the CBF is decreased from 90 % to 100% compared to normal. The neurons die by necrosis and damages are irreversible when CBF is below 10 mL/100g/min. Surrounding the ischemic core, the penumbra corresponds to severely ischemic but still viable cerebral tissue where the CBF is between 10-20 mL/100g/min corresponding to a 50% to 75% of decrease in CBF compared to normal. Above 20 mL/100g/min, but below the normal CBF (40 mL/100g/min), literature reported oligemia, a mildly hypoperfused area but not infarcted that recovers spontaneously (Baron, 2001; Bandera et al., 2006) (**Fig. 3**).

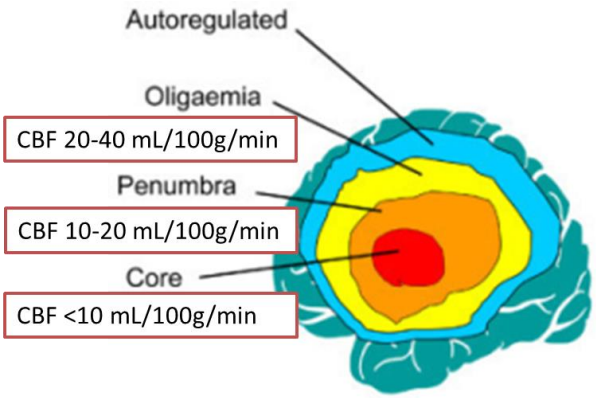


***Figure 3. Illustration of ischemic territory hemodynamics**. The ischemic core occurs when CBF is below 10 mL/100g/min, the penumbra area is perfused within 10-20 mL/100g/min and the oligaemia area is not infarcted with a CBF between 20-40 mL/100g/min (adapted from Moustafa and Baron (2007)).*

## 4. Cellular mechanisms of ischemia

Ischemia triggers an avalanche of cellular mechanisms that lead to short- and long-term consequences (Krnjevic, 2008). Following occlusion, a cascade of damaging events such as excitotoxicity, peri-infarct depolarizations, inflammation and apoptosis appears with a spatial and temporal progression in the ischemic infarct leading to neuronal death (Doyle et al., 2008) (**Fig. 4**).

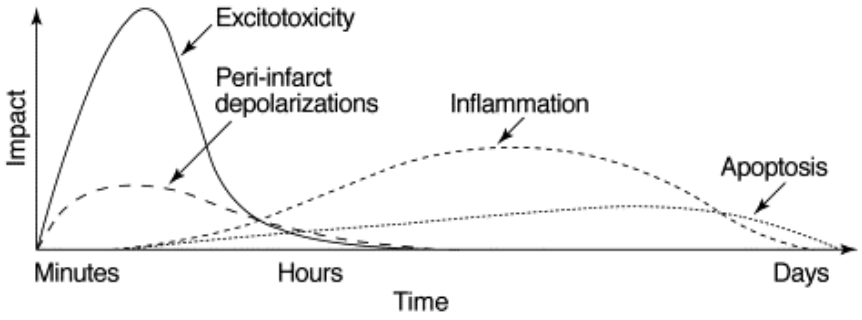


***Figure 4. Damaging cellular mechanisms in focal cerebral ischemia.** Following the focal perfusion deficit, a cascade of events damaging neurons and glia lethally occurs over time (x-axis) and has a differential impact on the final outcome depending of the nature of damaging elements (y-axis). Excitotoxicity triggers a number of events such as peri-infarct depolarizations, inflammation and apoptosis infarcted the tissue (from Dirnagl et al. (1999)).*

### 4.1. Excitotoxicity leading to neuronal death

Only few seconds to few minutes after interruption of the CBF, the neurons are impaired because of energetics substrates lacking (Hossmann, 1994). The viability of the cell is dependent on his environment, consequently the ionic gradient maintaining the membrane

potential is an important factor for the integrity of the cell. Neurons rely on adenosine triphosphate (ATP) as the main form of energy and the role of the ATP pump is to maintain this ionic gradient by activating ionic channels such as $Na^+/K^+$ ATPase. For this reason, a reduction of blood flow can significantly deprive brain cells of glucose and oxygen necessary for the production of ATP by oxidative phosphorylation, thereby leading to a decrease of ATP stock in the cell a few minutes after occlusion. When the cell is deprived in ATP, the ATPase pumps stop functioning and the ionic gradient is disturbed leading to accumulation of $K^+$ extracellular concentration and influx of $Na^+$, $Cl^-$ and $Ca2^+$ ions in the intracellular compartment. The augmentation of $K^+$ ion induces neuronal depolarization leading to activation of Ca2+ channels (Doyle et al., 2008). Because the neuron does not store an important amount of glycogen, this reduction of oxygen activates the anaerobic glycolysis that produces lactate and oxygen free-radicals burst, leading to ischemic damage and impaired electrical activity (Gloor, 1985; Hossmann, 1994). When the ionic gradients and the membrane potential cannot be maintained, it leads to the release of excitatory amino acids in the extracellular space and accumulation of glutamate due to impaired reuptake by the transporters. The augmentation of calcic concentrations leads also to glutamate accumulation into the perivascular environment (Rossi et al., 2007). The released glutamate activates NMDA (N-methyl-D-aspartate) receptor and AMPA (a-amino-3-hydroxy-5-methyl-4-isoxazolepropionic acid) receptor that overloads the $Ca^{2+}$ and causes an influx of $Na^+$ and $Cl^-$ into the neurons, leading to edema due to passive diffusion of water into the cell. Moreover, this influx of ions keeps depolarizing the cell membrane leading to necrosis of neurons (Doyle et al., 2008). Accumulation of glutamate is very deleterious for the cell (Choi et al., 1988; Nieber, 1999) (**Fig. 5**). It has been reported a correlation between extracellular glutamate concentration and the intensity of the neurological deficit as well as the infarct size observed in acute stroke (Castillo et al., 1996; Bullock et al., 1998).

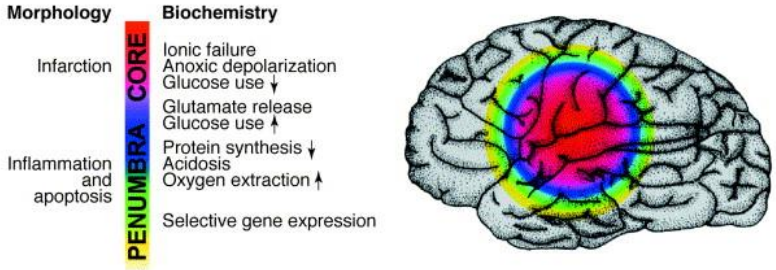


***Figure 5. Biochemistry events and morphology of the ischemic infarct.*** *Schematic representation of the ischemic core infarcted by ionic failure, anoxic depolarization leading to glutamate release. The penumbra area surrounding the core undergoes apoptosis (from Dirnagl et al. (1999)).*

### 4.2. Influx of calcium, oxidative stress and apoptosis

As a universal second messenger, the $Ca^{2+}$ regulates signaling pathways and expression of transcription factors (Seta et al., 2004). $Ca^{2+}$ activates proteolytic enzymes that degrade cytoskeletal proteins or extracellular matrix proteins. The generation of free-radicals or reactive oxygen species (ROS) by the activation of the phospholipase via $Ca^{2+}$ also produces membrane damage. In physiological conditions, ROS are released in few quantities and play an important role in signaling pathways and metabolism. The main ROS are the superoxide anion ($O_2^-$), the hydroxyl radical ($OH^-$) and the nitric oxide (NO). NO produced by $Ca^{2+}$-dependent enzyme neuronal nitric oxide synthase (nNOS) forms peroxynitrite (ONOO-) after reacting with an hydrogen peroxide ($H_2O_2$) that damages the tissue (Dirnagl et al., 1999; Crack and Taylor, 2005). Also, NO can capture electron leading to ATP production inhibition by mitochondria (Brookes et al., 1999). The high intracellular concentrations of $Ca^{2+}$ and $Na^+$ induce mitochondrial production of ROS leading to brain damage. Cells are impaired by peroxidation and degradation of membrane lipids via the action of the lipoxygenase, by degradation of proteins via the action of the peroxinitrite and by degradation of nucleic acid (Chan, 2001; Nakka et al., 2008). Moreover, ROS can block the mitochondrial respiration by inhibiting an enzyme involved in the electron transport chain which leads to accumulation of ROS (Boveris et al., 2000). Reperfusion occurring after removing the embolus in the artery can also increase the ROS production (Gursoy-Ozdemir et al., 2004).

In addition, the influx of $Ca^{2+}$ activates the caspase reaction leading to apoptosis. In cerebral ischemia, necrosis is the main phenomenon inducing neuronal death in the ischemic core but apoptosis is the major phenomenon of cellular death in the penumbra. Apoptosis is a condensation of the cytoplasm induced by the modification of the membrane cell, the cytoskeletal reorganization, chromatin condensation and nuclear fragmentation (Nakka et al., 2008). Multiple pathways such as energetic deprivation, excitotoxicity (Zhang and Bhavnani, 2006), oxidative stress (Liu, 2003) or proteases activation lead to death of neurons and glia cells (Mattson et al., 2000) (Doyle et al., 2008) (**Fig. 6**).

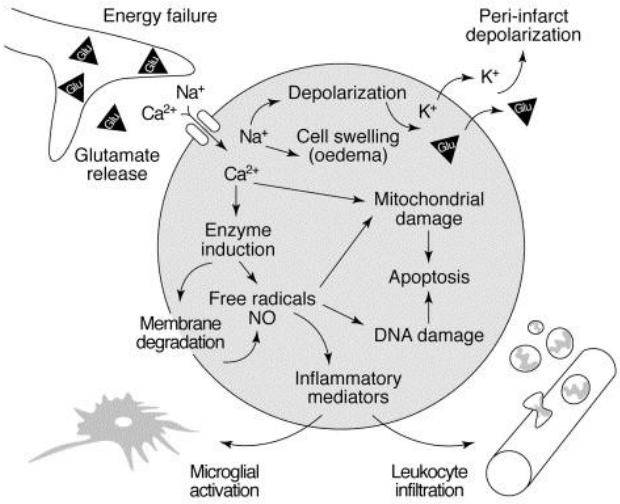


***Figure 6. Pathophysiological mechanisms occurring in focal ischemia.*** *Schematic representation of mechanisms leading to neuronal death are depicted. Energy failure leads to glutamate release that activate glutamate receptors leading to calcium, sodium influx and potassium efflux. These ions flux depolarize the neuron. In addition, calcium induces free radicals production and mitochondrial damages that leads to apoptosis (from Dirnagl et al. (1999)).*

## 5. Models of ischemia in vivo and in vitro

In order to study the underlying mechanisms of stroke, animal models were developed to reproduce etiological, anatomical, metabolic, cellular and functional impairments reported in human stroke. This panel of animal models enabled the science field to test new hypotheses and develop new rehabilitation therapies. In vitro models allow exploring cellular mechanisms whereas in vivo models are more adapted to study potential behavioral impairments. Briefly, in vitro models consist in incubating cell cultures in pathological conditions. Oxygen and glucose can be controlled to induce deprivation supply (OGD models) whereas chemical ischemia uses pharmacological inhibitors to suppress energetic production. Two main inhibitors are the iodoacetate, a glycolysis inhibitor which reproduces an hypoglycemia and cyanide salts which interrupt the ATP production of mitochondria mimicking an hypoxia (Endres and Dirnagl, 2002).

We wish to detail here in vivo models of stroke because the core objective of this thesis is to unravel the mechanisms underlying ischemia-induced memory impairments. Such a model has to be simple, reproducible, and as less invasive as possible to mimic clinical stroke adequately. Moreover, physiological parameters such as body temperature, blood pressure, glycemia or blood gases have to be easily controlled and brain extraction achievable easily to perform histology as well as biochemical and immunohistological analyzes

(Hossmann, 1998; Durukan and Tatlisumak, 2007; Howells et al., 2010). Rodents stand as excellent candidates for stroke models due to their accessibility, their housing, and their price. However, mice seem more vulnerable to stroke and mortality is higher than rats (Hoyte et al., 2004). We can distinguish two types of in vivo models: 1) global ischemic models in which the entire CBF is interrupted and 2) focal ischemic models in which the CBF can be blocked in a targeted brain territory. In addition, duration of artery occlusion as a permanent or a transient occlusion followed by a reperfusion period is also decisive for choosing the pertinent model. Focal transient models are generally preferred to study the deleterious effect of reperfusion observed in human stroke (Hallenbeck and Dutka, 1990). To model human stroke, multiple surgical techniques are used such as permanent or transient artery occlusion with pharmacological or mechanic tools targeting mainly the middle cerebral artery territory which is the most infarcted area in stroke patients (del Zoppo et al., 1992) (**Fig. 7**).

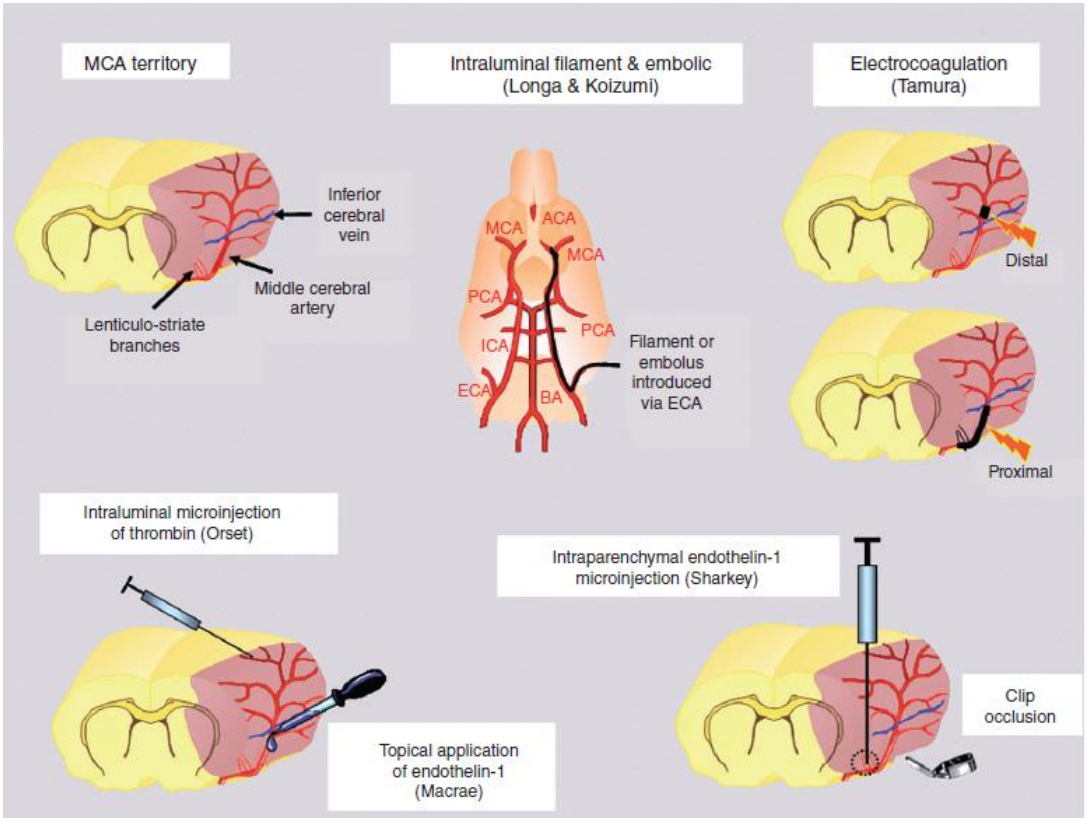


***Figure 7. Illustrations of middle cerebral artery (MCA) occlusion models in rodents.*** *Pink shading represents the territory supplied by the MCA and the infarcted tissue following distal or proximal electrocoagulation, intraluminal or intraparenchymal microinjection of blocking drugs and clip occlusion (from Macrae (2011)).*

### 5.1. Global transient ischemia models

In these models, the global CBF is temporary interrupted and followed by reperfusion.

Complete brain ischemia or incomplete brain ischemia can be performed depending on which artery is occluded (Hossmann, 1998). In general, a ligature or a permanent coagulation of the two common carotid arteries (CCA) associated with an hypotension or an occlusion of the four vessels located in the neck (4-VO model) are used to induce cerebral hypoperfusion (Howells et al., 2010). When global ischemia is performed for a short period of occlusion, neuronal death occurs only in sensitive areas such as the hippocampus (CA1, DG), cortical layers II and V and the striatum.

### 5.1.1. Complete brain ischemia model

Global brain ischemia is a reduction or an interruption of global CBF. Cardiac arrest can induce this type of ischemia by ventricular fibrillation or intracardiac injection of cardioplegic agents. Other techniques have also been developed such as occlusion of blood vessels in the neck by strangulation, inflation of a pneumatic cuff, clamping of subclavian arteries or fluids perfusion into the cisterna magna under high pressure to increase the intracranial pressure. To avoid collateral supply of blood to the ischemic brain, additional occlusion of the main arterial supply is applied by impairing internal mammary arteries, the pterygopalatine arteries or by retrograde drainage of the occluded vessels. (Ginsberg and Busto, 1989; Hossmann, 1998). Because all these techniques are invasive and impaired not only the brain but also the whole body leading to a variability of the stroke infarct, incomplete global ischemia is preferred to the complete global ischemia.

### 5.1.2. Incomplete brain ischemia

Incomplete global ischemia also called ‘oligemia’ (deficiency in the amount of blood in a tissue due to hypoperfusion for instance) involves decreasing the CBF without injuring the brain stem. Manipulations such as extracranial ligation of the carotid and vertebral arteries, increase of intracranial pressure or reduction of arterial blood pressure associated with occlusion of the bilateral carotid artery can be performed to produce incomplete global ischemia. The two most frequently used models of incomplete brain ischemia are outlined below.

#### 5.1.2.1. Two-vessel occlusion model of forebrain ischemia

Because of the incomplete circle of Willis in gerbils and the lack of connection between the basilar and the internal carotid artery, a severe oligemia can be produced by

ligation of CCAs without clamping additional vertebral arteries (Levine and Payan, 1966). This model of occlusion leads to reproducible cortical, striatal or hippocampal injuries in which the size of the infarct depends on the time of occlusion (Tomida et al., 1987). In non-gerbil species, the transient bilateral CCA occlusion is associated with hypotension to reduce CBF down to the ischemic range (Ginsberg and Busto, 1989).

#### 5.1.2.2. Four-vessel occlusion model of forebrain ischemia

The four-vessel occlusion model involves transiently occluding the bilateral CCAs in addition to permanently occluding the vertebral artery in order to avoid the blood supply of the circle of Willis. Indeed, the circle of Willis in human or rodent brains is an artery arrangement with numerous collaterals in the cerebral circulation allowing supplying the brain with sufficient blood despite the occlusion of one given artery. The occlusion of four-vessels is necessary to induce brain damage comparable to those observed after performing the two-vessel occlusions in gerbils (Pulsinelli and Brierley, 1979). Vertebral arteries are cauterised permanently and CCAs are clamped during a predetermined time depending on the size of the infarct to be achieved. Vulnerable areas such as CA1 of hippocampus, striatum and cortical layers III and V are the first impaired by blood impairment (Hossmann, 1998).

### 5.2. Models of focal cerebral ischemia in rats

To be closer from human ischemia, models inducing localized focal ischemia have been developed and especially the MCA occlusion model which mimics the most frequent form of human stroke reported (del Zoppo et al., 1992). The transient ischemia model reproduces the transient occlusion followed by the reperfusion phase induced by thrombolysis of the blood clot typically observed in the clinic. . Infarct size depends on the time of occlusion but can also vary according to the species being used. Several species such as rabbits, rats, mice, cats, non-human primates, or dogs have been employed but rats remain widely used when focal cerebral ischemia is needed because of their vascular system similar to that of humans and easily accessible for surgery (bigger than mice). Multiple surgical techniques of focal cerebral ischemia provide permanent or transient occlusion followed by a reperfusion period, but close examination of the literature reveals that the intraluminal filament technique is primarily used (Howells et al., 2010) (**Fig. 8**). When common carotid arteries are occluded, the anterior part of the brain is hypoperfused while occlusion of vertebral arteries impairs predominantly the posterior circulation of the brain.

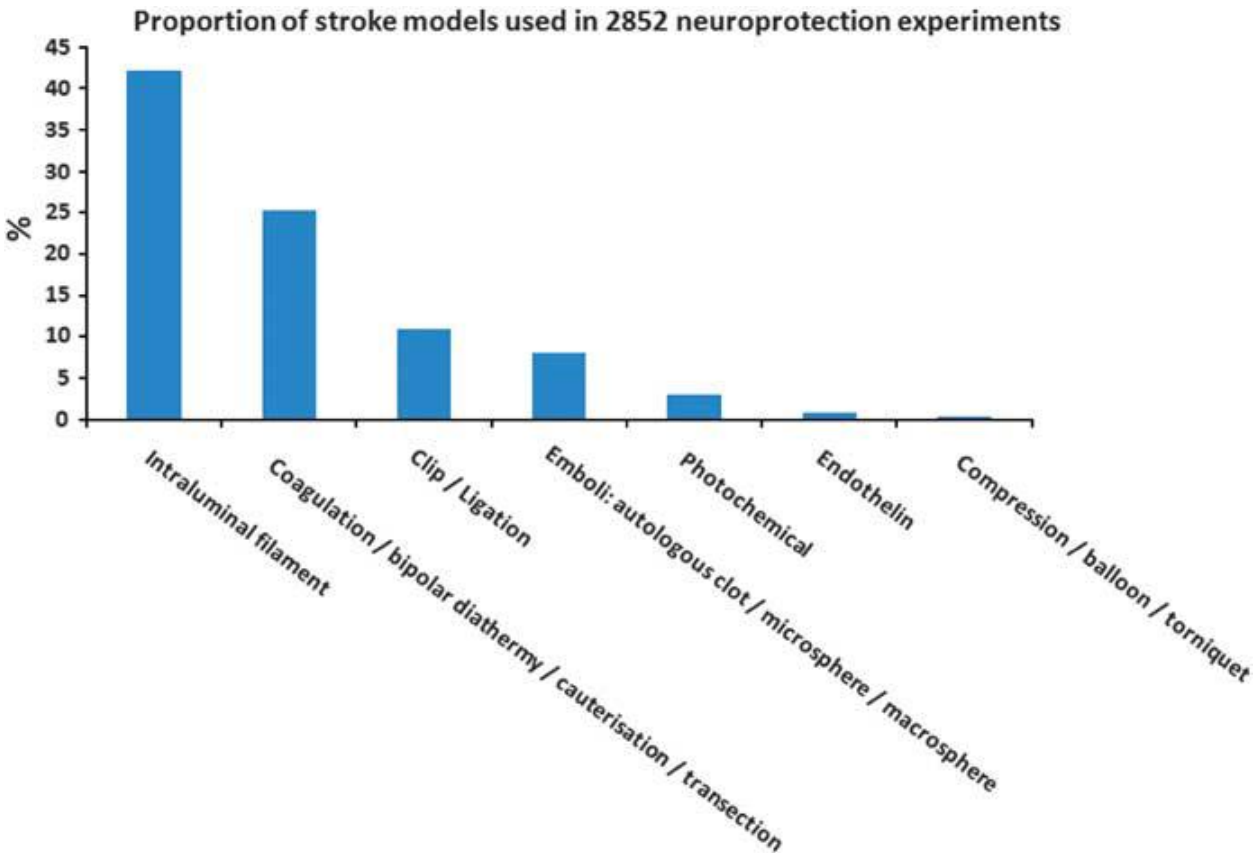


***Figure 8. Intraluminal filament method is widely used to induce focal cerebral ischemia.*** *Among 2852 studies performing focal brain ischemia, the intraluminal filament model is the first method used followed by coagulation or cauterization method. The mechanical obstruction such as clip or ligation of artery appears in third place (from Howells et al. (2010)).*

### 5.2.1. Middle cerebral artery occlusion (MCAO) model

A range of MCAO techniques have been developed using mechanical (clip or ligature) (van Bruggen et al., 1999), electrocoagulation of the blood vessel (Tamura et al., 1981) or pharmacological (vasoconstrictor endothelin-1 used) (Macrae et al., 1993) occlusion of the MCA after craniotomy. To avoid craniotomy, an intravascular approach can be used by inserting an intrafilament or embolus in the carotid artery up to the origin of the MCA (Brinker et al., 1999; Zhang et al., 2004). Each of these stroke MCAO techniques has his own advantages and disadvantages described in the following table (**table 1**) adapted from Macrae's in Sprague-Dawley rats (Macrae, 2011). In all of our experiments, we have chosen the dMCAO model with permanent occlusion of the distal MCA and a transient occlusion of CCA adapted from the Chen technique (Chen et al., 1986; Roof et al., 2001; Wang et al., 2008). This technique permits to have a low mortality and a good reproducibility of the infarct size localized in a small cortical part which includes the somatosensory cortex. Moreover, the

dMCAO model has been reported to spare hippocampal integrity and to induce cognitive impairments (Zvejniece et al., 2012; Li et al., 2013).

| Stroke model | Mortality (rat SD) / references | Advantages | Disadvantages |
|---|---|---|---|
| Permanent MCA occlusion by electrocoagulation | 0 % (6h-8 days) (Yonemori et al., 1999) | Good reproducibility.<br>Visual confirmation of the occlusion site.<br>Control of the size of the infarct depending on the size of MCA occluded.<br>24h-48h size infarct maximal.<br>Low mortality | Craniectomy required and technically challenging.<br>Cannot explore transient ischemia and thrombolysis studies. |
| MCA occlusion by an intraluminal filament | 0 % (24h)-33% (48h)-42 %( 72h).<br>(Aspey et al., 1998)<br>(Scholler et al., 2004) | Good reproducibility.<br>Permanent or transient ischemia.<br>Do not need craniectomy. | No visual confirmation of the success.<br>Reproducibility depends of the size or the dimension of the filament and the strains used.<br>Haemorrhagic risk increase.<br>Significant mortality.<br>Not suitable for thrombolysis studies. |
| Transient MCA occlusion by endothelin-1 (topical or intraparenchymal injection) | <5% (4h)<br>7% (24h)<br>15% (4h)<br>(Nikolova et al., 2009) | Good reproducibility.<br>Visual confirmation in topical model.<br>Conscious rat in intraparenchymal model. | Variability of the endothelin-1 vasoconstrictor potency from batch to batch.<br>Craniectomy required for topical administration.<br>Not suitable for thrombolysis studies. |
| Transient MCA occlusion by clip/mechanical device | 6.3% (24h), 6.3% (28 days)<br>(Wang et al., 2003) | Visual confirmation.<br>Permanent or transient ischemia. | Craniectomy required and technically challenging.<br>Hypotension or CCAO for reproducibility. |
| Transient MCA occlusion by autologous blood clot | 30-50% (24h)<br>44% (14 days)<br>(Rasmussen et al., 2008) | Mimic human ischemic stroke.<br>Suitable for thrombolysis studies. | Reproducibility variable.<br>Less control of location and duration of ischemia.<br>Clot breakdown can induce 2$^{nd}$ microclot formation. |
| Transient MCA occlusion by intravascular thrombin injection | Mouse 1% (24h)<br>(Orset et al., 2007) | Good reproducibility.<br>Visual confirmation.<br>Suitable for thrombolysis | Craniectomy required.<br>Clot breakdown can induce 2$^{nd}$ microclot |

| Stroke model | Mortality (rat SD) / references | Advantages | Disadvantages |
|---|---|---|---|
| | | studies.<br>Low mortality compared to autologous clot models. | formation.<br>Small size and location of infarct limit sensorimotor deficit. |
| Photochemical ischemia | Low (not defined) | Good reproducibility.<br>Skull is intact.<br>Suitable for thrombolysis studies. | Blood vessels damaged by photocoagulation.<br>Small size and location of infarct limit sensorimotor deficit. |

***Table 1. Advantages and disadvantages of MCAO techniques*** *(adapted from Macrae (2011)).*

### 5.2.2. Techniques of MCA occlusions

#### 5.2.2.1. MCA occlusion by electrocoagulation or ligature

Craniotomy and section of dura mater is necessary to expose the MCA, then permanent occlusion is performed using an electrical current passed through fine diathermy forceps to coagulate blood into the proximal artery inducing cortical and sub-cortical infarct. The occluded section is cut after complete coagulation. Ligature or clamp is used for transient occlusion (Tamura et al., 1981). The distal occlusion of the artery does not include the lenticulostriate branches and induces only cortical lesion, for this reason we have favoured in our experiments the distal MCA occlusion (dMCAO) model developed by Chen and colleagues (1986). Distal MCA is ligatured permanently and CCAs are clamped for a determined period of time, then clamp are removed to reperfuse CCAs (Chen et al., 1986; Roof et al., 2001) (**Fig. 9**).

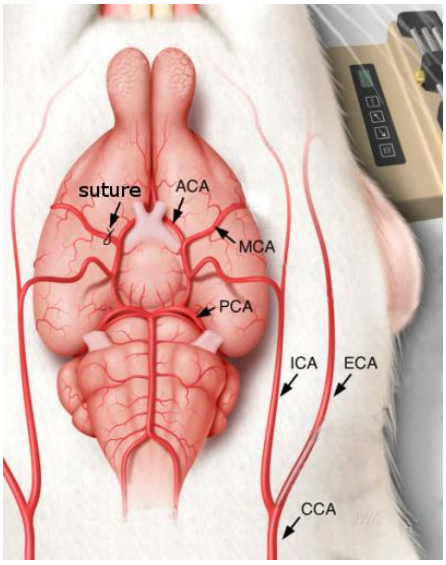

***Figure 9. Illustration of the dMCAO model****. Both CCAs are clamped for a transient period and distal MCA is ligatured permanently (adapted from Crumrine et al. (2011)).*

Transorbital surgery is atraumatic to the brain because tissue is not retracted to expose the MCA after removing the eyeball. This approach is used for bigger animal such as cat, dog or monkey (O'Brien and Waltz, 1973). Advantages of the MCA occlusion model are the reproducibility of infarct size and functional deficit, the possibility to adapt the size and the location of the infarct, low mortality and visual confirmation of the success of the occlusion. Due to permanent focal ischemia, this model is not adapted to investigate thrombolytic agents or drugs to reperfuse the blood flow following ischemia.

#### 5.2.2.2. MCA occlusion by thromboembolic agents

In humans, focal ischemia is caused by thrombus or embolus, for that reason thromboembolic stroke is closer to pathological situation. Moreover, the effect of thrombolytic agents such as rt-PA can be studied for the reperfusion. Occlusion can be performed by injecting a blood clot or a microsphere into the MCA or into the carotid (Steiner et al., 1980; Brinker et al., 1999; Zhang et al., 2004) or by injecting locally chemical agents initiating thromboembolism. The artificial or blood clot embolization approach can induce variability in the infarct due to the lack of control in the obstruction location of the clot. Systemic injection of a photosensitive dye in combination with irradiation through the animal skull with a specific light induces localised thrombosis. Photochemically agents such as the Rose Bengal or erythrosine B release oxygen radical causing peroxidation of blood elements leading to platelet aggregation and thrombosis following light stimulation (Watson et al., 1985; Ginsberg and Busto, 1989; Sugimori et al., 2004).

#### 5.2.2.3. MCA occlusion with endothelin-1 model

Endothelin-1 (Et-1) is a vasoconstrictor peptide of 21 amino-acids produced by endothelial cells. A localised injection of this substance induces a profound and severe vasoconstriction of the cerebral vessels (Asano et al., 1989; Robinson and McCulloch, 1990). If Et-1 is applied on the abluminal surface of the exposed MCA, a severe and reproducible infarct can be produced in rats (Macrae et al., 1993) or marmosets (Virley et al., 2004). Focal ischemia can also be induced following stereotaxic surgery and injection into the region of interest of the brain (Sharkey et al., 1993). Disadvantages of this model are the craniectomy surgery, control of duration by light stimulation and concentration of Et-1 that can vary due to the instability of the peptide. Advantages are the visual confirmation of ischemia and the

gradual reperfusion (Howells et al., 2010).

#### 5.2.2.4. MCA occlusion using an intraluminal filament

The intraluminal filament method is the most widely used model in rats and mice to induce permanent or transient ischemia. This approach avoids the craniectomy surgery by inserting a nylon filament into the vascular system and occluding the MCA. Different variants exist depending on authors (Longa et al., 1989; Mhairi Macrae, 1992). Koizumi et al introduced this method, and then Longa et al modified it. The approach consists in inserting a flexible monofilament into the internal or external carotid artery and advanced this filament until occlusion of the MCA origin. Choosing the diameter of the filament permits to occlude MCAs or CCAs. Advantages are that surgery does not imply craniectomy and the duration of the ischemia can be easily control. Indeed, reperfusion occurred just by removing the microfilament of the MCA (**Fig. 10**).

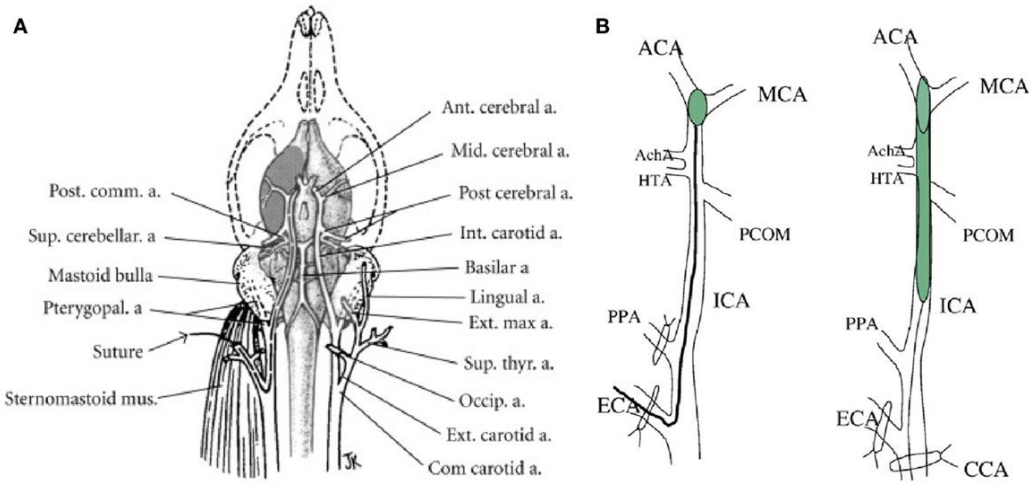


***Figure 10. Use of the intraluminal filament to occlude the MCA. (A)*** *Vascular system of the rat.* ***(B)*** *Left schema represents the Longa variant of the MCA occlusion via the external carotid artery. Right side represents the silicon-coated suture into common carotid artery, blocking MCA, AchA and HTA. ACA, anterior carotid artery; AchA. anterior choroidal artery; CCA, common carotid artery; ECA, external carotid artery; ICA, internal carotid artery; HTA, hypothalamic artery; PPA, pterygopalatine artery; PCOM, posterior communicating artery (from Canazza et al. (2014)).*

# Part II: Memory functions

## 1. Memory systems

Understanding memory functions has always been a central challenge since the field of neuroscience exists. For two centuries, neuroscientists tried to define what memory is and how it works. The profile of memory impairment (anterograde and temporally graded retrograde amnesia for declarative memories while non declarative memories are preserved) observed in patient H.M. following ablation of part of his medial temporal lobe to abolish epileptic seizures revealed for the first time the crucial role of the hippocampus in memory processing and highlighted the fact that memory is not a unitary process (Scoville and Milner, 1957). Nowadays, even if the boundaries of memory systems are still debated within the cognitive neuroscience field, there is a general consensus about the principal types of memory. First, we can distinguished short-term memory which last for seconds to minutes and long-term memory which last for fours to last time (Baddeley, 2001). The most frequently used classification for long-term memory (or remote memory) was proposed by Squire (Squire, 2004; Squire et al., 2004) (**Fig. 11**).

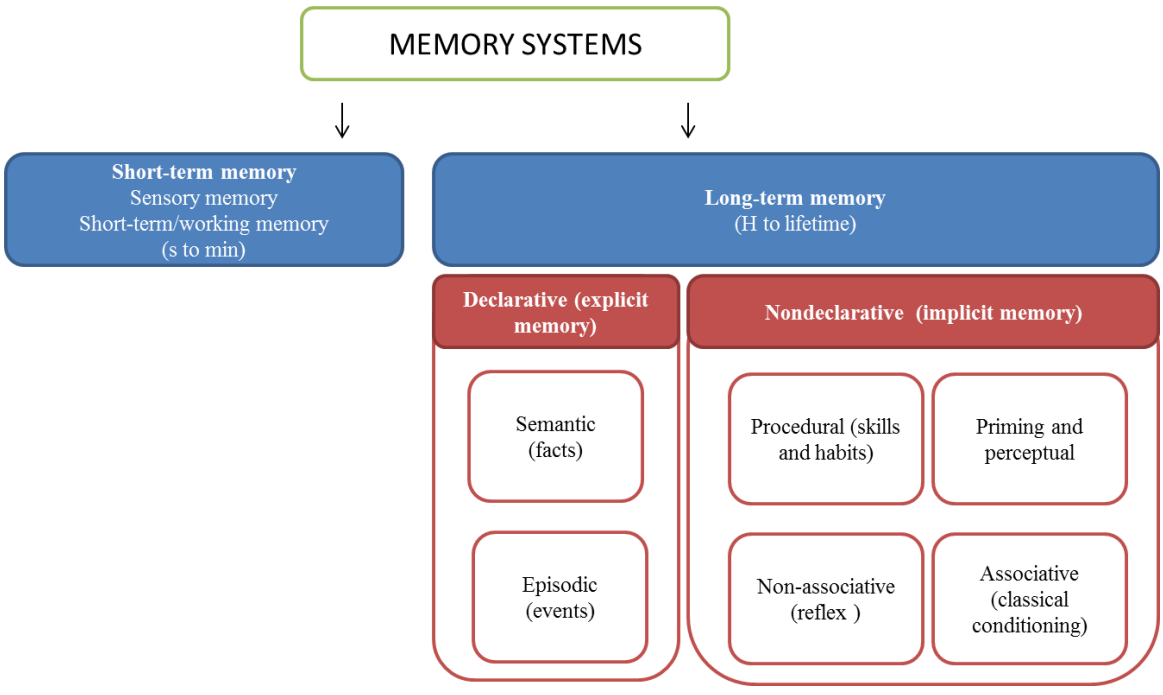


***Figure 11. Classification of memory systems***. *Memory can be divided into short-term memory (scale of seconds to minutes) and long-term memory (hours to lifetime). Declarative memory such as semantic or episodic memory and non declarative memory such as procedural, perceptual, non-associative and associative memories are part of long-term memory (adapted from Squire (2004)).*

Short-term memory is very sensitive to disruption. Because working-memory supports the transient storage that permits to manipulate information, the new acquired information has to be consolidated in order to become a long-term memory. This consolidation process requires attention and active repetition (Baddeley, 2001). Non declarative memory is implicit, i.e. it does not require a conscious stimulus to retrieve the memory and learning is acquired through experience (Squire, 2004). Declarative memory is explicit because memory refers to events (episodic) and facts (semantic) collected in a conscious learning episode. This memory is particularly sensitive to amnesia due to establishment of connections between events and its flexibility (Tulving and Schacter, 1990; Squire, 1992). Each memory system is defined by a network of connections and implication of one or several brain structures to process the information (Sporns et al., 2000), however memory systems are not independent to each other and they interact through competition, synergism and independence (Kim and Baxter, 2001).

## 2. Declarative memory and the medial temporal lobe

After removal of parts of its medial temporal region, patient H.M highlighted the importance of the medial temporal lobe in processing declarative memories referring to facts and events of this patient's life (Scoville and Milner, 1957). Brain structures implicated in declarative memory are located in the medial temporal lobe and consist of the hippocampal region (CA fields, dentate gyrus and subicular complex, the adjacent perirhinal, entorhinal and parahippocampal cortices (Squire et al., 2004). The anatomical studies performed in rats and monkeys permitted to describe the boundaries and the connectivity between these different areas (Insausti et al., 1987; Burwell et al., 1995; Lavenex and Amaral, 2000). Perirhinal and parahippocampal cortices received unimodal and polymodal inputs from the associative areas of the frontal, temporal and parietal cortices. The entorhinal cortex (EC) is the major source of cortical projections and convey information to the hippocampus (**Fig. 12**).

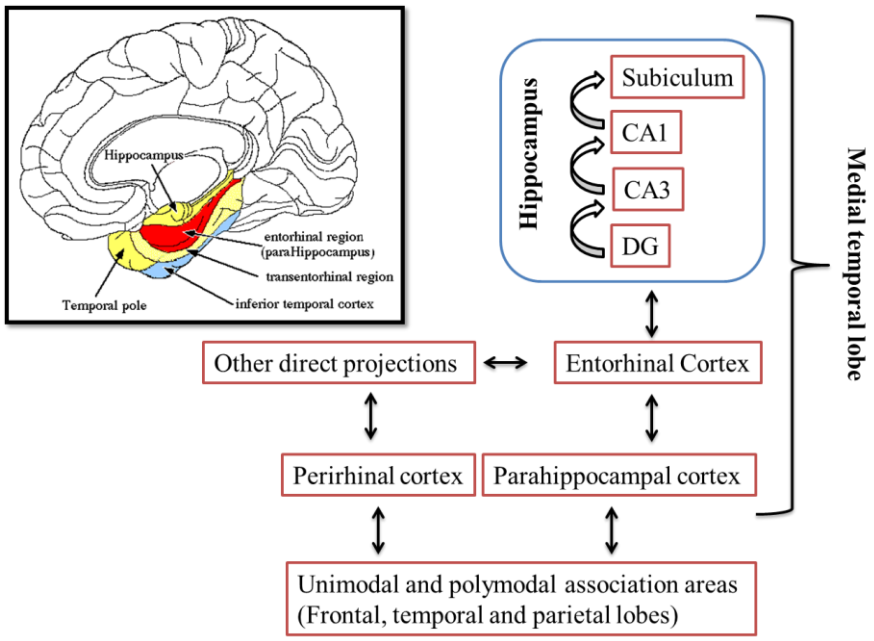


***Figure 12. Simplified representation of connectivity between brain structures of the medial temporal lobe thought to support declarative memory.*** *Left panel represents the location and the anatomy of the medial temporal lobe in the human brain. Hippocampus receives major information sources from entorhinal cortex (EC) which in turn receives information from the adjacent perirhinal and parahippocampal cortex. This information is processed by unimodal and polymodal association areas. At the hippocampus level, EC projects to all different substructures (DG, CA3, CA, subiculum); in turn CA1 and subiculum project to EC (adapted from Squire et al. (2004)).*

### 2.1. Somatosensory cortex

Somatosensory cortex (SS1) is an unimodal association area located in the parietal lobe (Mendoza, 2011) and constituted of three parts. The primary somatosensory cortex is located in the post central gyrus and receives somatotopic input from the thalamus (ventral posterior complex and ventro-postero-lateral nucleus) in the layer IV. The laminar organization of the neocortex is composed of 6 layers different by their cytoarchitecture and classed as follows: layer I is the molecular layer, layer II is the external granular layer, layer III is the external pyramidal layer, layer IV is the internal granular layer, layer V is the internal pyramidal layer and layer VI is the multiform layer. They are interconnected to each other receiving and projecting input-outputs to subcortical structure via the columnar vertical organization (Douglas and Martin, 2004). The layer II and VI are composed by 80% of glutamatergic excitatory neurons and 20% of GABAergic (gamma-aminobutyric acid) inhibitory neurons. Pyramidal neurons compose the layer II, III, V and VI, whereas layer IV contains stellate and granule cells. In the SS1, the layer IV receives a lot of input and this

layer is more developed than other layers. A sensory map was described for the first time by Penfield who introduced the “cortical homunculus”. The sensory homunculus in human refers to the body representation based on the sensory innervation degree (**Fig. 13**) (Penfield, 1950). As a parallel to the homunculus in humans, the somatosensory barrel field cortex in rodents represents nerve projection of each whisker (Woolsey and Van der Loos, 1970). The secondary somatosensory cortex (SS2) located in the lower parietal lobe receives projection from the SS1 and in turn projects to amygdala and hippocampus. Finally, the somatosensory association cortex located in the superior parietal lobe synthetizes all the projections from the SS1 and the SS2 to convey the information to subcortical structures including thalamus, cerebellum, hippocampus and entorhinal cortex (Koralek et al., 1990).

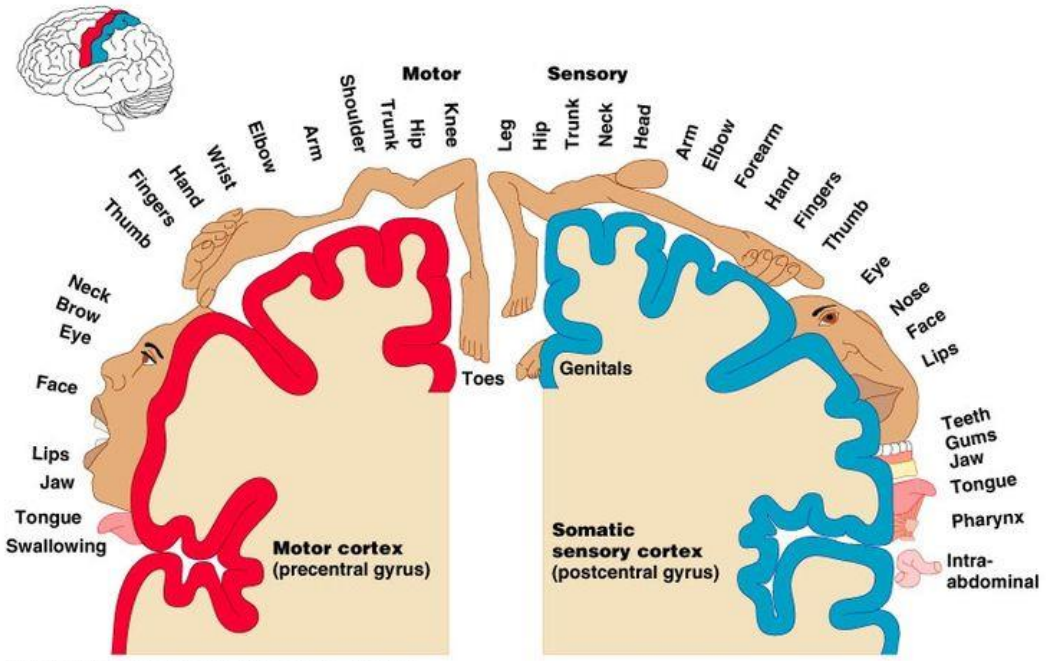


***Figure 13. Homunculus representation in the primary somatosensory cortex.*** *In blue, the sensory map is represented depending on the nerve afferents. In red, the primary motor cortex is a mirror of the sensory map (from Cognitive Psychology: Mind and Brain, Pearson Education 2013).*

### 2.2. Entorhinal cortex

The entorhinal cortex located in the medial temporal lobe is subdivided into medial entorhinal cortex (mEC) and lateral entorhinal cortex (lEC). This structure plays a pivotal role for processing bidirectional information: inputs from associative areas to hippocampus via the parahippocampal cortex and outputs from hippocampus to neocortex (Burwell and Amaral, 1998; Witter et al., 2000). EC processes and splits cortical inputs depending on spatial information and non spatial information. Unimodal sensory information related to qualities of

object (the “what”) travel from neocortical layer to the perirhinal cortex whereas polymodal spatial information (the “where”) are processed from neocortex to parahippocampal cortex (postrhinal cortex in rodents). Subsequently, the lEC receives projections from the perirhinal cortex whereas the mEC receives projection from the parahippocampal cortex (Eichenbaum et al., 2007; Kerr et al., 2007). The lEC receives more inputs from the piriform and insular cortex whereas the mEC receives more input from the visual, posterior parietal, and retrospenial cortices (**Fig. 14**) (Hunsaker et al., 2007; Eichenbaum and Lipton, 2008; Ranganath, 2010).

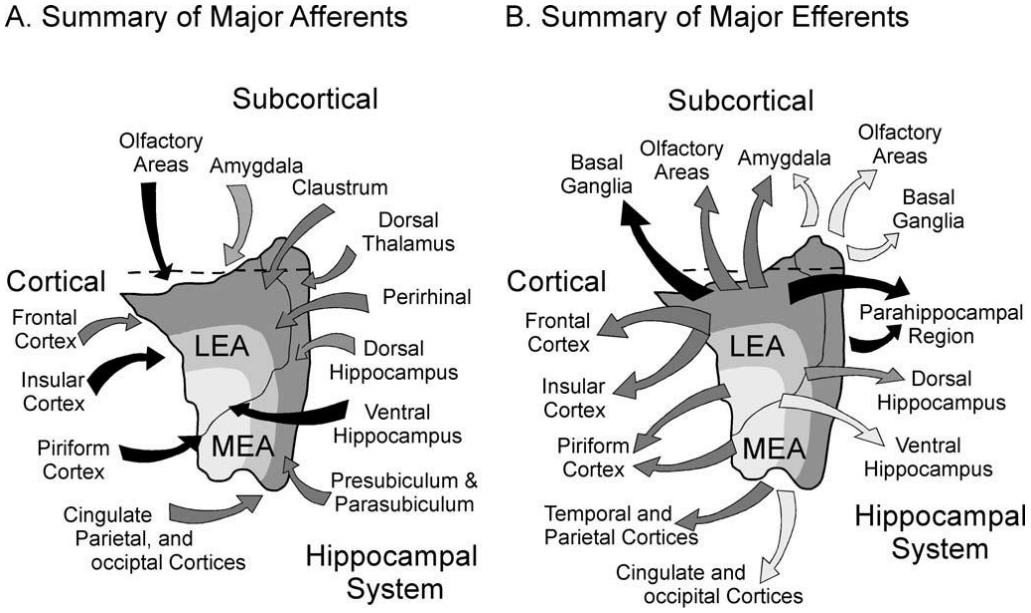


***Figure 14. Major connections of the lEC (LEA) and the mEC (MEA). (A)*** *Diagram representing the afferent connections of the EC.* ***(B)*** *Diagram representing the efferent connections of the EC. Black arrows represent strong connections whereas white arrows indicate weak connections (from Kerr et al. (2007)).*

Layer II of the EC projects to hippocampal subregions, the dentate gyrus and CA3 via the perforant pathway whereas layer III projects to the CA1 field of hippocampus. Additional inputs from layer III to the CA1 and the subiculum are provided via the temporoammonic pathway (Steward, 1976). Subiculum and CA1 field project back to deep layers of the EC which targets the cortical associative area (Kohler, 1985; Dolorfo and Amaral, 1998; van Haeften et al., 2000). Finally, the EC seems to act as a relay because of its bidirectional role between cortex and hippocampus and EC lesion lead to memory impairment. For example, mEC lesion induces spatial memory, recognition memory and working memory impairment in rat studies (Aggleton et al., 2000; Parron et al., 2004; Parron and Save, 2004) whereas lEC lesion induces spatial and non spatial memory impairment (Coutureau and Di Scala, 2009;

Van Cauter et al., 2013).

### 2.3. Hippocampal circuitry

The hippocampal formation is a bilateral and symmetrical complex consisting of dentate gyrus (DG), hippocampus (CA1, CA2, CA3, CA4) and subicular complex (presubiculum, parasubiculum and subiculum). Hippocampal cells are arranged in a C-shaped fashion which is interlocked with the DG layers. The pyramidal cells located closest to the subiculum are the CA1 field whereas the CA4 field is located within the hilus of the DG. CA2 and CA3 fields are located between the CA1and CA4. Usually, CA1 and CA3 are the most studied in literature because of the short length of CA2 and CA4. Pyramidal cells are the major type of cells within the hippocampus constituted by different cell layers as follows: 1) The external layer located in the inferior horn of the lateral ventricle is the plexiform layer. Axons of the pyramidal layer from the adjacent down layer project outside the hippocampus in this plexiform layer as well as the entorhinal cortex afferent fibers through the alvear pathway. 2) The stratum oriens is composed of basal dendrites and basket cells. 3) The pyramidal cells layer with basal and apical dendrites. Basal dendrites extend laterally and in the ventricular surface whereas apical dendrites project from the ventricular surface toward the dentate gyrus. 4) The deepest layer consists of stratum radiatum and stratum lacunosum-moleculare. These layers contain the apical dendrites of the pyramidal cells and the hippocampal afferents from the EC (i.e. performant pathway) (**Fig. 15**). (Lavenex and Amaral, 2000; Moscovitch et al., 2005).

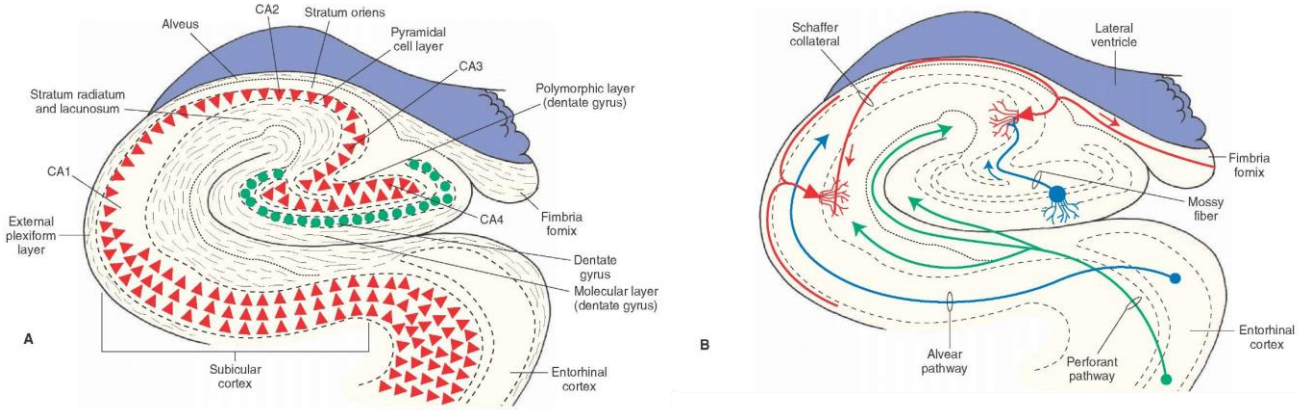


***Figure 15. Hippocampal anatomy and connectivity. (A).*** *coronal view representing a schematic histology of the hippocampal field (CA1-CA4), dentate gyrus and subicular complex.* ***(B)****. Connectivity into the hippocampal formation. Entorhinal cortex projects to DG and CA1, CA3 neurons via the performant pathway and the alvear pathway (connect only to CA1). CA3 neurons received input from the DG via the mossy fibers. The schaffers collateral pathway connects the CA1 to the CA3 and to the*

*contralateral hippocampus via the commissural pathway. CA1 neurons also receive input directly from the perforant pathway and project to the subicular cortex. In turn, all the hippocampal CA1 and subicular neurons project back to entorhinal cortex (from http://what-when-how.com/neuroscience).*

The DG is a part of the hippocampal formation and can be considered as part of hippocampus in the Amaral classification (Amaral, 1999). This structure is also composed of three layers in which granular cells are the principal cell type. Superficial layer is the molecular cell layer composed of axons of hippocampal afferent fibers. Then, mossy fiber is composed of the axon of granular cells and makes synaptic contact with pyramidal cells located in the CA3. Deeper layer to the granular cell layer is a polymorphic layer composed of modified pyramidal cells. Finally, the subicular complex is a transitional region between the entorhinal cortex and the hippocampus (Schultz and Engelhardt, 2014).

### 2.4. Hippocampal projections

The majority of hippocampal afferent connections are from the EC via the perforant pathway and the alvear pathway, which receives inputs from neocortex (temporal, parietal and frontal lobes). Lateral and medial EC project through the alveus to the molecular layer of the hippocampus and the DG, whereas the lateral perforant pathway passes through the molecular layer of the hippocampus and originates from the lateral EC. The medial perforant pathway projects from the medial EC to the alveus of the hippocampus via the white matter adjacent to the subiculum. Olfactory bulb and perirhinal cortex project to the layers II and III of the EC, whereas deeper layers of the EC receive the insular cortex, anterior cingulate, medial prefrontal cortex and the retrosplenial cortex afferents (Insausti et al., 1987; Schultz and Engelhardt, 2014). A second group of fibers considered as a feedback circuit to the hippocampal formation from the septal area make connection to the hippocampal formation through the diagonal band of Broca, in turn the septal area receives input from hippocampal formation through the precommissural fornix (Leranth and Hajszan, 2007).

The hippocampal formation has also many efferent connections. The axons of the pyramidal cells located into the CA1 project to the fornix system through the subicular cortex (Amaral et al., 1991). The subicular cortex also projects to retrosplenial structures such as the EC, the orbitofrontal cortex and the prefrontal cortex, whereas the hippocampal CA1 directly projects to perirhinal cortex and prelimbic areas (Jay et al., 1996; Burette et al., 1997). The fornix system also connects subiculum to the thalamus, nucleus accumbens, mammillary bodies and amygdala (Sorensen, 1985).

## 3. Long-term potentiation and long-term depression

Memory storage involving the hippocampus relies on persistence of the strength of synaptic connections among neurons. In 1894, Ramon Y Cajal suggested that structural changes or reorganization of the connectivity of neuronal networks by changes of strength between two active neurons could be a mechanism for memory storage. Phenomena inducing changes in synaptic activity (neuronal plasticity) are referred to as long-term potentiation (LTP) and long-term depression (LTD) of excitatory and inhibitory synapses. They also support the synaptic consolidation detailed in the next paragraph.

Bliss and Lomo were the first to identify, in 1973, the phenomenon of LTP by applying high frequency stimulation on the perforant path. The electrical stimulation induced a persistent increase of the excitatory postsynaptic potential in the DG (Bliss and Gardner-Medwin, 1973; Bliss and Lomo, 1973) (**Fig. 16**). This neuronal plasticity has also been observed in other brain structures such as amygdala, striatum, somatosensory cortex and prefrontal cortex (Bennett, 2000).

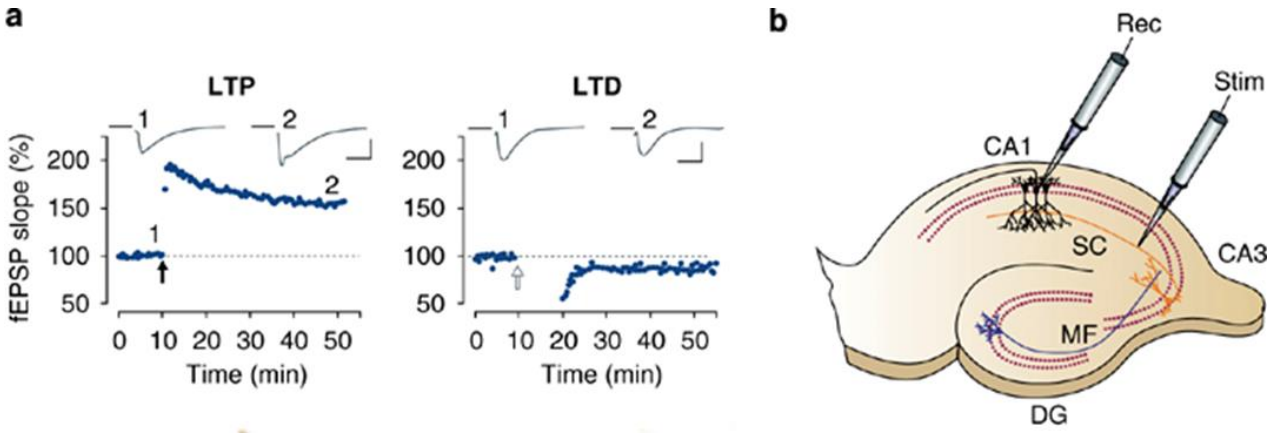


***Figure 16. LTP and LTD models in the CA1 region of the hippocampus. (A)*** *Sample experiments illustrating LTP and LTD in the CA1. Field excitatory postsynaptic potential (fEPSP) recorded in CA1 increase after high frequency stimulation (100Hz, 1s) of stratum radiatum layer of the Schaffer collateral (SC) for LTP (black arrow). LTD (decrease of fEPSP) is induced by low frequency stimulation (5Hz, 3 min) (white arrow). The two phenomena are persistent in time* ***(B)*** *Schematic diagram representing the recording electrode (Rec) into the pyramidal cell of the CA1 and the stimulation electrode (Stim) into the Schaffer collateral (SC). MF: mossy fiber (from Citri and Malenka (2008)).*

Cellular and molecular basis of synaptic plasticity is supported in both excitatory and inhibitory synapses and relies on different neurotransmitters. LTP is classically divided into two phases: 1) Phase of induction, in which the molecular cascade results in increasing the

intracellular calcium (Bliss and Collingridge, 1993) and 2) the maintenance phase in which the molecular mechanisms persist to maintain the increase of the synaptic efficiency (Kandel, 2001; Malinow and Malenka, 2002; Nguyen and Woo, 2003). LTD is the opposing process to LTP because it involves a persistent decrease of the excitatory postsynaptic potential (decrease of synaptic strength) induced by low frequency stimulation of the presynaptic neuron (1-5Hz) (Dudek and Bear, 1992). LTD has been also observed in many brain structures such as hippocampus or cerebellum (Massey and Bashir, 2007) but the underlying molecular processes are quite different from LTP. After glutamate is released from the presynaptic neuron, the post-synaptic NMDA receptors are activated which induce $Ca^{2+}$ entry into the cell (Dudek and Bear, 1992). Calcium will activate phosphatase leading to dephosphorylation and internalisation of post-synaptic AMPA receptor (Mulkey et al., 1994; Carroll et al., 1999; Morishita et al., 2005). This early phase decreases the post-synaptic density of AMPA receptors and the long-term consequence of these changes is the regression of the dendritic arborisation (Beattie et al., 2000; Zhou et al., 2004).

It has been reviewed that LTP or LTD impairments induce memory deficit in laboratory animals (Staubli et al., 1989; McGaugh, 2000; Kandel, 2001; Zhang and Linden, 2003; Lynch, 2004; Malenka and Bear, 2004; Massey and Bashir, 2007). For example, suppressing LTP with an NMDA receptor antagonist (AP5) impairs memory performance in the water maze (Morris et al., 1986). Spatial memory is compromised in mutant mice lacking NMDA receptors and exhibiting impaired LTP in CA1 (Tsien et al., 1996). LTD has been suggested to participate to memory forgetting (Dudek and Bear, 1992; Tsumoto, 1993) but LTD supports also the motor learning in the cerebellum and spatial learning in the hippocampus (Manahan-Vaughan and Braunewell, 1999; Kemp and Manahan-Vaughan, 2004).

## 4. Memory consolidation

The term “consolidation” was first introduced by Müller & Pilzecker in 1900 (Dewar et al., 2007) to describe the stabilization of memory trace after its acquisition. Consolidation refers to two types of processes. Synaptic consolidation occurs within the first minutes or hours following information encoding and relies on LTP and LTD phenomena. It involves stabilization of changes in synaptic connectivity in localized neuronal networks (for instance the growth of new synaptic connections together with the remodeling of existing ones) (Malenka and Bear, 2004). In contrast, systems-level consolidation operates over a much

longer time scale (from several days to weeks or months depending on the species). It involves a gradual reorganization of the brain regions that support memory stabilization (Dudai, 2004; Squire and Bayley, 2007; Wang and Morris, 2010). Interestingly, a temporal gradient exists to memorize the information and if a disturbing event or a lesion occurs during this period, it can lead to memory impairment.

The following diagram proposed by Dudai (2004) highlights the time course of the two forms of memory consolidation processes (**Fig. 17**).

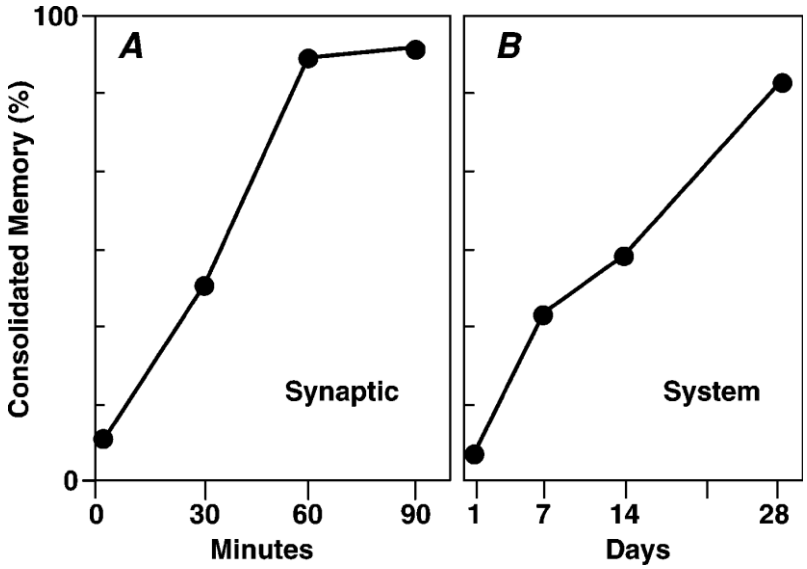


***Figure 17. Time course of synaptic and system consolidation. (A)*** *Consolidated memory at the synaptic level is defined as a treatment-resistant long-term memory after exploring the inhibition of protein synthesis.* ***(B)*** *System consolidation refers to the sensitivity of long-term memory after hippocampal lesion. The hippocampus is no longer engaged in the declarative memory process after one month (from Dudai (2004)).*

### 4.1. Synaptic consolidation

At the cellular level, this process starts by the activation of synaptic receptors such as brain-derived neurotrophic factor (BDNF) and glutamate receptors including AMPA and NMDA receptors (McGaugh, 2000; Izquierdo et al., 2006). Indeed, AMPA receptors permit the synaptic transmission of the activity whereas NMDA receptors regulate the efficiency of the transmission. The theory of Hebb describes the importance of the coincidence-detection function played by NMDA receptors for memory formation, i.e. the activated NMDA receptor

detects the activity coincidence between the presynaptic and the postsynaptic neuron leading to an influx of $Na^{+}$ and the $Ca^{2+}$ ions, and an efflux of the K+ ion in the postsynaptic neuron. This flux of ions and the high $Ca^{2+}$ concentration in the cell depolarize the neurons and activate a cascade of transduction to stabilize the synapse (Tsien et al., 1996; Rampon and Tsien, 2000) **(Fig. 18)**. LTP, synaptic plasticity and consolidation are interconnected phenomena involved in memory formation. NMDA receptors are necessary for the induction of LTP that increases the strength of the synapse between two neurons, making them more sensitized to each other. After the release of glutamate from the presynaptic neuron, both AMPA and NMDA receptors are activated and induce a cascade of molecular events among which the Ca2+/calmodulin-dependent protein kinase II (CamKII) plays an important role to regulate the early phase of expression of LTP (Malinow et al., 1989; Mayford et al., 1995; Lisman et al., 2002). Indeed, Ca2+ which enters the postsynaptic neuron after NMDA receptor activation binds to the CamKII and this activated kinase induces AMPA receptor insertion to the synapse which increase the calcium conductance (Nicoll and Malenka, 1999). In parallel, other kinases are also activated by calcium binding such as the protein kinase C (PKC) and the mitogen-activated protein (MAP) kinase (Sweatt, 1999). After this early phase of potentiation, LTP needs to be maintained by protein synthesis induction during the late-phase of LTP. This maintenance involves the protein kinase A (PKA) and the MAPK/ERK pathways leading to gene translation and protein synthesis (Frey and Morris, 1997; Sweatt, 2001; Abel and Nguyen, 2008).

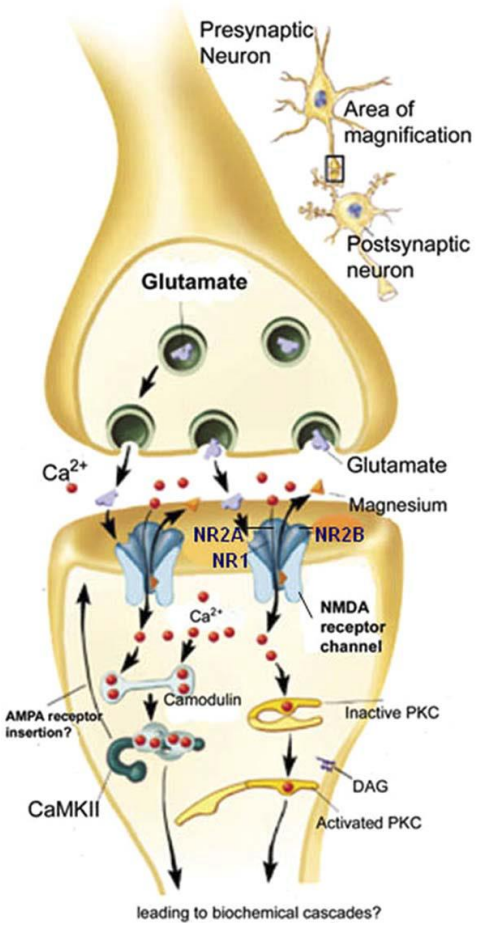


***Figure 18. Molecular cascades underlying changes in synaptic plasticity during cellular consolidation.*** *Glutamate release from the presynaptic neuron activates post-synaptic NMDA and AMPA receptors that in turn induce calcium influx into the cell. Synaptic transmission is enhanced when NMDA receptor detects the co-activity of the presynaptic and postsynaptic neurons. At the post-synaptic level, glutamate binds to the NMDA receptor and the magnesium is expelled from the channel pore if the postsynaptic membrane is sufficiently depolarized which induces $Na^{+}$,$Ca^{2+}$,and $K^{+}$ ions flux. The calcium into the cells binds to different type of kinase which activates protein synthesis necessary for the LTP (from Wang et al. (2006)).*

### 4.2. System consolidation

System consolidation refers to a gradual process of reorganization of the brain regions that support memory. It seems to be a feature of different types of memory: both declarative (Scoville and Milner, 1957) and non-declarative (Shadmehr and Holcomb, 1997) memories in humans show time-dependent reorganization at a system level, although their timescales are markedly different.

Examples of temporally-graded retrograde amnesia in both humans and animals have led to system-based models of consolidation. Marr formulated the first model to account for system consolidation (Marr, 1970, 1971). He proposed that the hippocampus rapidly stores

the day's events before the information is transferred to the cortex for subsequent reorganization and reclassification. Marr further proposed that the transfer process depended on REPLAY of waking patterns of neural activity during sleep. The ideas that the hippocampus is a temporary repository, that waking patterns of neural activity are reinstated or replayed during sleep, and that the cortex is important in extracting statistical structure (semantic knowledge) form the bases of contemporary models of memory formation (McClelland et al., 1995; Squire and Alvarez, 1995) (**Fig. 19**). According to these models, experience is initially encoded in parallel in hippocampal and cortical networks. Subsequent reactivation of the hippocampal network reinstates activity in different cortical networks. This coordinated replay across hippocampal-cortical networks leads to gradual strengthening of cortico-cortical connections, which eventually allows new memories to become independent of the hippocampus and to be gradually integrated with pre-existing cortical memories. In these models, memories are assumed to decay more rapidly in the hippocampus than in the cortex. An alternative view is based on two observations. First, medial temporal lobe damage can produce ungraded retrograde amnesia for some types of declarative memory, such as autobiographical/episodic (Cipolotti et al., 2001; Viskontas et al., 2002) and detailed spatial memories (Rosenbaum et al., 2000; Martin et al., 2005). Second, the recall of detailed, remote autobiographical/ episodic memories engages the hippocampus (Ryan et al., 2001; Maguire and Frith, 2003; Gilboa et al., 2004). To account for these observations, the multiple trace theory proposes that, although experience is initially encoded in distributed hippocampal-cortical networks, the hippocampus is always required for rich contextual or spatial detail (Nadel and Moscovitch, 1997). This theory predicts that complete hippocampal lesions should produce temporally-graded retrograde amnesia for only semantic (and not episodic) memories. However, the finding that patient E.P., who has extensive bilateral medial temporal lobe lesions, has excellent autobiographical and spatial memories from his youth (Teng and Squire, 1999) is inconsistent with this prediction. At present, there is some debate about whether spared remote memories in patients like E.P. are as vivid and detailed as in healthy subjects (Rosenbaum et al., 2000).

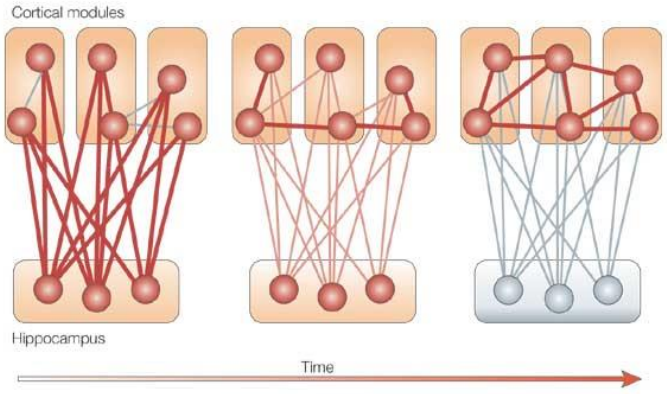


***Figure 19. Standard consolidation model.*** *Encoding of perceptual, motor and cognitive information initially occurs in several specialized primary and associative cortical areas. The hippocampus integrates information from these distributed cortical modules that represents the various features of an experience, and rapidly fuses these features into a coherent memory trace. Successive reactivation of this hippocampal–cortical network leads to progressive strengthening of cortico-cortical connections (for example, by strengthening existing cortico-cortical connections or establishing new ones). Incremental strengthening of cortico-cortical connections eventually allows new memories to become independent of the hippocampus and to be gradually integrated with pre-existing cortical memories. A key feature of this model is that changes in the strength of the connections between the hippocampal system and the different cortical areas are rapid and transient, whereas changes in the connections between the cortical areas are slow and long-lasting ( from Frankland and Bontempi (2005).*

Multiple trace theory was proposed in 1997 as an alternative to standard consolidation models (Nadel and Moscovitch, 1997). At the heart of the debate is how to account for instances where medial temporal lobe damage produces extensive retrograde amnesia. Although one argument is that flat gradients are associated with extensive damage to extra-hippocampal regions, which affect possible sites of permanent storage (Squire and Alvarez, 1995; Squire et al., 2004), Nadel and Moscovitch argued that the length of the gradient depended on the extent of hippocampal damage as well as the type of memory being probed. In particular, they noted that when damage included the whole hippocampal formation, retrograde amnesia for autobiographical (episodic) information was extensive, spanning much of a subject's lifetime. These observations led to the formulation of multiple trace theory (**Fig. 20**). The main features of the multiple trace theory are: 1) Memories are encoded in hippocampal–cortical networks; 2) Memory reactivation leads to the generation of multiple traces in the hippocampus, which are linked to cortical networks; 3) Traces in the hippocampus provide spatial and temporal context; 4) Traces in the cortex are context-free (or semantic) in nature; 5) Retrieval of contextually rich episodic memories always depends on hippocampal–cortical networks; and 6) Retrieval of remote semantic memories is possible in

the absence of a functional hippocampus.

According to this model, there are two conditions in which hippocampal damage might be associated with temporally-graded retrograde amnesia. Incomplete hippocampal lesions should preferentially affect recent rather than remote episodic or semantic memories, as trace proliferation should render older memories more resistant to hippocampal damage. Complete hippocampal lesions should abolish all episodic memories, regardless of their age. Furthermore, semantic components of remote memories might be spared even after complete hippocampal lesions. Predictions of standard models (a) and multiple trace theory (b) are contrasted (**Fig. 20**).

This theory shares one important assumption with standard consolidation models, that is, reactivation of memories initiates a process of reorganization. Where it differs is in terms of the locus of this reorganization. Although standard models predict that reorganization occurs in cortical networks, multiple trace theory predicts that reactivation should also lead to the generation of new traces within the hippocampus.

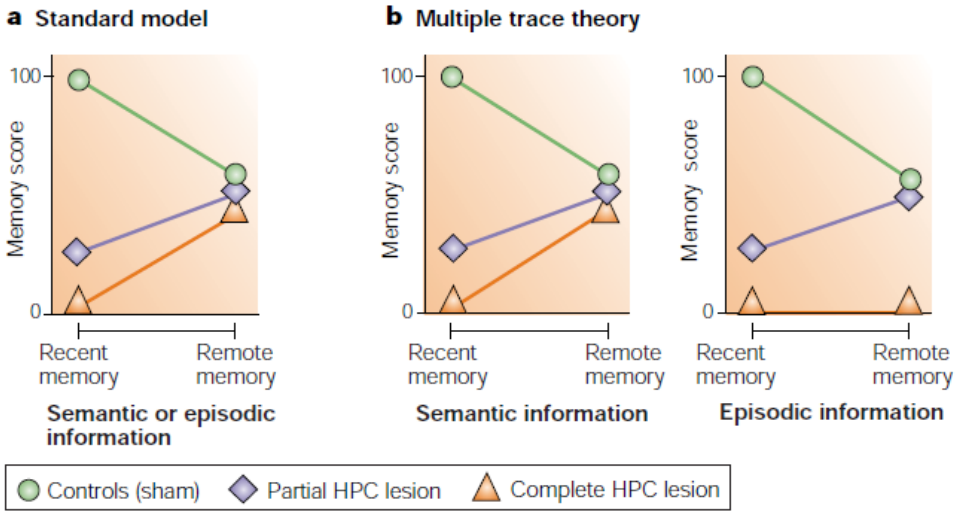


***Figure 20. Predictions made by the standard model of memory consolidation and the multiple trace theory.*** *From Frankland and Bontempi (2005).*

## 5. Memory impairment after stroke

After stroke, more than one half of patients suffer from cognitive impairments (Dennis et al., 2000; Barker-Collo et al., 2012) and 30 % of stroke patients develop dementia within one year of stroke onset (Cullen et al., 2007). The observed deficits result from a variety of causes such as location of the brain lesion, brain hypoperfusion, functional impairment of

connected areas distant from the infarcted brain (diaschisis phenomenon), pressure in the areas surrounding the lesioned tissue (Ferro, 2001). Cognition is complex and incorporates multiple concept such as attention (focusing, shifting, and flexibility), executive function (planning, inhibition, organizing of thoughts), visuospatial ability, memory (recognition and recall of visual/verbal information) and language (expressive and receptive). About 12-56% of stroke patients exhibit faster cognitive decline (Ebrahim et al., 1985; Tatemichi et al., 1994) compared to only (-10% of healthy adult of the same age range. (Luxenberg and Feigenbaum, 1986; Hamilton and Granger, 1994). Among the cognitive impairments induced by stroke, some are of vascular origin such as vascular dementia (VaD) occurring with a 20-30% rate in stroke survivors (Tatemichi et al., 1990; Barba et al., 2000; Desmond et al., 2000). VaD is the second leading cause of dementia in the world after Alzheimer disease and 1-4% of 65 years old people or older suffer from this form of dementia (Ruitenberg et al., 2001; McVeigh and Passmore, 2006). VaD is characterized by cognitive function impairments induced by vascular lesion and stroke infarct. These impairments vary depending on the stroke location and size of the cerebral damage (McVeigh and Passmore, 2006). The most impaired cognitive abilities three months following the stroke are short-term memory (31%), long term-memory (23%), constructive and visuospatial functions (37%), executive functions (25%) and aphasia (14%) (Pohjasvaara et al., 1997). These impairments are still present one year following the stroke with deficits in attention (48.5%), language (27%), short-term memory (24.5%) and executive functions (18.5%) (Lesniak et al., 2008). Executive deficit, aphasia and long-term memory impairments tend to decrease after one year post-stroke period compared to the acute period. Post-stroke memory impairment varies from 23% to 55% three months after stroke (Pohjasvaara et al., 1997; Sundar and Adwani, 2010; Sun et al., 2014) and decreases from 11% to 31% one year after stroke onset (Rasquin et al., 2004; Snaphaan and de Leeuw, 2007; Cumming et al., 2013). Because memory is directly linked to attention, these memory impairments can be a consequence of attention deficit observed in 46-92% of acute stroke survivors (Hochstenbach et al., 1998; Hyndman et al., 2008). Moreover, 20-50% of stroke patients suffer from memory deficits during the immediate period following a stroke diagnosis (acute period of the stroke). These deficits during this period of time are called mild cognitive impairments (MCI) and they are followed by a decline in the episodic memory performance if dementia occurs (Cooper and Greene, 2005; Lim and Alexander, 2009; Snaphaan et al., 2009; Al-Qazzaz et al., 2014). Focal cerebral ischemia induced by MCA occlusion increases the probability to develop cognitive dysfunction (Jaillard et al., 2010) such as mental slowing, memory problems and executive deficits exacerbated by the diffuse

neural dysfunction induced by diaschisis phenomena (de Haan et al., 2006). Finally, lesion effects can be increased by changes in neuronal plasticity and functional reorganization of the brain in early and later phases of stroke resulting in 20% to 50% of stroke patients complaining about memory impairments (Lim and Alexander, 2009).

In rats, several studies showed learning and memory impairments following MCA occlusion which induces focal cerebral ischemia. For example, spatial memory was impaired in rats overcoming 60 to 120 min of distal ischemia. Spatial memory impairment is observed 6 days (Zvejniece et al., 2012) but also 30 days (Li et al., 2013) after the stroke episode during the retention test in the water maze. Learning is also impaired 30 days following the ischemia onset as illustrated by the decline of performance during acquisition trials in the water maze (Dahlqvist et al., 2004). Moreover, when rats learned a spatial task in the Barnes maze (14 days of training) or the water maze (4 weeks of training) prior to the ischemic surgery, the MCA occlusion impairs retrieval of the acquired training (Sakai et al., 1996) (Yonemori et al., 1996; Yonemori et al., 1999). This spatial memory impairment is usually associated with important cortical brain lesion or decrease of LTP in the hippocampus (Yonemori et al., 1996; Yonemori et al., 1999; Zvejniece et al., 2012; Li et al., 2013). Altogether, these studies show that focal distal ischemia impairs learning as well as short-term and long-term memory retrieval. It can impair memory formation by inducing anterograde amnesia but also retrograde amnesia by impairing ongoing consolidation processes involved in the strengthening of memory acquired prior to the onset of stroke.

# Part III: Electrical brain activity and ischemic stroke

## 1. Electrical brain activity

By using penetrating and scalp electrodes, electroencephalography (EEG) has provided us with invaluable information regarding the generation, propagation, patterns and functions of brain oscillations for more than a century, with the first animal publication dating back to 1890 (by Adolf Beck) and the first humans investigation in 1929 (by Hans Berger), respectively. It is our current understanding that brain oscillations resulting from electrical currents propagate in all mammalian brains within the frequency range of 0.05 to 500 Hz. For all intents and purposes, the oscillations are categorized into 5 main frequency groups (Buzsaki and Draguhn, 2004) (**Fig. 21**):

- Delta: 1-4 Hz
- Theta: 4-8 Hz

The frequency of the theta band from superficial layers of the brain (4-8 Hz) differs from that recorded in the hippocampal layers (4-10 Hz) (Pignatelli et al., 2012).

- Alpha: 8-12 Hz

The mu rhythm (8-13 Hz) shares a great deal of similarity in frequency with that of the alpha band. However, unlike alpha which is recorded in the visual cortex in the occipital lobe, mu is not only recorded at various locations in the motor cortex such as the central and parietal areas, but also as a sinusoidal, regular and rhythmic waveform that is distinct from the sharp, negative peak and rounded positive phase observed in the alpha band.

- Beta: 12-30 Hz
- Gamma: 30-80 Hz

Apart from those commonly observed in the conventional EEG, there are other oscillations outside this spectrum. For example, there exists slow oscillations (0.3-1 Hz) that are slower than the delta band (Steriade et al., 1993b) and high-frequency oscillations (HFO) (80-200 Hz) that are faster than the gamma band, also known as fast oscillations that include ripples (100-200 Hz) (Bragin et al., 1999). Data from human sleep study suggest that the slow (<1 Hz) and delta bands are two different oscillatory types that are distinct in their evolution;

i.e. power of the delta waves decline from the first to the second non-REM sleep episode, while power of the slow wave remains unchanged (Ferri et al., 2001). In the low frequency range, some confusion may arise due to inconsistent nomenclature in reference to the slow oscillations that exist during slow-wave sleep, anesthesia or after stroke and the delta oscillations present during slow-wave sleep or after stroke. Indeed, these two low frequency waves differ by their frequency range because the slow oscillations refer to activity between 0.3-1 Hz in an adult awake EEG (Steriade et al., 1993b) whereas the delta wave refers to activity between 1-4 Hz (Ball et al., 1977; McCormick and Pape, 1990).

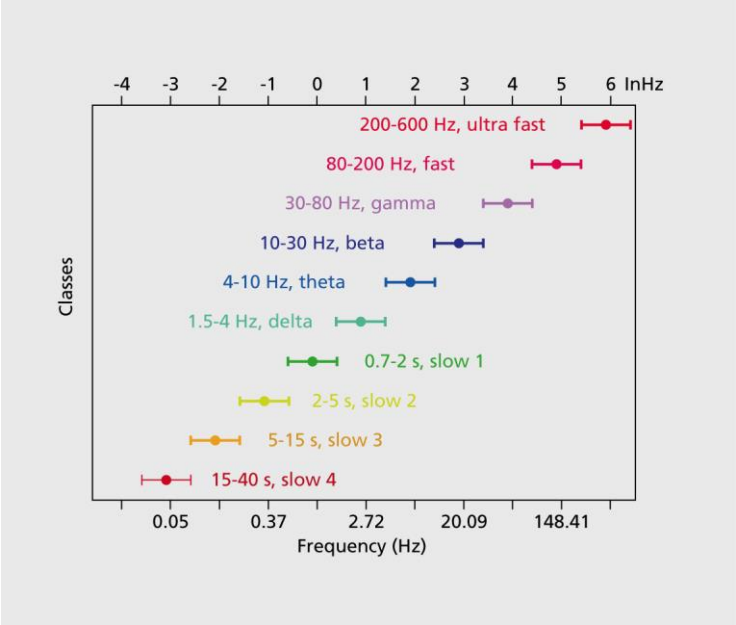


***Figure 21. Brain activity is classified according to frequency oscillation***. *Diagram showing the brain oscillations classification according to Buszaki. We can note that the alpha band is not included in this classification (from Buzsaki and Draguhn (2004)).*

## 2. Recording techniques

### 2.1. Electroencephalography technique

EEG is a widespread technique to study brain activity under physiological as well as pathological conditions. In humans, EEG records the electrical activity of the superficial layers of the brain using electrodes placed on the skull. Classically, the location of the electrodes is determined according to the ’10-20 System of Electrode Placement’ method that refers to a 10 % or 20% inter-electrode distance of the total front-back or right-left distance of the skull. Electrodes are distributed on the scalp and identified by the first letter of the brain regions (e.g. F,T,C,P and O for Frontal, Temporal, Central, Parietal and Occipital lobe) and

electrode number (1,3,5,7 assigned for left hemisphere and 2,4,6,8 for right hemisphere). The letter Z usually refers to an electrode placed on the midline (**Fig. 22**). The summation of the currents from cortical neurons can be detected by using two electrodes about 5 mm in radius that permit measurement of small current potential up to 100 µV (Sanei and Chambers, 2013). Due to the simplicity of this approach, EEG is one of the most widespread non-invasive techniques for neural activity recording as a diagnostic tool for clinical purposes (Acar et al., 2007). However, this technique does have some caveats mainly related to the tissue barrier of the scalp that prevents the detection of low-energy brain activity, such as frequencies higher than 100 Hz and those lower than 0.1 Hz. Furthermore, artifacts can be created by eye blinks, movements, or muscle activity such as respiration.

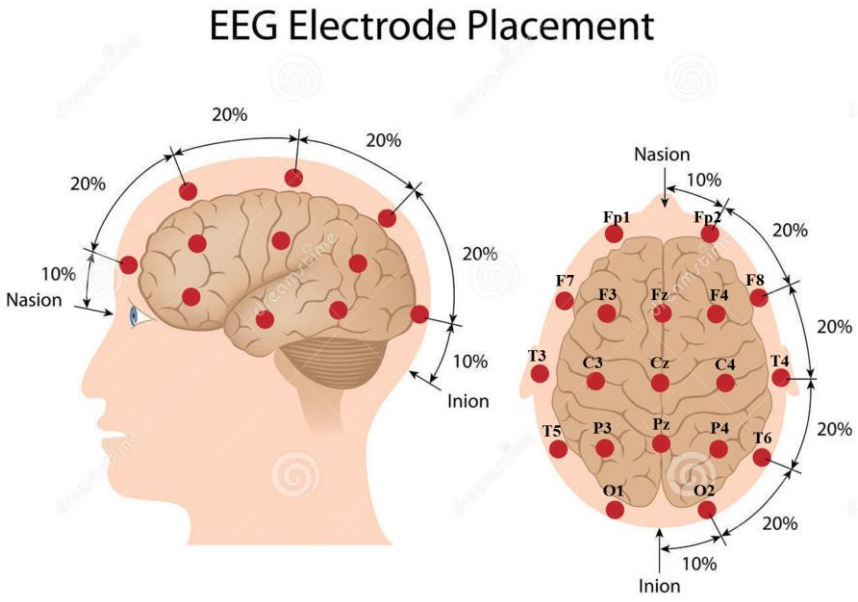


***Figure 22. EEG electrode placement to record brain electrical activity in humans.*** *Adapted from Gloor (1985).*

The utility of EEG as a diagnostic tool or in getting high-quality data is reduced when it comes to laboratory animals like rodents due to the following limitations: 1) lack of adequate space to accommodate the electrodes because of the small size of the rodent brains, 2) difficulty in locating the anatomic source of neural activity in epidural EEG recordings, and 3) lack of real time capability to extract signal characteristics due to the requirement of extensive computational analysis.

### 2.2. Microelectrode arrays

To circumvent the EEG limitations, the use of an invasive technique, such as probe

insertion, permits exploration of the activity of deeper structure in the brain including the thalamus or hippocampus. In particular, the use of microelectrode arrays can register activity of small groups of neurons, referred to as “local field potentials” (LFP), or a single neuron, known as “single-unit action potential”, with a signal frequency up to 5000 Hz. LFP is the summation of the action potential (AP) and the graded potential such as excitatory postsynaptic potential (EPSP) and inhibitory postsynaptic potential (IPSP). The electrode diameter inserted into the brain ranges from 10 to 30 μm, affording a great deal of tissue coverage up to 50 $mm^2$ on average (Normann et al., 1999) and a high spatial resolution that is required to analyze the neural substrates for complex tasks. Despite this enhanced sensitivity and specificity, which justifies their use in the experiments described in this thesis, the downside of using these penetrating electrodes still remains due to the invasive aspect of this technique, as insertion of a probe several millimeters deep into the brain can destroy neurons along the pass (Lebedev and Nicolelis, 2006).

## 3. Background electrical activity and signal processing

In order to determine the changes in brain oscillation associated with behavior-specific neural activity or pathological processes, it is critical to first understand the EEG patterns in a variety of normal physiological conditions including sleep, awake, immobile and highly mobile states from various brain regions in the cortex, brainstem, thalamus, and limbic areas. The normal range of the EEG frequency, also called background activity, is around or above 8.5 Hz in the posterior head regions in awake adults humans. In contrast, the background activity is dominated by the beta rhythm in the anterior brain regions, and by the beta, alpha and theta rhythms in the central and temporal regions, respectively. Due to rapid changes in EEG features during early development with respect to temporal and spatial organization and age-specific unique patterns in the pediatric brains that are not linked to pathology, we will limit our discussion of this chapter to adult EEG only (Plouin et al., 2013; Staba and Worrell, 2014).

EEG translates a three-dimensional electrical wave into a two-dimensional electrical wave using two electrodes as reference points. Thus, an epoch of EEG recording represents a time-varying dynamic of voltage difference (i.e., potential in mV or μV) between two locations (e.g., a target site vs. reference/ground). EEG signals in the time domain often contain slow and fast oscillations, amplitudes of which wax and wane in a complex fashion; hence the raw EEG information is not intuitive to the naked eye. As such, a Fourier

transformation is frequently used to parcel out specific frequency bands simultaneously and to reveal the unique characteristics of EEG from its complex time domain. As a frequency domain representation of the original data, the Fourier transformation provides information in the amplitude (mV or V) or power ($mV^2$ or $V^2$) of any frequency band over a period of time. In principle, data of a longer period generates a parcellation of frequency bands with finer resolution, and in turn results in a more precise estimate of amplitude at a given frequency. However, in practice, data of interest often do not last for a long time. Therefore, the parameters of the Fourier transformation are often dictated by specific scientific questions or the exact protocol that may vary between studies. The distribution of each wave throughout the entire brain under normal physiological condition following Fourier transformation spectrum excluding the gamma band is as following: 25-45 % of delta oscillations, 40 % of theta oscillations, 12-15 % of alpha oscillations and 3-20 % of beta oscillations in rodent EEG in the global frequency band (0-30 Hz) (Lu et al., 2001; Zhang et al., 2013).

## 4. EEG in normal conditions

EEG signal can be obtained by the volume conduction of the brain with the electrical current propagating from the generators to the recording electrode through brain tissue. Due to the physics of waves, slower oscillations propagate more than higher frequency ones, recruiting a larger network as in the case of theta and delta waves (Steriade, 2001; Csicsvari et al., 2003). Although it is established that EEG records the currents from the cortical neurons, the exact origin of the electrical activity or intermediate partners involved in driving these events are not well understood. Because EEG translates a three-dimensional signal into a two-dimensional one, it is not possible to precisely localize the electrical sources of the oscillations (Olejniczak, 2006). It is hypothesized that certain brain structures or neuronal networks serve as the generators of various oscillation frequencies similar to pacemakers, while others act like the resonators that respond to certain firing frequencies (Llinas, 1988). It appears that the locations of the generators may vary depending on the frequencies. The reticular activating system (RAS), known as the arousal system, originates from the midbrain reticular formation and potentiates thalamic and cortical responses during both waking and REM sleep, a state of dream consciousness. Interestingly, among the comatose patients there were simultaneous changes between EEG and other vital physiological parameters including cardiorespiratory and blood pressure (Evans, 1976; Steriade, 1996), suggesting that there might be a common origin in the inherent periodicity of the arousal mechanisms. The RAS serves to modulate all the spectrum rhythms depending on sensory inputs and ongoing

activity in the brain, in which ascending inhibition or decreasing excitation slows down the brain oscillations whereas excitation or disinhibition accelerates rhythms (Garcia-Rill et al., 2013).

Since the EEG technique was invented, efforts have been made to understand the association between a specific brain oscillation and corresponding behavior with some success. This chapter provides an overview in the amplitude or power of dominant waves observed during a specific behavior in humans and in animals with either scalp EEG or inserted electrodes in deeper structures allowing to explore the generators of the oscillations.

### 4.1. Alpha oscillations

Alpha oscillations have a frequency between 8-12 Hz and they are generated by the cells in layers IV and V of the cortex (Hari et al., 1997; Roopun et al., 2006; Buffalo et al., 2011). However, contradicting results raise the possibility that the alpha wave is generated from locations other than the cortex. The alpha wave frequency is present after sensory stimulation in the auditory and visual pathways, as well as in subcortical regions like the hippocampus or the reticular formation (Başar, 1998; Basar et al., 2001). It is also prominent in the thalamus and can be seen in isolated thalamic networks (Steriade et al., 1993a). Further evidence suggests that the cortical alpha wave is driven by thalamic pacemaker cells (Basar et al., 1997) and the thalamo-cortical-thalamic network (da Silva et al., 1973; Sauseng et al., 2007). As a direct support for the thalamic origin of alpha waves, thalamic lesions lead to alpha rhythm disorganization or suppression in humans (Ohmoto et al., 1978; Terao et al., 1993). In addition, occipital alpha rhythm episode is associated with an increase in the thalamic activity as measured by blood oxygenation (Goldman et al., 2002; Feige et al., 2005) or blood flow (Sadato et al., 1998).

The alpha band, also known as the mu rhythm in the motor cortex, is present in the occipital cortex during aroused states with eyes closed (Destexhe and Sejnowski, 2003) or relaxed wakefulness. A form of alpha wave can also be observed during sensory, cognitive and motor processes (Basar et al., 1997; Başar, 1998; Basar et al., 2001) and could play a role in the neuronal communication (Palva and Palva, 2007).

### 4.2. Beta oscillations

As alpha oscillations, beta oscillations (12-30Hz) are also generated by the cells in

layers IV and V of the cortex (Hari et al., 1997; Roopun et al., 2006; Buffalo et al., 2011). Beta power is observed in awake, attentive states that require working memory or in the motor cortex during the preparation of movements (Engel and Fries, 2010). It has been suggested that the function of the beta oscillation could highlight a novel stimulus that would require further attention (Kisley and Cornwell, 2006; Uhlhaas et al., 2008) based on its presence during novelty detection in the auditory system (Haenschel et al., 2000), reward evaluation (Marco-Pallares et al., 2008) and sensory gating (Kisley and Cornwell, 2006).

### 4.3. Theta oscillations

The generators of the theta wave (4-8Hz) have been proposed in several locations. To investigate deeper structure that can act as potential generators, electrode implants were particularly pertinent. One report suggests that structures like the entorhinal cortex and medial septum may act like pacemakers, inhibiting or exciting certain subregions of the hippocampus to synchronize the theta wave (Green and Arduini, 1954; Sirota et al., 2008; Pignatelli et al., 2012). In comparison, the hippocampus acting like a resonator generates the theta oscillation that propagates via the volume conduction through the septo-temporal axis (Monmaur et al., 1990). Hence, the inactivation or lesion of the septum perturbs the hippocampal theta oscillations (Green and Arduini, 1954). However, a discrepant report implicated the source of theta to originate from within the hippocampus (i.e. in the CA1 and DG, propagating the current into the superficial and deep layers of the brain, respectively). Despite the fact that theta oscillation has also been observed in the perirhinal cortex, cingulate cortex, subiculum and amygdale (Adey, 1967; Mitchell and Ranck, 1980; Alonso and Garcia-Austt, 1987; Leung and Borst, 1987; Pare and Collins, 2000), these structures are generally not considered as proper generators but rather as resonators of the currents (dipoles) because they cannot generate theta activity by themselves.

The role of the theta rhythm seems associated with the brain activity synchronization. Indeed, theta rhythm could organize the hippocampal activity of each field to synchronize the whole structure. Hippocampal interneurons participate to the synchronization of the pyramidal cell firing activity during theta oscillations (Buzsaki, 2002; Klausberger and Somogyi, 2008). CA1 theta rhythm is altered if interneurons are pharmacologically inactivated (Gillies et al., 2002; Rotstein et al., 2005). The hippocampal theta is also associated with memory functions (Hasselmo, 2005), as theta power increases during cognitive tasks as well as during verbal and spatial tasks due to an increase in memory load (Burgess and Gruzelier, 2000; Krause et

al., 2000; Kahana et al., 2001). Ample experimental studies have focused on the understanding of oscillations in the hippocampus and corresponding behavior. For example, in the rat hippocampus, theta state occurs during walking, running, rearing and exploratory sniffing as well as during REM sleep (Vanderwolf, 1968; Kahana et al., 2001; Buzsaki, 2002; Harris and Thiele, 2011). Hippocampal theta is associated with stimuli in working memory instead of reference memory condition (Kahana et al., 2001), thus it could be a tag for short-term memory (Vertes, 2005). Additional evidence also suggests that the hippocampal theta rhythm is associated with spontaneous movements in monkeys (7-9 Hz) (Stewart and Fox, 1991) and locomotion in rodents (Vanderwolf, 1968). Compared to hippocampal theta, the role of cortical theta rhythm is less clear. At least in cats, this rhythm is associated with task orientation during coordinated response indicating its role in alertness, arousal or readiness to process information (Basar et al., 2001).

### 4.4. Delta oscillations

For slow wave state present during non-REM sleep (frequency inferior at 1 Hz), the two main oscillations generators are in the neocortex (pyramidal neurons in the layers II/III, V and VI) and the thalamus (TC and NRT neurons). A synchronization is established between these two generators via corticothalamic, thalamocortical and intracortical connections (Crunelli and Hughes, 2010). The delta wave is generated by the thalamus and pyramidal cells located in the layer II-VI of the cortex.

Slow oscillations (0.3-1 Hz) and delta oscillations (1-4 Hz) are present during anesthesia and slow-wave sleep suggesting their role in the consolidation of neuronal connections and new memories acquired during wakefulness (Steriade and Timofeev, 2003). Increased amplitude in delta wave has also been detected after auditory target stimuli during oddball experiments in which presentations of repetitive audio/visual stimuli sequences were intermittently interrupted by a deviant stimulus, implicating its involvement in signal detection and decision making (Basar et al., 2001). Although delta oscillation is dominant during the sleep state in animals (Basar et al., 2001), it is also observed during immobility and drowsiness in awake animals (Harris and Thiele, 2011).

### 4.5. Gamma oscillations

The gamma rhythm (30-80 Hz) seems to be present in several different brain structures associated with visual, auditory and motor tasks (Tallon-Baudry et al., 1996; Basar

et al., 1998; Crone et al., 1998; Basar et al., 2000). The cortical gamma seems to be generated by the superficial layers II/III (Gray and McCormick, 1996; Buhl et al., 1998; Roopun et al., 2006) and networks of interconnected inhibitory interneurons (Whittington et al., 1995). At the network level, tetanic stimulation of the thalamic reticular nucleus induces focal cortical gamma oscillations via primary sensory pathways (Macdonald et al., 1998). Further, following the stimulation of the pacemaker cells located in the reticular nucleus of the thalamus (another reported location of generator), there is an increase of the gamma oscillation (35-55 Hz) in the somatosensory and auditory cortex (Macdonald et al., 1998). An alternative school of thought suggests that gamma oscillations are generated by synaptic activity via the interaction between neurons (Bringuier et al., 1997; Cardin et al., 2005). For example, gamma oscillations can be generated by pacemaker cells located in the hippocampus that entrain the "chattering cells" in the cortex to fire at the same frequency (Gray and McCormick, 1996). In vitro studies have shown that the gamma rhythm can be elicited in cortical and hippocampus slice preparations after stimulation of the metabotropic glutamate receptors for a long period of time (Buhl et al., 1998) or by activation of these receptors with bursts of afferent stimulation for transient amounts of time (Whittington et al., 1995; Whittington et al., 1997; Traub et al., 1999). Likewise, the subiculum can generate gamma oscillations via the local inhibitory neuronal network following stimulation evoked either locally or in the nearby hippocampus CA1 (Colling et al., 1998).

Gamma power often increases during problem solving, yet a 40 Hz frequency (gamma band) is present during the rapid eye movement (REM) dream state sleep that interrupts the delta power dominant-slow wave sleep (Llinas and Ribary, 1993; Destexhe and Sejnowski, 2003), suggesting its role in modulating other oscillations. Given its omnipresence across different brain regions and its implication in a variety of cognitive functions, the gamma rhythm may serve to provide the synchronization between different neuronal networks (Singer, 1999; Varela et al., 2001). The gamma wave has been commonly observed after sensory stimulation (auditory and visual) in the cortex, the hippocampus, brain stem and cerebellum in cats (Schurmann et al., 1997; Başar, 1999; Basar et al., 2001). Interestingly, the gamma amplitude in the rat hippocampus is larger during theta-associated behaviors such as exploration, sniffing, rearing and the paradoxical phase of sleep than it is during non-theta associated behaviors, suggesting that the gamma oscillation is synchronized with the theta oscillation (Bragin et al., 1995b)

### 4.6. Sharp-waves ripples

During slow wave sleep and resting wakefulness in humans and rodents, the hippocampus generates special burst of high frequency field oscillations called “sharp-waves ripples” (SWRs) (Buzsaki et al., 1992; Skaggs et al., 2007; Le Van Quyen et al., 2008). Stimulation protocols using LTP can induce SWRs and this LTP is a popular neurophysiological artificial model of learning and memory. Sharp-waves are large amplitude negative polarity deflections (40-100 ms) generated in the CA1 stratum radiatum. The current sink is located in this layer whereas current source is in the pyramidal cell layer (Buzsaki et al., 1983; Buzsaki, 1986; Sullivan et al., 2011). Sharp-waves are often associated with fast oscillations frequency events known as “ripples” with duration of less than one second. Ripples are generated in the CA1 stratum pyramidal and sink-source current pairs are both located in the pyramidal layer (Ylinen et al., 1995; Csicsvari et al., 1999b) . SWRs occurred mainly in CA1 but they also occur in CA3 or in the parahippocampal region such as entorhinal cortex, subiculum, para- and pre-subiculum cortices (Chrobak and Buzsaki, 1994, 1996) with a fast oscillation frequency ranging between 90-250 Hz (Csicsvari et al., 1999c). We can distinguish ripples by their frequency in CA1, they are positively correlated to the amplitude of the sharp-wave as follows: large sharp-wave are associated with ripples of 140-250 Hz and small sharp-wave (in the fast gamma range) are associated with ripples of 90-140 Hz frequency (Sullivan et al., 2011; Patel et al., 2013). Classical vision presents the CA3 as a generator of ripples propagating to CA1, and then to subiculum, parahippocampal region and EC (**Fig. 23**). Interestingly, it seems that ripples might be also generated locally because of the lack of coherence between CA1-CA3 ripples (Ylinen et al., 1995), the fact that CA3 ripples are smaller than CA1 ripples (Buzsaki et al., 1992; Ylinen et al., 1995), decreasing ripple coherence along the septotemporal hippocampal axis (Patel et al., 2013), and the lack of coherence between CA3 unit firing and CA1 ripples (Csicsvari et al., 1999c). We can mention that frequency of SWR differs between rodents and humans, indeed ripples has a frequency around 200 Hz in the CA1 subregion of rodent hippocampus (Buzsaki et al., 1992) whereas lower frequencies of around 80-100Hz are observed in human hippocampal recordings (Bragin et al., 1999; Axmacher et al., 2008).

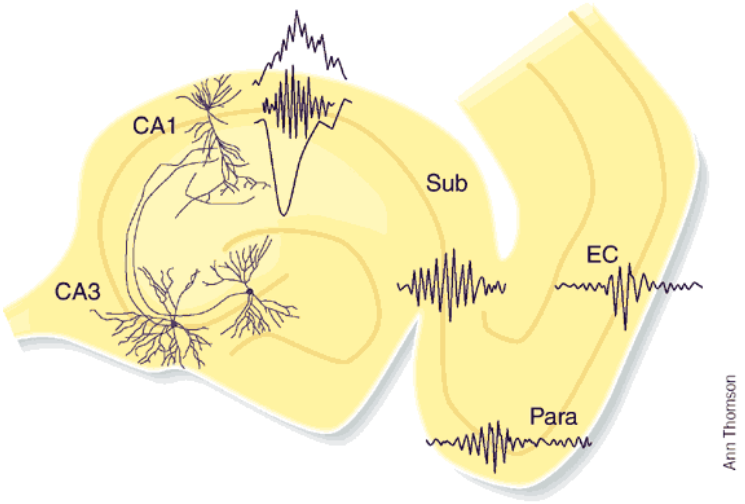


***Figure 23. Occurrence of ripples in hippocampus and parahippocampal regions***. *Representation of a sagittal view of the rat hippocampus. Burst of activity in CA3 induces SWR in CA1 pyramidal layer followed by similar SWR complexes in the subiculum (Sub), parasubiculum (Para) and entorhinal cortex (EC) (from Buzsaki and Chrobak (2005)).*

The underlying cellular and network mechanisms underlying the generation of SWRs are still unclear. Ten to twenty percent of all the pyramidal neurons in the rat hippocampus produce action potentials during SWRs (Csicsvari et al., 2000). The excitation of a minimum of 80 pyramidal cells is necessary to generate a detectable ripple. Computational models suggest the recruitment of pyramidal cells and interneurons over time. Spikes of CA1 pyramidal cells are phase-locked to the ripple cycles, and SWRs could occur when pyramidal cells fire by 90 ° before the interneuron firing (Brunel and Wang, 2003; Stark et al., 2014). The intrinsic circuits of an isolated hippocampus seems sufficient to generate SWRs. Buzsaky suggested that "the SWRs are not induced but "released" in the absence of suppression mechanisms because the default mode of the CA3 recurrent system is burst generation" (Buzsaki, 2015). The suppressive effect of the subcortical neuromodulators might be provided by the entorhinal cortex and the septum because lesions of these structures increase the incidence of SWRs (Buzsaki et al., 1983; Ylinen et al., 1995). In vitro study reported that both excitatory postsynaptic current **(**EPSC) and inhibitory postsynaptic current (IPSC) begin to increase 50 to 100 ms before the SWR event with a bigger amplitude of EPSC. Then, periodic and phase-shifted oscillations of EPSC and IPSC occur during the ripple (Stark et al., 2014). Hippocampal SWRs are more frequent to appear at the transition between down and up-states (Sirota et al., 2003; Battaglia et al., 2004; Isomura et al., 2006; Molle et al., 2006).

Role of SWRs are still discussed, however those events are correlated with memory consolidation and widespread changes in activity throughout the cortical network (Logothetis

et al., 2012; Atherton et al., 2015). HFO, ripples in particular, play a crucial role in the information processing and the consolidation of memory (Bragin et al., 2010). They might "transfer" labile memories from hippocampus to neocortex to stabilize memories during offline states such as sleep and periods of quiet wakefulness (Buzsaki et al., 1983; Buzsaki, 1996), but also in deeper structures such as ventral striatum (Pennartz et al., 2004; Lansink et al., 2009). It has been reported that SWRs occurrence increase in rat hippocampus following a learning task such as an odor-learning association task (Eschenko et al., 2008) or radial maze task (Ramadan et al., 2009). SWRs play a critical role in memory consolidation, possibly by promoting the hippocampal-cortical dialogue involved in memory storage at the cortical level, of which the selective elimination during post-learning sleep results in impairment of memory (Girardeau et al., 2009; Jadhav et al., 2012). For example, suppression of SWRs by electrical stimulation following learning impairs the formation of spatial memory (Girardeau et al., 2014). Interestingly, replay sequences occurring during slow wave sleep are shorter (faster) and frequency burst are higher (~200 Hz) than during the learning task which is comparable to the experimental protocol of LTP induction (Bliss and Collingridge, 1993). As a reminder, LTP is a cellular and molecular mechanisms involved in memory processes (Pastalkova et al., 2006; Whitlock et al., 2006). Theory mentioning the memory trace replay is emerging, indeed studies reported that memories are encoded during wake behavior by neurons which burst in a coordinated fashion in cell assemblies (McGaugh, 2000; Harris et al., 2003). To consolidate this new trace, activity of neurons need to be maintained, for this reason the network which was activated during the learning task is re-activated during subsequent offline periods in the same sequence of firing patterns observed during initial learning. To illustrate this phenomenon, place cells of the hippocampus which are activated sequentially when an animal perform a spatial task in an arena are reactivated and replayed in the same sequence during SWRs occurring in the slow-wave sleep period, or period of immobility of the animal (O'Neill et al., 2010; Carr et al., 2011).

The benefit of sleep in memory consolidation can be better appreciated from the perspective of slow wave activity. Apparently the amplitude and slope of EEG slow waves is related to the number of neurons that enter in near-synchrony state, which is directly linked to the number and strength of synaptic connections among these neurons. Thus, per synaptic homeostasis hypothesis, spontaneous activity renormalizes net synaptic strength and restores cellular homeostasis during sleep (Tononi and Cirelli, 2014). Plasticity-dependent recovery

could be improved by managing sleep quality, while monitoring EEG during sleep may help to explain how specific rehabilitative paradigms work (Gorgoni et al., 2013).

In stroke patients or stroke models, literature does not report any SWRs disturbance but pathological HFOs (200-600 Hz) that are distinct from normal ripples are often recorded in the dentate gyrus during seizure generation (Engel et al., 2009).

### 4.7. Synchronized versus. desynchronized cortical state and behavior

Apart from the conventional classification of brain activity based on frequency range, a new definition of the dynamics of network activity has emerged, known as the synchronized versus. desynchronized cortical states. A strong synchronization between the different networks consisting of both slow and large amplitude fluctuations as seen in slow wave sleep is referred to as a synchronized state, characterized by up phases during which neurons fire, followed by down phases during which neurons are silent. The low frequency power is high (slow oscillation and delta oscillation) whereas the gamma rhythm may decrease during this synchronized state. In contrast, the desynchronized state is present during waking or REM sleep, and it shows fast and low amplitude deflections during which the theta oscillations are dominant and the neurons fire continuously and irregularly without synchronization at the population level. Between these two opposing brain states, there is a continuum of intermediate states with varying degrees of synchronization. The transition between these two extreme states are mediated by neurotransmitters such as serotonin, noradrenaline and acetylcholine that modulate the excitability of the neurons (Harris and Thiele, 2011).

In general, the synchronized state is associated with immobility and quiescence in addition to slow wave sleep and anesthetized state (Clement et al., 2008; Renart et al., 2010; Ribeiro et al., 2010), albeit it is also present during waking. The amplitudes of oscillations in the synchronized state are usually smaller relative to those during slow wave sleep (Crochet and Petersen, 2006; Poulet and Petersen, 2008). Unlike the synchronized state, the desynchronized state is present in active and behaving rodents (Okun et al., 2010; Poulet et al., 2012), and is often associated with an increase in the gamma power among behaving animals (Niell and Stryker, 2010), or during stimulation of subcortical structures (Munk et al., 1996) and attention (Fries et al., 2001). However, some studies have shown contradicting results, in which the gamma power decreases in the desynchronized state (Chalk et al., 2010; Puig et al., 2010).

### 4.8. Phase locking and oscillation coupling

In light of the continuum represented by brain oscillations, using conventional approach by treating them as individual "explicit" entities seems to reach an impasse for advancement. The ability of one oscillation in modulating another across brain regions adds even more dimensions to the already complex relationship. Since low frequency waves propagate more than high frequency ones that tend to stay localized to small structures (Steriade, 2001; Csicsvari et al., 2003), theta and delta waves are found to propagate through the entire brain as directional waves, whereas alpha, beta and gamma waves are localized and driven by theta and delta rhythms. Ample studies sought to understand the interaction between gamma and theta oscillations. For example, it has been shown that neocortical neurons were modulated by the hippocampal theta rhythm, with increased firing when the phase of theta is down in the CA1. Interestingly, a greater proportion of interneurons, e.g. 32 % in parietal cortex and 46 % in prefrontal cortex were modulated by theta waves, compared to that in pyramidal neurons (11 % in parietal cortex and 28 in prefrontal cortex) (Sirota et al., 2008). Another study demonstrated that the gamma oscillation was phasically modulated by the theta cycle and the amplitude of gamma oscillation varied as a function of theta cycle. Moreover, the amplitude of gamma activity was larger and the hippocampal interneurons in the hilus of the dentate gyrus fired rhythmically with a higher rate during theta-associated behaviors such as exploration, sniffing, rearing, and the paradoxical phase of sleep. It should be mentioned that after entorhinal cortical lesion, the amplitude of the hippocampal theta (5-10 Hz) decreased by 50-70% and the frequency of gamma oscillations reduced in the dentate gyrus from 40-100 to 40-60 Hz (Bragin et al., 1995b). Additional studies further suggest that the gamma oscillation in the cortex is driven by theta oscillation from the hippocampus (Bragin et al., 1995b; Chrobak and Buzsaki, 1998; Sirota et al., 2008).

Evidence showing modulation between other oscillatory bands has just begun to emerge. A recent study investigated how slow activities such as delta rhythm coordinate fast oscillations such as gamma rhythm over time and space. One study recorded the local field potentials in the cortico-basal ganglia structure of freely moving, healthy rats and showed that the phase of delta waves modulates the amplitude of gamma activity (Lopez-Azcarate et al., 2013). The complexity of the relationship between various band frequencies and how it can be modified under pathological conditions is best exemplified for the alpha wave in the thalamus. An increased depolarization in the thalamocortical neurons that discharge in the range of 2-13 Hz can lead to oscillation in the alpha frequency (8-13 Hz), while a reduced

depolarization of the same neuronal subpopulation gravitates brain waves towards the theta rhythm (2-7 Hz) (Hughes and Crunelli, 2005). Modification in oscillation coupling has indeed been reported in pathological conditions including schizophrenia, Parkinson's disease, or autism (Voytek and Knight, 2015). Given that theta-gamma coupling seems necessary for working memory (Park et al., 2013), and that working memory is disturbed in stroke patients (Qureshi et al., 2013), it is surprising that there is no evidence showing an impaired theta-gamma or other oscillatory couplings in these patients or experimentally-induced stroke in rodents. Some factors might have contributed to the paucity of data in this area; for example, theta phase calculation relies on the sinusoidal assumption, while human theta (either EEG or hippocampal theta) is not sinusoidal-like. Although rodent theta is sinusoidal and an increase in delta power does occur after experimental stroke, deciphering clear theta epochs from other frequency bands is no easy task.

## 5. Cellular mechanisms of electrical brain activity

The conventional EEG records the summation of currents of pyramidal neurons located at the surface of the scalp in the cortical layers. Similar to pacemaker cells, neurons are electrically excitable cells that can generate pulse and are able to propagate an incoming current via electrical and chemical signals sent from the axon of one presynaptic neuron to the dendrites of another postsynaptic neuron in a network. The neuron has a resting membrane potential about -60 to -70 mV resulting from flux of ions in the neuronal environment. Neurons have high concentrations of potassium ($K^+$) and chloride ($Cl^-$) ions inside, while high concentrations of sodium ($Na^+$) and calcium ($Ca^{2+}$) ions are outside. These concentration gradients are maintained by a sodium-potassium pumping system. The closing or opening of ions channels induced by chemical or electrical stimuli modifies the flux of ions and leads to a modification of the membrane potential. An influx of positively charged ions into the cell reduces the charge separation across the membrane and results in a less negative membrane potential termed depolarization, whereas an efflux of positively charged ions increases the charge separation leading to a more negative membrane potential called hyperpolarization.

Once activated, a neuron releases neurotransmitters into the synaptic cleft that either excite (depolarize) or inhibit (hyperpolarize) the adjacent postsynaptic neuron depending on the nature of the neurotransmitters. EPSP depolarizes the post-synaptic neurons resulting from the release of excitatory neurotransmitters such as glutamate or acetylcholine, while IPSP hyperpolarizes neurons resulting from the release of inhibitory neurotransmitters such as

GABA and glycine. An EPSP produces a flow of positive charges into the cell (current sink), while an IPSP acts in the opposite way by inducing a flow of positive charges out of the cell (current source). The summation of IPSP and EPSP induces a graded potential in the neuron so that when this membrane potential reaches the threshold potential, it induces an action potential that can propagate between neurons. The AP is produced by a critical amount of $Na^+$ entering into the cell and the opening of additional $Na^+$ channels. This fast depolarizing event corresponds to the rising phase of the action potential, followed by the repolarization of the cell induced by an efflux of $K^+$ ions and a decrease of $Na^+$ influx. After an AP, there is a refractory period during which another AP cannot be generated due to a transitory inactivation of $Na^+$ channels (**Fig. 24**).

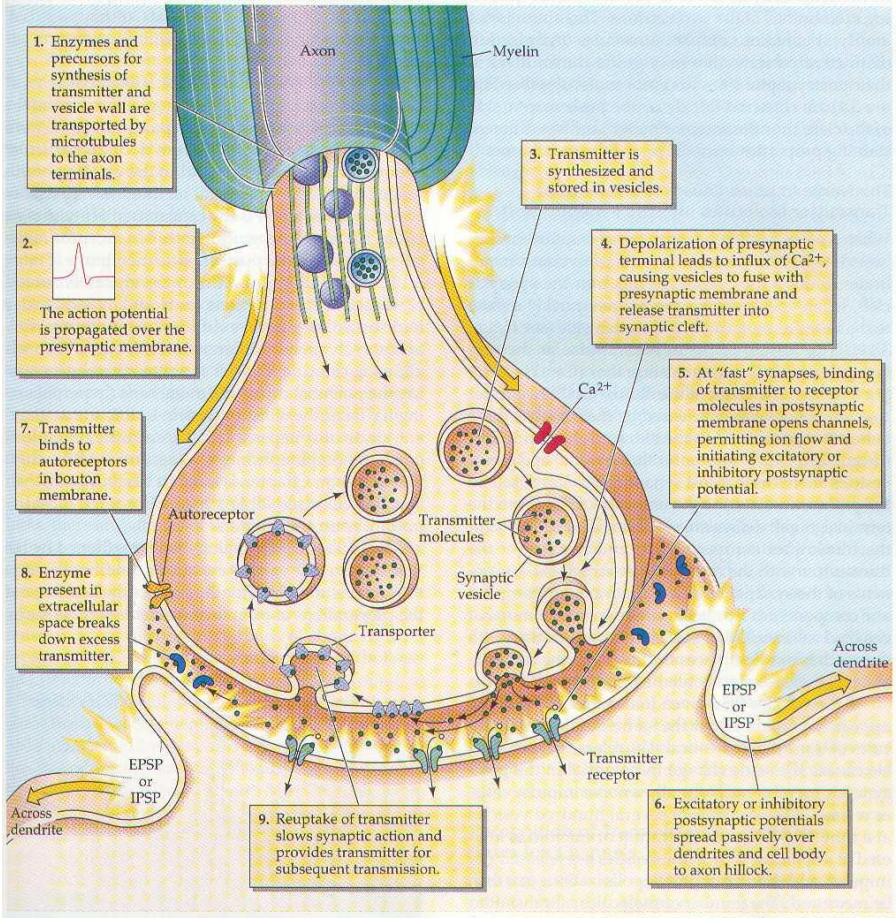


***Figure 24. Transmission and creation of EPSP and IPSP following presynaptic action potential.*** *Schematic representation of the synaptic activity. Neurotransmitters are released into the synaptic cleft following a presynaptic action potential, and then they bind to a postsynaptic receptor which open the ion gate and initiate EPSP or IPSP. Summation of EPSP or IPSP leads to an action potential if the threshold is crossed (from Purves D (2001)).*

EEG detects field potential as IPSP or EPSP generated by neurons because those events are longer in duration than action potentials (up to 10 milliseconds versus. few

milliseconds). To summarize the mechanisms of current flow, EPSP that depolarizes the membrane results from excitatory currents, involving $Na^+$ or $Ca^{2+}$ ions, flowing inward toward an excitatory synapse (i.e., from the activated postsynaptic site to the other parts of the cell) and outward away from it. The outward current is referred to as a passive return current (from intracellular to extracellular space). IPSP, which hyperpolarizes the membrane, is caused by inhibitory loop currents that involve $Cl^-$ ions flowing into the cell and $K^+$ ions flowing out of the cell (Olejniczak, 2006).

The vertically orientated pyramidal neurons located in the cortex laminae are considered as a dipole that can generate extracellular voltage fields from graded synaptic activity. The dipole is created with separation of charge vertically orientated in the cortex, and with apical dendrites extending upward to more superficial laminae and axons projecting to deeper laminae. The EEG detects the extracellular electrical fields generated closer to the cortical surface. The cortex is composed of several cortical laminae that can generate an opposite current for the same synaptic event depending on the layer being excited. For example, an EPSP at the apical dendrite in the layer II/III is associated with an extracellular negative field (active current field) and an extracellular positive field (passive current source) in the basal dendrite located in layer V. On the contrary, an EPSP on the proximal apical dendrite located in the cortical layer IV is associated within extracellular negative field (active current sink) and an extracellular positive field in the distal apical dendrite in layers II/III (passive current source) (**Fig. 25**) (Olejniczak, 2006). So, a deep IPSP and a superficial EPSP will both generate a negative field in the scalp and vice versa. Therefore, large population of neurons can be considered as a collection of oscillating dipoles (Ebersole, 2003).

The EEG tracings reflect the mean excitatory state of a pool of neurons rather than individual neurons, because the extracellular space beneath the electrode is traversed by currents from many cells. The interaction of signals of excitatory and inhibitory neurons explains why EEG waves oscillate (Freeman, 1991), in which alternating rises and falls in amplitude come from negative feedback circuits formed by this complex interaction as the following: 1) the excitatory neurons are stimulated or ceased to be inhibited; 2) the excitatory neurons stimulate the inhibitory neurons, dampening excitation; 3) the inhibitory neurons inhibit the excitatory neurons, reducing the electrical activity; 4) when the activity falls to minimal level, the inhibitory neurons rest, releasing excitatory neurons from inhibition and cycle resumes. In support of this conceptual framework depicting the collective activity underlying odor perception, another computational study further illustrates how synchronous

rhythmic spiking in neuronal networks can be brought about by the interaction between excitatory and inhibitory cells in generating the pyramidal-interneuronal gamma rhythm, in which the inhibitory neurons inhibit the pyramidal neurons that themselves project to the inhibitory neurons (Borgers and Kopell, 2005).

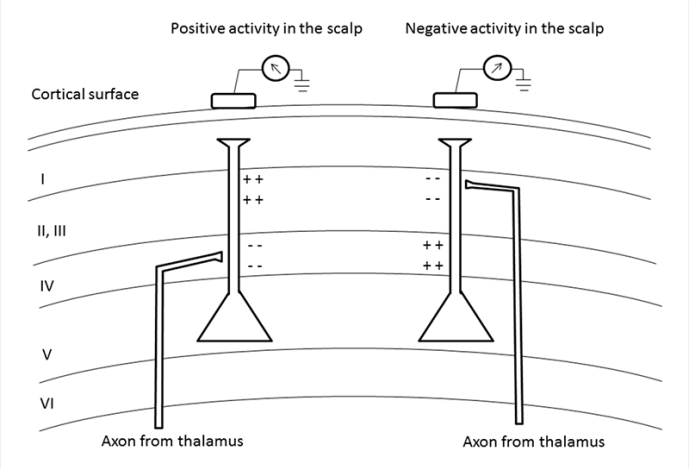


***Figure 25. Generation of extracellular voltage fields.*** *Relationship between the polarity of surface potentials and the location of dendritic postsynaptic potentials. EPSP depolarizing cell membrane induces a local negative local field potential and a positive local field potential far away from the source. EPSP can also induce negative or positive activity in the scalp depending on the cortical layers excited (adapted from Olejniczak (2006)).*

## 6. EEG in stroke conditions

Evidence suggests that ischemic stroke, a direct consequence of CBF impairment in local cerebral areas, is associated with brain oscillations fluctuations. Due to the non-invasive and real-time nature of the technique used to record the changes in brain activity, EEG has been widely employed in both the clinical and research fields.

### 6.1. Cerebral blood flow and EEG

Due to the great complexity and variation in brain ischemia-induced pathophysiology, a general consensus regarding the modifications of the brain oscillations after stroke is hard to reach, except that the electrical activity appears to correlate with cerebral blood flow (Astrup et al., 1981; Jordan, 2004; Foreman and Claassen, 2012; O'Gorman et al., 2013), oxygen and glucose level (Lennox et al., 1938; Faught, 1993).

EEG abnormality begins to emerge when the CBF decreases to 25-30 mL/100 g/min compared to the normal range of 50-70 mL/100 g/min. (Astrup et al., 1981). **Table 2**

illustrates the critical levels of CBF for categorical reduction or loss in EEG amplitude and frequency, with corresponding changes in cellular metabolism and neuronal morphology (Branston et al., 1974; Faught, 1993; Jordan, 2004; Foreman and Claassen, 2012). When CBF falls below 18 mL/100 g/min, it crosses the ischemic threshold and induces neuronal death while when it reaches 12 mL/100 g/min or below, infarction becomes evident because of the progressive loss of transmembrane potential gradients of neurons. If the CBF is below the ischemic threshold but maintained above the infarction threshold, the effect on metabolism or cell survival is still reversible, with visible electrical activity as delta oscillations. When the CBF falls below the threshold of infarction for a substantial amount of time, say more than 45 min at 14 mL/100 g/min or less, the spontaneous neuronal activity never returns even after reperfusion, and the damages are irreversible (Sharbrough et al., 1973; Gloor, 1985; Hossmann, 1994; Jordan, 2004). A blood reduction of 20 % inhibits the protein synthesis, 50 % of CBF reduction is associated with an accumulation of neurotoxic elements such as glutamate and lactate in the extracellular space and under 50 % of blood reduction, the ATP is not anymore available in the cell which leads to the arrest of electrical transmission associated with a water flux inducing an oedema. The neuronal death appears after 80 % of blood reduction because of the loss of the ionic gradient and a rapid depolarization of the neuronal cells (Hossmann, 2006).

| **CBF level (mL/100g/min)** | **EEG abnormality** | **Cellular response** | **Degree of neuronal injury** |
|---|---|---|---|
| 35-70 | Normal | Decreased protein synthesis | No injury |
| 25-35 | Loss of fast beta frequencies and decreased amplitude of somatosensory evoked potentials | • Anaerobic metabolism<br>• Neurotransmitter release (glutamate) | Reversible |
| 18-25 | Slowing of theta rhythm and loss of fast frequencies | • Lactic acidosis<br>• Declining ATP | Reversible |
| 12-18 | Slowing of delta rhythm, increases in slow frequencies and loss of post synaptic evoked responses | • Sodium-potassium pump failure<br>• Increased intracellular water content | Reversible |

| | | | |
|---|---|---|---|
| <8-10 | Suppression of all frequencies, loss of presynaptic evoked responses | • Calcium accumulation<br>• Anoxic depolarization | Neuronal death |

***Table 2. The relationship of cerebral blood flow to electrical brain activity and pathophysiology.*** *Adapted from Foreman and Claassen (2012) and Jordan (2004).*

While the CBF is directly correlated with the brain oscillations, it has been shown that the glutamate concentration (excitatory neurotransmitter) is associated with the theta waves (4-7 Hz) in the frontal lobe and the hippocampus in humans undergoing cognitive tasks (Gallinat et al., 2006). Abnormal release of glutamate coincides with CBF level of 20-30 mL/100g/min and is associated with peri-infarct depolarization (Hossmann, 1994; Dreier et al., 2009). Parallel experimental data show that a reduction in EEG power across all frequency ranges 1 to 3 hours after permanent middle cerebral artery occlusion (pMCAO) in the ischemic ipsilateral cortex of rats is associated with a decrease of 30 % of CBF compared to baseline and an increase of 1400 % of glutamate release (Guyot et al., 2001). Moreover, CBF and cerebral rate of oxygen metabolism studied with Xenon computed tomography and positron emission tomography show that regional EEG changes reflect the coupling of CBF and metabolism in ischemic stroke (Nagata et al., 1989). In early subacute stroke, the EEG correlates with the CBF because the oxygen extraction fraction increases to preserve the cerebral rate of oxygen metabolism (described as the “misery perfusion or stage 2 hemodynamic failure”). During the period of luxury perfusion or stage 3 hemodynamic failure, the EEG is no longer correlated with the CBF but instead with the rate of cerebral oxygen metabolism (Nagata et al., 1989; Powers, 1991). It should be noted that the cellular damages such as decreased protein metabolism and neuronal death appear even before the critical stage of CBF in the peri-infarct area (Hossmann, 1994). To recapitulate, increased power in slower frequency bands (as theta or delta) and decreased power in faster frequency bands (as alpha and beta) are seen with the reduced rate of cerebral oxygen metabolism (Nagata et al., 1989). Second, the delta rhythm seems to be the most reliable parameters correlating with CBF and metabolism changes during focal ischemia.

### 6.2. Core and penumbra associated with the electrical brain activity

The ischemic core and penumbra areas are two distinct areas of the infarct according to the time course of the impairment. After a focal ischemia, the core is the first to appear where neurons die due to necrosis. Neuronal survival is threatened by acidosis, lipolysis,

proteolysis, and disaggregation of membrane microtubules after the bioenergetics failure and the ion homeostasis breakdown. Besides, because of the $K^+$ and glutamate release, the neurons depolarize but cannot repolarize. Damages are irreversible and occur a few minutes after the hypoperfusion. Unlike the core, neurons in the penumbra struggle to maintain function but exhibit perturbed electrical activity due to partial energy metabolism preservation. Since repolarization of neurons following depolarization consumes energy, the succession of "peri-infarct depolarization" occurs at the expanse of the valuable and scarce energy remained in the penumbra, leading to a perpetual depletion of the energy, and hence a further expansion of the core and penumbra (Dirnagl et al., 1999). The penumbra area is less deleterious than the core because the cerebral tissue is still viable but electrically impaired. Size of the core and penumbra is time-dependent of the hypoperfusion (**Fig. 26**). Ischemic core can expanse overlapping the peri-infarct penumbra, indeed a wave of depolarization propagates from the core to the penumbra area (Hossmann, 1994, 1996). In the core, the neurons are dead and the cell membrane cannot repolarize, whereas in the penumbra area, the neurons can still repolarize requiring an important consumption of energy. Those depolarizations are multiple and successive which is deleterious for the neurons and expand the size of the infarct, the phenomenon is called peri-infarct depolarizations (Dirnagl et al., 1999). The size of the ischemic core increases with the period of occlusion. Few minutes after occlusion, excitotoxicity induces neuronal necrosis in the ischemic core. Due to inflammation and apoptosis, two mechanisms which are longer to appear, the neurons in the penumbra zone can be rescued if the reperfusion appears less than 4 h 30 min post-ischemia (Gonzalez, 2006; Doyle et al., 2008; Paciaroni et al., 2009).

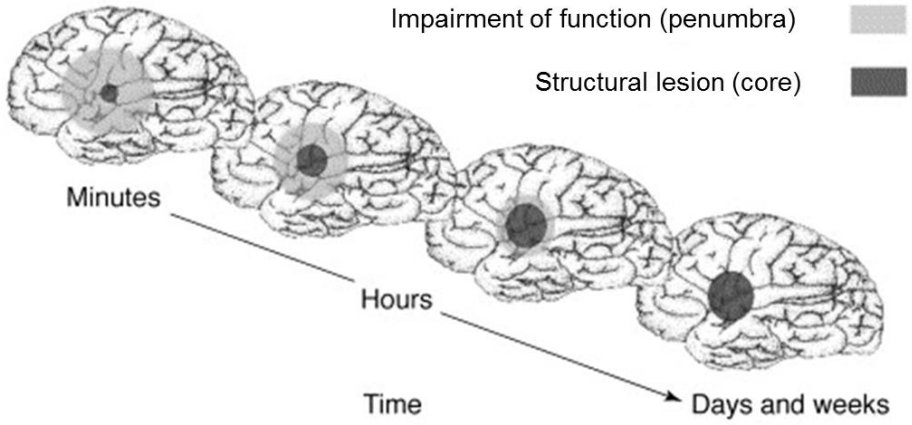


***Figure 26. Illustration of the dynamic state of penumbra and core ischemic territory over time.*** *Over time, the ischemic core extends to penumbra area (from Dirnagl et al. (1999)).*

The nature of the brain oscillation perturbation can provide insight into the pathophysiology and evolution of ischemic core and penumbra. For example, patients with acute unilateral ischemic stroke in the MCA territory experience an increase in the delta activity (low frequency band) whereas a decrease in the alpha activity (high frequency band) in the ipsilateral parieto-occipital cortex and the contralateral medial and posterior cortex occur (Machado et al., 2004), reflecting the state of brain metabolism as well as neural activity in the core and penumbra, respectively (Sheorajpanday et al., 2010; Sheorajpanday et al., 2011). Consistent with this concept, the power of high frequency oscillation like the beta band was found to decrease proportionally with the size and proximity of the infarct in patients one day after stroke (Wang et al., 2013). However, as an exception to the rule, penumbra could also generate slow activity like delta or theta rhythms (Finnigan and van Putten, 2013).

Alternative interpretations regarding the origin of the slow frequency activity after brain ischemia have emerged since the witness of a delta variant known as the polymorphic delta activity. The core support for the alternative theory derives from the fact that a direct lesion to the cortical gray matter alone does not produce slow wave activity due to the coincidental destruction of the neuronal generators located in the cortex; hence a lesion in the subcortical white matter induces irregular delta activity in the cortex overlying the infarct (Gloor et al., 1977). Evidence suggests that the polymorphic delta activity is cortical and it results from a disruption of corticocortical and thalamocortical connections (Ginsburg et al., 1977), since deafferentation of cortical neurons with thalamic lesion leads to the increase of delta-like activity in unilateral or bilateral cortex, bilateral hypothalamus, or bilateral mesencephalon (Gloor et al., 1977; Schaul et al., 1981). Furthermore, surface positive delta waves may represent an inhibitory phenomenon such as a hyperpolarization, based on the following possibilities: 1) the presence of synaptic IPSPs at the soma or basal dendrites, and 2) an influx of the calcium mediated by the efflux of potassium after hyperpolarization. Given the fact that the administration of the cholinergic antagonist atropine leads to polymorphic delta activity, the apparition of the slow-wave activity or the increase of the power of delta oscillations after stroke could result from an impairment of the cholinergic pathways (Schaul et al., 1978).

To summarize, the EEG changes observed after ischemia are caused by an electrical impairment of the neurons due to the changes of the membrane potential induced by energy deprivation. This energy deprivation results from the reduction of the CBF and leads to

irreversible neuronal damages if the CBF is not restored in time. However, the neuronal origin of the increase of slow or delta oscillations and the decrease of high frequencies oscillations after stroke is still under debate.

### 6.3. Excitotoxicity and brain electrical activity

The ischemia-induced excitotoxicity was well studied in the hippocampus and neocortex. In the CA1, short ischemia induces electrophysiological changes in pyramidal cells as a transient small depolarization followed by an increase in the excitability that leads to a hyperpolarization that changes the membrane resistance and abolishes the spontaneous or evoked spikes. Following ischemic reperfusion, the return of $O_2$ and glucose induces a transient hyperpolarization before restoring to baseline conditions (Krnjevic, 2008). This post-stroke hyperexcitability is present during first week to one month of recovery, and plays an essential role in post-stroke neuroplasticity. In rodents, it is manifested by expanded and less specific receptive fields as well as increased spontaneous activity (Schiene et al., 1996; Winship and Murphy, 2008). This increased neuronal excitability also occurs in vitro following oxygen-glucose deprivation, leading to down regulation of the GABAa receptor involved in the inhibitory pathway (Kelley et al., 2008). This hyperexcitability in surviving neurons contributes to a low frequency spontaneous activity (0.1-1 Hz) that fosters a permissive environment for axonal sprouting among rats with focal ischemia (Carmichael and Chesselet, 2002). The modification of neuronal connections resulting from stroke-induced plasticity change in axons and dendrites (Carmichael, 2006; Brown et al., 2007; Bender et al., 2009) can persistently alter the generation and propagation of brain oscillations for weeks after stroke.

A variety of pathological states can cause aberrant changes in brain electrophysiological recordings. For example, hypoxia induces a reversible hyperpolarization in the CA1 region of the hippocampus via a rise in $K^+$ conductance. It has been shown that similar events are seen during hypoglycemia in the neocortex (Luhmann and Heinemann, 1992), the striatum (Calabresi et al., 1995) and substantia nigra (Jiang et al., 1994), as well as in the hippocampus subregions such as CA1 (Spuler and Grafe, 1989) and CA3 (Knopfel et al., 1990) soon after the onset of ischemia (Harata et al., 1997; Tanaka et al., 1997). Interestingly, hypoxia induces moderate depolarization instead of hyperpolarization (Rosen and Morris, 1991) in some brain regions including the neocortex, dentate gyrus (Krnjevic and Xu, 1989), striatum (Calabresi et al., 1995), and thalamus (Erdemli and Crunelli, 1998). It has

been shown that inducing anoxia with cyanide can depolarize or hyperpolarize the same CA1 neuron depending on its resting potential (Englund et al., 2001), providing the neural basis for the diverse EEG changes seen after stroke.

### 6.4. Modifications of the brain oscillations in experimental stroke

A recent comprehensive review documented the EEG changes commonly observed after focal cerebral ischemia in rodents (Moyanova and Dijkhuizen, 2014). In essence, during the acute phase of ischemia in a transient MCAO model, the distribution of the power of the EEG spectrum (0-30 Hz) after Fourier transformation in animals is as follows: 85 % of delta oscillations, 7 % of theta oscillations, 5 % of alpha oscillations and 3 % of beta oscillations. Thus, ischemia has resulted in an increase of low frequency and a decrease of high frequency oscillations, or specifically a decrease of the alpha-to-delta ratio (Williams et al., 2003; Zhang et al., 2013), considering the baseline distribution as 25-45 % of delta, 40 % of theta, 12-15 % of alpha and 3-20 % of beta oscillations (Lu et al., 2001; Zhang et al., 2013). In particular, an increase in delta power in the ipsilateral hemisphere after transient MCA stroke was reported in both subacute and chronic phase from 24 hours to 7 days or beyond (Moyanova et al., 1998; Lu et al., 2001; Moyanova et al., 2007; Moyanova et al., 2008; Moyanova et al., 2013; Zhang et al., 2013). Another study reported that an increase of the ipsilateral delta and theta power occurred as early as one minute following intraluminal filament occlusion of the proximal part of MCA that leads to impairment in the subcortical brain regions (Zhang et al., 2006). The increase of both delta and theta activity was also reported 8 days after tMCAO in rats in fronto-parietal, occipital and temporal regions, whereas alpha and beta activity were depressed (Bhattacharya et al., 2013). Diaschisis frequently occurs after focal brain ischemia (von Monakow, 1914; Finger et al., 2004), of which the transhemispheric diaschisis refers to changes in the contralateral hemisphere detected after unilateral stroke (Andrews, 1991). Some studies suggest that an increase of the delta activity in the contralateral sensorimotor cortical areas correlated with an ipsilateral increase 1-7 days after MCAO in rodents (Lu et al., 2001; Hartings et al., 2003; Williams et al., 2003; Moyanova et al., 2013). On the other hand, other studies have shown that an increase in the contralateral EEG power in the somatosensory cortex accompanied a suppression of the EEG activity in the ipsilateral side 15 minutes after tMCAO in rats. Due to the lack of consensus in the evolution of the contralateral side, asymmetric index is often used to reflect changes of rhythms in both hemispheres over time. This asymmetry calculated by the brain symmetry index (BSI) or the global pairwise derived brain symmetry index (pdBSI) is also present in experimental studies as reported

during both acute (1 hour post stroke) and chronic phases (up to 14 days post stroke) in young and one-year old rats, respectively (Moyanova et al., 2013).

The literature is less clear concerning the modifications of the power of gamma, beta and alpha bands. In general, these three bands decrease after stroke in rodents, although contradicting results do exist. For example, a 35% reduction of the amplitude of alpha and beta waves in the ipsilateral hemisphere was reported 3-7 days after tMCAO (Moyanova et al., 1998; Moyanova and Dijkhuizen, 2014). The alpha band power decreased from day 1 to day 28 after pMCAO (Lammer et al., 2011; Moyanova and Dijkhuizen, 2014), whereas other studies reported an increase of delta, beta and rhythmic alpha activity by 7 days in the contralateral cortex in a rat model of tMCAO (Lu et al., 2001). Since gamma oscillations have been implicated in higher cognitive processes and might critically depend on proper mitochondrial function, they are highly sensitive to decrease in $pO_2$, thus likely to the reduction in blood flow (Huchzermeyer et al., 2008; Kann et al., 2011).

Some evidence seems to implicate that an increase of the infarct volume is correlated with an increase of the delta power and neurological deficits (Williams and Tortella, 2002; Williams et al., 2003). The volume of infarction is also correlated with the acute delta change index (Finnigan et al., 2004), the pdBSI (Sheorajpanday et al., 2009), relative alpha percentage, relative alpha-beta percentage, relative delta-theta percentage, delta/alpha ratio or delta-theta/alpha-beta ratio (Sheorajpanday et al., 2010). It is likely that the loss of the fast frequencies and the increase of slow wave activity is caused by the pathological neural tissue, leading to an impairment of the communication between the affected neuronal networks (Gloor et al., 1977)

# Objectives of the thesis

Due to the high incidence of chronic disabilities following stroke, rehabilitation therapy has become increasingly important in promoting recovery in the stroke patients. However, effective rehabilitation strategies rely on a thorough understanding of the mechanisms underlying the cause of functional deficits and pathways to recovery. As we mentioned in the general introduction (part I), focal cerebral ischemia has consequences for the entire brain because the brain operates as a network with multiple and intricate connections between different regions. In addition to the infarct zones that suffer the deadly consequence of ischemic stroke, penumbra surrounding the lesion site and some brain regions remote to ischemic area are also affected by the insult via a diaschisis-like mechanism (i.e. reduced cerebral function resulting from deafferentation or the interruption of normal input to a region not directly involved in the stroke (von Monakow, 1914)).

Although the frequency of post-stroke dementia is low, post-stroke MCI is common even among the first-ever stroke patients (Srikanth et al., 2003; Rasquin et al., 2004; Srikanth et al., 2004). In addition to the high prevalence, the rate of cognitive decline after ischemic stroke is also significantly greater than that of individuals without one. However, the neural pathways involved in the post stroke MCI as well as the recovery of cognition are not well understood.

The crucial role played by the hippocampus in memory functions is compelling (see introduction part II). However, this brain region is often spared in human stroke or in many rodent models of cerebral focal ischemia. As a core objective of this thesis, we thus aimed at unravelling the mechanisms responsible for the memory impairments observed after the induction of cerebral focal ischemia. We raised the working hypothesis that loss of functional activity in anatomically intact brain regions, connected to but remote from the ischemic infarct, could be the mechanism underlying the observed memory deficits accompanying stroke. We focused our attention on the hippocampus and speculated that hippocampal functional activity could be impaired despite a preserved integrity (lack of damage after ischemic stroke).

We adopted an integrative approach to test the validity of this “hippocampal diaschisis” hypothesis. To mimic MCI, we selected the dMCAO model of focal ischemia in rats that produces mild memory deficits and no hippocampal damage and combined this model to multidisciplinary approaches including behavioural assays tailored to examining memory functions, immunohistochemistry, imaging of the c-fos activity-depending gene,

intracerebral injections and cutting-edge in vivo electrophysiology recordings.

In a first part of our result section, we established the anatomical and behavioural phenotypes of our dMCAO model (unilateral infarct located in the somatosensory cortex) and map the distant brain regions potentially impaired during memory challenges following experimental stroke in rats. To this end, we compared the expression of the activity-dependent gene Fos in key limbic brain regions involved in memory function between sham and ischemic rats following pharmacological, novel context exploration and spatial (Barnes maze) and non-spatial (social transmission of food preference task (STFP)) memory testing.

In a second part, we further explored the mechanistic bases of our hippocampal diaschisis hypothesis. Since the diaschisis concept is based on reduced afferent inputs to a given region (i.e. deactivation), we attempted to reproduce the phenotypes of our dMCAO model by performing localized pharmacological inactivation of specific brains regions in behaving rats exploring a novel environment or submitted to the STFP task. To this end, rats were equipped with guide cannulas to enable discrete inactivation with the AMPA receptor antagonist CNQX of either the somatosensory cortex which is infarcted in our model of focal ischemia, or the dorsal hippocampus. An experimental design combining unilateral or bilateral cortical and hippocampal inactivations with memory testing enabled us to provide converging evidence indicating that hippocampal hypofunction do occur after silencing neuronal activation in the somatosensory cortex and produces cognitive deficits similar to that observed in dMCAO rats, thus identifying hippocampal diaschisis as an important contributing deleterious mechanism.

In a last part of our result section, we investigated the extent of disruption in the activity of neocortical-hippocampal neuronal networks after experimental stroke. In order to have a more thorough understanding of stroke related cognitive deficits, we examined in dMCAO rats the neuronal circuits known to critically participate in memory functions. Global network patterns (theta and sharp-wave-ripples) as well as discharge activity of multiple individual neurons were recorded in the hippocampus and cortex using multi-site extracellular recordings with in vivo during acute and chronic stroke. We particularly focussed on theta oscillations and sharp-wave ripples (see introduction part III) because of their roles in memory function and additionally explore these two electrophysiological readouts during pharmacological inactivation of the somatosensory cortex.

Overall, our integrative approach was successful in establishing hippocampal

diaschisis as a crucial mechanism responsible, at least in part, for the memory deficits observed after ischemic stroke. This mechanism is further discussed in light of the existing knowledge on cerebral focal ischemia, and a putative model of hippocampal hypofunctioning following cortical dysfunction incorporating our main findings, is proposed.

# General Materials & Methods

Common procedures for part I and II such as animals housing, food deprivation, behavioral testing and immunostaining are described in the following section. More specific procedures are described in the corresponding chapter. Part III, which is dedicated to electrophysiology recordings, is independent from this general Materials & Methods section.

## 1. Ethical considerations

All experimental procedures complied with official European Guidelines for the care and use of laboratory animals (directive 2010/63/UE) and were approved by the ethical committee of the University of Bordeaux (protocol A50120159). All ischemic experiments were conducted in accordance with the animal care guidelines issued by the National Institutes of Health and by the SFVAMC Institutional Animal Care and Use Committee.

## 2. Animals

All the ischemic experiments were conducted in adult male Sprague-Dawley rats (9 weeks of age, 250-300 g) obtained from Charles River Laboratories (Wilmington, MA). Adult male Sprague-Dawley rats (8 weeks of age, 200-250 g) from Janvier Laboratories (Le Genest-St-Isle, FR) were used for pharmacological experiments which consisted in region-specific cerebral inactivations. Upon arrival in the animal facility, rats were habituated to their new housing conditions for a minimum of 3 days (2 rats per cage) Because some of our learning and memory procedures required specific testing and food deprivation procedures, all rats were then housed individually (1 rat per cage) for the entire duration of the behavioral experiments. After being single housed for 5 days, each rat underwent a 2-day handling procedure in order to be habituated to the experimenter and to minimize as much as possible stress responses which would interfere with subsequent memory testing. This procedure lasted about 5 min per day and consisted in removing the rat from its cage and holding it in the experimenter's hands until the rat felt comfortable. Rats then underwent surgery (ischemia or intracerebral implantation of guide cannula) as described in the Materials & Methods section of part I and II. After a recovery period of 15 days in which rats had access to water and food ad libitum, each rat was submitted to a progressive food deprivation protocol prior to memory testing. Animals were kept on a 12:12 h light-dark cycle and experiments were conducted during the light phase of the cycle.

## 3. Food deprivation procedure

Some memory testing procedures used in this thesis such as the social transmission of food preference task or the odor discrimination task (see below special procedure) were appetitive in nature and required the rats to undergo a partial and gradual food deprivation protocol in order to increase their motivation for food during the entire duration of the experiment. Rats were submitted to a partial food deprivation protocol to increase their motivation 5 days prior to the beginning of the memory task. They were first weighed for 3 days (once a day at the same time of the day) to determine their average reference weight before food deprivation. Then the amount of food available in their home cage was gradually reduced to bring them to 85-90% of their baseline (ad libitum) weight and never more than 15%. An adequate food amount (about 15 g) was then distributed daily to maintain a level of food deprivation constant in all animals which were weighed once daily. An individual weight sheet was kept for all the animals until completion of the experiment.

## 4. Behavioral experiments

### 4.1. Spatial exploration of a novel environment

Five minutes after receiving an intracerebral injection, rats explored a novel environment during 10 minutes (one single session). The spatial exploration occurred in an open field that consisted of a circular table (120 cm in diameter).

### 4.2. Odor discrimination test

Rats were placed in a square Plexiglas enclosure Open Field (110 x 110 cm) equipped with a Noldus Instruments EthoVision video tracking system enabling to record the time spent by each animal exploring 4 cups placed in a 40 cm square. Because this task is appetitive and need motivation for food, rats were gradually food deprived 5 days before the beginning of experiment (see food deprivation protocol) and received a delay amount of 15 of food during the entire duration of the experiment. Prior to the open field arena shaping, rats were habituated for two days to consume and discriminate flavored powdered chow from two cups placed in their home cage for 20 min (height: 4 cm; diameter: 7 cm carefully cleaned between each experiment to prevent olfactory cues). One cup was filled with cumin-flavored powdered chow (0.5% cumin mixed with plain powdered chow) and cover with a thin bedding layer. The second cup was filled with bedding only. The third and fourth day, rats were shaped in the open-field arena for 10 minutes to locate the cup flavored with cumin (0.5% in plain

powdered chow) among 3 other cups filled with bedding only. The flavored cup was covered with bedding to force the rat to dig into the cup. Location of the flavored cup was changed the second day of shaping. After these 2 days of shaping, rats performed the odor discrimination test for 10 minutes and time exploring the 4 cups in the arena was recorded. Rats had to discriminate the cup flavored with cumin (0.5% cumin in bedding) among 3 others cups filled with non flavored bedding (**Fig. 27**). Because chow powder was not present this day of the test, rats had to dig into the flavored cup. For analysis of exploratory behavior, percentage of time exploring the flavored cup versus the non-flavored cups was used as a discrimination index.

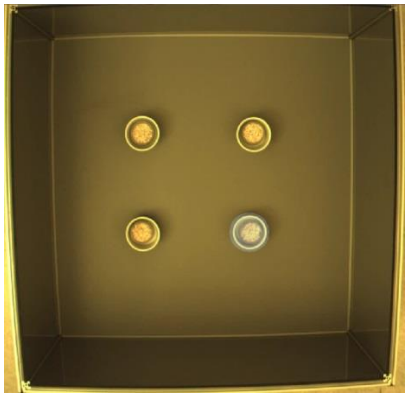

***Figure 27. Open field arena used for the odor discrimination task****. Rat had to explore the arena and discriminate the cumin flavored cup (0.5% cumin mixed with bedding) among 3 other cups filled with non flavored bedding.*

### 4.3. Social transmission of food preference task

The social transmission of food preference (STFP) paradigm involves an ethologically-based form of associative olfactory memory (Frankland and Bontempi, 2005) and the task was performed as described by Lesburguères et al. (Lesburgueres et al., 2011). This task is appetitive in nature and required the rats to undergo a partial and gradual food deprivation protocol in order to increase their motivation for food during the duration of the experiment. Rats were thus subjected to partial food deprivation to increase their motivation 5 days prior to the beginning of the memory task and an adequate food amount (about 15 g) was then distributed daily to maintain a level of food deprivation constant in all animals during the entire duration of experiment.

In the STFP task, within only one single interaction session of 30 min, rats learned rapidly about the safety of potential food sources by sampling the odor of those sources on the breath of their littermates. Food deprived rats underwent a three-step procedure as illustrated

in the figure below (**Fig. 28**). The task took place in the home cage of the animals. Rats called "demonstrators" were first presented with two cups (height: 4 cm; diameter: 7 cm carefully cleaned between each experiment to prevent olfactory cues) in their home cage and habituated to eating plain or flavored powdered chow (0.5% cumin) for three days (30 min session). Observer rats were also shaped for three days to consume plain powdered chow from two cups placed in their home cage for 20 min. Cups were then weighed and additional food was given to reach a daily amount of food of about 15 g. These shaping and eating procedures minimized novelty-induced stress that would interfere with memory performance during the experimental procedure described below.

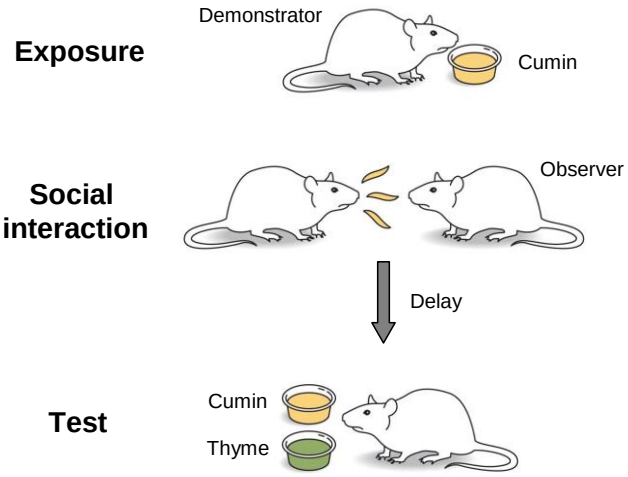


***Figure 28. The 3-step social transmission of food preference task. (1) Exposure*** *(30 min): a food-deprived demonstrator rat eats cumin flavored food (0.5%).* ***(2) Social interaction*** *(30 min): an observer rat forms an association between the cumin odor and some constituents of the breath of the demonstrator rat.* ***(3) Retention test*** *(20 min): When submitted to a choice between cumin and a novel food (thyme, 0.75%), the observer rat expresses a memory of the association by preferentially eating cumin because it was present in demonstrator's breath, considered without danger and therefore safe to eat.*

The detailed experimental procedure is described and illustrated (**Fig. 30**) below:

1) Exposure phase: Demonstrator rats were food-deprived and then habituated to eat plain or cumin (0.5 %, i.e. 0.5 g of cumin mixed in 99.5 g of plain chow) powdered chow for three days (30 min session). During these 30 min period, 40 g of powdered chow were available in a cup placed in the demonstrator's home cage. Water was removed from the cage. After the feeding session, the food was weighed, and the amount eaten was recorded. Observer rats were also shaped for three days to consume plain powdered chow from two cups placed in their home cage.

2) Interaction phase: the demonstrator rat was moved to the observer's cage fitted with a stainless steel wire mesh divider (**Fig.29**). Food-deprived observer rats and demonstrator rats were separated in opposite side of the cage for a 20 min interaction period, then they were allowed to interact freely for another 10 min when the divider was removed. The demonstrator rat was removed from the observer's cage at the end of this 30 min interaction period. Observer and demonstrator rats were always unfamiliar with each other.

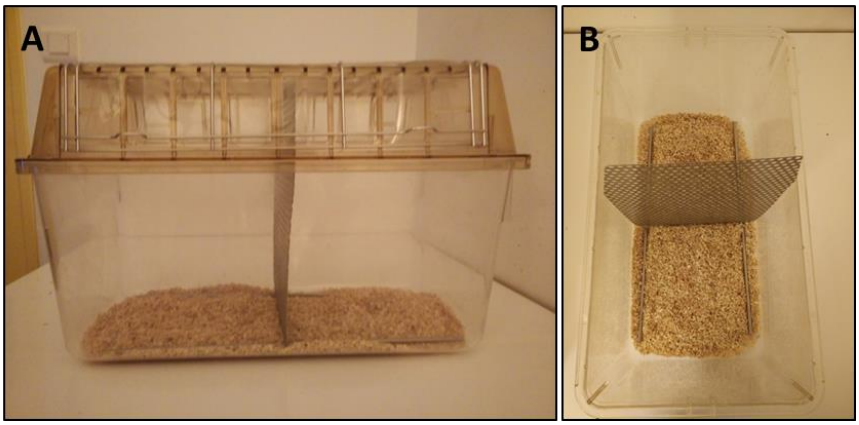


***Figure 29. Cage setup used for the STFP test. (A)*** *The home cage of the observer rat was divided into 2 areas by a stainless steel wire mesh divider for 20 minutes. A Filtered top was placed to avoid odor dispersal.* ***(B)*** *Top view of the steel wire mesh divider located in the observer rat home cage.*

3) Retention test: 7 days after the social interaction, food-deprived observer rats had to choose in their home cage between two cups containing a novel food (0.75% thyme) or the familiar food that the demonstrator rat had consumed before interacting with the observer rat (0.5% cumin). After 20 min, cups were removed, weighed and olfactory associative memory performance was expressed as percentage of familiar food eaten (% cumin) using the following formula: (amount of familiar food eaten / amount of total food) x 100. In addition the total amount of food eaten was examined to control that all the groups had the same motivation for eating food.

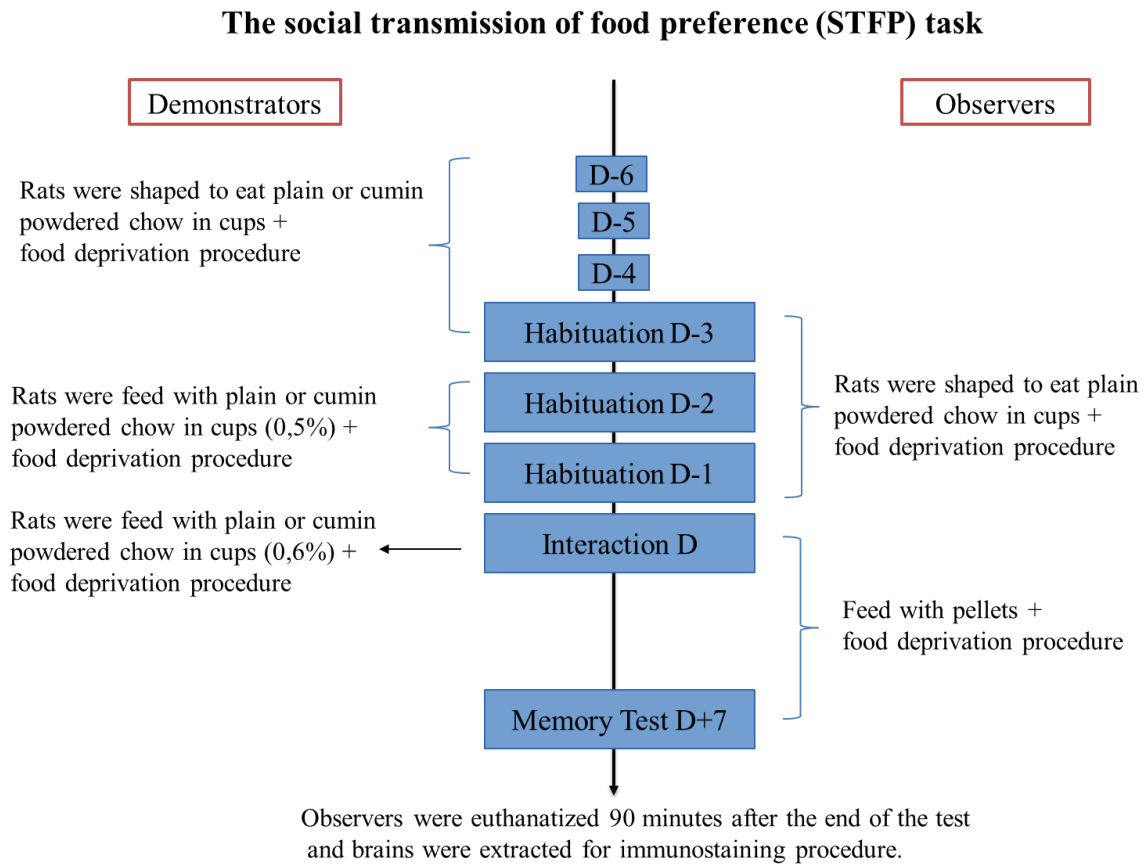


***Figure 30. Details of the STFP paradigm.*** *During the entire procedure, observer and demonstrator rats were food deprived and received a daily amount of food of 15g. Demonstrator rats were shaped 6 days in a row prior to interaction day to eat plain or cumin powdered chow in cups. Observer rats were shaped 3 days prior to interaction phase with 2 cups of plain powdered chow placed in their home cage. Seven days following the interaction phase, observer rats were submitted to the retention test <upon completion they were euthanized 90 minutes after the end of the test. Brain were collected and processed for Fos immunostaining.*

Flavor concentrations were chosen in pilot experiments to induce an innate preference for thyme (Lesburgueres et al., 2011). Because rats naturally prefer thyme over cumin at the concentrations used for the cumin/thyme flavor pair, use of these two biased flavored pairs permit to decrease the chance level at test and thus to optimize the possibility of detecting changes in memory performance across our various treatments. Indeed, interaction with a demonstrator that has eaten cumin powdered chow could reverse this innate preference so that observers chose cumin over thyme (up to 80% of the total food eaten, chance level of ~20%).

In addition to the experimental groups that interact with demonstrator who ate cumin flavor, “food preference” (FP) controls group were generated to ensure that CNQX injection or focal ischemia did not change the innate preference for thyme and did not impair the motivation to consume food. FP control groups were treated similarly as the experimental

groups, i.e. they were injected with CNQX or Acsf in specific brain regions prior to the interaction phase or submitted to dMCAO or sham surgery 15 days prior to the interaction phase except that they interacted with a demonstrator rat which had eaten plain powdered chow (**Fig. 31**).

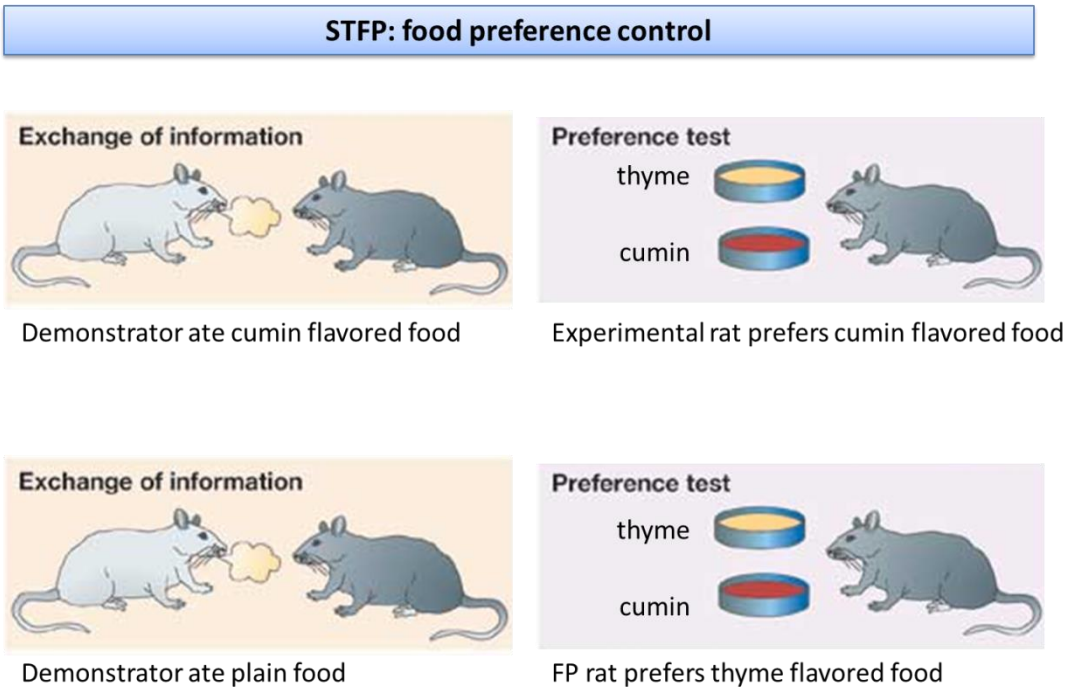


***Figure 31. Paradigm of the food preference control (FP) group in the STFP task.*** *By choosing naturally the thyme flavored food when interacting with a demonstrator rat fed with plain food, FP rats permit to control that treatment or surgery does not impair the motivation of the rat to consume food or the innate preference for the thyme flavor. Experimental chance levels were generated by pooling FP control groups (Acsf/CNQX rats or sham/dMCAO rats after verifying that there was no significant group difference).*

## 5. Euthanasia and tissue preparation

Rats were terminally anesthetized with lethal injection of pentobarbital (300 mg/kg i.p.) and perfused transcardially with 0.9% saline and 4% paraformaldehyde (PFA) in 0.1M phosphate buffer, pH 7.4 (PB). Euthanasia was done 90 min after completion of memory testing or right after electrophysiological recordings. After decapitation, brains were removed and fixed overnight in 4% PFA-PB and placed in 30% sucrose for 48hours (**Fig. 32**). Fifty µm coronal sections were cut on a microtome and collected serially in 4 section packs in 0.02% azide solution with 0.1M PB, pH 7.4. Brain sections were stored at 4°C.


***Figure 32. Example of brains fixed with 4% PFA.*** *Left brain was extracted from a sham rat and right brain was extracted from a dMCAO rat. The brown area visible at the surface of the somatosensory cortex highlights the ischemic core.*

## 6. Immunohistochemistry staining

Free-floating coronal sections were transferred in 6-well plates loaded with phosphate buffer solution 0.1 M (PBS) and washed 3 times with PBS 0.1M on a shaker (10 minutes/wash). Sections were incubated with fresh 0.3% $H_2O_2$ in PBS 0.1 M for 30 minutes at room temperature on a shaker to inactivate the endogenous peroxidase. Sections were rinsed 3 x 10 minutes with PBS 0.1 M on a shaker, then incubated with primary antibody (1:5000 dilution, Rabbit anti-Fos polyclonal IgG, Santa Cruz; 1:10000 dilution mouse anti-rat NeuN, Chemicon ; 1:10000 dilution mouse anti-rat ED1, Chemicon) diluted with blocking solution (PBS 0.1M, 0.1% BSA, 0.2% Triton X-100, 2% serum) overnight at room temperature on a shaker. The next day, sections were rinsed 4 x 10 minutes with PBS 0.1 M on a shaker and incubated with biotinylated secondary antibody (1:2000 dilution, Biotin-SP-conjugated affiniPure Goat anti-rabbit IgG, Jackson Immunoresearch; 1:2000 dilution sheep anti-mouse IgG, Amersham), diluted in blocking solution for 2 hours at room temperature on a shaker. Sections were rinsed 4 x 10 minutes in PBS 0.1 M and incubated in Avidin Biotin Complex (ABC) solution (kit Vectastain ABC diluted with PBS 0.1M, Vector Laboratories) for 2 hours at room temperature on a shaker. After 4 x 10 minutes wash with PBS 0.1M, sections were incubated in 3,3'-diaminobenzine-tetrachlorid solution (DAB 0.05% with PBS 0.1M, Sigma) for 8 minutes at room temperature on a shaker. To reveal staining, 3 drops of 0.3% $H_2O_2$ were added in each well for 2 minutes. Section were rinsed 4 x 10 minutes with PBS 0.1 M on a shaker to stop the reaction. Figure 7 illustrates the immunostaining reaction (**Fig.33**).

Coronal sections were mounted on gelatin-coated slides (Fischer Scientific) until dried, then slides were immersed in toluene solution (2 x 15 minutes) to dehydrate them. Mounting medium was added coverslips were placed on slides.

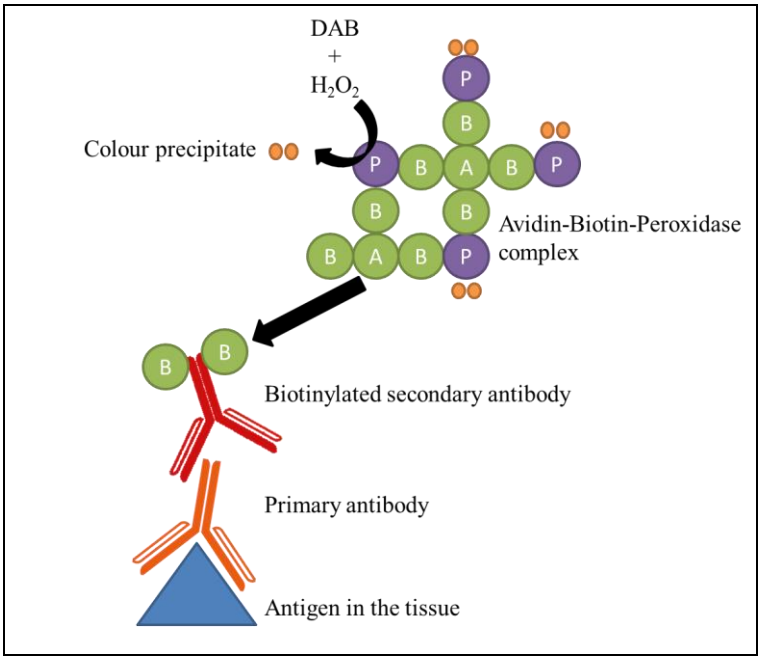


***Figure 33. Staining reaction using DAB oxidation by the peroxidase enzyme***. *First antibody recognizes the antigen of the tissue then the biotinylated secondary antibody binds to the first antibody. Avidin which has a high affinity for biotin will bind the biotin located on the second antibody. Biotinylated peroxidase binded to the avidin-biotin complex will oxidize the DAB by adding H2O2 and create a brown color precipitate.*

## 7. Cell counting

The number of Fos-positive cells was counted bilaterally in a minimum of three sections in structures of interest. The Biocom Visiolab 2000 software was used for counting. Optical microscope (Olympus BX51) was connected to the video camera (Sony DXC-950P) for capturing images. Structures were defined according to the Franklin and Paxinos atlas. Counts in each region of interest were expressed as number of cells/mm2 and average of the 3 coronal sections was made.

## 8. Structures of interest

Structures of interest were defined according to the Franklin and Paxinos atlas and illustrated in **Fig. 34**.

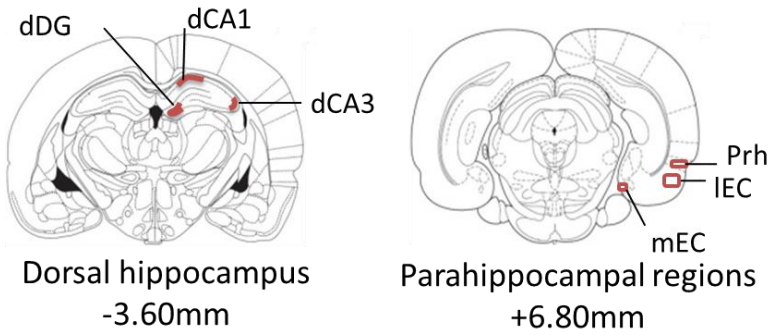


***Figure 34. Schematic drawings of rat coronal sections adapted from Paxinos and Watson atlas showing the regions of interest (red areas) selected for measurements of Fos-positive nuclei****. Numbers indicates the distance (in millimeters) of the section from bregma. dCA1: CA1 field of dorsal hippocampus; dCA3: CA3 field of dorsal hippocampus; dDG: dentate gyrus of dorsal hippocampus; Prh: perirhinal cortex; lEC: lateral entorhinal cortex, mEC: medial entorhinal cortex.*

## 9. Statistical analyses

Statistical analyses were performed using GraphPad Prism version 5.00 for Windows (http://www.graphpad.com). N represented the number of animals that were analyzed. Normal distribution was tested with Kolmogorov–Smirnoff tests. For normal distribution and independent samples, group comparisons were made using t-test, one-way and two-way ANOVAs analyses. Bonferroni's test was used for post hoc comparisons when appropriate. For paired samples, repeated measures ANOVA were performed. For non-normal distributed data sets, nonparametric tests were applied: Kruskal–Wallis for multiple comparisons and Mann-Whitney's test with significance correction for double comparisons of independent samples. Data were expressed as mean ± SEM. Values of $p<0.05$ were considered as significant.

# Results

# Part I : Ischemia-induced memory deficits: contribution of hippocampal diaschisis?

## 1. Introduction

Although motor impairment is often apparent and well documented in patients suffering from ischemic stroke, the cognitive consequences and the underlying mechanisms leading to cognitive impairments after cerebrovascular occlusive diseases are less understood. Multiple impairments are observed after ischemic stroke such as executive functions (25%), visuospatial (37%), short-term (31%) and long-term memory (23%) (Pohjasvaara et al., 1997). While the frequency of post-stroke dementia is low, post-stroke cognitive impairment is common even among the first-year stroke patients (Patel et al., 2003; Srikanth et al., 2003; Erkinjuntti, 2007). Hippocampus is an important operator in the complex organization of memory function (Martin and Clark, 2007) but this brain region is often spared in human stroke or in many rodent models of cerebral focal ischemia (Carmichael, 2005). A concept termed diaschisis describes the neurophysiological changes that can occur in anatomically connected brain regions distant from a focal lesion area (von Monakow, 1914). It has been proposed to contribute to cognitive impairments observed in stroke patients. Indeed, in addition to the infarcted zones that suffer the deadly consequence of ischemic stroke, penumbra surrounding the lesion sites and some brain regions more remote to the ischemic areas have been reported to be functionally affected to various degrees (Witte et al., 2000). To illustrate this diaschisis phenomenon, remote brain regions injury as thalamic and fornix lesions has been associated with hippocampal dysfunction and memory impairments (Vann et al., 2000a; Jenkins et al., 2002; Carrera and Tononi, 2014), however, the role in the hippocampal diaschisis in ischemic stroke remains unclear and development of adequate experimental models is necessary.

For this reason, the first part of this thesis explores the effect of focal cortical ischemia in rats. In order to study the functional connectivity between cortex and hippocampus in the context of ischemic stroke and investigate the neurobiological mechanisms of the hippocampal diaschisis, we used the dMCAO in rats which induces focal cortical infarct in the absence of direct hippocampal injury (Carmichael, 2005; Matsumori et al., 2006).

Using cellular imaging of the activity-dependent gene c-fos, classically used as an indirect correlate of neuronal activity (Vann et al., 2000a; Maviel et al., 2004), we first examined the dMCAO-induced reorganization of neuronal activation within the hippocampal formation (including the hippocampus proper and its most direct afferent cortical regions) of rats exploring a novel environment or confronted to hippocampal-dependent spatial and non-

spatial memory testing. Since the diaschisis concept is based on reduced afferent inputs to a given region (i.e. deactivation) rather than impaired synaptic transmission in that region, we also performed single unit recordings to establish the status of synaptic transmission in the hippocampus.

## 2. Materials & Methods

### 2.1. Groups

dMCAO surgery was performed 15 days before the beginning of the experiment. The following figures summarize the timeline for each experiment such as sulpiride challenge (**Fig. 35**), Fos stimulation by exploration test (**Fig. 36**), Barnes maze (**Fig. 37**) and STFP tests (**Fig. 38**), odor discrimination test (**Fig. 39**) and neuronal tracing with BDA (**Fig. 40**). Because STFP test and odor discrimination tests were already described in details in the previous chapter, timeline of those experiments are only presented here but not detailed in the following sections.

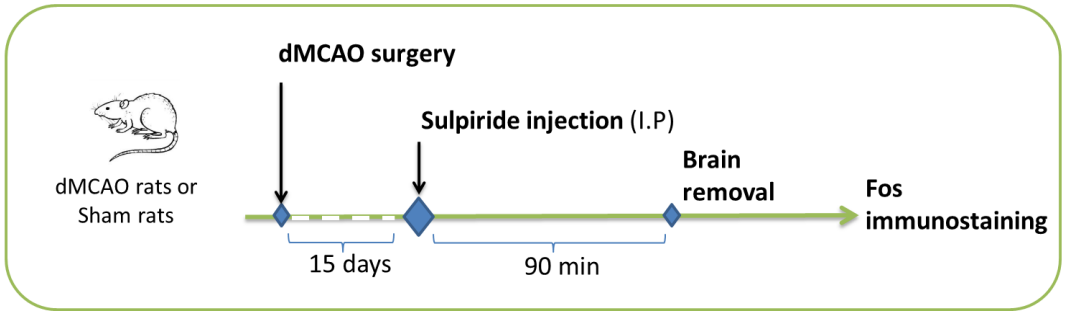


***Figure 35. Timeline of the Sulpiride challenge experiment****. 15 days prior to i.p. sulpiride injection (100 mg/kg), surgery was performed and rats were housed in their home cage. Rats were euthanatized 90 minutes after the sulpiride injection and their brains were processed for Fos immunostaining.*

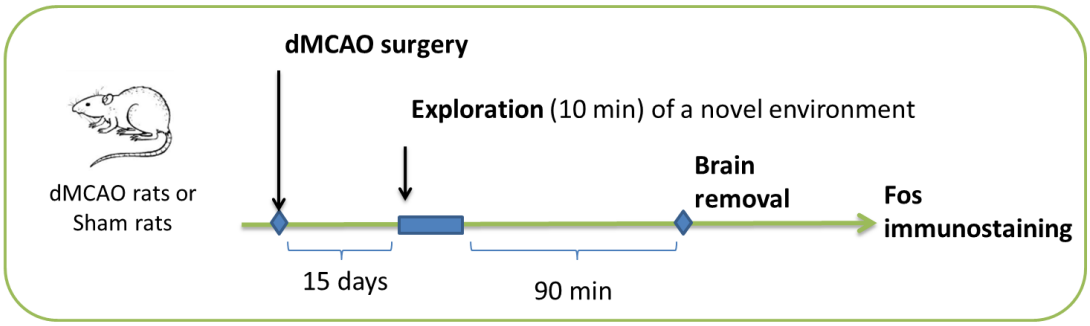


***Figure 36. Timeline of the spatial exploration experiment****. 15 days prior to exploration, surgery was performed and rats were housed in their home cage. Rats were euthanatized 90 minutes after the*

*spatial exploration and their brains were processed for Fos immunostaining.*

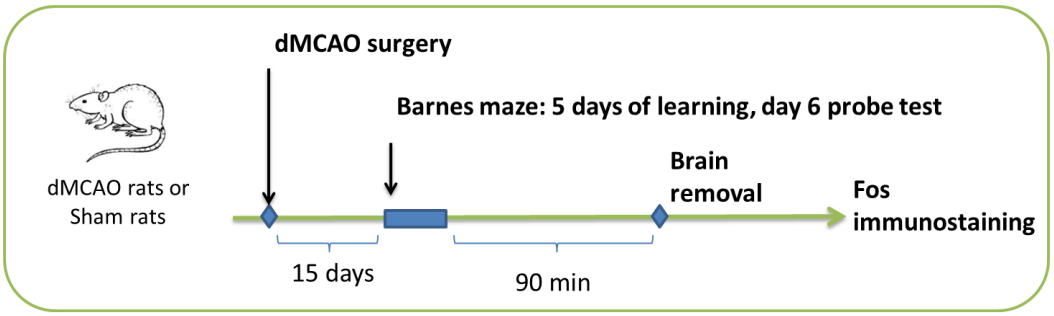


***Figure 37. Timeline of the Barnes maze experiment**. 15 days prior to the beginning of the Barnes maze test, surgery was performed and rats were housed in their home cage. Rats were euthanatized 90 minutes after probe the test in the Barnes maze (day 6) and their brains were processed for Fos immunostaining.*

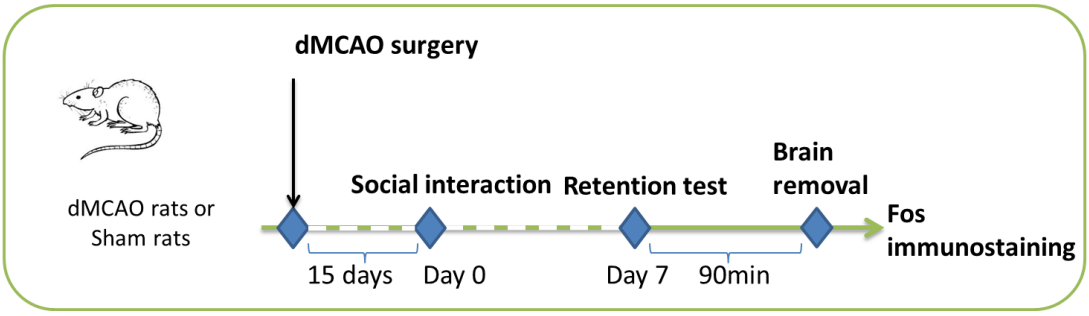


***Figure 38. Timeline of the STFP experiment**. 15 days prior to the beginning of the STFP task, surgery was performed and rats were housed in their home cage. Rats were euthanatized 90 minutes after retention test of the STFP test (7 days following the interaction phase) and their brains were processed for Fos immunostaining.*

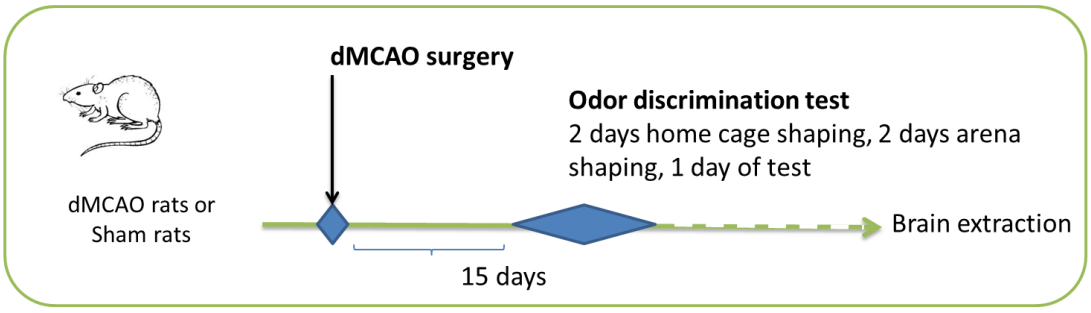


***Figure 39. Timeline of the odor discrimination task**. 15 days prior to the beginning of the Odor discrimination task, surgery was performed and rats were housed in their home cage. Rats were euthanatized 90 minutes after the last day of the test following 4 days of shaping and their brains were processed for Fos immunostaining.*

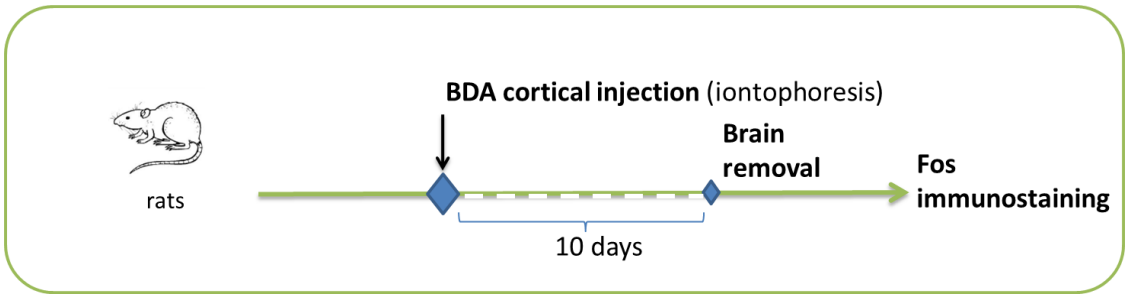


***Figure 40. Timeline of the neuronal tracing experiment with BDA**. Rats were euthanatized 10 days after the BDA injection and their brains were processed for immunostaining of the retrograde tracer.*

### 2.2. Distal MCA occlusion (dMCAO) surgery

Procedures to create the focal ischemia/reperfusion model were performed as described previously (Matsumori et al., 2006). Because a permanent distal ligation of MCA does not give reproducible infarct in most rat strains, we combined it with a CCAs occlusion. Anesthesia was induced with 3% isoflurane in a closed chamber and maintained with 2% isoflurane in 30% O2 and 70% N2O administered by using a facemask. Core temperature was maintained at 37±0"5 "C with a heating blanket and rectal thermistor servo-loop. The animal was placed in the supine position and a ventral cervical midline skin incision was made. After making a midline incision, both CCAs was carefully freed from the adjacent vagus nerve to make room for clip application. The animal was then placed in the lateral position, and a 1.5-cm scalp incision was made at the midpoint between eye and ear to separate the temporalis muscle. After exposing the zygomatic bone, a burr hole was made in 2 mm in diameter with a dental drill 1 mm rostral to the anterior junction of the zygoma and squamous bone. MCA was ligated using a 10-0 suture just above the rhinal fissure after piercing the dura mater and CCAs were occluded temporarily for 90 minutes by using micro clamps (**Fig. 41**). Then, the micro clamps were removed to restore blow flow and chest incision was closed. Rats were kept under anesthesia during occlusion and monitored for blood flow for 30 minutes following reperfusion. Animals were returned to recovery cage and be watched until they were fully recovered. Rats stayed in the recovery cage on a heating pad (40° C) for 2 hrs and be watched for the whole time. With the exception of MCA and CCAs occlusion, sham-operated animals were exposed to identical anesthetic and surgical procedures.

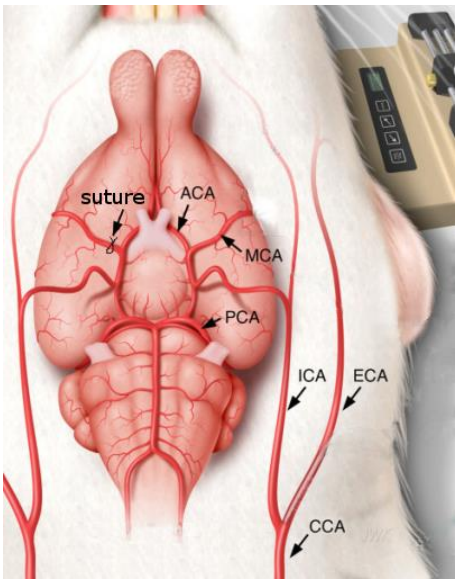


***Figure 41. Schematic representation of the rat vascular system in supine position***. *Right MCA is ligatured and CCAs are clamped for 90 minutes.*

### 2.3. Pharmacological challenge with sulpiride injection

dMCAO and sham animals received i.p. injections of sulpiride (100 mg/kg in 0.9% saline, Sigma, St. Louis, MO) then housed in their home cage during 90 minutes before euthanasia. The control group was injected with saline (0.9%) as vehicle. Sulpiride is a dopaminergic $D_2$ receptor antagonist that stimulates neuronal activity among the dopaminergic limbic system because D2 receptor is coupled to protein Gi which inhibits adenylyl cyclase activity.

### 2.4. Neuronal tracing with anterograde tracer injection.

Neuronal tracing was done according to the protocol described by Burwell et al (Burwell, 2000). Surgical procedures were performed under isoflurane anesthesia. Once anesthetized, breathing of rats was maintained by a small animal anesthesia machine. Core temperature was maintained between 37± 0.5 °C with a heating blanket and rectal thermistor servo-loop. Rats were placed in a stereotaxic frame (Kopf Instruments) equipped with a mask delivering 1.5-2%isoflurane/68%N2O/30%O2. The effectiveness of anesthesia was assessed by evaluating the paw reflex (paw withdrawal in response to briefly pinching the skin between toes of the hindlimbs). The incisor bar of the stereotaxic frame was positioned at -3.3 mm below the interaural line. After subcutaneous injection of bupivacaine (0.2 cc, 0.25%), the scalp was incised longitudinally to expose the animal's skull. A hole was drilled into the skull

above the injection site of the parietal cortex (AP:-5.0 mm, L:-5.0 mm, D:-0.9 mm) and a small incision was made in the dura to permit unobstructed penetration of the glass micropipette (Drummond capillary glass: outside diameter 1.14 mm ) following by iontophoretically injection of the anterograde tracer biotinylated dextranamine (BDA, Molecular Probes, Eugene, OR) with a Nanoject II Auto-injector. The wound was sutured after injection and animals were returned to recovery cage on a heating pad (40° C). They were regularly checked upon they fully recovered (2h) before being returned to the colony. Ten days following the injection, rats were euthanatized and brains were extracted for immunostaining.

### 2.5. Immunohistochemistry staining after BDA injection and confocal microscopy.

Serial coronal sections (480 µm apart) were immunostained with streptavidine Cy3-red goat anti-rat IgG conjugate (5µg/mL, Molecular Probes, Eugene , OR). Fluorescence signal was detected using a Zeiss LSM 510 confocal imaging system.

### 2.6. Barnes maze

In the Barnes maze test (Hamilton Kinder, Poway, CA), the ability of rat to locate a hidden escape box (10-cm diameter per hole, 18 possible locations) under a circular platform (120 cm in diameter) was assessed to measure spatial memory acquisition and retention. . In order to increase the motivation of the rat to find and get into the escape box, bright light (300- 350 LUC) and blowing fans (strong enough to see the furs moved) were provided. Rats were trained to locate the box in a 3-min trial, 6 trials daily for 5 days. Following 30 trials of acquisition test, a probe trial in which the hidden box was removed was conducted to test memory retention. Once the rats located the box by referring to distal visual cues, they were allowed to remain on it for 15 seconds (**Fig. 42**). Time to reach the box (latency), path length, and velocity were recorded with a Noldus Instruments EthoVision video tracking system (Noldus, Leesburg, Va) set to analyze two samples per second. Because the time required to locate the hidden box is a function of both path length and velocity, we also analyzed these parameters, in addition to latency.

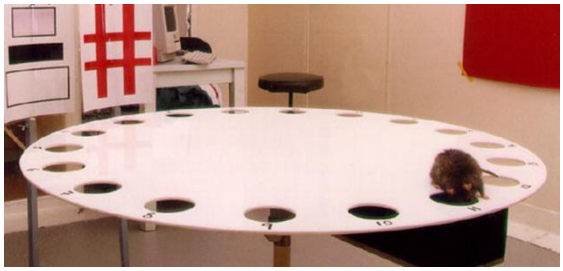

***Figure 42. The Barnes maze apparatus used in our experiments to assess spatial memory.*** *The rat had to locate the escape box hidden under one of the 18 holes of the platform using distal cues scattered in the room containing the maze.*

### 2.7. Infarct volume measurement

Infarct volume was measured by subtracting the volume of intact tissue in the ipsilateral hemisphere from that in the contralateral hemisphere on NeuN-stained serial sections. Coronal sections located between Bregma level -0.28 and +0.68 in dMCAO rats were used to determine the peri-infarct neuronal density detectable with NeuN-immunoreactive cells medial to the cortical lesion.

## 3. Results

### 3.1. dMCAO-induced brain damage are restricted to the cortex

In order to determine the extent of brain damage in our rat model of focal ischemia, we first examine the extent of the unilateral infarct zone in rats that underwent occlusion of the left distal middle cerebral artery. As shown in **Figure 43**, average of infarct volume was 66.66±6.52 $mm^3$ and restricted to unilateral motor and sensorimotor cortices, consistent with previous findings (Matsumori et al., 2006; Wang et al., 2008). No signs of hippocampal injury were observed. Indeed, immunohistochemistry with ED1, a cellular marker specific for activated rat microglia, did not reveal any inflammation in the hippocampus whereas strong expression was shown in the ipsilateral somatosensory cortex. Second, immunostaining with the neuronal biomarker NeuN did not reveal any detectable cell loss in the hippocampus while neuronal death in the ipsilateral somatosensory cortex was clearly visible (**Fig. 44**). Together, these findings indicate that damage following ischemia induced by left dMCAO is restricted to the ipsilateral cortex while sparing the hippocampus.

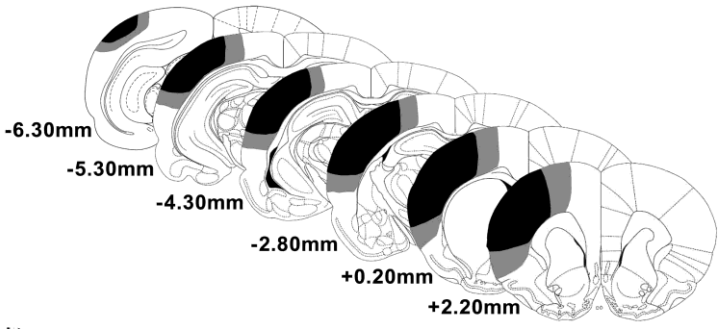


***Figure 43. Left dMCAO induced a focal ischemic infarct restricted to the ipsilateral cortex.*** *Ischemic size infarct in rat with dMCAO reconstructed by coronal sections. Smallest and largest damaged areas are represented in black and gray, respectively. The section distance in millimeters is indicated by numbers from Bregma.*

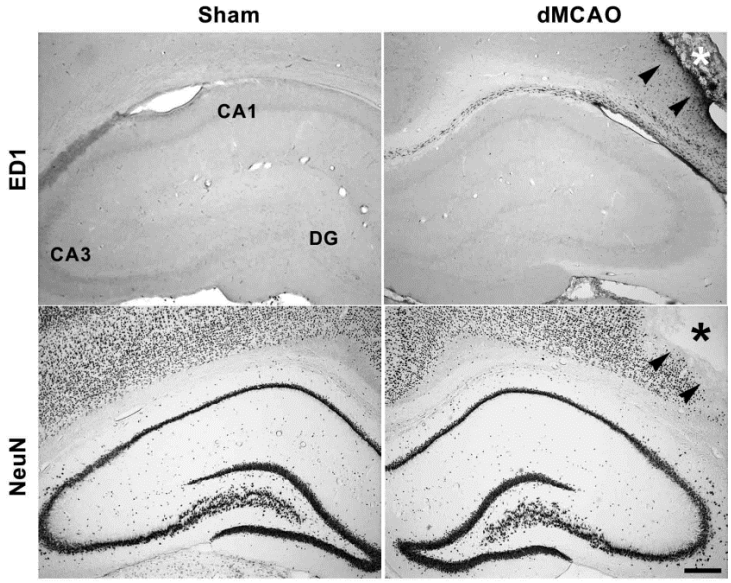


***Figure 44. Left dMCAO affected the ipsilateral cortex but spared the hippocampus.*** *No sign of injury throughout the hippocampus were revealed by the expression of ED1, a marker for activated microglia (left CA1, CA3 and DG areas are shown). However, infarcted and peri-infarcted somatosensory cortex ipsilateral to ischemic stroke expressed robust ED1 (arrowheads). Lack of hippocampal damage was confirmed by the similar expression of the neuronal marker NeuN throughout the hippocampus of shams and dMCAO rats. NeuN was not expressed in the right peri-infarcted cortex revealing complete cell loss (arrowheads). Star indicates the core of the infarct. Scale bar, 100 µm.*

### 3.2. dMCAO-induces hippocampal hypoactivation

Despite a preserved integrity of the hippocampus following dMCAO, we next tested the possibility that functional activity within the hippocampus was altered. To this end, we mapped the expression of the activity-dependent gene c-fos which is widely used as an indirect correlate of neuronal activation (Vann et al., 2000b; Maviel et al., 2004). Because,

this gene has been reported to be transiently expressed in response to brain injury, including ischemia (Honkaniemi et al., 1997), we added a delay of 4 days before examining its expression, therefore controlling for this potential confound. This delay was sufficient to enable cerebral Fos expression to return to baseline, including in the infarcted cortical areas (**Fig. 45**). We focused our attention to Fos expression in the subregions of the hippocampus (CA1, CA3 and DG) in sham and dMCAO animals that remained in their home cage. While we noted a trend for ischemic-induced reduced expression in the regions analyzed, none of these differences reach significance ($F < 1$ for all comparisons), likely because Fos proteins are not constitutively expressed which generates a floor effect (**Fig. 46B-D**). To circumvent this issue, we chose to stimulate Fos expression either pharmacologically or more physiologically by exposing ischemic rats to a novel environment (free exploration).

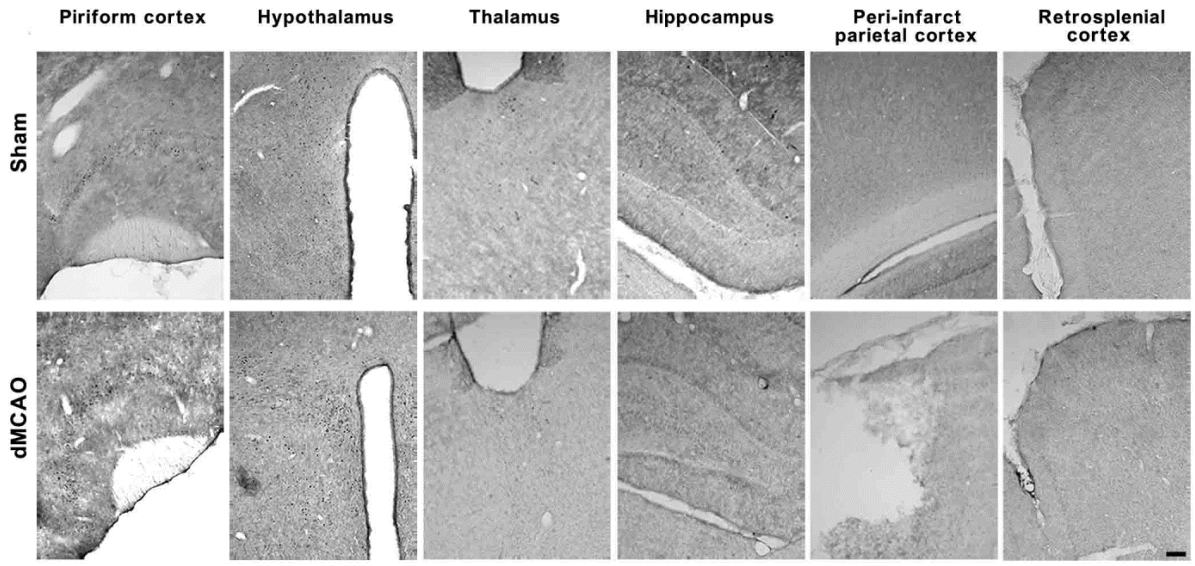


***Figure 45. Fos Protein expression is low in dMCAO rats 4 days after induction of focal ischemia.*** ***(A)*** *Photomicrographs of coronally-cut sections showing Fos protein expression throughout various brain regions in shams and dMCAO rats that remained in their home cage during 4 days after induction of focal ischemia. Scale bar, 100 µm.*

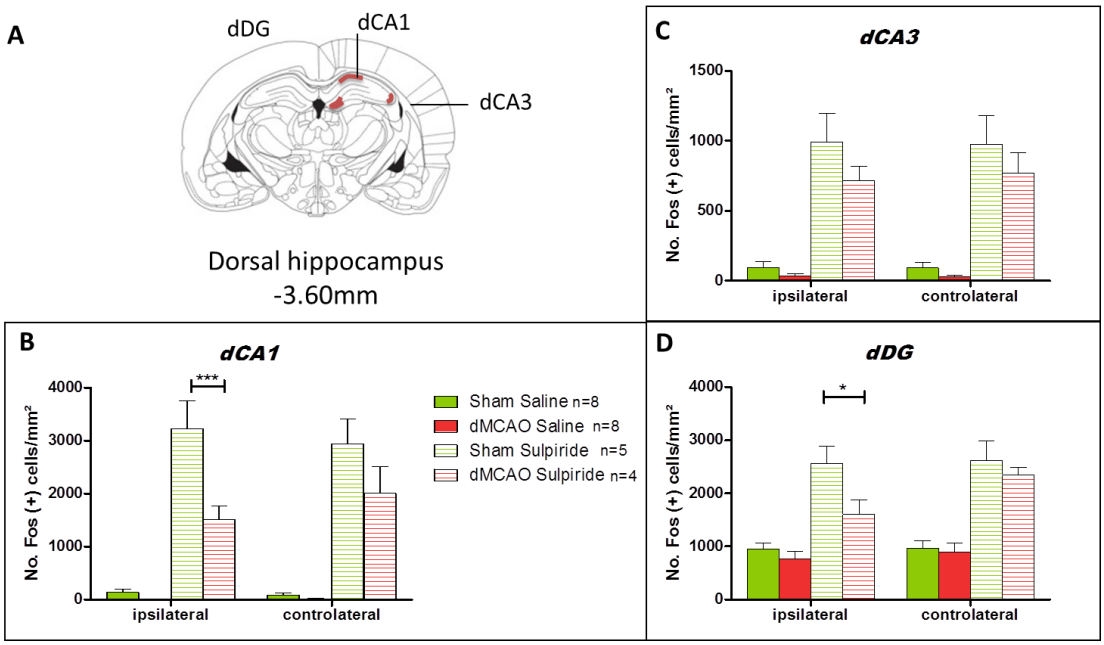


***Figure 46. Hippocampal activation is reduced in dMCAO rats after pharmacological challenge. (A)*** *Regions of interest (filled areas) selected for measurements of Fos labeling are shown. Number indicates the distance in millimeters of the section from Bregma. CA1: CA1 field of dorsal hippocampus; CA3: CA3 field of dorsal hippocampus; DG: dentate gyrus.* ***(B)*** *Expression of Fos-positive nuclei in the hippocampal CA1 region of shams and dMCAO rats injected in their home cage with saline or sulpiride (100 mg/kg, i.p.). Sulpiride treatment increased Fos expression in the ipsilateral side ($F_{1,21}$= 99.12; $p < 0.001$) and contralateral side ($F_{1,21}$= 89.55; $p < 0.001$), but this effect was less pronounced in ischemic rats is the ipsilateral side (interaction treatment x surgery: $F_{1,21}$ =11.66; $p <0.01$).* ***(C)*** *Sulpiride increased Fos expression in the CA3 region of the hippocampus compared to saline-injected rats ($F_{1,21}$ = 67.41; $p < 0.001$) but the treatment x surgery effect failed to reach significance ($F_{1,21}$ = 1.293; $p > 0.05$).* ***(D)*** *In the hippocampal DG, sulpiride stimulated Fos expression in the ipsilateral side ($F_{1,21}$ = 37.35; $p < 0.0001$) and the contralateral side ($F_{1,21}$ = 51.72; $p < 0.0001$). Hypoactivation occurred in dMCAO rats and affected predominantly the ipsilateral infarcted hemisphere (treatment x surgery: $F_{1,21}$ = 8.227; $p < 0.05$). *p < 0.05, ***p < 0.001; n = 4–8 rats/group.*

To increase Fos protein expression, we performed intraperitoneal injections of either sulpiride, a $D_2$ receptor antagonist known to enhance Fos expression throughout the limbic system (Ozaki et al., 1998), or saline (vehicle) in sham and dMCAO rats which remained in their home cages. While, as expected, sulpiride injections increased hippocampal Fos expression in sham rats compared to saline-injected rats (**Fig. 46B-D**), this compound failed to enhance Fos expression in hippocampal regions of dMCAO rats, suggesting hypoactivation of hippocampal regions following this pharmacological challenge (**Fig. 46B-D**). When required to explore a novel spatial environment (free exploration of a circular arena), dMCAO rats also exhibited Fos hypoactivation in hippocampal regions, a pattern which contrasted

with that of sham animals for which Fos expression was increased in all subfields of the hippocampus compared to rats that remained in their home cage. (**Fig. 47A-C**). Notably, Fos protein expression in dMCAO rats was reduced in a region- and hemisphere-specific manner. Reduced Fos activation was particularly prominent in the CA1 and DG regions and more important in the ipsilateral hemisphere (**Fig. 47A-C**). Importantly, these reduced levels of Fos expression in dMCAO rats were not observed in all brain regions, indicating region-specificity and the absence of a generalized impairment in the cerebral regulation of Fos expression due to ischemia (**Fig. 48**).

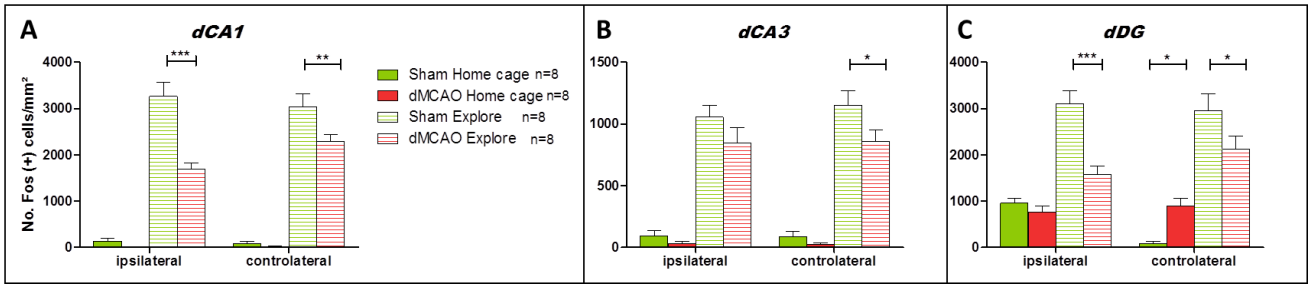


***Figure 47. Hippocampal activation is reduced in dMCAO rats after exploration of a novel environment. (A)*** *Expression of Fos-positive nuclei in the hippocampal CA1 region of shams and dMCAO rats remaining in their home cage or exploring a circular arena. Spatial exploration increased Fos expression in both hemispheres (ipsi: $F_{1,28}$=195.3; p<0.0001, contra: $F_{1,28}$=283.6; p<0.0001)but this effect was attenuated in ischemic rats. Reduction in Fos expression was predominant in the ipsilateral infarcted hemisphere (interaction treatment x surgery: $F_{1,28}$=17.69; p<0.001) compared to contralateral side (interaction treatment x surgery: $F_{1,28}$=4.823; p<0.05)* ***(B)*** *In the CA3 of the hippocampus, spatial exploration increased Fos expression compared to home cage controls in ipsilateral ($F_{1,28}$=122.2; p<0.0001) and contralateral sides ($F_{1,28}$=152.3; p<0.0001), an effect that was attenuated in dMCAO rats in contralateral side ($F_{1,28}$=5.131; p<0.05)****(C)*** *In the DG of the hippocampus, spatial exploration enhanced Fos expression in the ipsilateral ($F_{1,28}$=61.20; p<0.0001) and contralateral sides ($F_{1,28}$=67.29; p<0.0001) and revealed hypoactivation in dMCAO rats (interaction treatment x surgery: $F_{1,28}$=12.82; p<0.01). *p<0.05, **p<0.01, ***p<0.001; n = 8 rats/group.*

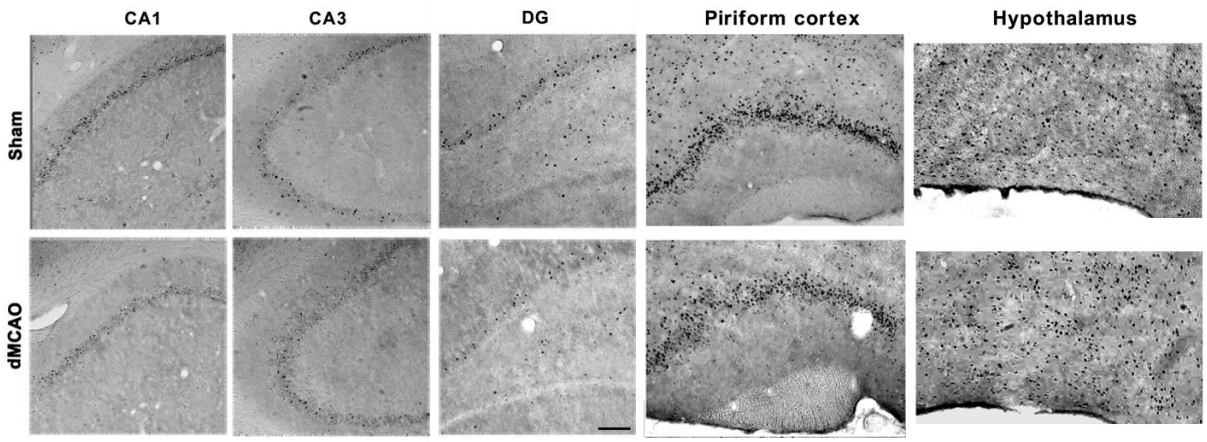

***Figure 48. Reduced Fos protein expression following focal ischemia is region-specific****. Photographs showing that Fos expression is reduced in dMCAO-Exploring rats in the ipsilateral CA1, CA3 and DG (bottom panel) compared to sham-Exploring controls (top panel). Fos expression did not vary in the ipsilateral piriform cortex and hypothalamus of the rats exploring a novel environment. Scale bar, 100µm.*

### 3.3. dMCAO-induced hippocampal hypofunction translates into memory dysfunction

We next tested whether the observed hippocampal hypofunctioning following focal ischemia after either a pharmacological challenge or exploration of a novel environment could translate into the induction of memory deficits. To this end, we submitted dMCAO rats to two types of hippocampal-dependent memory tasks, one spatial and aversive, the Barnes maze in which the animals is required to locate the position of an escape box (Sunyer et al., 2007), and one non spatial but appetitive, the social transmission of food preference task in which the animal learns about the safety of potential food sources by sampling those sources on the breath of littermates (Clark et al., 2002). While the Barnes maze relied on spatial memory, the STFP task required the formation of associative olfactory memory.

Spatial memory was tested in the Barnes maze, over the 5 days of training (2 sessions/day). While dMCAO animals managed to learn the location of the escape box, their acquisition rate was slower than sham rats (**Fig. 49**).

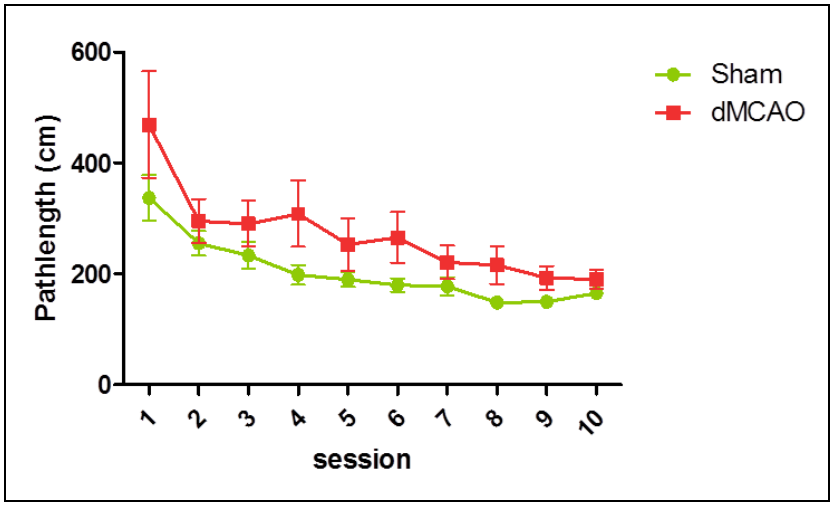


***Figure 49. Focal ischemia induces spatial memory impairment as measured in the Barnes maze.*** *Path length to locate the escape box in the Barnes maze decreased for both groups over trial blocks ($F_{9,252}$=10.77; p<0.0001). dMCAO rats were slower in mastering the task compared to sham controls ($F_{1,252}$=5.014; p<0.05). n= 14-16 rats/group.*

At the cellular level, Fos protein expression in the hippocampus was decreased in

dMCAO rats after completion of training in the Barnes maze (**Fig. 50B-D**), thus confirming the hippocampal dysfunction following spatial exploration of a novel environment we observed previously. In the STFP task, dMCAO rats were impaired upon memory retrieval probed 7 days following social interaction. While sham rats exhibited a preference for the cumin flavor, dMCAO rats failed to do so, indicating an inability to adequately form and/or retrieve long-term associative olfactory memory (**Fig. 51A**). This anterograde amnesia was memory-specific as motivation of the dMCAO rats to eat powdered food was similar to that of sham rats. Indeed, the total amount of food eaten was equivalent between groups (**Fig. 51B).** To rule out the possibility that dMCAO rats suffers from a deficit in olfactory sensitivity, we submitted dMCAO and sham rats to an additional odor discrimination task using the same concentration of cumin odor as in the STFP task and establish that the dMCAO rats were as efficient as sham rats in discriminating the cumin flavoured cup in the arena (**Fig. 52**).

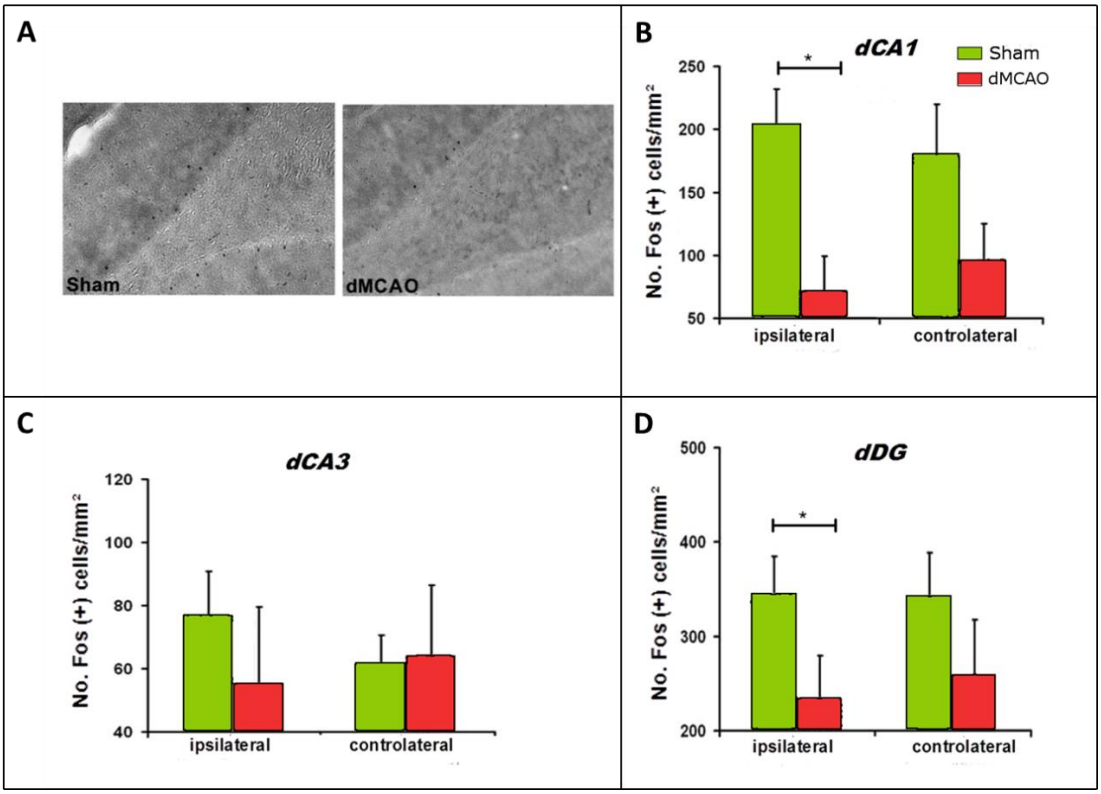


***Figure 50. Focal ischemia is associated with hippocampal hypoactivation following training in the Barnes maze. (A)*** *Photomicrographs of Fos staining in the ipsilateral DG from shams and dMCAO animals.* ***(B)*** *Expression of Fos-positive nuclei in the hippocampal CA1 region of shams and dMCAO rats after Barnes maze.* ***(C)*** *dMCAO did not affect neuronal activity in the CA3 ($F<1$, NS).* ***(D)*** *In the DG, dMCAO-STD rats showed reduced Fos counts compared to Sham-STD rats ($F_{1,30}=4.59$ ; $p<0.05$). This effect was predominant in the ipsilateral side (interaction: surgery x housing: $F_{1,30}=4.64$; $p<0.04$). *$p<0.05$; n= 11-16 rats/group.*

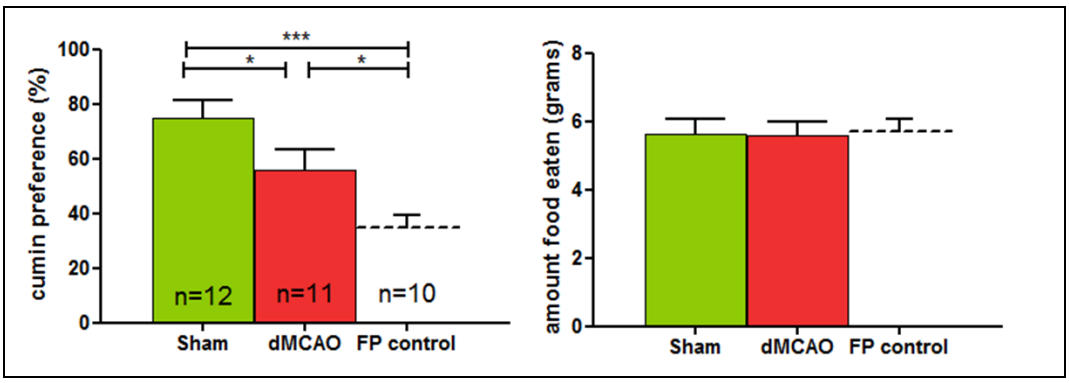


***Figure 51. Associative olfactory memory as measured in the STFP task is impaired following focal ischemia. (A)*** *dMCAO rats exhibited a lower preference score for cumin compared to sham controls during the retrieval test administered 7 day after social interaction ($F_{2,30}$=10.00; p<0.05). However, performance of ischemic rats was higher than that of food preference controls (experimental chance level) which interacted with a demonstrator fed with plain food.* ***(B)*** *The total amount of food consumed by all groups during test was similar, indicating no confounding effect of motivation. *p<0.05, ***p<0.001.*

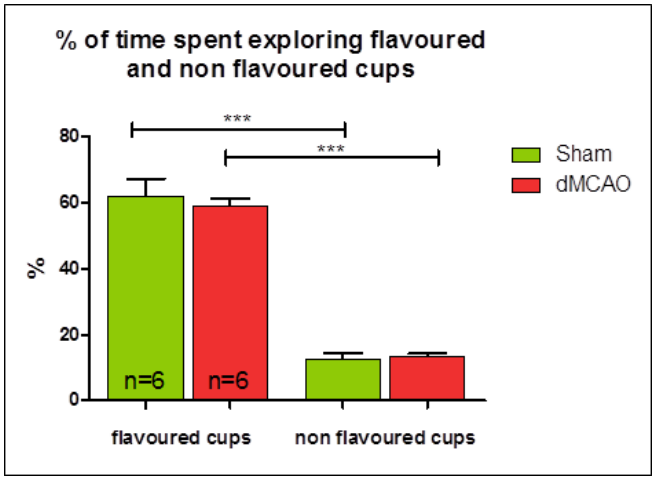


***Figure 52. Focal ischemia does not impair odor discrimination.*** *dMCAO rats and sham rats spend a similar time exploring the cumin cup compared to non-flavoured cups ($F_{3,20}$=9.175; p<0.005). **p<0.001.*

Experiments analyzing the level of hippocampal activation using the activity-dependent gene c-fos following acquisition and retrieval of associative olfactory memory in the STFP task are ongoing.

### 3.4. Electrical activity was preserved in the hippocampus but silent in parietal cortex after ischemia

Since there was no evidence of hippocampal damage following dMCAO, we sought to determine whether the hippocampal circuitry was affected in dMCAO rats. This was addressed directly by electrophysiological recordings from neocortex and hippocampus in anesthetized animals (n=5) within the 4 hours following a dMCAO episode. As expected, neuronal activity was virtually abolished in the ipsilateral, but not contralateral, somatosensory cortex (**Fig. 53A**). In the ipsilateral hippocampus, the presence of spontaneous SPW-ripples, a hallmark of functional CA3 to CA1 ongoing synaptic transmission via Schaffer collaterals (Csicsvari et al., 2000), as well as evoked responses to electrical stimulations of the commissural pathway, suggest that neuronal activity and synaptic transmission were not disrupted in the post-ischemic hippocampus (**Fig. 53B**). Thus, hippocampal hypofunction revealed by Fos imaging in ischemic rats confronted to behavioral challenges could be due, at least in part, to a deprivation of excitatory drive originating from the cortical infarct located in the somatosensory cortex.

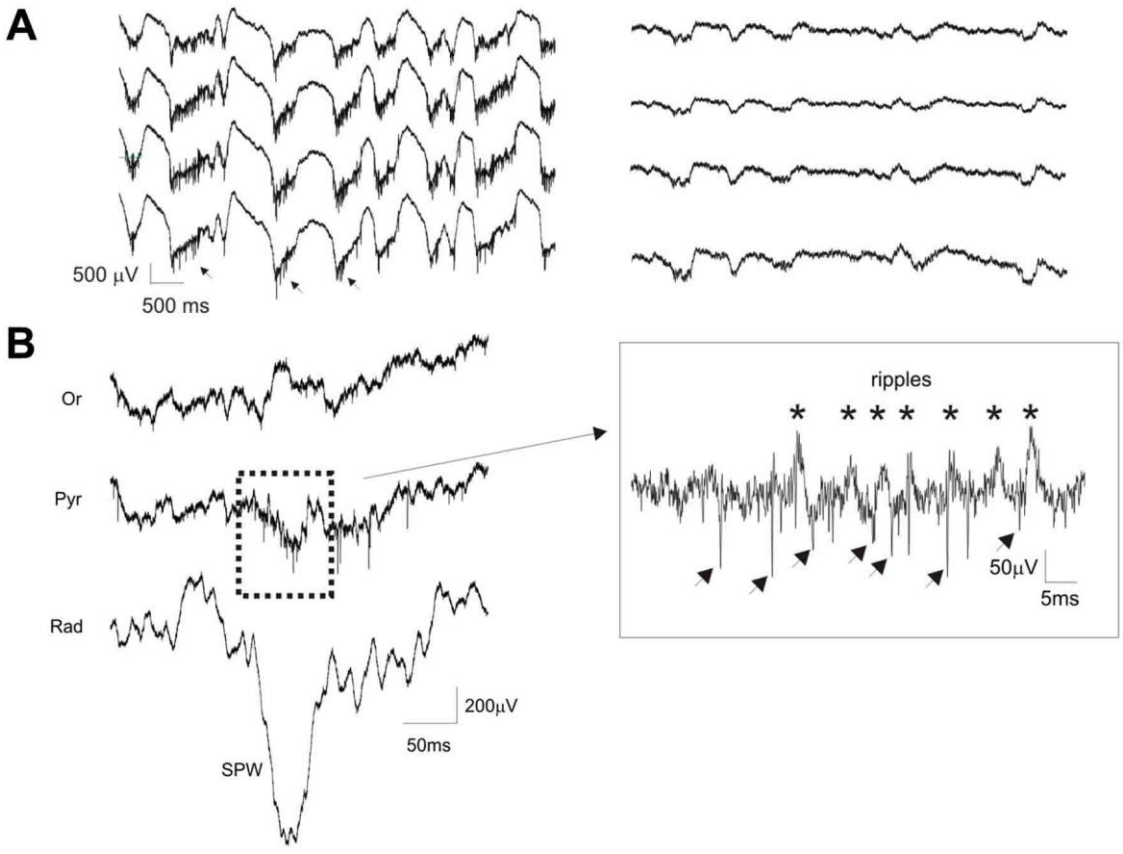


***Figure 53. Synaptic hippocampal activity is preserved during MCA occlusion***. ***(A)*** *Samples of bilateral multisite electrophysiological recordings made during induction of dMCAO in an urethane-*

*anesthetized rat. Depths of the 3 different traces are in the cortical layer V-VI (between 1550 and 1650µm). Left panel shows neocortical activity prior to the onset of focal ischemia. Slow oscillations (1Hz) in the contralateral hemisphere driving recurrent multi-unit bursting activity (arrows) can be observed. Right panel shows depressed neocortical activity upon ischemia in the ipsilateral cortex (infarct side. Note the absence of unit activity and the decrease of amplitude of local field potentials.* ***(B)*** *CA1 pyramidal layer (Pyr) and stratum radiatum (rad) recordings do not show disruption of the synaptic transmission in the hippocampus during ischemia. On the right, spontaneous Sharp Wave activity is shown characterized by a ripple burst in the pyramidal layer (transient fast oscillations of 200 Hz frequency depicted by stars), multi-unit burst of activity (arrows) and by a downward deflection in the radiatum layer (lower trace).*

### 3.5. Topographical characteristics of the somatosensory cortex

To examine the connectivity of the parietal cortex, the anterograde tracer biotinylated dextranamine was microinfused in the somatosensory cortex of intact rats. The somatosensory cortex did not project directly to the hippocampus supporting previous tracing studies (Burwell, 2000). However, it projected to the parahippocampal region (entorhinal, perirhinal and postrhinal cortices) (**Fig. 54**). This result further supports our hippocampal diaschisis hypothesis in which hippocampal hypofunction could be the consequence of reduced cortical inputs (i.e. deactivation) or increased inhibition through the parahippocampal region that acts as relay structure for information exchange between cortical areas and the hippocampus. Thus, the possibility that hippocampal dysfunction and associated memory impairment could be the consequence of impaired neuronal activation in the parahippocampal region in response to altered cortical inputs could be expected. Such a possibility was confirmed when we examined Fos expression in the entorhinal cortex (**Fig. 55A-B**), and the perirhinal cortex (**Fig. 55C**) which innervates the entorhinal cortex. Reduced levels of Fos expression in these two regions were observed in dMCAO animals compared to shams (**Fig. 55**).

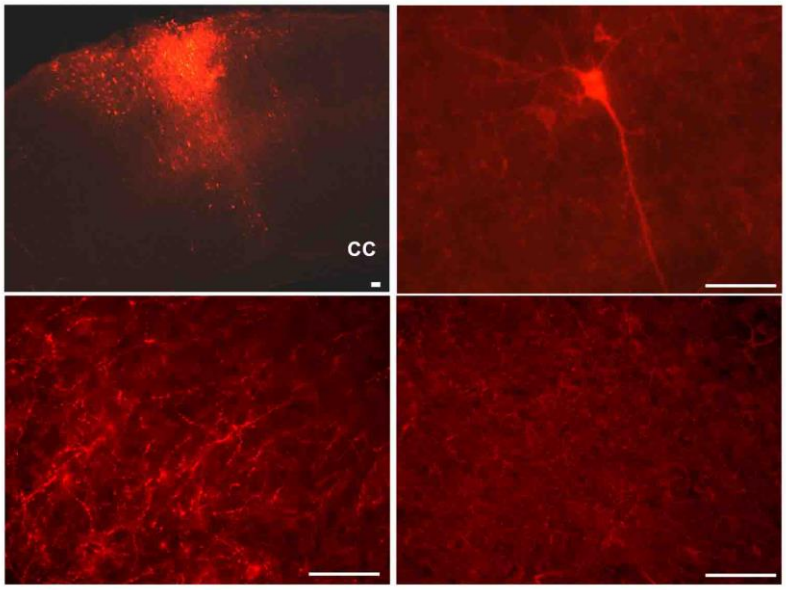


***Figure 54. The somatosensory cortex is anatomically connected to parahippocampal areas****. After unilateral injection of the anterograde tracer BDA into the parietal cortex of intact rats, fibers were labeled in the ipsilateral perirhinal cortex. Cy3-red immunofluorescence was used to stain coronal sections. Upper left panel shows the injection site. Upper right panel illustrates a fluorescent neuron in the cortex. Labeled fibers in the perirhinal cortex (lower left) were apparent in the side ipsilateral to the cortical injection with no trace of staining contralaterally (lower right). CC: corpus callosum. Scale bars, 100 µm.*

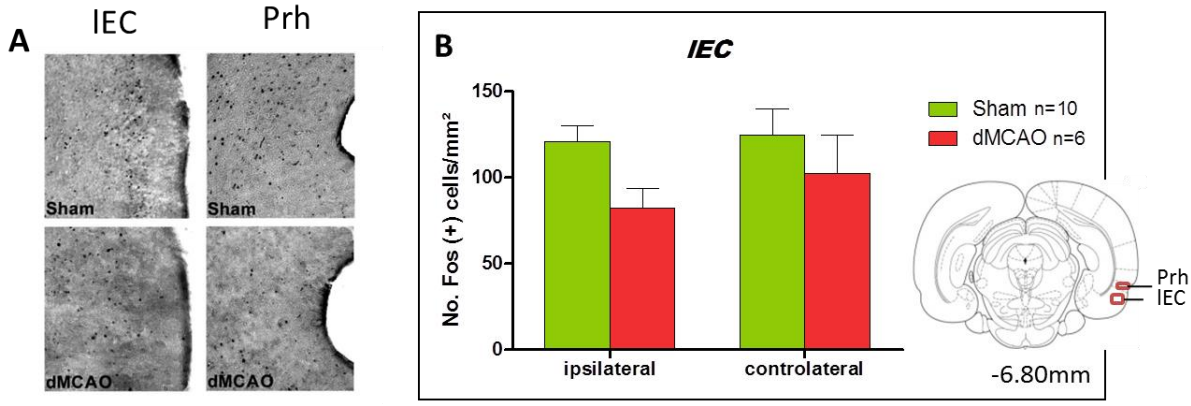


***Figure 55. Hypoactivation in the parahippocampal region occurs following dMCAO. (A)*** *Photomicrographs showing Fos labelling in the ipsilateral entorhinal cortex (left panel) and perirhinal cortex (right panel) of shams and dMCAO animals. Fos expression in dMCAO rats was attenuated in these two brain regions.* ***(B)*** *Expression of Fos-positive nuclei in the entorhinal cortex of shams and dMCAO rats tested for spatial memory in the Barnes maze. Fos counts in the entorhinal cortex ipsilateral to the ischemic infarct of dMCAO rats was reduced compared to sham rats. ($F_{1,28}$=3.970; p=0.0562). n= 6-10 rats/group.*

Experiments analyzing the level of activation within the parahippocampal regions

using the activity-dependent gene c-fos following acquisition and retrieval of associative olfactory memory in the STFP task are ongoing.

## 4. Discussion

In our dMCAO model, we found that the infarct area was restricted to the unilateral parietal cortex while the integrity of the hippocampus or subcortical regions was preserved as described in previous study (Chen et al., 1986; Matsumori et al., 2006). Despite an intact hippocampus, ischemic animals exhibited hippocampal hypoactivation. Because hippocampus is anatomically connected with the somatosensory cortex via the perirhinal cortex projecting to entorhinal cortex (Lavenex and Amaral, 2000), cortical infarct could induce hippocampal hypofunction via a diaschisis-like mechanism. Anatomical connectivity between the somatosensory cortex and perirhinal cortex was confirmed in our anterograde tracing study. This observation of an hippocampal diaschisis extends previous findings showing that focal ischemia can also induce dysfunction in remotely connected brain regions such as the cerebellum (Gold and Lauritzen, 2002). In line with our findings, hippocampal dysfunction and memory impairments resulting from injury to remote brain regions has been demonstrated in animals with thalamic or fornix lesions (Vann et al., 2000a).

Supporting the hippocampal hypoactivation revealed by fos staining, dMCAO rats were impaired when submitted to spatial learning in the Barnes Maze. Similar to water maze, processing of information in this spatial apparatus is dependent on the functional interaction between several brain regions among which the hippocampus and parietal cortex (Save et al., 2005). Although the ipsilateral parietal cortex is consistently damaged following dMCAO-induced focal ischemia (Carmichael, 2005), bilateral lesions are usually required to impair long-term storage and/or expression of spatial memory (Kesner et al., 1991).

dMCAO rats were slower in acquiring the spatial discrimination task in the Barnes maze. These rats also exhibit (1) hippocampal neuronal discharge and synaptic transmission were not disrupted following dMCAO, (2) no hippocampal damage could be revealed 4 weeks post dMCAO, (3) dMCAO rats exhibited reduced expression of the activity-dependent gene c-fos within several regions of the hippocampal formation. Altogether, these results suggest hippocampal neuronal hypofunctioning in response to experimental inputs. We thus suggest that although unilateral, concomitant impaired functioning of hippocampus and parietal cortex is sufficient to induce cognitive impairment. Parietal cortex lesions have been

reported to induce hippocampal place cell firing instability suggesting that this associative cortical region actively participates in the elaboration of hippocampal spatial maps that support navigation though space (Save et al., 2005). Therefore, we propose that hippocampal diaschisis is likely to participate in the dMCAO-induced cognitive impairments and appears as a crucial mechanism underlying, at least in part, memory deficits following focal cerebral ischemia.

Further supporting the spatial memory deficit observed in the Barnes maze, we found dMCAO rats to also exhibit a deficit in non-spatial associative olfactory memory which we assessed using the STFP task. In this paradigm, rats learn about the safety of potential food sources by sampling those sources on the breath of conspecifics. Interestingly, this paradigm does exhibit some of the key features of human declarative memory affected in stroke patients (Rasquin et al., 2002), that is information about potential food sources can be encoded rapidly and expressed flexibly in a test situation different from the circumstances encountered during initial learning (Alvarez et al., 2001). The STFP task has been shown to be dependent on hippocampal function and is particularly well-suited for the investigation of recent and remote memory formation because one single interaction session produces long-lasting memories resistant to forgetting (Lesburgueres et al., 2011).

dMCAO rats were impaired when required to retrieve olfactory associative memory acquired 7 days earlier during social interaction, suggesting that ischemic rats were unable to form and stabilize information over time. This anterograde amnesia was also observed after bilateral lesions of hippocampus (Clark et al., 2002) supporting that hippocampus is needed to acquire and subsequently stabilize and consolidate new information learned during the social interaction. Graded retrograde amnesia has also been reported in the STFP task after either permanent lesion or targeted pharmacological inactivation administered at various delays after social interaction. Hippocampal dependency during the course of systems-level memory consolidation has been shown to be required for at least 15 days post-interaction (Clark et al., 2002; Lesburgueres et al., 2011) until cortical regions become capable of sustaining remote memory retrieval independently of the hippocampus. Diaschisis-induced hippocampal hypofunctioning in ischemic rats could therefore interfere with consolidation processes leading to an altered memory trace potentially less accessible and/or more difficult to retrieve. Alternatively, the ischemic-induced hippocampal dysfunction at the time of retrieval might have prevented memory expression since hippocampal inactivation prior to recent memory retrieval up to 7 days impairs memory performance (Lesburgueres et al., 2011). Fos counts in

dMCAO rats submitted to the SFTP task (after social interaction or retention at 7 days) are in progress. Although speculative at this point, we anticipate that these animals should exhibit reduced hippocampal activation.

Importantly, we found that (1) hippocampal neuronal discharge and synaptic transmission were not disrupted following dMCAO, (2) no hippocampal damage could be revealed 4 weeks post-dMCAO. Electrophysiological recordings reveal that synaptic electrical activity is preserved in the hippocampus but, as expected, silent in cortical layer during ischemia. However, the pattern of electrical events might be changed and this possibility is addressed in details in chapter 3 of this thesis. At the cellular level, freezing-induced damage limited to the cortex induces changes in GABA subunit receptors not only in the cortex, but also in remote brains regions including the hippocampus (Redecker et al., 2000). These remote regions often exhibit reduced metabolic rates routinely detected by PET in human patients (Fiorelli et al., 1991), which has led to the proposal that diaschisis is presumably caused by a disruption of afferent excitatory input originating from distant infarcted areas (Witte et al., 2000; Gold and Lauritzen, 2002). Our data further extend these findings and suggest that hippocampal deactivation resulting from decreased excitatory inputs originating in the cortex, a form of focal ischemia-induced diaschisis in the hippocampus, was likely to be responsible for ischemic-induced memory dysfunction.

Altogether, our results point to hippocampal neuronal hypofunctioning in response to experimental inputs processed by cortical primary and associative areas. Our results further suggest that although unilateral, concomitant impaired functioning of hippocampus and parietal cortex is sufficient to induce cognitive impairment. Parietal cortex lesions have been reported to induce hippocampal place cell firing instability suggesting that this associative cortical region, in addition to the hippocampus, actively participates in the elaboration of hippocampal spatial maps that support navigation though space (Save et al., 2005). Therefore, in light of our findings in this chapter, we propose that parietal dysfunction together with hippocampal hypofunctioning via a diaschisis-like mechanism are likely to participate in the dMCAO-induced cognitive impairments. Hippocampal diaschisis thus appears as a crucial mechanism underlying, at least in part, memory deficits following focal cerebral ischemia. Our data provide novel insights to explain the neurobiological mechanisms underlying to focal ischemic stroke and inducing memory impairments. Hippocampal diaschisis seems a good candidate to explain the observed deficits. In order to further investigate the dynamics between parietal cortex and hippocampus following stroke, additional studies will be

presented in the part II and III, including pharmacological inactivation of targeted structures and electrophysiological electrode recordings.

# Part II : Targeted pharmacological inactivations of somatosensory cortex and hippocampus support hippocampal diaschisis in mediating ischemia-induced memory deficits

## 1. Introduction

In the previous part, we reported memory impairments in dMCAO rats submitted to the STFP task and hippocampal hypoactivation after spatial exploration of a novel environment. Our findings suggest that focal ischemia induces hippocampal diaschisis by decreased functional activation of the hippocampus as revealed by Fos imaging in ischemic rats behaviorally challenged. We propose that decreased excitatory inputs to the hippocampus could be responsible for the observed hippocampal hypofunctioning (deactivation) since hippocampal integrity and intrinsic connectivity was preserved. To provide further mechanistic support to the hippocampal diaschisis phenomenon, we attempted, in a new series of experiments, to reproduce the effects of focal ischemia by adopting a targeted pharmacological strategy. It consisted in performing a combination of region-specific inactivations of cortical and hippocampal regions and in determining the outcome of these manipulations on memory performance in the STFP task and hippocampal activation using Fos imaging. We hypothesized that parietal (somatosensory) cortex infarct could induce hippocampal diaschisis leading to memory impairment after stroke, for this reason we explored the effect of specific inactivation of this brain region on cognitive function using two type of drugs. First, rats were inactivated with lidocaine, a sodium channel blocker that blocks the synaptic transmission (Onizuka et al., 2008) for 10 to 30 minutes (Martin, 1991; Pereira de Vasconcelos et al., 2006), and explored a novel environment in order to map the neuronal activation of the hippocampus and the parahippocampal region with c-fos, an indirect marker of neuronal activation. Second, the somatosensory cortex of rats were inactivated with CNQX, a competitive AMPA/kainate receptor antagonist that blocks synaptic transmission for 10 to 60 min (Attwell et al., 1999) and performed a hippocampal-dependent memory test, the STFP task (Ross and Eichenbaum, 2006) before mapping neuronal activation in hippocampal and entorhinal regions. Such targeted inactivations offered a number of advantages. First, it mimicked an ischemic infarct whose boundaries were localized in the somatosensory cortex. Second, by enabling a very localized inactivation, the ischemic-induced general decrease of blood flow that inevitably impact the global brain metabolism during the occlusion of the carotid could be avoided (Roof et al., 2001; Jordan, 2004; Foreman and Claassen, 2012). Last, this acute and reversible pharmacological approach enabled to examine the validity of the hippocampal diaschisis concept in the absence of extended permanent cell loss and associated vicariance phenomena secondary to the ischemic core.

## 2. Materials & Methods

### 2.1. Groups

Inactivated (CNQX or lidocaine) rats and vehicle (Acsf) rats underwent each experiment listed as follows : Fos expression stimulation following spatial exploration (**Fig. 56**), STFP (**Fig. 57**) and odor discrimination tests (**Fig. 58**). Protocols were described in detail in the General Materials & Methods.

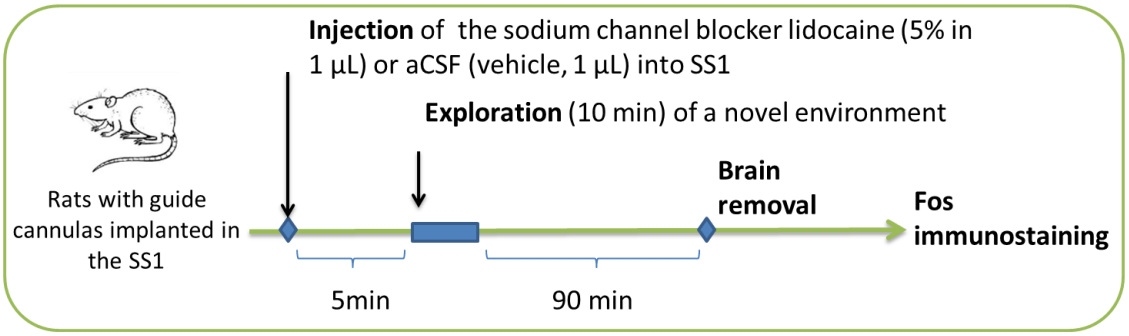


***Figure 56. Timeline of exploration of a novel environment protocol.*** *Rats were injected with lidocaine or vehicle 5 minutes prior to a 10 minute exploration of a novel environment . Rats were then returned to their home cages for 90 minutes. After this period corresponding to the peak of Fos expression, rats were anesthetized and perfused intracardially with PFA. Their brains were removed and processed for Fos immunostaining.*

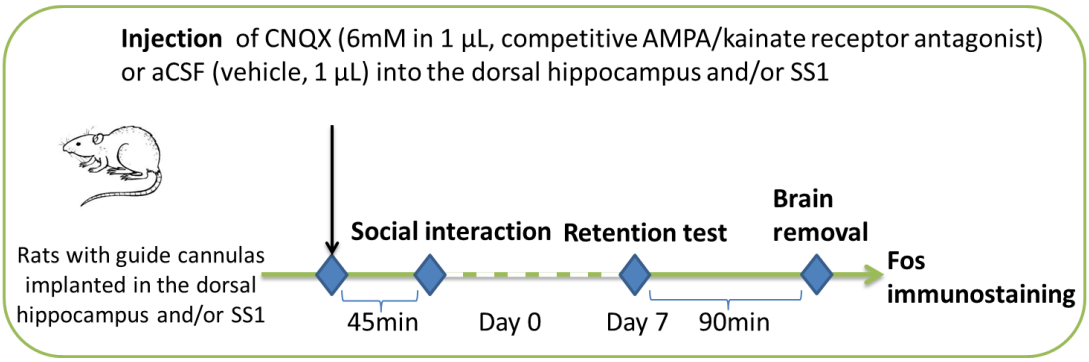


***Figure 57. Timeline of the STFP test.*** *Rats were injected intracerebrally 45 minutes prior to social interaction (Day 0). Ninety minutes after the retention test (Day 7), rats were euthanized and and their brains were processed for Fos immunostaining.*

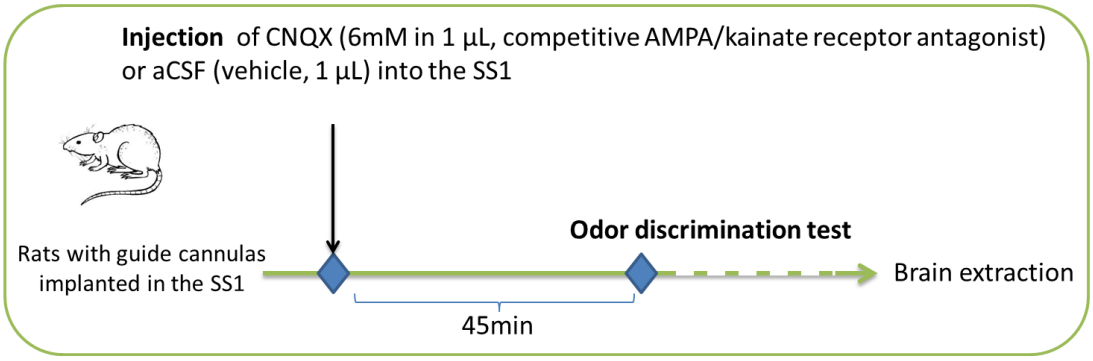


***Figure 58. Timeline of the odor discrimination test.*** *Rats were injected intracerebrally 45 minutes prior to the odor discrimination test and housed in their home cage until the beginning of the task.*

### 2.2. Intracerebral implantation of guide cannulas

We implanted and secure guide cannulas in the brains of rats to enable intracerebral injections of drugs in specific brain regions of awake, freely moving, animals and to modulate neuronal activity prior to memory testing.

Five different groups of rats were implanted as follows : (1) bilateral hippocampus, (2) unilateral hippocampus, (3) unilateral somatosensory cortex (SS1), (4) ipsilateral SS1 and ipsilateral hippocampus, and (5) ipsilateral SS1 and contralateral hippocampus (**Fig. 59**). All implanted groups did not perform the 3 paradigms described in the previous section. Spatial exploration of a novel environment was performed by unilateral SS1 implanted rats . STFP task was performed by all implanted groups. Odor discrimination test was performed by unilateral hippocampus and unilateral SS1 implanted rats.

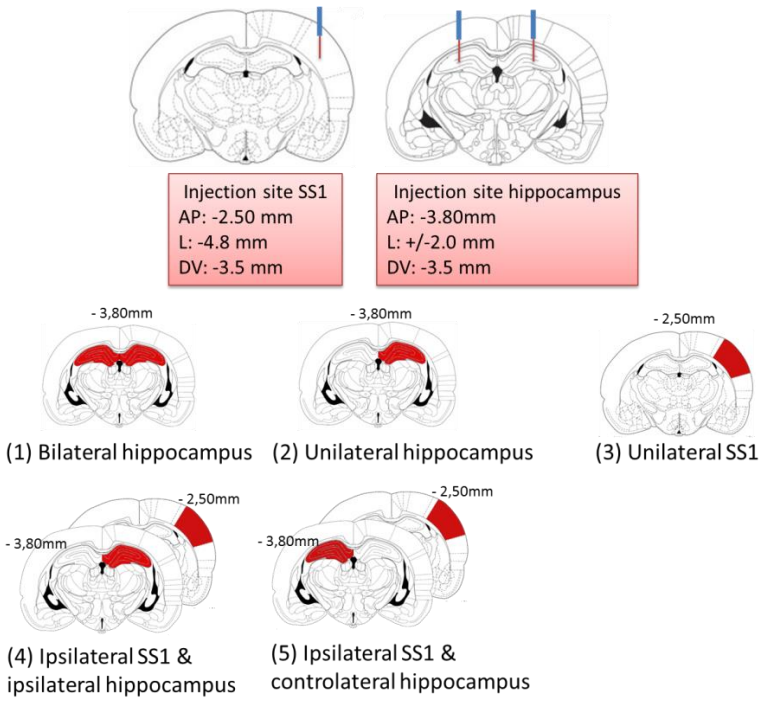


***Figure 59. Schematic representation of inactivated areas.*** *Rats were implanted unilaterally or bilaterally in 2 different locations: SS1 or hippocampus. Red areas represent the inactivated structures that were targeted.*

All surgical tools were autoclaved prior to surgery. The guide cannulas and dummy cannulas were sterilized in Cidex, rinsed with sterile water and stored in a sterile tube until use for stereotaxic implantation. Stereotactic implantations of guide cannulas were conducted two weeks before the beginning of the behavioral procedures. Surgical procedures were performed under isoflurane anesthesia. Once anesthetized, breathing of rats was maintained by a small animal anesthesia machine. Core temperature was maintained between 37± 0.5 °C with a heating blanket and rectal thermistor servo-loop. Rats were placed in a stereotaxic frame (Kopf Instruments) equipped with a mask delivering 1.5-2% isoflurane/68%N2O/30%O2. The effectiveness of anesthesia was assessed by evaluating the paw reflex (paw withdrawal in response to briefly pinching the skin between toes of the hindlimbs). The incisor bar of the stereotaxic frame was positioned at -3.3 mm below the interaural line. After subcutaneous injection of bupivacaine (0.2 cc, 0.25%), the scalp was incised longitudinally to expose the animal's skull. The bone surface was cleaned and dried to ensure better adhesion of the dental cement and to make the different bone sutures easily visible in order to identify accurately the Bregma reference point. Two anchor stainless steel screws were then placed in the cranial bone. After selecting the proper stereotaxic coordinates, one or two holes (unilateral or bilateral) were carefully drilled in the skull using a mini-electric drill whose drill bits have been carefully autoclaved. One or two guide cannulas (8

mm long, od: 0.460 mm, id: 0,255 mm) were then gently implanted above the future site of injection. The different target structures were 1) the dorsal hippocampus, 2) the somatosensory cortex, 3) the entorhinal cortex. Coordinates were determined using the atlas of Paxinos and Watson for rats and were calculated relative to the Bregma reference point. To minimize tissue damage, each guide was positioned 1,5 mm above the target injection site and anchored to the skull with rapid-setting acrylic dental cement that covers the three stainless steel screws. Patency was maintained by inserting a 8 mm stylet.

After suture of the skin, intraperitoneal (i.p.) injection of buprenorphine (0.02 mg/kg) was administrated to each rat in order to minimize pain. Rats were monitored daily 72 hours after surgery, then they were weighed and the amounts of food and water consumed were checked until the beginning of behavioral experiments.

### 2.3. Intracerebral injection procedure prior to memory testing

Some rats underwent stereotaxic surgery to implant guide cannulas in regions of interest to enable intracerebral injections of drugs in awake, freely moving, rats and to modulate neuronal activity prior to memory testing. These rats were habituated to later intracerebral injections to minimize stress responses and maximize performance during subsequent memory testing. To this end, rats were first habituated for 3 days to being handled and maintained 2-3 min in the hand of the experimenter that will perform the intracerebral injection. During this period, we inspected whether healing had occurred on the skull and that the inside of the guide cannula was clean. The day of the experiment, local injections of the selected drug were made by inserting a 33 gauge-injection cannula through the guide cannula in awake, freely moving animals. The injection cannula projected 1,5 mm beyond the tip of the guide and was anchored to the guide by means of a plastic connector that was screwed onto the guide. Polyethylene tubing connected the injection cannula to a 5 µl Hamilton syringe mounted on a Harvard injection pump. The drug was injected at a rate of 0.8 µl/min, with a volume of 1 µl infused into the hippocampus, the somatosensory cortex, or the entorhinal cortex, respectively. The injection cannula was left in place for 2 min after the infusion. After removal of the cannula, animals were left in their cage until memory testing began.

### 2.4. Selected drug: lidocaine or CNQX

Rats were injected 5 minutes prior to the exploration of a novel environment. To inactivate

the neuronal activity, Lidocaine was injected into specific regions of the brain (5% in artificial cerebrospinal fluid (aCSF), 1µL). Lidocaine is a sodium channel blocker that block the synaptic transmission (Onizuka et al., 2008) for 10 to 30 min (Martin, 1991; Pereira de Vasconcelos et al., 2006). Controls received aCSF only (1µL, Sigma).

Because the drug effect of lidocaine was not appropriated for the behavioral tests, rats were injected with a long effect duration drug. Rats were injected 45 minutes prior to the beginning of the behavioral test (STFP task and odor discrimination test) and the outcome on performance measured either in the STFP paradigm or the odor discrimination task was determined (**Fig. 57-58**). Silencing of neuronal activity was achieved by injecting the AMPA receptor antagonist 6-cyano-7-nitroquinoxaline-2,3-dione (CNQX, 6 mM, 1µL, in artificial cerebrospinal fluid (aCSF), Sigma). CNQX blocks synaptic transmission for 10 to 60 min (Attwell et al., 1999). Controls received aCSF only (1µL).

### 2.5. Verification of guide cannula position

Cannula placements were examined after Fos staining and slide mounting to determine whether correct implantation was achieved. If brains were not used for Fos mapping, whole brains were collected and frozen at -80°C after euthanasia of rats. A cryostat was used to generate coronal sections (50 µm thick) proximal to guide and cannula tracts and mounted on PLUS slides (Fisher Scientific) until dried. Cannula placements were verified under a light microscope. If injection sites were not within the targeted region such as somatosensory cortex or dorsal hippocampus, rats were excluded from the data analyses (**Fig. 60**).

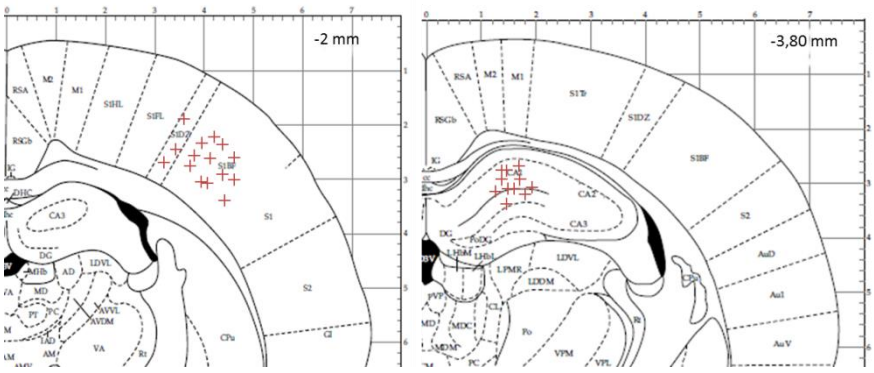


***Figure 60. Histological localization of cannulas in the SS1 cortex and dorsal hippocampus.*** *Red crosses represent the localization of the cannula used for the drug injection into the SS1 cortex (right) or dorsal hippocampus (right) (adapted from Paxinos and Watson, 1998).*

## 3. Results

### 3.1. Inactivation of the somatosensory cortex induced hippocampal hypoactivation and perirhinal hyperactivation following spatial exploration.

To reproduce the implication of the somatosensory infarct in the hippocampal disruption observed in dMCAO animals, we mimicked this lesion by injecting lidocaine, a sodium channel blocker that inactivated part of the somatosensory cortex by blocking the repolarization of the neurons and we examined Fos protein expression in subregions of the hippocampus (dorsal CA, dorsal CA3 and dorsal DG) following spatial exploration of a novel environment. Lidocaine injected in the somatosensory cortex induced hypoactivation of the hippocampus (**Fig. 61 A-C**) and hyperactivation of the parahippocampal region (perirhinal, lateral entorhinal and medial entorhinal cortices) ipsilaterally to the injection site (**Fig. 62 A-C**).

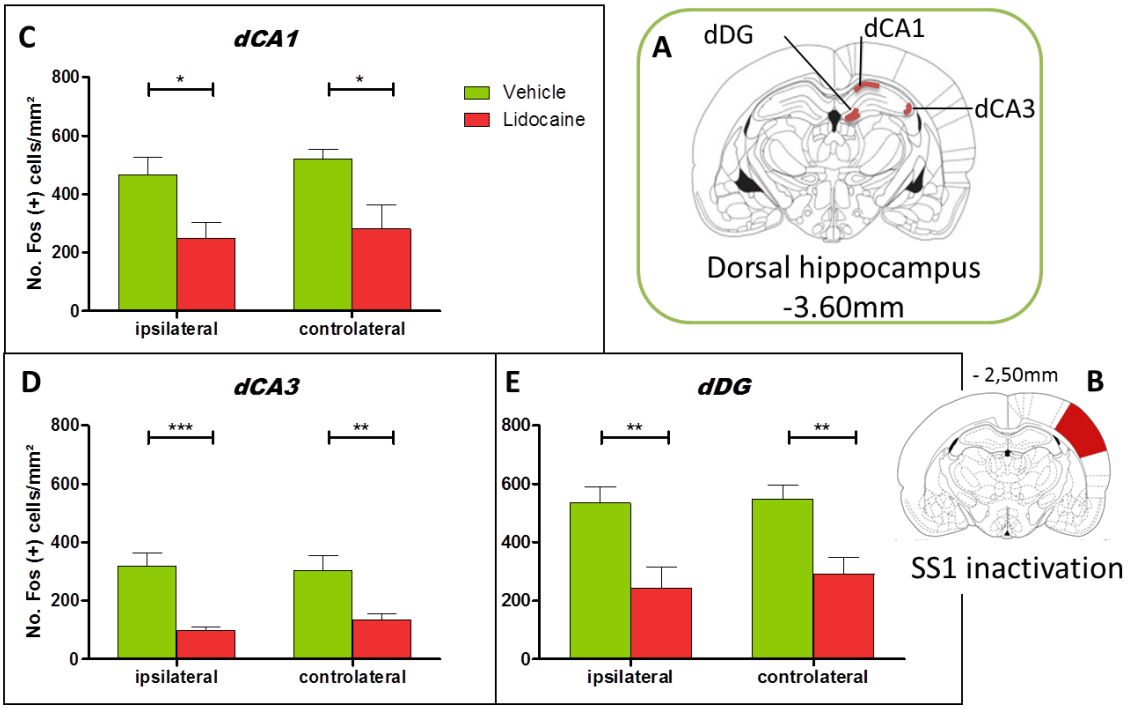


***Figure 61. Somatosensory cortex inactivation induced hypoactivation in the hippocampus following exploration of a novel environment.*** ***(A)*** *Regions of interest (filled areas) selected for measurements of Fos labeling on rat coronal sections. Number depicts the distance in millimeters of the section from Bregma. dCA1: CA1 field of dorsal hippocampus; dCA3: CA3 field of dorsal hippocampus; dDG: dentate gyrus of dorsal hippocampus.* ***(B)*** *The somatosensory cortex (SS1) was injected with either acsf (vehicle) or lidocaine (schematic inactivated area appears in red). Number represents the distance of the section from Bregma.* ***(C)*** *Expression of Fos-positive nuclei in the hippocampal CA1 region of vehicle- and lidocaine-injected rats following exploring a novel environment. Lidocaine injected unilaterally into the somatosensory cortex of rats reduced the Fos expression in the CA1 in*

*both sides ($F_{1,24}$=14.38; p<0.001).* ***(D)*** *Fos protein expression was reduced in both sides of the dCA3 in lidocaine-injected rats ($F_{1,24}$=28.43; p<0.0001).* ***(E)*** *Lidocaine injected in somatosensory cortex of rats also reduced Fos expression in both sides of the dDG ($F_{1,24}$=22.06; p<0.0001). *p<0.05, **p<0.01, ***p<0.001; n = 7 rats/group.*

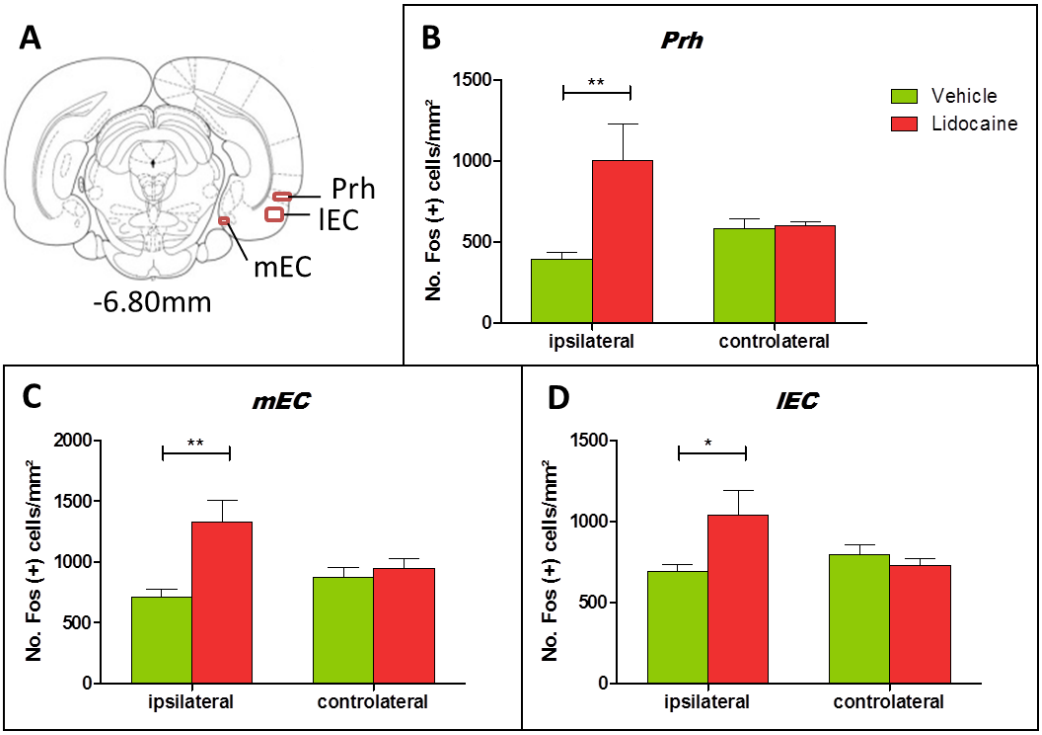


***Figure 62. Somatosensory cortex inactivation induced hyperactivation in the parahippocampal regions following exploration of a novel environment.*** ***(A)*** *Regions of interest (filled areas) selected for measurements of Fos labeling on rat coronal sections. Number indicates the distance in millimeters of the section from Bregma. Prh: Perirhinal cortex, mEC: medial entorhinal cortex, lEC: lateral entorhinal cortex.* ***(A)*** *Expression of Fos-positive nuclei in the perirhinal cortex of vehicle- and lidocaine-injected rats following exploration of a novel environment. Lidocaine injected into the somatosensory cortex of rats resulted in increased Fos expression in the ipsilateral perirhinal cortex (interaction injection x side: $F_{1,24}$=6.473; p<0.05).* ***(B)*** *Fos protein expression was increased in the ipsilateral mEC of the lidocaine-injected rats (interaction injection x side: $F_{1,24}$=5.765; p<0.05).* ***(C)*** *Lidocaine injected into the somatosensory cortex of rats increased Fos expression in the ipsilateral lEC (interaction injection x side: $F_{1,24}$=5.510; p<0.05). *p<0.05, **p<0.01, n = 7 rats/group.*

### 3.2. Somatosensory cortex inactivation induces associative memory deficits.

We next examined whether hippocampal dysfunction observed in SS1 inactivated rats following exploration could translate into memory deficits. We inactivated the SS1 unilaterally with CNQX, a competitive AMPA/kainate receptor antagonist and animals were submitted to memory testing using the STFP olfactory associative memory test. Additional groups were injected in the hippocampus bilaterally to establish that this memory paradigm do require the hippocampus for acquisition. We confirmed previous findings (Ross and

Eichenbaum, 2006) showing that hippocampal damage produce anterograde amnesia in the STFP task (**Fig. 63A-C**), highlighting the hippocampal dependent nature of the task.

Inactivation of the somatosensory cortex induced a memory impairment (**Fig. 63D-E**) similar to that observed in dMCAO rats suffering from an ischemic core located in the same brain region (**Fig. 51A-B**). No confounding effect of somatosensory cortex inactivation on odor discrimination was observed, indicating a true memory deficit (**Fig. 64**). Interestingly, this impairment was not as pronounced as for bilateral inactivation of the hippocampus, suggesting that compensatory mechanisms, possibly in the preserved contralateral hippocampus, were induced. If unilateral somatosensory cortex inactivation triggered hippocampal diaschisis, we predicted that the observed impairment in the STFP task could be mimicked by unilateral hippocampal inactivation forty-five minutes prior to social interaction. This was indeed the case, both groups exhibiting similar levels of impairments. Thus, an intact unilateral hippocampus was not sufficient for allowing complete successful execution of the STFP task 7 days following social interaction, a process which requires both hippocampi.

The deficit in associative olfactory memory observed in SS1-inactivated rats may be the result of the conjoint disruption of both cortical (direct inactivation) and hippocampal (distant inactivation via diaschisis) functions. To decipher between the functional roles of these two anatomical components, we performed conjoint unilateral inactivation of the somatosensory cortex and the hippocampus in the same hemisphere and probed associative olfactory memory 7 days post-interaction. This double inactivation did not exacerbate the memory deficit induced after single somatosensory inactivation, suggesting that the cortical component did not contribute significantly to the observed memory deficit. Thus, the deficit in SFTP induced by unilateral somatosensory cortex inactivation was predominantly attributable to hippocampal diaschisis leading to impaired hippocampal processing of information and was comparable to that observed after dMCAO.

To determine whether such a deficit was due to a genuine unilateral effect on hippocampal function or to impaired hippocampal function extending contralaterally, we next applied targeted inactivation of the somatosensory cortex and the hippocampus on opposite hemispheres and examined the outcome of this procedure on memory performance in the STFP task (**Fig. 65-66**). This asymmetrically placed double inactivation exacerbated the memory deficits observed in somatosensory cortex rats inactivated unilaterally. Magnitude of

the induced-deficit was comparable to that observed following bilateral inactivation of the hippocampus, indicating that unilateral inactivation of the somatosensory cortex induced restricted ipsilateral hippocampal diaschisis which did not spread contralaterally. Mapping of hippocampal Fos staining following unilateral inactivation of the somatosensory cortex of rats submitted to social interaction, which is still ongoing, should provide confirmatory evidence.

The greater impairment observed was thus attributable to a conjoint bilaterally-induced hippocampal dysfunction, one direct on one hemisphere, the other more distant which originated in the somatosensory cortex located in the other hemisphere.

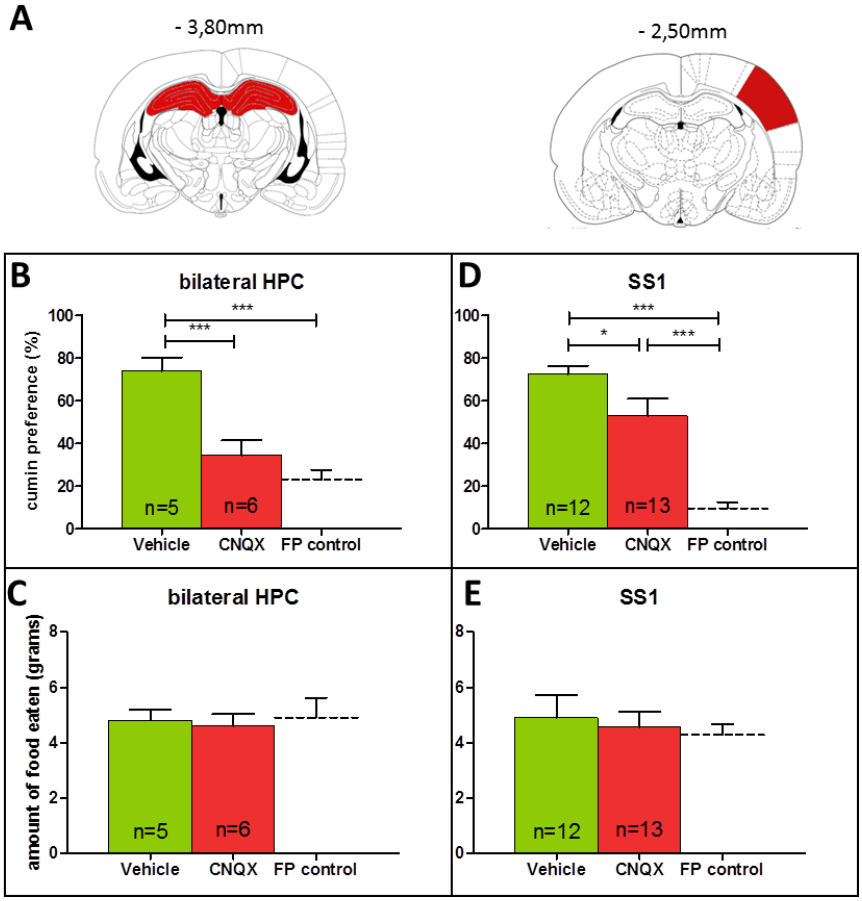


***Figure 63. Bilateral hippocampal inactivation or unilateral SS1 inactivation impaired the STFP test. (A)*** *Schematic representations of inactivated areas (in red) are shown on rat coronal sections (adapted from Paxinos and Watson, 1998).* ***(B)*** *Rats injected with CNQX bilaterally into the hippocampus one hour prior to social interaction showed reduced preference for cumin compared to rats injected with Acsf (Vehicle) when submitted to retrieval 7 days later in the STFP procedure ($F_{2,14}$=18.52; p<0.001).* ***(C)*** *Food consumption during the retrieval test was similar across groups. ($F_{2,14}$=0.085; p>0.05)* ***(D)*** *Rats injected unilaterally with CNQX into SS1 showed reduced preference for cumin compared to rats injected with Acsf (Vehicle) when submitted to retrieval 7 days later in the STFP procedure ($F_{2,38}$=37.92; p<0.0001).* ***(E)*** *Food consumption during the retrieval test was similar across groups ($F_{2,38}$=0.278; p>0.05) *p<0.05, ***p<0.001.*

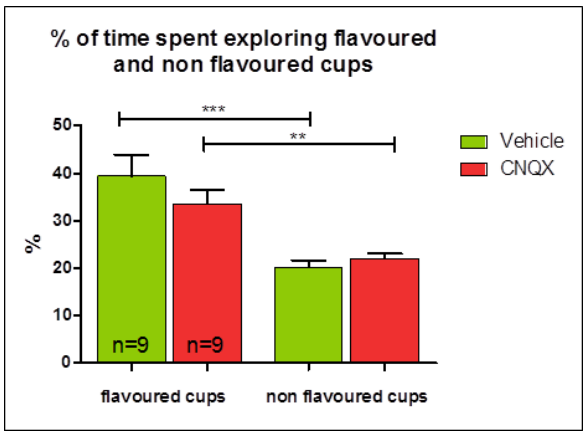


***Figure 64. Unilateral SS1 inactivation did not impair odor discrimination.*** *CNQX and vehicle-injected rats spent more time exploring the cumin cup compared to non-flavoured cups ($F_{3,35}$=10.73; p<0.0001). **p<0.01, ***p<0.001.*

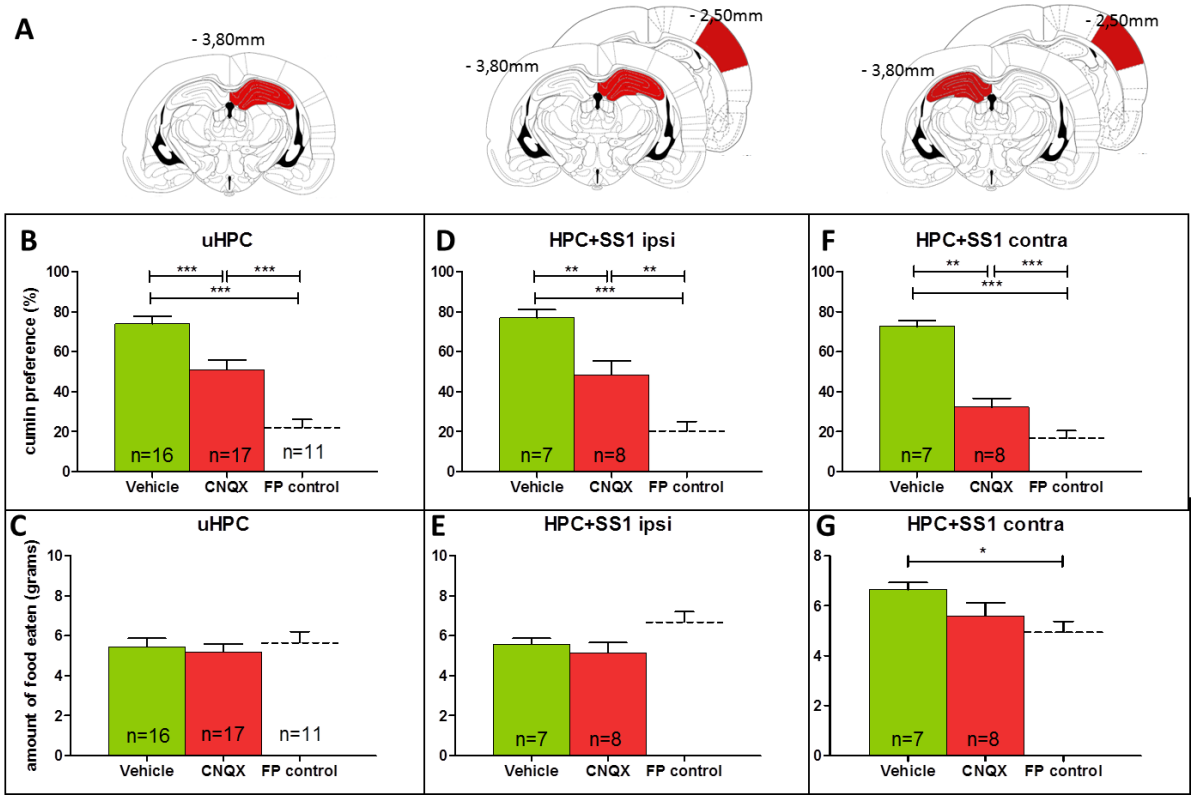


***Figure 65. Effects of anatomical disconnection procedures of the hippocampus and the somatosensory cortex on olfactory associative memory as measured in the STFP test (A)*** *Schematic representations of CNQX inactivated areas (in red) are shown on rat coronal sections (adapted from Paxinos and Watson, 1998).**(B)** Rats injected unilaterally with CNQX into the hippocampus one hour prior to social interaction showed reduced preference for cumin compared to rats injected with Acsf (Vehicle) when submitted to retrieval 7 days later in the STFP procedure ($F_{2,41}$=31.87; p<0.0001). **(C)** Food consumption during the retrieval test was similar across groups. ($F_{2,41}$=0.2541; p>0.05) **(D)** Rats injected unilaterally with CNQX into both the hippocampus and the somatosensory cortex of the same hemisphere one hour prior to social interaction showed reduced preference for cumin compared to rats injected with Acsf (Vehicle) when submitted to retrieval 7 days later in the STFP procedure*

*($F_{2,16}$=18.50; p<0.0001).* ***(E)*** *Food consumption during the retrieval test was similar across groups ($F_{2,16}$=02273; p>0.05)* ***(F)*** *Rats injected unilaterally with CNQX into the hippocampus and the somatasosensory cortex of opposite hemispheres one hour prior to social interaction showed reduced preference for cumin compared to rats injected with Acsf (Vehicle) when submitted to retrieval 7 days later in the STFP procedure ($F_{2,24}$=50.87; p<0.0001).* ***(G)*** *FP control rats ate less food than vehicle-injected rats ($F_{2,24}$=3.587; p<0.05)*p<0.05, **p<0.01, ***p<0.001.*

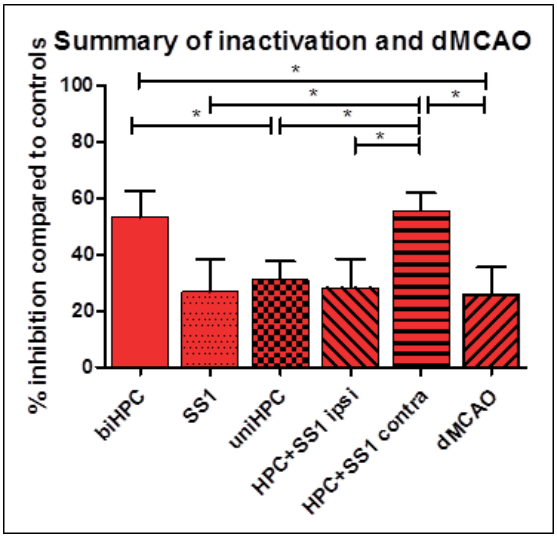


***Figure 66. Comparisons of the effects of dMCAO and anatomical disconnection procedures of the hippocampus and the somatosensory cortex on memory performance in the STFP task.*** *Percentage of impairment induced after induction of dMCAO or targeted inactivation with CNQX is relative to vehicle-injected controls of the corresponding group. One way-ANOVA did not show any differences between groups ($F_{5,62}$=1.677; p>0.05) but t-test revealed differences between bilateral hippocampal and unilateral hippocampal inactivated groups ($t_{21}$=1.787, p<0.05) as well as between bilateral hippocampal and dMCAO groups ($t_{15}$=1.822, p<0.05). Rats inactivated in the SS1 and contralateral hippocampus were more impaired than rats inactivated in the SS1 and ipsilateral hippocampus ($t_{14}$=2.293, p<0.05), unilateral hippocampus ($t_{23}$=2.338, p<0.05), SS1($t_{19}$=1.871, p<0.05) or dMCAO rats ($t_{17}$=2.347, p<0.05). *p<0.05.*

### 3.3. SS1 inactivation did not reduce Fos protein expression following the STFP task.

To investigate hippocampal activity following the retention test of the STFP task, we examined Fos protein expression in the SS1, hippocampus and lEC in inactivated rats and vehicle-injected rats. There was no evidence that neuronal activity is impaired 7 days after the injection of the CNQX despite the tendency shown in the SS1 (**Fig. 67**). Hippocampus or parahippocampal regions did not reveal any fluctuations between groups (**Fig. 68**). However due to a problem with our lot of Fos antibody, new sections are being stained in order to determine if hippocampal and parahippocampal Fos activity are impaired the day of the social interaction when the new odor is acquired. We also expect to detect hippocampal hypoactivation following social interaction in rats that underwent hippocampal inactivation

prior to the social interaction, an impairment which should result in anterograde amnesia when long-term memory is probed 7 days post-interaction.

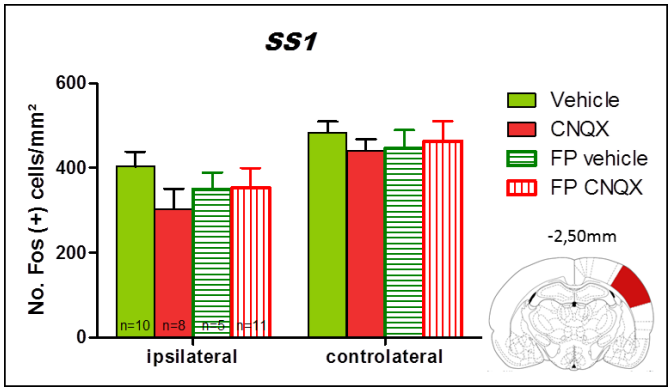


***Figure 67. SS1 unilateral inactivation tends to reduce Fos protein expression following STFP task 7 days after injection.*** *Two-way ANOVA did not show any significant difference between group differences in Fos protein expression in SS1 ($F_{3,60}$=1.033; p>0.05).*

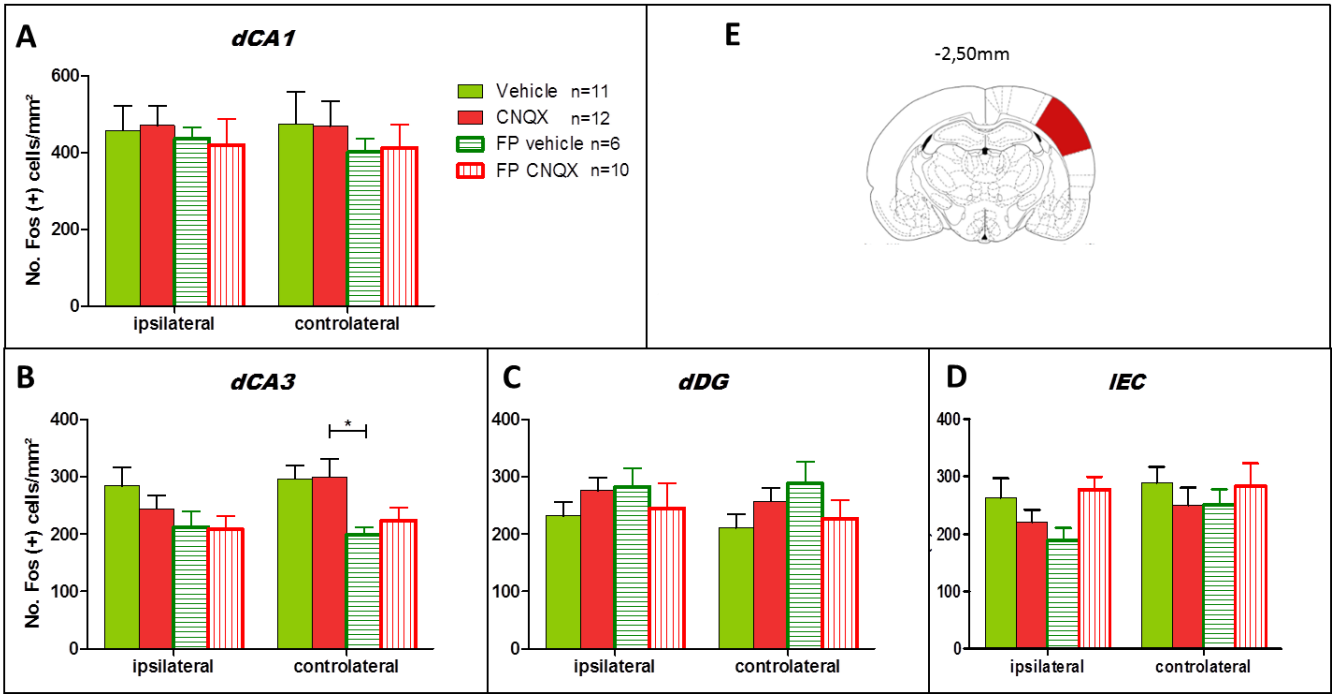


***Figure 68. SS1 inactivation did not reduce Fos protein expression following STFP task 7 days after CNQX injection. (A)*** *Two-way ANOVA did not show any differences between groups in Fos protein expression in the dorsal CA1 ($F_{3,70}$=0.399; p>0.05).* ***(B)*** *Two-way ANOVA revealed difference between CNQX experimental rats and FP vehicle rats but did not show any differences between other groups in Fos protein expression in the dorsal CA3 ($F_{3,70}$=4.401; p<0.01).* ***(C)*** *Two-way ANOVA did not show any differences between groups in Fos protein expression in the dorsal DG ($F_{3,70}$=1.671; p>0.05).* ***(D)*** *Two-way ANOVA did not show any differences between groups in Fos protein expression in the lEC ($F_{3,70}$=1.742; p>0.05).* ***(E)*** *Schematic brain coronal section representation of SS1 inactivated (red).*

## 4. Discussion

The pharmacological inactivation of the somatosensory cortex was developed to mimic the hippocampal hypoactivation and the memory deficits observed in the dMCAO model. SS1 inactivation induced hypoactivation of hippocampus and hyperactivation of the parahippocampal region after spatial exploration but not after associative memory task as STFP test. It should be interesting to analyze Fos protein expression after the interaction day of the STFP task followed by the SS1 inactivation. Brain slides from this experiment have been stained and analysis is ongoing. Interestingly, it was shown that the HPC contributes to the acquisition but is unnecessary for retrieval of the engram 1 week or 5 days following acquisition for STFP recall (Winocur, 1990; Winocur et al., 2001; Smith et al., 2007). Moreover, Fos expression was increased in the lateral entorhinal cortex following acquisition (Ross and Eichenbaum, 2006) as expected given the connectivity of this structure with olfactory association cortices (Burwell and Amaral, 1998). In our paradigm, we would expect that the hippocampus is engaged during the acquisition and the retrieval task highlighted by an increase of the Fos expression as reported before (Lesburgueres et al., 2011).

Our odor discrimination task indicated that olfaction was not impaired because of the inactivation of the SS1 cortex which processes inputs from the whiskers (Woolsey and Van der Loos, 1970). Memory impairments were similar after inactivation of either the ipsilateral hippocampus or the ipsilateral SS1. We can suggest that SS1 inactivation impaired predominantly information processing in the unilateral hippocampus via diaschisis and due to the connectivity between associative cortex and hippocampus (Lavenex and Amaral, 2000). Moreover, the contralateral hippocampus can, at least in part, counteract this impairment since rats with bilateral hippocampal inactivations are more severely impaired. According to literature, inactivation of one side of the hippocampus is not sufficient to induce memory impairment in a passive avoidance task or in a water maze task suggesting that contralateral side of the hippocampus counteract the deleterious effect (Fenton and Bures, 1993; Cimadevilla et al., 2007). This was not the case in our STFP task wherein only unilateral inactivation upon encoding of the hippocampus was sufficient to partly impaired memory performance upon retrieval. Another study reported that unilateral hippocampus inactivation increases electrical stimulation of the contralateral hypothalamus (Zimmermann et al., 1997) suggesting the same mechanisms of diaschisis by altering a remote structure of the infarcted area. The inactivation of the SS1 led to impairment in the STFP test comparable to that observed in dMCAO rats. Our set of **anatomical disconnection procedures** targeting either

the hippocampus or the somatosensory cortex provided converging evidence in favor of a hippocampal diaschisis phenomenon responsible, at least in part, of the memory deficits induced by focal ischemia which target preferentially the cortex. In addition to diaschisis, the memory deficits observed after dMCAO could be due, at least in part, to permanent damage and cell loss, or ongoing apoptosis, throughout the ischemic core and penumbra. Our inactivation approach, which only induced minimal cell damage, enabled to isolate this potential contributing factor. Hippocampal diaschisis occurred independently of permanent cell loss, further strengthening that distant regions, namely the hippocampus, is primarily responsible for ischemia-induced cognitive dysfunctions. By combining imaging of neuronal activity to region-specific pharmacological inactivation, we also identified the parahippocampal region which acts as a crucial gateway for information exchange between cortical areas and the hippocampus. As the hippocampus is a bilateral structure, the information can be process either by the unilateral or the contralateral side, leading to a mild memory impairment if only one side of the hippocampus is deleterious following the diaschisis. Taken together, our findings support the concept that hippocampal hypoactivation is the consequence of a reduced source of cortical information (i.e. deactivation).The following part III dealing about the hippocampal activity in anesthetized rats following stroke or SS1 inactivation could explore the diaschisis phenomenon in vivo.

# Part III : Exploring the impact of focal cerebral ischemia on hippocampal activity: effects on theta rhythm and sharp-wave ripples

## 1. Introduction

In stroke studies, it has been unclear whether the post-stroke cognitive impairment associated with ischemia induced by middle cerebral artery occlusion is due to hippocampal dysfunction. However, we provide evidence in chapter 1 that our model (distal MCAO) spares the integrity of hippocampus while impairing the functionality of this remote structure via a hippocampal diaschisis phenomenon. Because electrical activity measured by electroencephalography (EEG) is widely used to diagnose potential impairment for clinical purposes (Acar et al., 2007), we aimed to study brain activity in stroke condition by means of the probe insertion technique that allow to record deeper structure of the brain such as the hippocampus. We focused our study on the theta frequency band (3-7 Hz) because this frequency is modified in humans and animals submitted to cognitive challenges. For example, hippocampal theta is associated with memory function (Hasselmo, 2005) as theta power increases during cognitive tasks as well as during verbal and spatial tasks due to an increase in memory load in humans (Burgess and Gruzelier, 2000; Krause et al., 2000; Kahana et al., 2001). In the rat hippocampus, theta state occurs during walking, running, rearing and exploratory sniffing as well as during REM sleep (Vanderwolf, 1968; Kahana et al., 2001; Buzsaki, 2002; Harris and Thiele, 2011). Hippocampal theta is associated with stimuli in working memory but not with reference memory (Kahana et al., 2001), thus it could be a tag for short-term memory (Vertes, 2005). Additional evidence also suggests that hippocampal theta is associated with spontaneous movements in monkeys (7-9 Hz) (Stewart and Fox, 1991) and locomotion in rodents (Vanderwolf, 1968). Compared to hippocampal theta, the role of cortical theta is less clear. At least in cats, this rhythm is associated with task orientation during coordinated response indicating its role in alertness, arousal or readiness to process information (Basar et al., 2001). EEG changes were reported in a review dealing with focal cerebral ischemia in rodents (Moyanova and Dijkhuizen, 2014). Slow oscillations such as delta wave increase and high oscillations such as alpha, gamma, beta waves decrease after stroke. Theta frequency seems also to be decreased after stroke. For these reasons, we investigated the hippocampal theta frequency during occlusion and after stroke in dMCAO model and after SS1 inactivation in our pharmacological model.

We also investigated special activity events specific to the pyramidal layer of the CA1 (hippocampus), the SWRs. SWRs are 100-200 Hz field oscillations with duration of less than one second, present during awake immobility and slow-wave sleep in rat hippocampus and

EC (Bragin et al., 2010). SWRs play a critical role in the formation and subsequent stabilization of enduring memories at the cortical level during the course of systems-level memory consolidation, their selective elimination during post-learning sleep resulting in impairment of long-term memory (Girardeau et al., 2009; Jadhav et al., 2012). To what extent occurrence of SWRs is affected by stroke is unknown. To fill up this void, we analyzed their pattern of expression during dMCAO and after SS1 inactivation with CNQX in rats.

## 2. Materials & Methods

### 2.1. Animals

All the electrophysiology experiments were conducted with adult male Sprague-Dawley rats (9 weeks of age, 250-300 g) from Charles River Laboratories (Wilmington, MA). Upon arrival in the animal facility, rats were habituated to their new housing conditions for a minimum of 1 week (2 rats per cage) Each rat undergo a 2-day handling procedure in order to habituate it to the experimenter and to minimize as much as possible stress responses which would interfered with electrophysiology recordings. This procedure lasted about 5 min per day and consisted in removing the rat from its cage and holding it in the experimenter's hands until the rat feels comfortable. Rats then underwent electrophysiology surgery (ischemia or intracerebral CNQX injection) as described in the following sections. For chronic stroke rat, electrophysiology recordings were made 4 weeks after the dMCAO surgery. Animals were kept on a 12:12 h light-dark cycle and experiments were conducted during the light phase of the cycle

### 2.2. Groups

Electrophysiology recordings were performed on 4 groups: chronic dMCAO animals (2-4 weeks), acute dMCAO animals, CNQX injection into SS1 cortex (1µL, 6mM) and CNQX injection into SS1 cortex (3µL, 6mM). Timeline of each procedure is described below (**Fig. 69-71**).

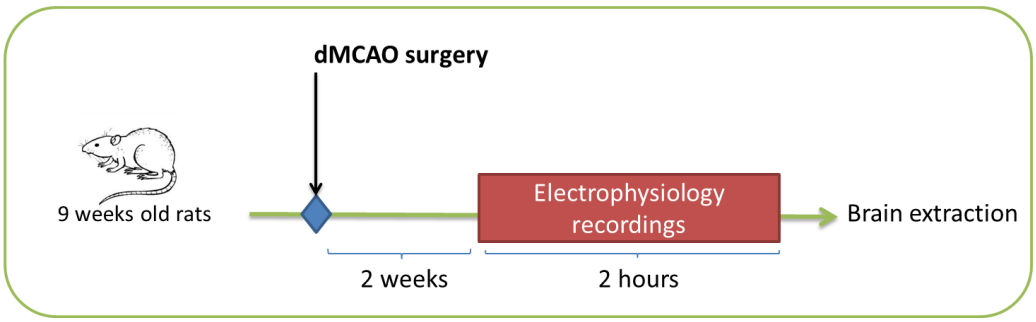


***Figure 69. Timeline of electrophysiological recordings in chronic dMCAO rats.*** *Rats underwent dMCAO surgery 2 weeks before the electrophysiology recordings. Brain electrical activity was recorded during 2 hours, then rats were euthanized and brains were extracted.*

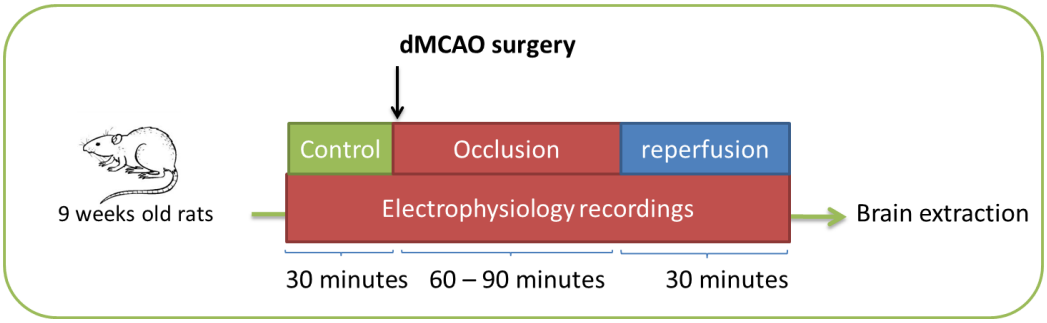


***Figure 70. Timeline of electrophysiological recordings in acute dMCAO rats.*** *Brain electrical activity was recorded for 30 minutes prior to the onset of ischemia. dMCAO surgery was performed and activity was recorded upon occlusion (60-90 minutes). After the occlusion period, brain activity was recorded for 30 minutes (reperfusion), then rats were euthanized and brains were extracted.*

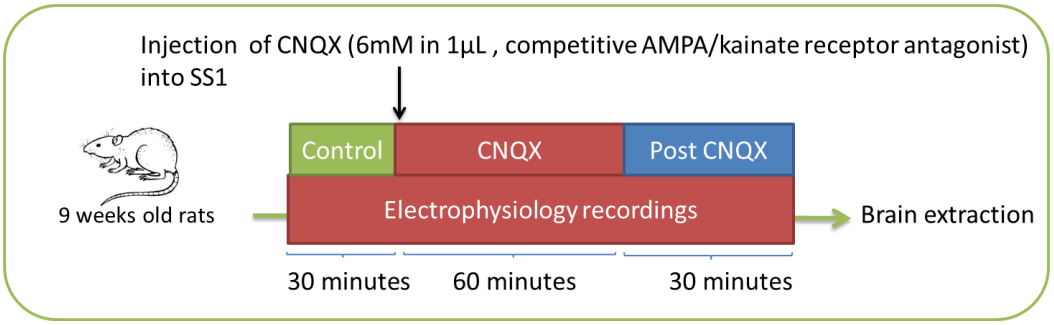


***Figure 71. Timeline of CNQX inactivation into SS1 rats.*** *After 30 minutes of control recording , 1µL of CNQX was injected into SS1 cortex and electrical brain activity was recorded during 90 minutes. Then, rats were euthanized and brains were extracted.*

### 2.3. Anesthesia and analgesia

Anesthesia was induced with 4% isoflurane in the induction chamber and maintained with 1.5% isoflurane in 30% O2 / 70% N2O using a face mask. The rectal temperature was monitored and maintained at 37°C with a thermal blanket throughout the surgical procedure and recording. Prior to skin incision, 0.2 cc of 0.25% bupivacaine was injected subcutaneously locally. After initial induction with isoflurane, animals was taken out of the

induction chamber, and urethane (5 ml/kg from a 30% urethane solution, equivalent to 15 mg/kg) was administrated via i.p. in a titrate-to-effect fashion over 5 min.

### 2.4. Electrophysiological recording

Electrophysiological recordings were performed using multisite extracellular silicon probes (NeuroNexus Technologies) in anesthetized rats. For recording under anesthesia, rats were anesthetized with urethane (Sigma, 15 mg/kg; i.p.) and were positioned in a stereotaxic frame (Kopf). A midline incision was made on the scalp to expose the skull. One or two burr holes were made over the somatosensory cortex (AP: -2.5 mm; AP: ±4.8 mm to Bregma), or the hippocampus (AP: -3.3 mm; ML: ±2 mm to Bregma) either unilaterally or bilaterally. One or two NeuroNexus silicon probes (16 channels; spacing: 100 microns) were inserted vertically to target the CA1, and then slowly inserted into the brain after the dura mater was resected. Real-time data display and an audio aid were used to determine recording depth while lowering electrodes until both the pyramidal and hippocampal fissure (at least 500 μm below the pyramidal layer) were recorded (**Fig. 72**). Continuous recordings lasted for up to 4 hrs depending on signal quality and the nature of manipulation (CNQX injection or stroke), but usually for 2.5 hrs. Full-spectrum electrical activity at the region of interest was recorded at a sampling rate of 32K Hz after band-pass filtering (0.1-9K Hz) with an input range of ± 3 mV (Digital Lynx SX, Neuralynx, USA). Recordings were at various depths corresponding successively to neocortex and layer CA1 of dorsal hippocampus.

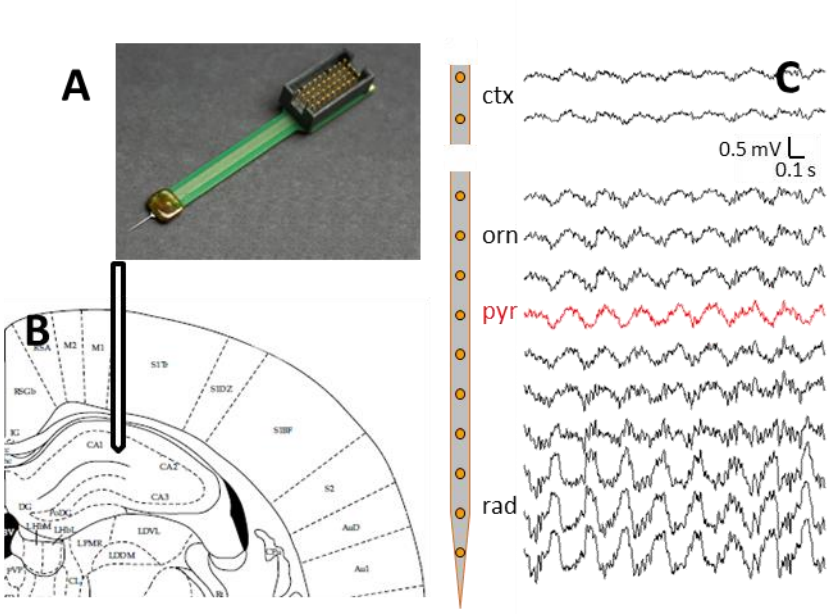


***Figure 72. Location of the silicon probe into the brain and example of recordings. (A)*** *Photograph of a 16 channel silicon probe (Neuronexus).* ***(B)*** *Location of the silicon probe to record cortical and hippocampal activity.* ***(C)*** *Example of electrophysiological activity recorded on each channel. Ctx: cortex layers, orn: oriens layer, pyr: CA1 pyramidal layer, rad: radiatum layer.*

### 2.5. Cortical inactivation with CNQX

Injection occurred simultaneously during the electrophysiological recording. After probe insertion, a micropipette (Drummond capillary glass: outside diameter 1.14mm) was inserted at a depth of 800 um in the somatosensory cortex (AP: -2.5 mm; AP: ±4.8 mm to Bregma). The micropipette was filled with 6 mM CNQX. After the 30 minutes recording for control, 1 µL of CNQX were injected into the somatosensory cortex with a Nanoject II Auto-injector. Micropipette stayed in place until the end of the recording. Brain activity was recorded during 90 min after injection.

### 2.6. dMCAO surgery during electrophysiology recordings

After 30 minutes of control recording, rats were removed from the stereotaxic frame and the recording system to undergo the dMCAO surgery described in the Materials & Methods of the part I. Then, when rats were still occluded, they were replaced in the stereotaxic frame and probes were reinserted at the previous length to record cerebral activity during the stroke period (60 to 90 minutes). During reperfusion, rats stayed on the frame and clamps were removed from CCAs. Recordings continued for 30 minutes.

### 2.7. Euthanasia and tissue preparation

Rats were terminally anesthetized with lethal injection of pentobarbital (300 mg/kg i.p.) and perfused transcardially with 0.9% saline and 4% PFA in 0.1M PBS, pH 7.4. Euthanasia was induced right after electrophysiological recordings. After decapitation, brains were removed and fixed overnight in 4% PFA-PBS and placed in 30% sucrose for 48 hours. Fifty µm coronal sections were cut on a microtome and collected serially in 4 section packs in 0.02% azide solution with 0.1M PB, pH 7.4. Brain sections were conserved in the fridge at 4°C.

### 2.8. Analyses

The recording channels of the CA1 pyramidal layer and the hippocampal fissure were determined manually based on the distinct electrophysiological features by using an off-line software program (Neuroscope, GNU). In particular, within the CA1, only the pyramidal layer showed robust unit activity, sharp waves and ripples, and theta amplitude peaks around the hippocampal fissure (Bragin et al., 1995b; Kamondi et al., 1998). More recent literature (using similar methods like ours) locate the maximal theta amplitude at the stratum lacunosum-moleculare layer in CA1 (Scheffer-Teixeira et al., 2012; Shinohara et al., 2013). Therefore, we used the CA1 stratum lacunosum-moleculare layer (lm) when referring to our hippocampal fissure recordings. The cortical channel was defined as the channel 800 µm above the CA1 pyramidal layer channel. To quantify LFP, raw recording was down-sampled to 1250 Hz, and then a Fourier transformation was used to compute time spectrogram at 5-sec resolution (50% overlap) using Chronux Toolbox (Medametrics, USA) in Matlab (MathWorks, USA). To investigate specific aspects of LFP changes associated with stroke and their relationship with brain states (i.e., theta and non-theta periods), several variables were computed as following. The theta-to-delta ratio (T/D ratio; in logarithm) was defined as the theta amplitude (the maximum between 3-7 Hz) divided by the delta amplitude (median between 0-2.5 Hz). To reduce noise, a smoothing process was applied to T/D ratio (Matlab). It is noteworthy that the exact frequency bands for computing delta and theta power (or amplitude) as well as T/D ratio varied slightly among studies (Csicsvari et al., 1999a; Barth and Mody, 2011; Del Pino et al., 2013). Since our mean theta frequency was around 3.8 Hz, an ad hoc theta frequency cut-off was set at 3 rather than 4 Hz, and accordingly, an ad hoc delta frequency cut-off was set at 2.5 Hz to avoid frequency leakage. The theta frequency was the frequency where theta amplitude peaks in theta period (theta amplitude > 0.12 mV or log

theta amplitude > -.91). To measure the network shift in time, the peak-to-peak phase (180 degree) duration were measured to estimate period. Every 5 seconds, the median peak-to-peak phase duration was defined as the period in degree (°) (**Fig. 73**). For statistical analysis in dMCAO conditions, each variable was binned to 10-min blocks with or without control for theta period. The change of theta frequency was defined as the standard deviation of theta frequency in each 10-min block. For statistical analysis in CNQX conditions, each variable was binned to 15-min blocks.

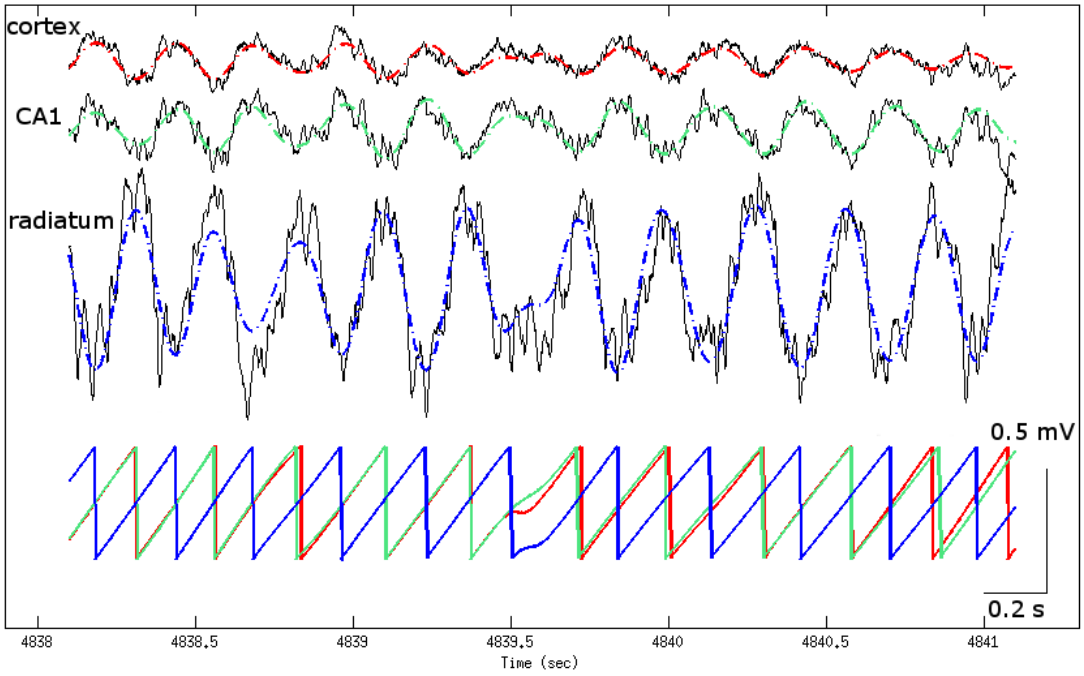


***Figure 73. Sample of electrical tracing during theta period.*** *The three tops traces represent the cortex layer, CA1 hippocampus layer and radiatum layer respectively during baseline recording. The bottom schema represents the periodicity of the theta frequency for each layer. Theta shift between cortical and CA1 layer is bigger between 4839.5 and 4840 seconds.*

SWRs were detected and analyzed only during non-theta period, i.e when delta frequency is 0.5 Hz-2.5 Hz. First, ripples were manually detected and tagged on CA1 pyramidal layer with Neuroscope software. Then, tags were imported in Matlab software to be analyzed automatically with the following parameters: lowpass filter 110Hz, highpass filter 200Hz, threshold amplitude detection (4 times baseline SD in mV) (Ylinen et al., 1995). Average of SWRs occurrence was examined between baseline and stroke/CNQX inactivation. Occurrence of SWRs was calculated using the following formula: numbers of SWRs / time of delta period (s).

### 2.9. Statistical analyses.

Normal distributions were tested with Kolmogorov–Smirnoff tests. For normal distributed data sets, one-way within-subject analysis of variance (ANOVA) was used to assess an acute-ischemia effect, a stroke effect, or a CNQX effect for each variable in dMCAO groups and CNQX groups, respectively. Post hoc multiple comparisons after error correction were used to characterize the temporal profile if necessary. If ANOVAs did not reveal any differences, t-test was used to compare ischemia or CNQX effect with baseline only. For non-normal distributed data sets, nonparametric paired tests were applied: Friedman test for multiple comparisons, post hoc Dunn's Multiple Comparison test and Wilcoxon signed rank test for double comparisons of paired samples. The alpha level was set at 0.05. All statistical analyses were performed using GraphPad Prism version 5.00 for Windows.

## 3. Results

### 3.1. Hippocampal theta frequency changes during and following acute distal focal ischemia

First, we determined the most adapted channel offering the best signal-to-noise ratio to explore potential changes in hippocampal theta frequency. The pyramidal layer of the CA1 is the most studied layer because of its special high frequency SWRs. However, this anatomical region is not the most suitable for analyzing low frequencies such as theta rhythm due to events creating noise in the signal. For this reason, the lm layer in CA1 is typically used in the literature because it presents the maximal theta amplitude (Scheffer-Teixeira et al., 2012; Shinohara et al., 2013). Therefore, we used the channel located 400-600 µm below the pyramidal layer corresponding to the lm layer. As expected, we obtained the best signal-to-noise ratio during theta period (**Fig. 74**).

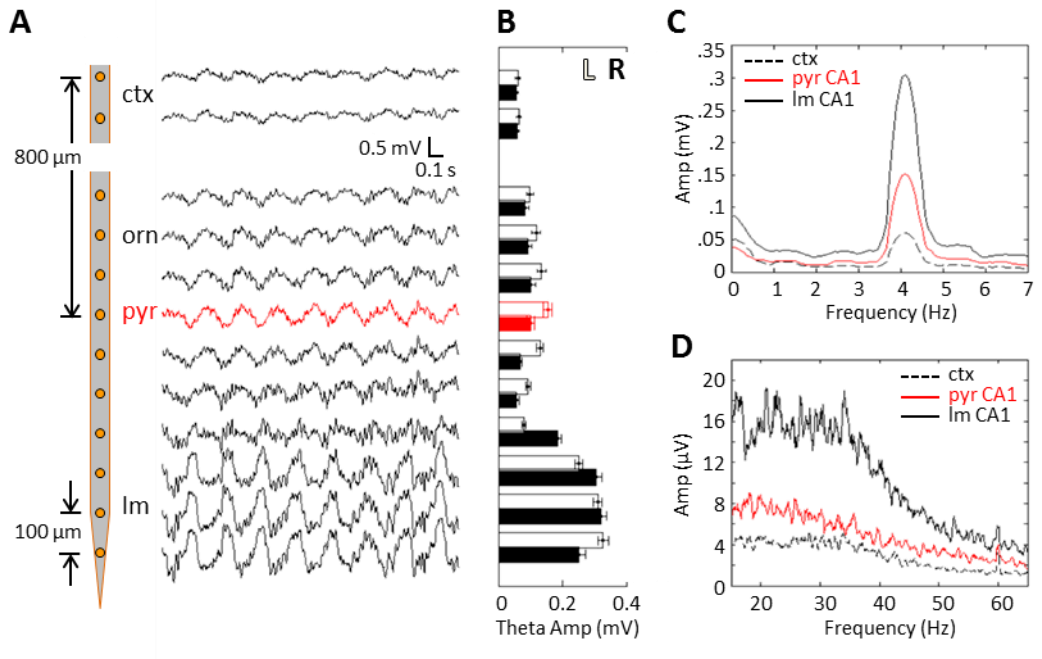


***Figure 74. Lacunosum-moleculare layer has the best signal-to-noise ratio during theta period. (A)*** *A sample of 2-sec multichannel recording using a 16-channel NeuroNexus probe (left) is shown during baseline in dMCAO rats prior to occlusion. Top two traces are in the cortex and bottom traces are in the hippocampal CA1. Red: pyramidal layer (pyr) of CA1, ctx : cortex layer, lm : lacunosum-moleculare layer.* ***(B)*** *In the frequency domain, theta- (max between 3 and 7 Hz) amplitude for each channel was computed using a 10-sec sliding window (50% overlap) for 1 min. Black and white bars: simultaneous bilateral recordings from the same animal (mean ± SD).* ***(C-D)*** *Mean spectrograms of the pyramidal layer channel (red), a cortical channel (dotted), and a lacunosum-moleculare layer channel (solid). Typically, our lm channels used for analysis were 400-600 µm below the pyramidal layer.*

Following occlusion of the MCA, the theta frequency decreased and progressively came back to the baseline level when the artery was reperfused. In parallel, the delta power seemed decreased after occlusion and the T/D ratio was lower (**Fig. 75**). Statistically, this visual theta changes were confirmed as shown in **Figure 76** (**C-D**). Indeed, 60-90 minutes after the beginning of recording, that is 30-60 minutes after the beginning of dMCAO, both ipsilateral and contralateral theta frequencies decreased compared to sham-control rats. These changes were still observable during the reperfusion period but their magnitude was smaller. Moreover, the amplitude of theta frequency decreased during dMCAO in the hemisphere ipsilateral to the infacted side. These observed theta changes were not coupled with a significant diminution of the delta power, however the T/D ratio decreased during occlusion and reperfusion periods (**Fig. 76 A-B**).

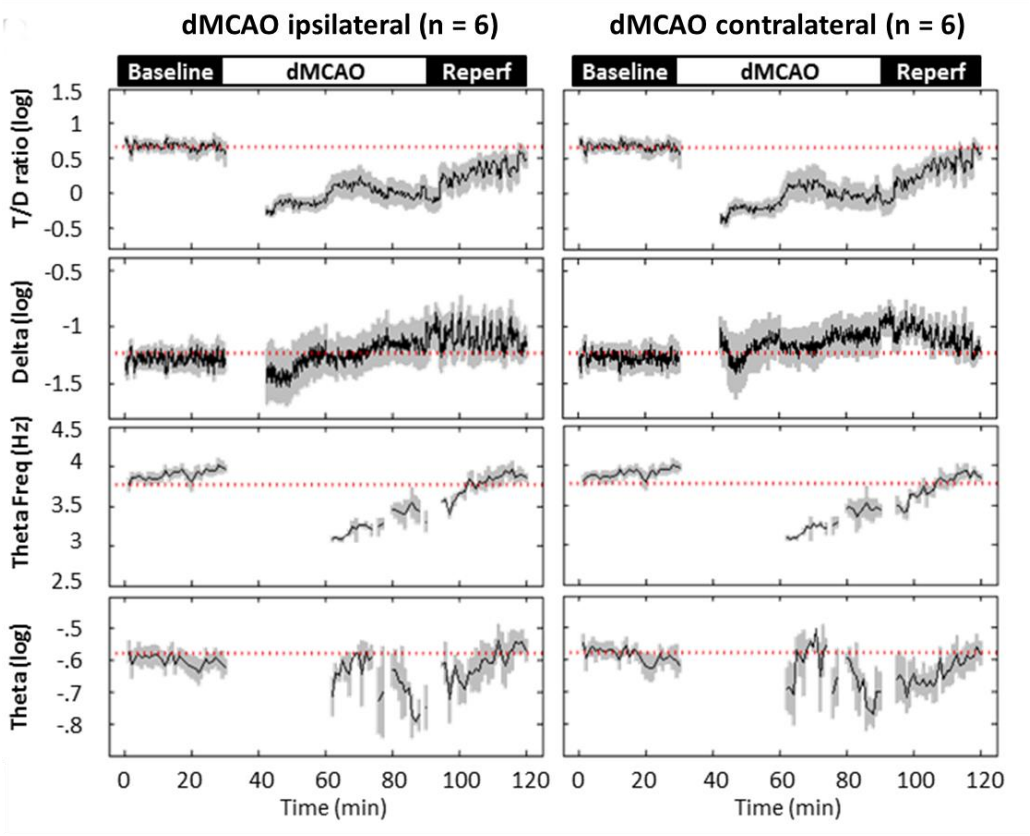


***Figure 75. The hippocampal response to an acute cortical stroke.*** *From top to bottom: 2-hr time series of theta/delta ratio (T/D ratio), delta, theta frequency and theta in ipsilateral and contralateral sides of dMCAO rats. Red dotted lines: average of 2-hr recording from sham-controls (n = 8). Black lines: mean. Grey bars: SEM. Note that the first couple of minutes of recording after dMCAO induction are missing due to surgery. Also, theta frequency and amplitude were not available in the presence of strong delta (max amplitude between 3-7 Hz less than 0.12 mV, -.91 in logarithm).*

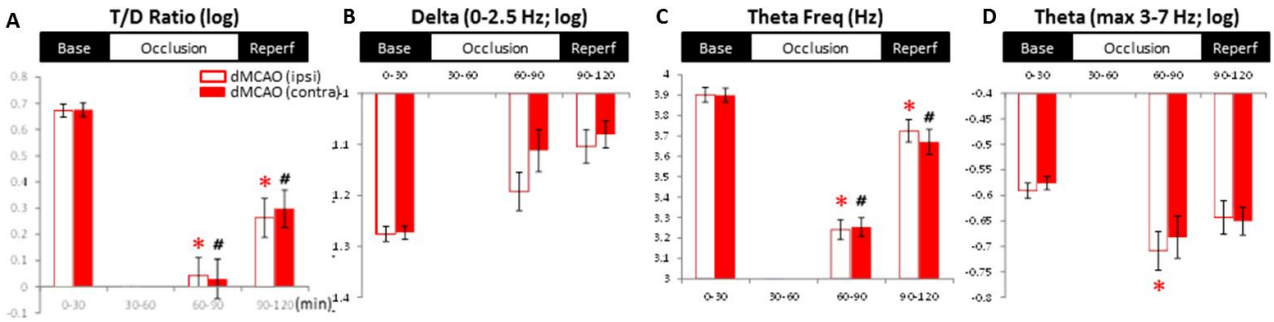


***Figure 76. Theta frequency decreases during distal focal ischemia.*** *Statistics on the bilateral T/D ratio, delta and theta (white: ipsilateral; red: contralateral to dMCAO). Each variable was first binned every 10 min (up to 12 samples per rat) and then grouped into four time levels: baseline (0-30 min), 1st 30-min occlusion (30-60 min), 2nd 30-min occlusion (60-90 min), and the subsequent reperfusion of CCA (90-120 min). Due to the missing data, only three time levels were used to balance the design.* ***(A)*** *T/D ratio decreased after occlusion and during reperfusion compared to baseline in ipsilateral side ($F_{2,10}$ = 13.774; p<0.001) and contralateral side ($F_{2,10}$ = 15.535; p<0.001).* ***(B)*** *There was no significant change of delta power after occlusion (ipsilateral, $F_{2,10}$= 1.865; p>0.05; contralateral $F_{2,10}$= 2.78; p>0.05). * p < 0.05 compared to ipsilateral baseline, # p < 0.05 compared to contralateral baseline.* ***(C)*** *Theta frequency decreased during occlusion and reperfusion in both*

*sides (ipsilateral, $F_{2,7.5}$ = 28.056; p <0.001; contralateral, $F_{2,8}$ = 34.15; p < 0.001), but **(D)** Theta amplitude decreased just during occlusion in ipsilateral side ($F_{2,7.3}$= 4.963; p<0.05) but not in contralateral side ($F_{2,8}$= 2.003; p>0.05).*

### 3.2. Theta frequency is less stable two weeks after dMCAO

To further characterize theta changes, we recorded hippocampal activity in dMCAO rats which underwent stroke fourteen days earlier (D14 dMCAO). To reduce variability of the recorded signal, we used for our analysis either the ipsilateral or the contralateral side, depending on the best signal-to-noise ratio that could be obtained. Indeed, the ipsilateral or contralateral theta frequency signal was not significantly different in control or D14 dMCAO rats (**Fig. 77 A-B**).

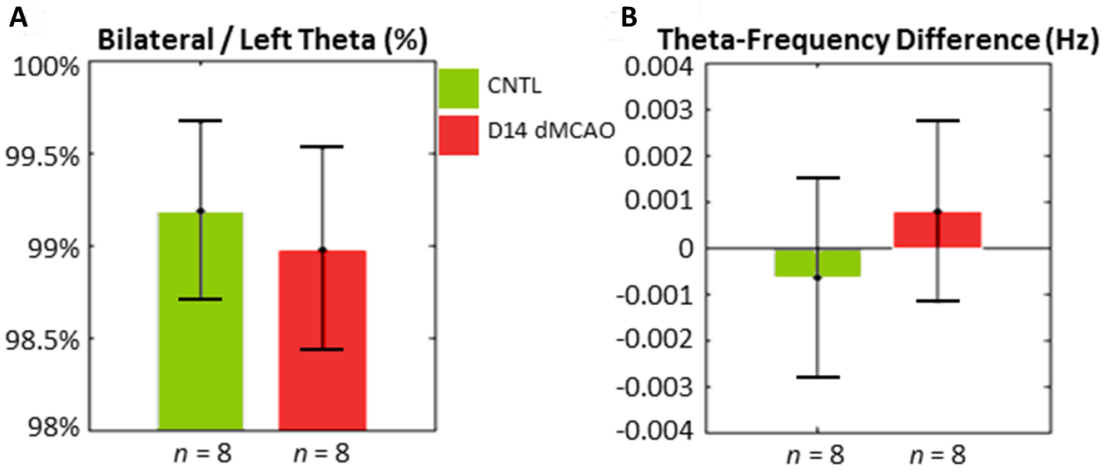


***Figure 77. No difference between the ipsilateral and contralateral hippocampal theta was observed.*** ***(A)*** *Averaged (2 hr) bilateral-theta percentage.* ***(B)*** *Averaged (2 hr) theta-frequency difference between hemispheres. 99% of our theta was bilateral (100% for strong theta); the bilateral theta had an equivalent frequency.*

Frequency or amplitude was not decreased compared to sham-controls, suggesting that theta oscillations were not impaired 14 days after dMCAO (**Fig. 79 A, C**). However, the dynamic of these oscillations seemed altered as shown in a 14D dMCAO rat (**Fig. 78**). This instability of the theta frequency over time was confirmed by the significant difference of the theta frequency change in 14D dMCAO rats compared to sham-control rats (**Fig. 79 B**). Note that the behavioral test was performed two weeks after stroke surgery as shown in these recordings.

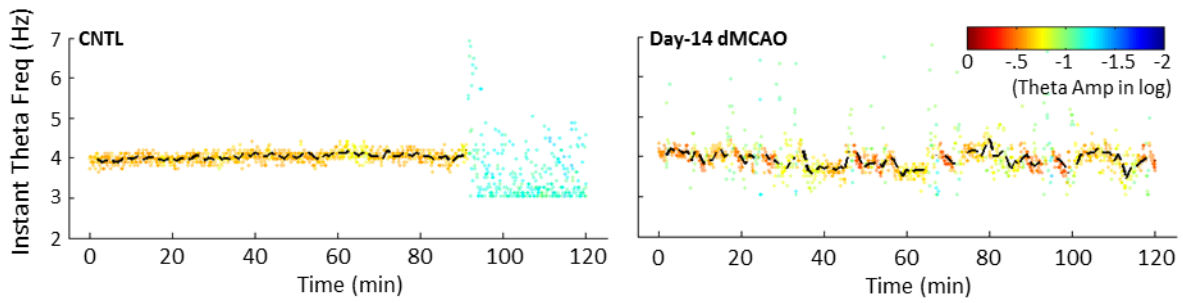


***Figure 78. Theta frequency is less stable 14 days after focal ischemia.*** *Representative time series of instant theta frequency from a sham-control (left), and a Day-14 dMCAO rat (right). Instant theta frequency: instant frequency (every 5 sec) between 3-7 Hz at which amplitude peaks. Color indicates amplitude at the instant theta frequency. Dotted lines: theta frequency, 1-min average instant theta frequency after thresholding instant theta amplitude (> 0.12 mV; -0.91 in logarithm).*

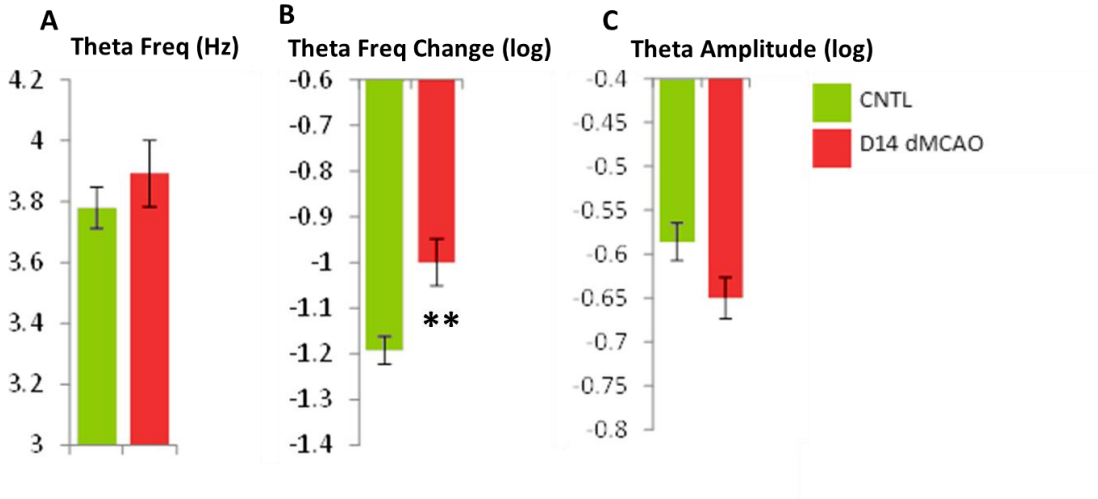


***Figure 79. Characterization of the hippocampal response to a chronic cortical-stroke.*** *Data were averaged over a 2-hr period after separating theta and non-theta periods in sham-control (n = 8) and Day-14 dMCAO (n = 9) rats. Only recordings contralateral to the infarcted side were used . Theta frequency change: average of 2 hour recordings (120 bins), standard deviation of theta frequency in 10-min bin.* ***(A)*** *There was no theta frequency difference between sham and D14 dMCAO groups ($t_{15}$=0.850, p>0.05).* ***(B)*** *Theta frequency was less stable 14 days after focal ischemia ($t_{15}$=3.128, p<0.01)* ***(C)*** *Theta amplitude did not vary between groups ($t_{15}$=1.993, p>0.05). **: p < 0.01 versus sham-controls.*

### 3.3. Hippocampal theta frequency is altered following SS1 inactivation

We found that hippocampal theta frequency was altered during acute focal ischemia as well as two weeks following stroke. We next examined whether this oscillation could be altered after inactivation of the SS1 with 1µL of CNQX injected into the hippocampus. Inactivation did not impair the frequency of theta oscillations. However, their amplitude decreased in the hippocampus during the first fifteen minutes following the inactivation.

However the change in theta frequency appeared more variable over time 60-75 minutes after the CNQX injection (**Fig. 80A-C**). When the coupling of the theta phase between hippocampus and parietal cortex was compared, we observed a shift in the theta phase 30-45 minutes after the SS1 inactivation highlighting a potential desynchronization between the two structures (**Fig. 81**).

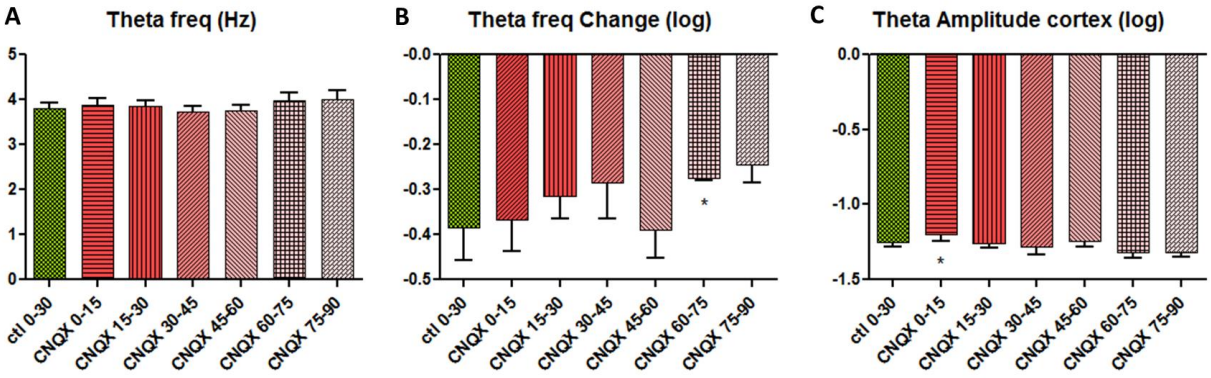


***Figure 80. The hippocampal theta frequency was more variable after SS1 inactivation.*** *(A) There was no theta frequency differences after SS1 inactivation ($F_{6,37}$=0.439, p>0.05). (B) Theta frequency was less stable 60-75 minutes after CNQX injection compared to vehicle-injected rats ($F_{6,37}$=0.622, p>0.05, $t_2$=3.028). (C) Cortical theta amplitude decreased 15 minutes following CNQX injection ($F_{6,37}$=0.798, p>0.05, $t_4$=2.360). * p<0.05 versus controls; n=3-7 values/groups obtained from 7 animals.*

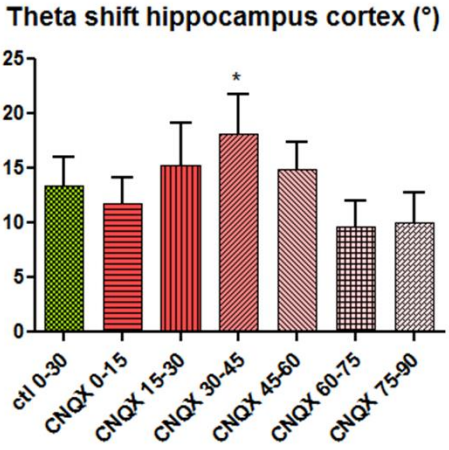


***Figure 81. The shift between the hippocampal theta and the cortical theta frequencies increased after SS1 inactivation.*** *The theta shift increased 30-45 minutes after CNQX injection between the oriens layer of CA1 and the cortical layer of somatosensory cortex (SS1) ($F_{6,37}$=0.793, p>0.05, $t_6$=2.997). * p<0.05; n=3-7values/groups obtained from 7 animals.*

### 3.4. Sharp-waves ripples are altered following acute ischemia

SWRs are high frequency oscillation events occurring during slow-wave sleep which are associated with learning (Girardeau et al., 2014), we investigated potential changes in duration, amplitude or occurrence of SWRs during dMCAO surgery. We observed that the occurrence of SWRs increased during the reperfusion period compared to controls (**Fig. 82**).

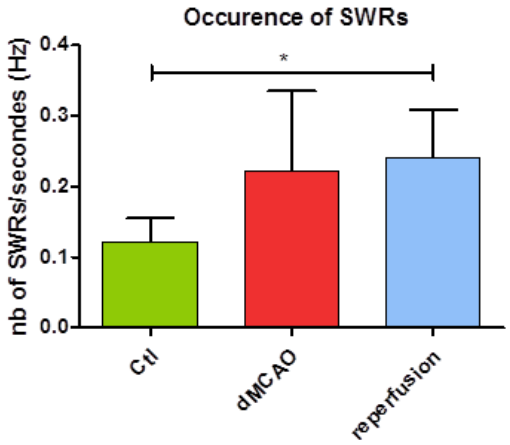


***Figure 82. Occurrence of SWRs increased during the reperfusion of the MCA.*** *The occurrence of ripples increased during the reperfusion compared to baseline ($\chi^2(2) = 6.000$, $p<0.05$). * $p<0.05$; n=7values/groups.*

### 3.5. Inactivation of SS1 reduced the occurrence of SWRs

We inactivated the SS1 cortex with CNQX in order to inactivate the neuronal activity mimicking the neuronal death occurring during dMCAO. The occurrence of SWRs was not significantly impaired when we analyzed the three groups together, but Wilcoxon test showed a significant diminution when control and CNQX 0-60 min groups were compared (**Fig. 83**).

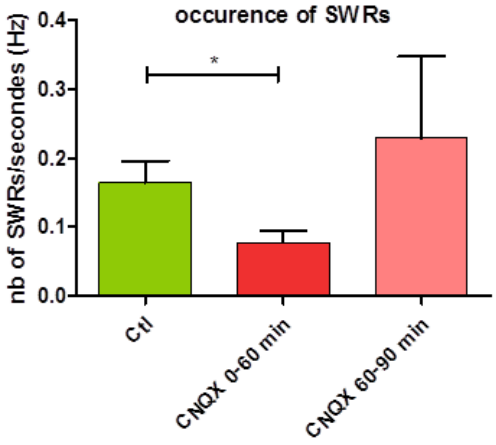


***Figure 83. Occurrence of SWRs decreased within the first hour of SS1 inactivation.*** *Wilcoxon matched pairs test reveal a significant difference after CNQX inactivation compared to control ($p<0.05$). * $p<0.05$; n=6values/groups.*

## 4. Discussion

We observed that focal ischemia induced theta frequency diminution in acute stroke which persisted following reperfusion. Two weeks after stroke, this diminution was not observed anymore but the theta frequency was less stable over time, just like the SS1 inactivation induced one hour following the CNQX injection, suggesting a desynchronization of the oscillation within neuronal networks (Colgin, 2011). The theta frequency diminution was not associated with an increase of the delta power, however the T/D ratio was lower. Usually, an increase in delta power in the ipsilateral hemisphere after transient MCAO is observed during stroke close to the infarct territory (Lu et al., 2001; Zhang et al., 2013; Moyanova and Dijkhuizen, 2014). An increase of the delta power and a decrease of the theta power in cortex and CA1 following 20 minutes of transient global ischemia in Wistar rats (Mariucci et al., 2003), as well as a decrease of the theta amplitude in CA1 following 20 minutes of global ischemia in rats have been reported (Monmaur et al., 1990). In healthy animal, it is known that frequency of the hippocampal theta varies with movement speed (Whishaw and Vanderwolf, 1973; Slawinska and Kasicki, 1998), visual novelty (Jeewajee et al., 2008), and nasal respiration (Yanovsky et al., 2014), suggesting that the time-varying property of theta frequency reflects a neural process at a network level (in need of communicating between brain regions particularly when the animal is engaged in cognitive performance). Another piece of evidence for the theta frequency being a manifestation of network activity is that frequency of the hippocampal theta in animal under anesthesia is much smaller than that in the awake state (Buzsaki, 2002). Here, in pathological conditions

where connections between the cortex and the hippocampus were experimentally disrupted (either by time-limited dMCAO or SS1 inactivation with CNQX), the hippocampal theta frequency seems also disrupted. This assumption is further supported by the shift of the theta phase between hippocampal theta and cortical theta (in the non infarcted area) which increased after SS1 inactivation. However, future investigation is needed to explore whether in stroke animal the theta shift between parietal cortex and hippocampus can be observed during acute stroke and can persist a few weeks after the onset. Also, it seems important to differentiate whether the theta frequency change underlies network re-wiring (neural plasticity) or atypical cognitive processes in a permanently disrupted network in learning conditions.

SWRs constitute the second parameter explored in this study because of their involvement in memory consolidation (Buzsaki, 1996; Girardeau et al., 2009). We found an increase in the occurrence of SWRs following reperfusion, whereas the inactivation of the SS1 was associated with a decrease of SWR occurrence. Interestingly, literature reports an increase of SWR during slow-wave sleep following an odor-learning association task (Eschenko et al., 2008) or radial maze task (Ramadan et al., 2009). Our stroke observations can be due to the cerebral blood flow (CBF) fluctuations. Indeed, the electrical brain activity is directly correlated with the CBF (Foreman and Claassen, 2012; O'Gorman et al., 2013). We can hypothesized that the hyperexcitability of the neuron induced by the 90 minutes of ischemia can be increased by the injury damage associated with the reperfusion (Hallenbeck and Dutka, 1990; Hammerman and Kaplan, 1998; Winship and Murphy, 2008). The cortical excitability by the phenomenon of diaschisis would lead to hippocampal hyperactivity. It would be interesting to explore the SWR pattern several weeks after stroke in order to observe if this hippocampal hyperactivation persists. The stroke-induced increase in SWRs can also be interpreted by a mechanism of defense in order to re-introduce the communication between the cortex and the hippocampus. Indeed, SWRs might be implicated in the “transfer” of labile memories from hippocampus to neocortex to stabilize information and consolidate the memory (Buzsaki, 1996). However SWRs occur during slow-wave sleep (SWS) and awake immobility in rat hippocampus (Buzsaki et al., 1992). During these periods, the delta power is dominant (Basar et al., 2001; Harris and Thiele, 2011). Interestingly, an increase of the delta power is associated with stroke (Lu et al., 2001; Zhang et al., 2013; Moyanova and Dijkhuizen, 2014) and the benefit of SWS in neuronal plasticity has been highlighted by several studies (Tononi and Cirelli, 2012, 2014), suggesting that the increase of SWRs

occurring during stroke might be helpful for neuronal plasticity.

The bias of the CBF reperfusion can be avoided by performing a CNQX inactivation of the SS1, thus stopping the synaptic activity between neurons due to the AMPA receptor antagonism action of the CNQX. We reported a decrease of the SWR occurrence during the first hour following the injection. The hippocampal hypoactivation is more in adequacy with the expected results which might occurred few weeks after stroke and the memory impairment observed after the deletion of SWR during post-learning sleep (Girardeau et al., 2009; Jadhav et al., 2012).

In conclusion, the hippocampal theta frequency and the SWR alteration following focal ischemia and SS1 inactivation located in the parietal cortex and sparing the hippocampus support our diaschisis hypothesis. The cortical impairment leads to a modification of the hippocampal activity, a structure distant from the infarcted area. In the general discussion chapter, we will further compare the alterations of hippocampal activity with the cognitive impairment observed in ischemic and SS1 inactivated rats.

# General Discussion

Ischemic stroke is the second cause of mortality and the first cause of handicap in industrialized countries (Donnan et al., 2008). About 30 % of patients exhibit cognitive deficits and dementia for within 1 year of the stroke onset (Dennis et al., 2000; Cullen et al., 2007; Barker-Collo et al., 2012). Stroke occurs most often in the MCA territory which supplies the parietal cortex but not the hippocampus located in the medial temporal lobe. Because the mechanisms underlying the observed ischemia-induced memory impairments, especially following an MCA stroke, are still unclear, we explored the anatomical pathways allowing the communication between the somatosensory cortex and the hippocampus. We found that dMCAO rats were cortically infarcted but no signs of hippocampal injury were observed. Still, we were able to provide evidence for memory deficits in these ischemic rats. In particular, the formation and stabilization of associative olfactory memory was impaired in the STFP task and spatial learning was slower during training in the Barnes maze. These results support previous studies that have reported spatial memory impairments following MCA stroke in rats (Dahlqvist et al., 2004; Zvejniece et al., 2012; Li et al., 2013). Moreover, hippocampus and lEC showed reduced functional activation in ischemic rats submitted to spatial exploration of a novel environment or spatial discrimination in the Barnes maze, supporting our hippocampal diaschisis hypothesis associated with stroke. To investigate the neural pathways involved in the post-stroke memory impairments, targeted pharmacological inactivations of the somatosensory cortex and the dorsal hippocampus were performed in rats before spatial exploration or associative memory testing. Just like for dMCAO rats, hypoactivation of the hippocampus occurred following spatial exploration of a novel environment in rats bearing inactivation of the somatosensory cortex, thus further supporting the contribution of a diaschisis phenomenon to the observed memory deficits. The hippocampal hypoactivation was not reproduced in rats with an inactivated parietal cortex following the retention test in the STFP task (7-day retention period). Ongoing Fos analyses explore neuronal activity in hippocampal and parahippocampal regions following social interaction (day of the somatosensory cortex inactivation), the period during which observer rats make the association between the flavored food eaten by the demonstrator and the fact that this particular food is without danger and therefore safe to eat. By injecting an anterograde neuronal tracer into the somatosensory cortex, we confirmed that this area is anatomically connected to the parahippocampal regions including the entorhinal cortex, a pivotal gateway between the hippocampus and the cortex for processing information bilaterally (inputs and outputs) (Burwell and Amaral, 1998; Canto et al., 2008). Following spatial exploration , the EC and connected structures such as parahippocampal and perirhinal

cortices of somatosensory cortex inactivated rats were hyperactivated whereas hippocampus was hypoactivated. Interestingly, this pattern was not reproduced in the stroke condition for the lateral entorhinal cortex (lEC). Indeed, dMCAO rats exploring a novel environment exhibited hypoactivation in the hippocampus as also observed after CNQX inactivation of the somatosensory cortex, but this stroke-induced hippocampal hypoactivaty was associated with lEC hypoactivation. These opposite patterns of activity in the lEC highlight the difference of our pharmacological inactivation of the parietal cortex compared to focal ischemia. Indeed, our ischemic model induces chronic impairment due to the permanent cortical infarct which could induce extensive brain plasticity changes and associated compensatory phenomena throughout the brain circuitry whereas the effects of pharmacological inactivations are reversible and acute in essence and thus less likely to induce a drastic reorganization of the brain connectivity. Also, the pharmacological inactivation is region-specific whereas the size of the infarcted zone in dMCAO rats is more extensive. Moreover, the ischemic infarct is not a uniform area but constituted of a core and a penumbra zone. While the former area is "electrically dead", the latter is impaired but still functional (Hossmann, 1994; Dirnagl et al., 1999). Following reperfusion, return of oxygen and glucose leads to an hyperexcitability of the neurons which can persist from one week to one month after the onset of ischemia (Schiene et al., 1996; Krnjevic, 2008; Winship and Murphy, 2008). This neuronal hyperexcitability could lead to a reorganization of the synaptic strength or neurotransmitter receptor density as previously reported in seizure models (Zhang et al., 2012; Lopes et al., 2013; Mollajew et al., 2013). Different mechanisms could take place leading to opposite activation of the entorhinal cortex. We can propose that inhibitory pathways connecting parietal cortex and EC are predominantly recruited in stroke condition because located in the penumbra area, thus leading to EC hypoactivation. In contrast the SS1 inactivation could suppress the inhibitory activity of this pathway inducing hyperactivation of the EC. Therefore, the entorhinal cortex would react depending on the excitability of cortical inputs (filter or amplifier) leading in fine to the hypoactivity of the hippocampus. How then an opposite neuronal activity of the EC (activation or inhibition) can lead to a similar reduction of hippocampal activity as revealed by Fos expression?

Homeostasis is a key feature of a healthy brain and neural hyperexcitability is known to be associated with pathological syndrome such as focal dystonia, epileptic seizure or auditory hallucinations (Hoffman and Cavus, 2002). For this reason, the potential hippocampal hyperexcitability highlighted by the increase of SWR occurrence following

acute focal ischemia and supported by c-fos induction a few hours after MCA occlusion in the hippocampus (Kinouchi et al., 1994; Kinouchi et al., 1999) might be reversed 2 weeks following the ischemic onset as the reduction of the c-fos expression we observe in the hippocampus suggests. This decrease of the hippocampal activity could occur via a downregulation of neuroreceptors inducing synaptic plasticity as a defense mechanism. We can suggest that a chronic cortical stimulation following ischemia might decrease the entorhinal activity by activating an inhibitory pathway. Then, the lack of inhibitory inputs from EC could induce 1) in acute condition, an increase of the hippocampal activity and 2) in chronic condition, a decrease of hippocampal activity. For example, hippocampal c-fos expression is decreased 40 days following lEC lesion and associated with a decrease of the AMPA receptor subunit (GLUR1) and an increase of NMDA receptor subunit (NR2B and NR1) density into the CA1 layer and DG respectively. The alteration of the expression and molecular organization of hippocampal glutamate receptors can be induced by the suppression of EC inputs (Kopniczky et al., 2005). Synaptic expression of AMPA receptor is also down-regulated after light-controlled excitation at individual synapse by homeostatic adjustment (Hou et al., 2011) suggesting that a high excitation can lead to a drastic down-regulation outside of the physiological range. In the pharmacological model, all this synaptic mechanism might not occur because of the ephemerality of the drug effect and because the inactivation induces inhibition of the cortical neurons instead of hyperexcitability. Overall, we can suggest that the diaschisis mechanism induced by the lesion or the inactivation of the SS1 which impairs the functional involvement of the hippocampus occurs via distant anatomical projections including those arising from the entorhinal cortex (**Fig. 84**). The ongoing Fos analyses after acquisition and retention of the STFP test in dMCAO rats and inactivated rats in the SS1 should bring further explanations.

The electrophysiological exploration of the hippocampus enabled us to provide some novel insights into the hippocampal diaschisis mechanism occurring in dMCAO rats and SS1 inactivated rats, even if we have to keep in mind that our recordings were obtained from anesthetized animals and not from awake animals actively engaged in a memory task. We found that the theta oscillation which is a brain wave associated with cognitive, attentional and memory behavior (Burgess and Gruzelier, 2000; Kahana et al., 2001; Buzsaki, 2002) was impaired during acute ischemia and fourteen days following its onset. Moreover, this brain oscillation modulates synaptic plasticity (Holscher et al., 1997) and memory functions in the cortex (Winson, 1978; Macrides et al., 1982; Givens and Olton, 1990; Vertes, 2005; Rizzuto et

al., 2006). This impairment of theta oscillations was also observed in SS1 inactivated rats. The stability of the hippocampal theta frequency seemed particularly impaired after focal ischemia. The theta oscillation is a wave travelling throughout the hippocampus (Lubenov and Siapas, 2009; Patel et al., 2012; Zhang and Jacobs, 2015) and seems to entrain cortical gamma rhythm. The firing of cortical neurons located in sensory and associative areas of parietal (Sirota et al., 2008) or prefrontal cortices (Siapas et al., 2005; Bitzenhofer et al., 2015) are also synchronized with the theta rhythm. Moreover, it was reported that hippocampal theta loss after electrolytic lesions of the medial septal nucleus (generator of theta rhythm) in rats is associated with spatial memory deficit (Winson, 1978). Altogether, the theta shift between the cortex and the hippocampus observed following SS1 inactivation and the variability of the theta frequency dynamics observed 2 weeks after stroke could contribute, at least in part, to the impaired memory profile of our dMCAO rats. If we make the assumption that this theta impairment is also present in an awake rat, we can hypothesized that the cognitive impairment observed in STFP task is due, at least in part, to a perturbation of the communication between the cortex and the hippocampus. Thus, the lack of stability of the theta frequency might be a neural supports of the diaschisis.

We found that dMCAO rats exhibited anterograde amnesia in the STFP task, a memory profile pointing to an inability to form and stabilize, or retrieve, long-lasting memories. At the neuronal level, we also observed dysfunctional patterns of post-ischemia hippocampal SWRs in anesthetized rats recorded during and after the onset of focal ischemia. Post-learning hippocampal SWRs generated during slow wave sleep are thought to play a crucial role in memory formation. Accordingly, when disrupted experimentally, abnormal SWR signatures lead to impaired spatial learning (Ego-Stengel and Wilson, 2010; Girardeau and Zugaro, 2011; Girardeau et al., 2014). At the mechanistic level, memory reactivation is considered as the core iterative mechanism in contemporary consolidation models. Hippocampal cells that were co-active during a cognitive challenge exhibit correlated firing patterns during slow-wave sleep, revealing a replay mechanism. Importantly, hippocampal replay retains the original temporal order, and occurs preferentially during the occurrence of SWRs (Frankland and Bontempi, 2005), thus conferring to these specific offline oscillations a privileged role in promoting weight and wiring synaptic plasticity and in coordinating memory consolidation across hippocampal-cortical networks. Thus, SWRs dysfunctional patterns in dMCAO rats likely impacted predominantly consolidation processes involved in the subsequent stabilization of the hippocampal memory trace. An altered hippocampal-

cortical dialogue during the course of systems-level memory consolidation may have resulted in a memory trace not properly stabilized (faster forgetting) or an impaired access to a partially degraded trace.

The entorhinal cortex might explain how a remote structure such as the hippocampus can be impaired by the cortical infarct. Indeed, the entorhinal cortex is known to act as a theta generator providing inputs to the hippocampal rhythm and this structure also controls hippocampal SWRs (Chrobak and Buzsaki, 1996; Dickson et al., 2000). It is believed that intrinsic circuits of the hippocampus are sufficient to generate alone the SWRs originating from CA3 and spreading to CA1, then coming back to the EC as an output event (Sullivan et al., 2011; Buzsaki, 2015). This auto-generation of SPWs is controlled by inhibitory interneurons, for example large bilateral lesions of the EC lead to an increase of SWRs occurrence (Bragin et al., 1995a). So, when the suppressing effects of the subcortical neuromodulators are removed, the hippocampal neurons are not inhibited anymore which leads to SWRs burst. In summary, the default mode of CA3 generates SWRs bursts and these events are "released" in the absence of suppression mechanisms (Buzsaki et al., 1983). It has been shown that the median raphe region projects to the hippocampus and its activation or inhibition leads to a reduction or enhancement of SWR activity (Wang et al., 2015). Based on the same mechanisms, the EC may control the triggering of hippocampal SWRs due to the projections of the EC layers II-III to the hippocampal CA1 and DG via the activation of inhibitory interneurons. For example, the temporo-ammonic pathway which originates from cells located in the entorhinal cortex and excites a diverse population of inhibitory neurons located in the CA1 (Maccaferri and McBain, 1995; Elfant et al., 2008) or the perforant pathway which connects the EC to all fields of hippocampal formation could be recruited (Jones, 1994; Kajiwara et al., 2008). Several studies suggested that 'silent' epochs in the DG (i.e when SWRs do not burst) reflect neocortical slow oscillation changes relayed by the EC (Isomura et al., 2006; Wolansky et al., 2006; Hahn et al., 2007) and the activity of the CA1 neurons is driven by inputs from layer III of the EC (Charpak et al., 1995). Moreover, the EC (lateral and medial) receives cortical input arising from the layer II, V and VI (Burwell and Amaral, 1998). We found that the neuronal activity of the entorhinal cortex, revealed by Fos imaging, was altered following distal ischemia or inactivation of the SS1. This impairment of the EC might thus be responsible, at least in part, for the observed alterations impairments of the hippocampal theta rhythm and occurrence of SWRs. An hyperactivation of the lEC was associated with CNQX cortical inactivation whereas an hypoactivation of the lEC was

associated with cortical ischemia (2 weeks of post-stroke). Our cortical inactivation was associated with a decrease of the hippocampal SWRs whereas acute ischemia was associated with an increase of the hippocampal SWRs. These results can confirm the inhibitory role of the lEC on the hippocampal SWRs (**Fig. 84**).

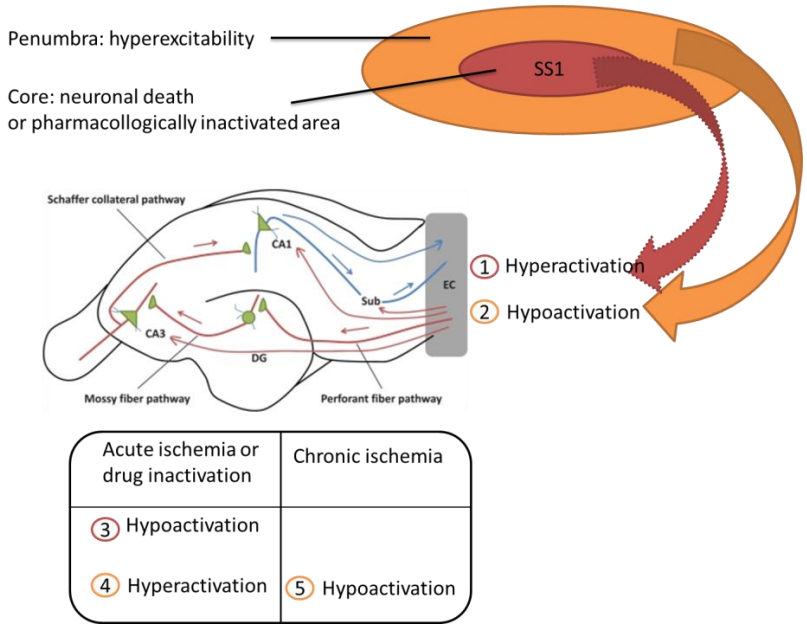


***Figure 84. Potential mechanisms leading to hippocampal diaschisis after cortical alteration.*** *Contrary to ischemia which predominantly triggers inhibitory pathways, the lack of inputs from the SS1 induced by a localized cortical inactivation, which mimics the ischemic core, preferentially recruit activatory pathways leading to hyperactivation of the EC (1). The penumbra area generated by the ischemic episode is hyperexcitable (in both acute and chronic conditions) and triggers inhibitory pathways , leading to hypoactivation of the EC (2). Projections of the EC recruit in turn hippocampal interneurons which regulate SWRs triggering. EC hyperactivation (1) can lead to hippocampal hypoactivation (3) (as shown by decrease Fos expression and SWR occurrence) whereas EC hypoactivation can induce hippocampal hyperactivation (4 ) (as shown by increase of SWR occurrence following the acute phase of ischemia). In contrast, during chronic ischemia, the hippocampus is hypoactivated (5) (as shown by decreased Fos expression possibly resulting from downregulation of neuroreceptors inducing synaptic plasticity as a consequence of the initial acutely-induced ischemic hyperexcitability).*

As for the SWRs which seem to be controlled by the lEC, the hippocampal theta rhythm is directly dependent of the lEC because it is a generator of the theta oscillations (Pignatelli et al., 2012). The theta rhythm is mediated by the entorhinal cortex, for example the theta dipole is suppressed in the hippocampal fissure and in the stratum lacunosum moleculare of the CA1 after EC lesion (Kamondi et al., 1998; Buzsaki, 2002). It has been suggested that the EC provides periodic excitatory glutamatergic inputs to the pyramidal cells of the CA1, CA3 and molecular layer of the DG (Amaral and Witter, 1989; Kamondi et al.,

1998; van Groen et al., 2003), however it seems that the mEC is more implicated in the generation of the hippocampal theta oscillations than the lEC (Montoya and Sainsbury, 1985; Deshmukh et al., 2010). The temporo-ammonic pathway originating from the EC has been proposed to also play a critical role in the generation of theta rhythm (Ang et al., 2005).

The following figure summarizes the electrical mechanisms supporting the memory process occurring during the awake state or non-REM sleep (ON condition) and during immobility or slow-wave sleep (OFF condition) (**Fig. 85**).

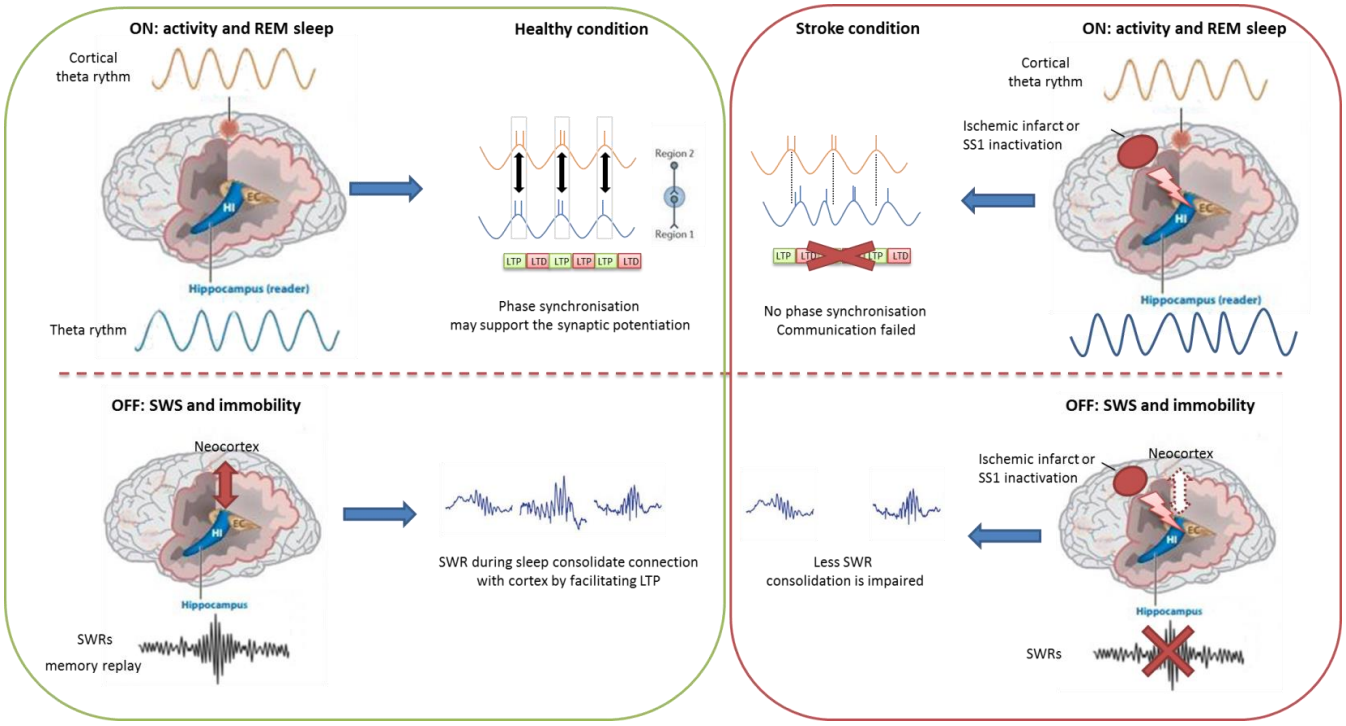


***Figure 85. Stroke or somatosensory cortex inactivation induces hippocampal theta rhythm and SWRs impairments leading to memory consolidation deficits.*** *In healthy conditions (green box), the hippocampal (HI) theta rhythm triggered during attentional task or rapid-eye movement (REM) sleep ("ON period") is synchronized with the cortical rhythm. The synchronization facilitates the communication between the two regions (black arrow) and the efficient information transfer during coincident activity (two coinciding spikes are surrounded by grey box). The phase synchronization may serve to recruit memory-related regions and facilitate the synaptic potentiation (LTP, LTD). This new information is consolidated during the "OFF period" (i.e. immobility or slow-wave sleep (SWS)) during SWRs replay. Focal ischemia or inactivation of the somatosensory cortex (SS1) induces hippocampal diaschisis (red box) via the entorhinal cortex (EC) which leads to a theta desynchronization between regions and a reduced occurrence of SWRs in hippocampus. Deficits in theta and SWRs may alter the cellular and molecular mechanisms underlying memory encoding and subsequent consolidation, for instance the synaptic potentiation.*

The occurrence of hippocampal diaschisis leading to deficits in encoding or memory consolidation may be explained at a system level (**Fig. 86**). According to the standard theory

of systems-level memory consolidation, the hippocampus is necessary to encode and integrate new information arising from cortical networks processing the sensory-motor inputs of the whole experience (Squire and Alvarez, 1995; Squire, 2004). Following ischemic stroke, the induced hippocampal hypoactivity would lead to anterograde amnesia because of the hippocampal incapacity to organize adequately the memory allocation and consolidate the different features of the memory trace into cortical networks.

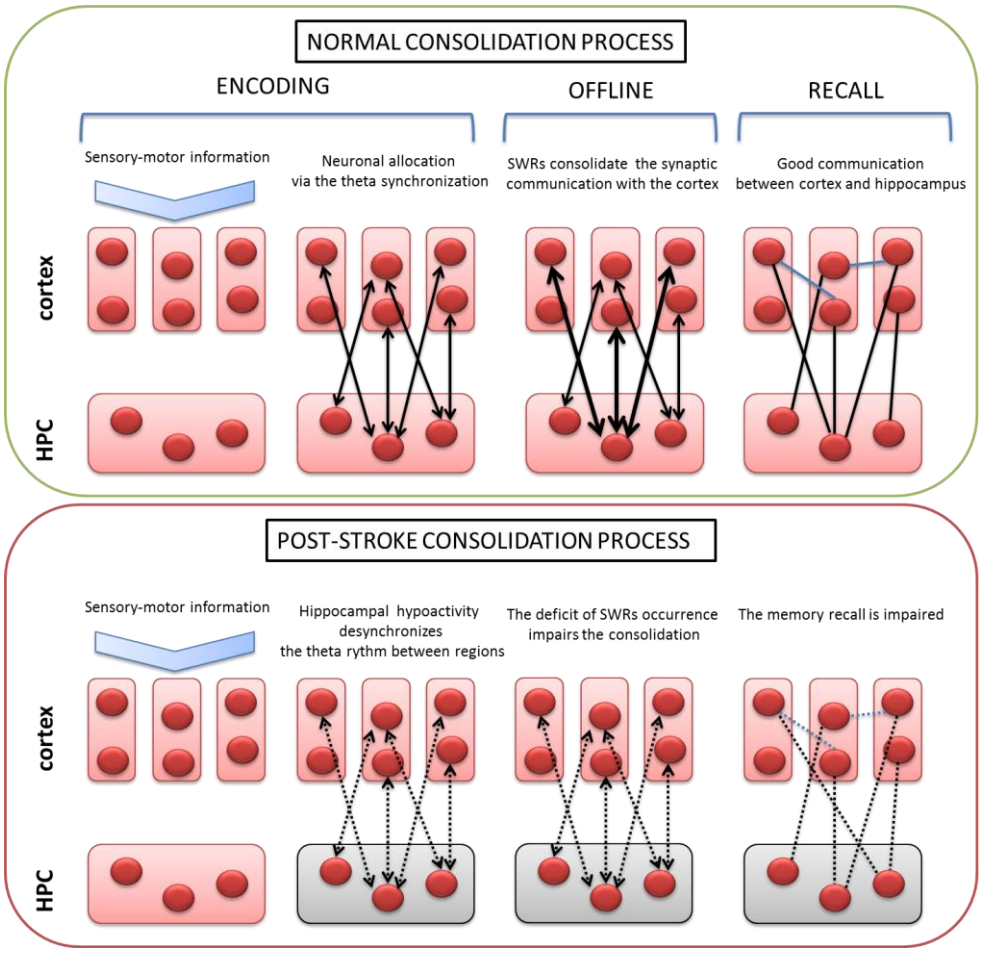


***Figure 86. A putative model of encoding memory deficit after ischemic stroke.*** *In physiological conditions (green box), the new information is encoded following sensory-motor inputs undergoes consolidation. During this process, the hippocampus organizes the different pieces of information into a coherent memory trace that will be progressively embedded into cortical networks. During offline periods (slow-wave sleep or quiet wakefulness), SWRs actively participate to the consolidation of the new memory trace by promoting weight and wiring synaptic plasticity among hippocampal-cortical connections.. The strength and stability of cortico-cortical connections is progressively increased to stabilize the memory trace. Upon memory recall, the hippocampus acts as a reactivator of hippocampal-cortical neuronal ensembles, enabling the reactivation of the whole features of the memory trace. In ischemic stroke (red box), the consolidation organizing function of the hippocampus is impaired by the phenomenon of diaschisis leading to hippocampal deactivation. This would lead to accelerated forgetting (anterograde amnesia) or the formation of an insufficiently detailed or coherent memory trace amenable for successful retrieval.*

A better understanding of these mechanisms leading to hippocampal diaschisis will help to design more efficient therapeutical strategies aimed at restoring hippocampal activity by 1) better preserving parietal cortex activity following ischemic stroke (e.g. reducing excitotoxicity), or 2) restoring hippocampal activity by stimulation with motor and mental activities (cognitive challenges) given as soon as possible to patients that underwent an ischemic episode

# Perspectives

Our current findings identify hippocampal diaschisis as a potential mechanism underlying memory dysfunction in focal cerebral ischemia. Because we explored the electrical activity of the brain in anesthetized rat, it would be particularly interesting to investigate the electrical brain activity in freely moving rats during a learning task by means of silicon probe insertion tailored to recording unit activity within large neuronal assemblies. Indeed, network oscillations have been assumed to integrate local computations to global networks (Engel et al., 2001; Sirota et al., 2003; Battaglia et al., 2011). A spatial task as the Barnes maze seems more adapted for freely-moving investigation because of the repetitions of the training and the presence of one single rat during the test avoiding technical problem with the wire connectivity. We could record the hippocampal and the parietal cortex during training and during the immobility period in the home cage of the animals. Hippocampal SWRs, hippocampal theta but also cortical gamma and cortical spikes known to be coupled for memory process could be collected.

First, the theta-gamma coupling could be explored during training in the Barnes maze in controls and ischemic rats. Multiple studies reported that slow rhythm such as theta waves engage large areas and modulate localized and fast oscillations such as gamma waves (Bragin et al., 1995b; Chrobak and Buzsaki, 1998; Lakatos et al., 2005; Sirota et al., 2008; Bitzenhofer et al., 2015). The benefit of the synchronization between the hippocampal theta and the cortical gamma represents a special case of global coordination which is necessary for working memory (Park et al., 2013). In stroke condition, we can suppose that this theta-gamma coupling is altered and leads to an impairment of memory encoding. The hippocampal theta oscillations could also act like a firing metronome for the cortical neurons (Benchenane et al., 2010). For example, activity of neurons in sensory and associative areas located in parietal cortex is entrained by the theta rhythm (Sirota et al., 2008). In addition to analyzing the theta-gamma coupling, we could explore the entrainment of the neuronal spiking activity in parietal cortex by the hippocampal theta rhythm.

Second, place cells in the hippocampus are known to fire during accomplishment of spatial tasks and the hippocampal replay of the SWRs might be a substrate for the memory consolidation (Girardeau et al., 2009; Carr et al., 2011). These hippocampal events could be recorded when rats rest after the spatial task and during sleep in order to evaluate a potential deficit in ischemic animals. Recent study reported that firings of prefrontal cortical neurons are phase-locked with hippocampal SWRs (Peyrache et al., 2011), the exploration of this same kind of correlation might thus be interested in the parietal cortex of controls and

ischemic rats submitted to spatial discrimination in the Barnes maze.

Third, the electrical activity of the entorhinal cortex (EC) which connects the parietal cortex to the hippocampus would deserve further investigation.. Because SWRs also occur in the EC (Bragin et al., 1999; Buzsaki and Chrobak, 2005) and that this structure is a theta generator (Pignatelli et al., 2012), it would be interesting to examine what extent theta rhythm and SWRs in the EC correlate with those occurring in cortical and hippocampal regions. This would provide converging evidence for the role of the EC as a crucial relay in mediating hippocampal diaschisis.

In addition to the exploration of the anterograde amnesia in ischemic rats, retrograde amnesia could also be examined. Few studies reported retrograde memory impairment in spatial tasks following stroke (Sakai et al., 1996; Yonemori et al., 1996; Yonemori et al., 1999). The ischemia could be induced at various delays after spatial learning in the Barnes maze in order to determine the impact on memory retrieval. Electrophysiological investigations detailed previously could also be reproduced in these specific experimental conditions.

Finally, a therapy based on environmental stimulation could be developed to counteract the deleterious effect induced by stroke. Enriched environment (EE) induces facilitation of LTP in the hippocampal CA1 neurons (Malik and Chattarji, 2012), enhances hippocampal neurogenesis (Matsumori et al., 2006) and improves motor skills and memory performance after brain injury or ischemia (Hamm et al., 1996; Johansson, 1996; Yu et al., 2014). For these reasons, EE might restore the cognitive function of the ischemic rats by restoring the hippocampal theta stability or the occurrence of the hippocampal SWRs.

Molecular investigations might be performed by analyzing the N-methy-D-aspartate (NMDA) receptor density in the hippocampus and in the cortical infarct. In stroke, NMDA receptors are intensively activated by the release of glutamate leading to neuronal death. Accordingly, multiple strategies have used NMDA receptor antagonists to induce neuroprotection of the infarcted area (Doeppner et al., 2015; Jaeger et al., 2015; Yu et al., 2015). Hippocampal diaschisis could also affect the density or the activation of the NMDA receptor on hippocampal neurons leading to impaired activity.

# Annexes

*Int. J. Mol. Sci.* **2015**, *16*, 1-x manuscripts; doi:10.3390/ijms160x000x

OPEN ACCESS
International Journal of
**Molecular Sciences**
**ISSN 1422-0067**
www.mdpi.com/journal/ijms

*Review*

# Perturbation of Brain Oscillations after Ischemic Stroke: A Potential Biomarker for Post-stroke Function and Therapy

**Gratianne Rabiller [1,2,3,4], Ji-Wei He [1,2], Yasuo Nishijima [1,2,5], Aaron Wong [1,2,6] and Jialing Liu [1,2,*]**

1 Department of Neurological Surgery, University of California at San Francisco and Department of Veterans Affairs Medical Center, 1700 Owens Street, San Francisco, CA 94158, USA; E-Mails: gratianne.rabiller@gmail.com (G.R.); jiwei.he@ucsf.edu (J.-W.H.); nishijima_yasu@yahoo.co.jp (Y.N.); aaronwong95@gmail.com (A.W.)
2 UCSF and SFVAMC, San Francisco, CA 94158, USA
3 Univ. de Bordeaux, Institut des Maladies Neurodégénératives, UMR 5293, Bordeaux 33000, France
4 CNRS, Institut des Maladies Neurodégénératives, UMR 5293, Bordeaux 33000, France
5 Department of Neurosurgery, Tohoku University Graduate School of Medicine 1-1 Seiryo-machi, Aoba-ku, Sendai 980-8574, Japan
6 Rice University, 6100 Main St, Houston, TX 77005, USA

***** Author to whom correspondence should be addressed; E-Mail: jialing.liu@ucsf.edu; Tel.: +1-415-575-0407; Fax: +1-415-575-0595.

Academic Editor: Xiaofeng Jia

*Received: 14 July 2015 / Accepted: 15 October 2015 / Published:*

---

**Abstract:** Brain waves resonate from the generators of electrical current and propagate across brain regions with oscillation frequencies ranging from 0.05 to 500 Hz. The commonly observed oscillatory waves recorded by an electroencephalogram (EEG) in normal adult humans can be grouped into five main categories according to the frequency and amplitude, namely δ (1–4 Hz, 20–200 μV), θ (4–8 Hz, 10 μV), α (8–12 Hz, 20–200 μV), β (12–30 Hz, 5–10 μV), and γ (30–80 Hz, low amplitude). Emerging evidence from experimental and human studies suggests that groups of function and behavior seem to be specifically associated with the presence of each oscillation band, although the complex relationship between oscillation frequency and function, as well as the interaction between brain oscillations, are far from clear. Changes of brain oscillation patterns have long been implicated in the diseases of the central nervous system including ischemic stroke, in which the reduction of cerebral blood flow as well as the progression of tissue damage have direct spatiotemporal effects on the power of several oscillatory bands and their

interactions. This review summarizes the current knowledge in behavior and function associated with each brain oscillation, and also in the specific changes in brain electrical activities that correspond to the molecular events and functional alterations observed after experimental and human stroke. We provide the basis of the generations of brain oscillations and potential cellular and molecular mechanisms underlying stroke-induced perturbation. We will also discuss the implications of using brain oscillation patterns as biomarkers for the prediction of stroke outcome and therapeutic efficacy.

**Keywords:** electroencephalography; action potential; MCAO; CBF

---

## Table of Contents

## 1. Introduction

Electroencephalography (EEG) has commonly been used as a non-invasive method of recording and analyzing electrical activity of the brain via electrodes attached to the scalp. This test is most often used to diagnose and monitor various neurological diseases including ischemic stroke and seizures. In particular, EEG has been instrumental in differentiating acute ischemic stroke from stroke mimics. This review summarizes the current knowledge of brain oscillatory wave changes recorded by either conventional EEG or penetrating electrodes during human or experimental stroke from extracellular recordings to molecular events. It will first describe the fundamentals and utility of using EEG in a normal mammalian adult brain, as well as discuss neural oscillations as being the primary basis of analysis of EEG. Next, it will focus on both how stroke conditions modify the brain oscillations typically observed in EEG and which biomarkers can be used to detect and predict these outcomes. While acknowledging the variability reported by different sources of literature regarding EEG changes after stroke, this review will conclude by considering both the molecular events that occur during ischemia and the structures that generate neural oscillations in an attempt to draw conclusions about brain oscillations and give a new approach to brain connectivity. Although most experimental data were collected by using penetrating electrodes instead of scalp EEG, the term EEG is still used in the relevant context throughout this review in order to make reference to the frequency groups originally identified by conventional EEG.

## 2. EEG Signals and the Spectrum of Oscillations

EEG is a widespread technique to study brain activity under physiological as well as pathological conditions. In humans, EEG records the electrical activity of the superficial layers of the brain using electrodes placed on the skull. Classically, the location of the electrodes is determined according to the "10–20 System of Electrode Placement" method that refers to a 10% or 20% inter-electrode distance of the total front-back or right-left distance of the skull. Electrodes are distributed on the scalp and identified by the first letter of the brain regions (e.g., F, T, C, P and O for frontal, temporal, central, parietal and occipital lobe) and electrode number (1, 3, 5, 7 assigned for the left hemisphere and 2, 4, 6, 8 for the right hemisphere). The letter Z usually refers to an electrode placed on the midline. The summation of the currents from cortical neurons can be detected by using two electrodes about 5 mm in radius that permit measurement of small current potential up to 100 μV [1]. Due to the simplicity of this approach, EEG is one of the most widespread non-invasive techniques for neural activity recording as a diagnostic tool for clinical purposes [2]. However, this technique does have some caveats that are mainly related to the tissue barrier of the scalp that prevents the detection of low-energy brain activity, such as frequencies higher than 100 Hz and those lower than 0.1 Hz. Furthermore, artifacts can be created by eye blinks, movements, or muscle activity such as respiration.

The utility of EEG as a diagnostic tool or in getting high-quality data is reduced when it comes to laboratory animals like rodents due to the following limitations: (1) lack of adequate space to accommodate the electrodes because of the small size of the rodent brains, (2) difficulty in locating the

anatomic source of neural activity in epidural EEG recordings, and (3) lack of real time capability to extract signal characteristics due to the requirement of extensive computational analysis. To circumvent the first two limitations, the use of an invasive technique, such as probe insertion, permits exploration of the activity of deeper structures in the brain including the thalamus or hippocampus. In particular, the use of microelectrode arrays can register the activity of small groups of neurons, referred to as "local field potentials", or a single neuron, known as "single-unit action potential", with a signal frequency up to 5000 Hz. The electrode diameter inserted in the brain ranges from 10 to 30 μm, affording a great deal of tissue coverage up to 50 $mm^2$ on average [3] and a high spatial resolution that is required to analyze the neural substrates for complex tasks. Despite this enhanced sensitivity and specificity, the downside of using these penetrating electrodes still remains due to the invasive aspect of this technique, as insertion of a probe several millimeters deep into the brain can destroy neurons along the pass [4].

By using penetrating and scalp electrodes, EEG has provided us with invaluable information regarding the generation, propagation, patterns and functions of brain oscillations for more than a century, with the first animal publication dating back to 1890 (by Adolf Beck [5]) and the first human investigation in 1929 (by Hans Berger [6]), respectively. It is our current understanding that brain oscillations resulting from electrical currents propagate in all mammalian brains within the frequency range of 0.05 to 500 Hz. For all intents and purposes, the oscillations are categorized into five main frequency groups, namely δ (1–4 Hz), θ (4–8 Hz), α (8–12 Hz), β (12–30 Hz) and γ (30–80 Hz) [7]. Apart from those commonly observed in the conventional EEG, there are other oscillations outside this spectrum. For example, there exist slow oscillations (0.3–1 Hz) that are slower than the δ band [8] and high frequency oscillations (HFO) (80–200 Hz) that are faster than the γ band, also known as fast oscillations that include ripples (100–200 Hz) [9]. Data from human sleep studies suggest that the slow (<1 Hz) and δ bands are two different oscillatory types that are distinct in their evolution; *i.e.*, the power of the δ waves declined from the first to the second non-Rapid Eye Movement (REM) sleep episode, while the power of the slow wave remained unchanged [10]. Furthermore, pathological high frequency oscillations (pHFOs) (200–600 Hz) that are distinct from normal ripples are often recorded in the dentate gyrus during seizure generation [11]. It should be mentioned that the frequency of the θ band from superficial layers of the brain (4–8 Hz) differs from that recorded in the hippocampal layers (4–10 Hz) [12]. In addition, another oscillation band known as the mu rhythm (8–13 Hz) shares a great deal of similarity in frequency with that of the α band. However, unlike α which is recorded in the visual cortex in the occipital lobe, mu is not only recorded at various locations in the motor cortex such as the central and parietal areas, but also as a sinusoidal, regular, and rhythmic waveform that is distinct from the sharp negative peak and rounded positive phase observed in the α band. In the low frequency range, some confusion may arise due to inconsistent nomenclature in reference to the slow oscillations that exist during slow-wave sleep, anesthesia or after stroke and the δ oscillations present during slow-wave sleep or after stroke. Indeed, these two low frequency waves differ by their frequency range because the slow oscillations refer to activity between 0.3 and 1 Hz in an adult awake EEG [8] whereas the δ wave refers to activity between 1 and 4 Hz [13, 14].

In order to determine the changes in brain oscillations associated with behavior-specific neural activity or pathological processes, it is critical to first understand the EEG patterns in a variety of normal physiological conditions including sleep, awake, immobile, and highly mobile states from various brain regions in the cortex, brainstem, thalamus, and limbic areas. The normal range of the EEG frequency, also called background activity, is around or above 8.5 Hz in the posterior head regions in awake adults. In contrast, the background activity is dominated by the β rhythm in the anterior brain regions, and by the β, α, and θ rhythms in the central and temporal regions, respectively. Due to rapid changes in EEG features during early development with respect to temporal and spatial organization and age-specific unique patterns in pediatric brains that are not linked to pathology, we will limit our discussion of this review to adult EEG only [15].

EEG translates a three-dimensional electrical wave into a two-dimensional electrical wave using two electrodes as reference points. Thus, an epoch of EEG recording represents a time-varying dynamic of voltage difference (*i.e.*, potential in mV or μV) between two locations (e.g., a target site *vs.* reference/ground). EEG signals in the time domain often contain slow and fast oscillations, amplitudes of which wax and wane in a complex fashion; hence, the raw EEG information is not intuitive to the naked eye. As such, a Fourier transformation is frequently used to parcel out specific frequency bands simultaneously and to reveal the unique characteristics of the EEG from its complex time domain. As a frequency domain representation of the original data, the Fourier transformation provides information in the amplitude (mV or V) or power ($mV^2$ or $V^2$) of any frequency band over a period of time. In principle, data of a longer period generates a parcellation of frequency bands with finer resolution, and in turn results in a more precise estimate of amplitude at a given frequency. However, in practice, data of interest often do not last for a long time. Therefore, the parameters of the Fourier transformation are often dictated by specific scientific questions or the exact protocol that may vary between studies. The distribution of each wave throughout the entire brain under normal physiological conditions following the Fourier transformation spectrum excluding the γ band is as following: 25%–45% of δ oscillations, 40% of θ oscillations, 12%–15% of α oscillations, and 3%–20% of β oscillations in rodent EEG in the global frequency band (0–30 Hz) [16, 17].

## 3. EEG in Normal Conditions

### *3.1. Generators of Oscillations*

The EEG signal can be obtained by the volume conduction of the brain with the electrical current propagating from the generators to the recording electrode through brain tissue. Due to the physics of waves, slower oscillations propagate more than higher frequency ones, recruiting a larger network as in the case of θ and δ waves [18, 19]. Although it is established that EEG records the currents from the cortical neurons, the exact origin of the electrical activity or intermediate partners involved in driving these events are not well understood. Because EEG translates a three-dimensional signal in a two-dimensional signal, it is not possible to precisely localize the electrical sources of the oscillations [20]. It is hypothesized that certain brain structures or neuronal networks serve as the generators of various oscillation frequencies similar to pacemakers, while others act like the resonators that respond to certain firing frequencies [21]. It appears that the locations of the generators may vary depending on

the frequencies. For the slow-wave state present during non-REM sleep (frequency inferior at 1 Hz), the two main oscillation generators are located in the neocortex (pyramidal neurons in the layers II/III, V, and VI) and the thalamocortical (TC) and nucleus reticularis thalami (NRT) neurons in the thalamus. A synchronization is established between these two generators via corticothalamic, thalamocortical, and intracortical connections [22].

The generators of the θ wave have been proposed in several locations. To investigate deeper structures that can act as potential generators, electrode implants were particularly pertinent. One report suggests that structures like the entorhinal cortex and medial septum may act like pacemakers, inhibiting or exciting certain subregions of the hippocampus to synchronize the θ wave [12, 23, 24]. In comparison, the hippocampus acting like a resonator generates the θ oscillation that propagates via the volume conduction through the septo-temporal axis [25]. Hence, the inactivation or lesion of the septum perturbs the hippocampal θ oscillations [23]. However, a discrepant report implicated the source of the θ to originate from within the hippocampus (*i.e.*, in the cornu ammonis 1 (CA1) and dentate gyrus (DG), propagating the current into the superficial and deep layers of the brain, respectively). Despite the fact that θ oscillation has also been observed in the perirhinal cortex, cingulate cortex, subiculum, and amygdale [26-30], these structures are generally not considered as proper generators but rather as resonators of the currents (dipoles) because they cannot generate θ activity by themselves.

The δ wave is generated by the thalamus and pyramidal cells located in layers II–VI of the cortex, whereas higher frequency oscillations like α or β are believed to be generated by the cells in layers IV and V of the cortex [31-33]. However, contradicting results raise the possibility that the α wave is generated from locations other than the cortex. For example, it is present in subcortical regions like the hippocampus or the reticular formation [34]. It is also prominent in the thalamus and can be seen in isolated thalamic networks [35]. Further evidence suggests that cortical α is driven by thalamic pacemaker cells [34] and the thalamo-cortical-thalamic network [36, 37]. As a direct support for the thalamic origin of α, thalamic lesions lead to α rhythm disorganization or suppression in humans [38, 39]. In addition, an occipital α rhythm episode is associated with an increase in the thalamic activity as measured by blood oxygenation [40, 41] or blood flow [42].

The γ rhythm seems to be present in several different brain structures associated with visual, auditory, and motor tasks [43-46]. The cortical γ seems to be generated by the superficial layers II/III [33, 47, 48] and networks of interconnected inhibitory interneurons [49]. At the network level, tetanic stimulation of the thalamic reticular nucleus induces focal cortical γ oscillations via primary sensory pathways [50]. Further, following the stimulation of the pacemaker cells located in the reticular nucleus of the thalamus (another reported location of generator), there is an increase of the γ oscillation (35–55 Hz) in the somatosensory and auditory cortex [50]. An alternative school of thought suggests that γ oscillations are generated by synaptic activity via the interaction between neurons [51, 52]. For example, γ oscillations can be generated by pacemaker cells located in the hippocampus that entrain the “chattering cells” in the cortex to fire at the same frequency [48]. *In vitro* studies have shown that the γ rhythm can be elicited in cortical and hippocampus slice preparations after stimulation of the metabotropic receptors for a long period of time [47] or by activation of

metabotropic glutamate receptors with bursts of afferent stimulation for transient amounts of time [49, 53, 54]. Likewise, the subiculum can generate γ oscillations via the local inhibitory neuronal network following stimulation evoked either locally or in the nearby hippocampus CA1 [55].

### *3.2. Oscillations and Behavior*

Since the EEG technique was invented, efforts have been made to understand the association between a specific brain oscillation and corresponding behavior with some success. This chapter provides an overview in the amplitude or power of dominant waves observed during a specific behavior in humans and in animals with either scalp EEG or inserted electrodes in deeper structures. We also highlight a different aspect of the cortical state known as the synchronized *vs.* desynchronized state, in addition to the classical view of oscillation defined by the frequency range.

#### 3.2.1. In Humans

Slow oscillations (0.3–1 Hz) and δ oscillations (1–4 Hz) are present during anesthesia and slow-wave sleep, suggesting their roles in the consolidation of neuronal connections and new memories acquired during wakefulness [56]. Increased amplitude in the δ wave has also been detected after auditory target stimuli during oddball experiments in which presentations of repetitive audio/visual stimuli sequences were intermittently interrupted by a deviant stimulus, implicating its involvement in signal detection and decision-making [57]. High levels of cortical spontaneous neuronal activity are observed in animals during natural sleep and this behavioral state is associated with global inhibition of the cerebral cortex to suppress consciousness, suggesting that neuronal activity observed during slow-wave sleep may be the basis for neuronal plasticity and to consolidate memory traces acquired during wakefulness [58]. The link between neural plasticity and slow waves is further supported by a recent human study in which intermittent θ burst stimulation inducing long-term potentiation in the left primary motor cortex in awake adults was followed by an increase of δ wave power in the same area [59].

The benefit of sleep in memory consolidation can be better appreciated from the perspective of slow-wave activity. Apparently, the number of neurons bursting in synchrony is directly correlated with the amplitude and slope of EEG slow waves. Moreover, this near-synchrony state is also directly related to the number of strength of synaptic connections among these neurons. Thus, per the synaptic homeostasis hypothesis, cellular homeostasis is restored and synaptic strength is renormalized via spontaneous slow-wave activity occurring during sleep [60]. Plasticity-dependent recovery could be improved by managing sleep quality, while monitoring EEG during sleep may help to explain how specific rehabilitative paradigms work [61].

γ power often increases during problem-solving, yet a 40 Hz frequency (γ band) is present during the rapid eye movement (REM) dream state sleep that interrupts the δ power-dominant slow-wave sleep [62, 63], suggesting its role in modulating other oscillations. Given its omnipresence across different brain regions and its implication in a variety of cognitive function, the γ rhythm may serve to provide the synchronization between different neuronal networks [64, 65]. High frequency oscillations, ripples

in particular, play a crucial role in the information processing and consolidation of memory [66]. β power is observed in awake, attentive states that require working memory or it is found in the motor cortex during the preparation of movements [67]. It has been suggested that the function of the β oscillation could highlight a novel stimulus that would require further attention [68, 69] based on its presence during novelty detection in the auditory system [70], reward evaluation [71], and sensory gating [68]. The hippocampal θ is also associated with memory function [72], as θ power increases during cognitive tasks as well as during verbal and spatial tasks due to an increase in memory load [73-75]. The α band is present in the occipital cortex during aroused states with eyes closed [63] or relaxed wakefulness. A form of α wave can also be observed during sensory, cognitive, and motor processes [34, 57] and could play a role in the neuronal communication [76].

The reticular activating system (RAS), known as the arousal system, originates from the midbrain reticular formation and potentiates thalamic and cortical responses during both waking and REM sleep, a state of dream consciousness. Interestingly, clinical studies reported simultaneous changes between EEG and other vital physiological parameters including cardiorespiratory and blood pressure among the comatose patients [77, 78], suggesting that there might be a common origin in the inherent periodicity of the arousal mechanisms. The RAS serves to modulate all the spectrum rhythms depending on sensory inputs and ongoing activity in the brain, in which ascending inhibition or decreasing excitation slow down the brain's oscillations whereas excitation or disinhibition accelerates rhythms [79].

### 3.2.2. In Animals

Ample experimental studies have focused on the understanding of oscillations in the hippocampus and corresponding behavior. For example, in the rat hippocampus, θ state occurs during walking, running, rearing, and exploratory sniffing, as well as during REM sleep [73, 80-82]. Hippocampal θ is associated with stimuli in the working memory instead of the reference memory condition [73], thus it could be a tag for short-term memory [83]. Additional evidence also suggests that the hippocampal θ is associated with spontaneous movements in monkeys (7–9 Hz) [84] and locomotion in rodents [82]. Compared to hippocampal θ, the role of cortical θ is less clear. At least in cats, this rhythm is associated with task orientation during coordinated response, indicating its role in alertness, arousal, or readiness to process information [57]. The α frequency is present after sensory stimulation in the auditory and visual pathways, as well as in the hippocampus and reticular formation [57]. Although δ oscillation is dominant during the sleep state in animals [57], it is also observed during immobility and drowsiness in awake animals [80]. Sharp-wave associated ripples (SPW-Rs) are 100–200 Hz field oscillations with a duration of less than one second, present during awake immobility and slow-wave sleep in rat hippocampus and entorhinal cortex [66]. They are produced by inhibitory postsynaptic potentials (IPSP) occurring during bursts of interneurons, which converge on principal neurons and synchronize with the hippocampal sharp waves [85]. SPW-Rs play a critical role in memory consolidation and transferring memory from the hippocampus to the neocortex, of which the selective elimination during post-learning sleep resulted in the impairment of memory [86, 87]. The γ wave has been commonly observed after sensory stimulation (auditory and visual) in the cortex, the

hippocampus, the brain stem, and cerebellum in cats [57, 88]. Interestingly, the γ amplitude in the rat hippocampus is larger during θ-associated behaviors such as exploration, sniffing, rearing, and the paradoxical phase of sleep than it is during non-θ-associated behaviors, suggesting that the γ oscillation is synchronized with the θ oscillation [89].

3.2.3. Synchronized *vs.* Desynchronized Cortical State and Behavior

Apart from the conventional classification of brain activity based on frequency range, a new definition of the dynamics of network activity has emerged, known as the synchronized *vs.* desynchronized cortical states. A strong synchronization between the different networks consisting of both slow and large amplitude fluctuations as seen in slow-wave sleep is referred to as a synchronized state, characterized by up phases during which neurons fire, followed by down phases during which neurons are silent. The low frequency power is high (slow oscillation and δ oscillation), whereas the γ rhythm may decrease during this synchronized state. In contrast, the desynchronized state is present during waking or REM sleep, and it shows fast and low amplitude deflections during which the θ oscillations are dominant and the neurons fires continuously and irregularly without synchronization at the population level [80]. Between these two opposing brain states, there is a continuum of intermediate states with varying degrees of synchronization. The transitions between these two extreme states are mediated by neurotransmitters such as serotonin, noradrenaline, and acetylcholine that modulate the excitability of the neurons [90-92].

In general, the synchronized state is associated with immobility and quiescence in addition to slow-wave sleep and anesthetized state [93-95], albeit it is also present during waking. The amplitudes of oscillations in the synchronized state are usually smaller relative to those during slow-wave sleep [90, 91]. Unlike the synchronized state, the desynchronized state is present in active and behaving rodents [96, 97], and is often associated with an increase in the γ power among behaving animals [92], or during stimulation of subcortical structures [98] and attention [99]. However, some studies have shown contradicting results in which the γ power decreases in the desynchronized state [100, 101].

Finally, it has been well documented that the EEG signal contains rich characteristics in its temporal, spectral, and spatial aspects that tightly correlate with behaviors. Behavioral state or brain state, as a loose term, is therefore often used to describe EEG patterns in various aspects that strongly correlate to a group of behavior (a.k.a. “state”) instead of to a limited set of performance (e.g., a sensorimotor task). For example, a strong oscillation at θ frequency (3–12 Hz) across the brain (particularly in the hippocampus and neocortex) has been referred to as a wakefulness state in both rodents [81, 102] and humans [103], albeit with distinct electrophysiological characteristics between species such as central frequency, duration, and network coherence [103, 104]. Accumulating evidence from human studies suggests that specific patterns (e.g., cross-frequency modulation, coherent network activity, *etc.*) during θ oscillation manifest cognitive processes [105-107]. Another example is a spectral change in the human motor cortex during motor movement [108], in which a decrease in power at a low frequency band (8–32 Hz) occurs with movement of a concomitant increase at a high frequency band (76–100 Hz). It is noteworthy that such spectral change occurs only at specific regions within the

motor cortex, whereas the θ state (analogous to the desynchronized state) often involves multiple regions. In this regard, it remains unclear whether the movement-related spectral change is directly related to the θ state. Nonetheless, these region-, and behavior-specific changes of EEG may depict a general pattern when a certain kind of behavior (e.g., motor or cognition) is engaged.

## 4. EEG and the Cellular Origins of Oscillations

### *4.1. Under Physiological Conditions*

#### 4.1.1. Cellular Mechanisms

In order to delve further into the electrophysiological perturbations in response to stroke, we will first address the normal cellular mechanisms underlying the genesis of the electrical activity detected by EEG. The conventional EEG records the summation of currents of pyramidal neurons located at the surface of the scalp in the cortical layers. Similar to pacemaker cells, neurons are electrically excitable cells that can generate pulse and are able to propagate an incoming current via electrical and chemical signals sent from the axon of one presynaptic neuron to the dendrites of another postsynaptic neuron in a network. The neuron has a resting membrane potential of about −60 to −70 mV resulting from flux of ions in the neuronal environment. Neurons have high concentrations of potassium ($K^+$) and chloride ($Cl^-$) ions inside, while high concentrations of sodium ($Na^+$) and calcium ($Ca^{2+}$) ions are outside. These concentration gradients are maintained by a sodium-potassium pumping system. The closing or opening of ion channels induced by chemical or electrical stimuli modifies the flux of ions and leads to a modification of the membrane potential. An influx of positively charged ions into the cell reduces the charge separation across the membrane and results in a less negative membrane potential termed depolarization, whereas an efflux of positively charged ions increases the charge separation, leading to a more negative membrane potential called hyperpolarization.

Once activated, a neuron releases neurotransmitters into the synaptic cleft that either excite (depolarize) or inhibit (hyperpolarize) the adjacent postsynaptic neuron, depending on the nature of the neurotransmitters. Excitatory postsynaptic potential (EPSP) depolarizes the post-synaptic neurons resulting from the release of excitatory neurotransmitters such as glutamate or acetylcholine, while inhibitory postsynaptic potential (IPSP) hyperpolarizes neurons resulting from the release of inhibitory neurotransmitters such as γ-amino butyric acid (GABA) and glycine. An EPSP produces a flow of positive charges into the cell (current sink), while an IPSP acts in the opposite way by inducing a flow of positive charges out of the cell (current source). The summation of IPSP and EPSP induces a graded potential in the neuron so that when this membrane potential reaches the threshold potential, it induces an action potential that can propagate between neurons. The action potential is produced by a critical amount of $Na^+$ entering in the cell and the opening of additional $Na^+$ channels. This fast depolarizing event corresponds to the rising phase of the action potential, followed by the repolarization of the cell induced by an efflux of $K^+$ ions and a decrease of $Na^+$ influx. After an action potential, there is a refractory period during which another action potential cannot be generated due to a transitory inactivation of $Na^+$ channels.

EEG detects field potential as IPSP or EPSP generated by neurons because those events are longer in duration than the action potential (up to 10 milliseconds *vs.* a few milliseconds). To summarize the mechanisms of current flow, EPSP that depolarizes the membrane results from excitatory currents, involving $Na^+$ or $Ca^{2+}$ ions, flowing inward toward an excitatory synapse (*i.e.*, from the activated postsynaptic site to the other parts of the cell) and outward away from it. The outward current is referred to as a passive return current (from intracellular to extracellular space). IPSP, which hyperpolarizes the membrane, is caused by inhibitory loop currents that involve $Cl^-$ ions flowing into the cell and $K^+$ ions flowing out of the cell [20].

The vertically orientated pyramidal neurons located in the cortex laminae are considered as a dipole that can generate extracellular voltage fields from graded synaptic activity. The dipole is created with a separation of charge vertically oriented in the cortex, and with apical dendrites extending upward to more superficial laminae and axons projecting to deeper laminae. The EEG detects the extracellular electrical fields generated closer to the cortical surface. The cortex is composed of several cortical laminae that can generate opposite current for the same synaptic event depending on the layer being excited. For example, an EPSP at the apical dendrite in layer II/III is associated with an extracellular negative field (active current field) and an extracellular positive field (passive current source) in the basal dendrite located in layer V. On the contrary, an EPSP on the proximal apical dendrite located in cortical layer IV is associated with an extracellular negative field (active current sink) and an extracellular positive field in the distal apical dendrite in layers II/III (passive current source) (Figure 1) [20]. Thus, a deep IPSP and a superficial EPSP will both generate a negative field in the scalp and *vice versa*. Therefore, a large population of neurons can be considered as a collection of oscillating dipoles [109].

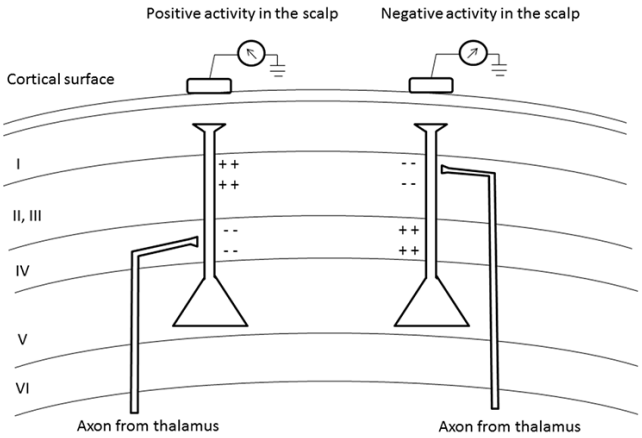


**Figure 1.** Generation of extracellular voltage fields. Relationship between the polarity of surface potentials and the location of dendritic postsynaptic potentials. EPSP depolarizing cell membrane induces a local negative local field potential (- -) and a positive local field potential (+ +) far away from the source. EPSP can also induce negative or positive activity in the scalp depending on the cortical layers excited.

The EEG tracings reflect the mean excitatory state of a pool of neurons rather than individual neurons, because the extracellular space beneath the electrode is traversed by currents from many cells. The interaction of signals of excitatory and inhibitory neurons explains why EEG waves oscillate [110], in

which alternating rises and falls in amplitude come from negative feedback circuits formed by this complex interaction as the following: (1) the excitatory neurons are stimulated or cease to be inhibited; (2) the excitatory neurons stimulate the inhibitory neurons, dampening excitation; (3) the inhibitory neurons inhibit the excitatory neurons, reducing the electrical activity; (4) when the activity falls to a minimal level, the inhibitory neurons rest, releasing excitatory neurons from inhibition and the cycle resumes. In support of this conceptual framework depicting the collective activity underlying odor perception, another computational study further illustrates how synchronous rhythmic spiking in neuronal networks can be brought about by the interaction between excitatory and inhibitory cells in generating the pyramidal-interneuronal γ rhythm, in which the inhibitory neurons inhibit the pyramidal neurons that themselves project to the inhibitory neurons [111].

### *4.2. Under Pathological Conditions of Energy Failure*

#### 4.2.1. Cellular Events after Ischemia

Because the pyramidal neurons located in the cortical layers III, V, and VI that generate graded EPSP and IPSP have been shown to be vulnerable to hypoxia and ischemia [112], we will discuss the cellular events occurring after ischemia and present evidence underlying the cause of EEG changes observed after stroke. Ischemia triggers an avalanche of cellular mechanisms that lead to short- and long-term consequences [113]. Given that neurons rely on adenosine triphosphate (ATP) as the main form of energy, a reduction of blood flow can significantly deprive brain cells of the glucose and oxygen necessary for the production of ATP. This reduction of oxygen activates the anaerobic glycolysis that produces lactate and the oxygen free-radicals burst, leading to ischemic damage and impaired electrical activity [114]. When the ionic gradients and the membrane potential cannot be maintained, it leads to the release of excitatory amino acids in the extracellular space and the accumulation of glutamate due to impaired reuptake by the transporters. The released glutamate activates the *N*-methyl-D-aspartate (NMDA) receptor that overloads the $Ca^{2+}$ and causes an influx of $Na^{+}$ and $Cl^{-}$ into the neurons, leading to edema due to the passive diffusion of water into the cell.

As a universal second messenger, the overloaded $Ca^{2+}$ activates proteolytic enzymes that degrade cytoskeletal proteins or extracellular matrix proteins. The generation of free radicals by the activation of the phospholipase via $Ca^{2+}$ also produces membrane damage. Nitric oxide (NO) produced by $Ca^{2+}$-dependent enzyme neuronal nitric oxide synthase (nNOS) forms peroxynitrite (reacted with a superoxide anion) that damages the tissue [115].

The ischemia-induced excitotoxicity has been well studied in the hippocampus and neocortex. In the CA1, short ischemia induces electrophysiological changes in pyramidal cells as a transient small depolarization followed by an increase in the excitability that leads to a hyperpolarization that changes the membrane resistance and abolishes the spontaneous or evoked spikes. Following ischemic reperfusion, the return of $O_2$ and glucose induces a transient hyperpolarization before restoring to baseline conditions [113]. This post-stroke hyperexcitability is present during the first week to one month of recovery, and plays an essential role in post-stroke neuroplasticity. In rodents, it is manifested by expanded and less specific receptive fields as well as increased spontaneous activity [116, 117].

This increased neuronal excitability has also occurred *in vitro* following oxygen-glucose deprivation, leading to the down-regulation of the GABAa receptor involved in the inhibitory pathway [118]. This hyperexcitability in surviving neurons contributes to a low frequency spontaneous activity (0.1–1 Hz) that fosters a permissive environment for axonal sprouting among rats with focal ischemia [119]. The modification of neuronal connections resulting from stroke-induced plasticity change in axons and dendrites [120-122] can persistently alter the generation and propagation of brain oscillations for weeks after stroke.

A variety of pathological states can cause aberrant changes in electrophysiology. For example, hypoxia induces a reversible hyperpolarization in the CA1 region of the hippocampus via a rise in $K^+$ conductance. It has been shown that similar events are seen during hypoglycemia in the neocortex [123], the striatum [124], and substantia nigra [125], as well as in the hippocampus subregions such as CA1 [126] and CA3 [127] soon after the onset of ischemia [128, 129]. Interestingly, hypoxia induces moderate depolarization instead of hyperpolarization [130] in some brain regions including the neocortex, dentate gyrus [131], striatum [124], and thalamus [112]. It has been shown that inducing anoxia with cyanide can depolarize or hyperpolarize the same CA1 neuron depending on its resting potential [132], providing the neural basis for the diverse EEG changes seen after stroke.

4.2.2. Cerebral Blood Flow (CBF) and EEG

Due to the great complexity and variation in brain ischemia-induced pathophysiology, a general consensus regarding the modifications of the brain oscillations after stroke is hard to reach, except that the type of electrical activity appears to correlate with cerebral blood flow [133-136], oxygen, and glucose levels [137, 138].

EEG abnormality begins to emerge when the CBF decreases to 25–30 mL/100 g/min compared to the normal range of 50–70 mL/100 g/min. [134]. Table 1 illustrates the critical levels of CBF for categorical reduction or loss in EEG amplitude and frequency, with corresponding changes in cellular metabolism and neuronal morphology [133, 135, 138, 139]. When CBF falls below 18 mL/100 g/min, it crosses the ischemic threshold and induces neuronal death. When it reaches 12 mL/100 g/min or below, infarction becomes evident because of the progressive loss of transmembrane potential gradients of neurons. If the CBF is below the ischemic threshold but maintained above the infarction threshold, the effect on metabolism or cell survival is still reversible, with visible electrical activity as δ oscillations. When the CBF falls below the threshold of infarction for a substantial amount of time, specifically for more than 45 min at 14 mL/100 g/min or less, the spontaneous neuronal activity never returns, even after reperfusion, and the damages is irreversible [114, 133, 140, 141].

While CBF is directly correlated with brain oscillations, it has been shown that the glutamate concentration (excitatory neurotransmitter) is associated with the θ waves (4–7 Hz) in the frontal lobe and the hippocampus during cognitive tasks in humans [142]. Abnormal release of glutamate coincides with CBF levels of 20–30 mL/100 g/min and is associated with peri-infarct depolarization [140, 143]. Parallel experimental data show that a reduction in EEG power across all frequency ranges 1–3 h after permanent middle cerebral artery occlusion (pMCAO) in the ischemic ipsilateral cortex of rats is

associated with a decrease of 30% of CBF compared to baseline and an increase of 1400% of glutamate release [144]. Moreover, CBF and the cerebral rate of oxygen metabolism studied with Xenon computed tomography and positron emission tomography show that regional EEG changes reflect the coupling of CBF and metabolism in ischemic stroke [145]. In early subacute stroke, the EEG correlates with the CBF because the oxygen extraction fraction increases to preserve the cerebral rate of oxygen metabolism (also known as misery perfusion or stage 2 hemodynamic failure). During the period of luxury perfusion or stage 3 hemodynamic failure, the EEG is no longer correlated with the CBF but instead with the rate of cerebral oxygen metabolism [145, 146]. It should be noted that the cellular damages such as decreased protein metabolism and neuronal death appear even before the critical stage of CBF in the peri-infarct area [140].To recapitulate, increased power in slower frequency bands (as θ or δ) and decreased power in faster frequency bands (as α and β) are seen with the reduced rate of cerebral oxygen metabolism [145]. Second, the δ rhythm seems to be the most reliable parameter correlating with CBF and metabolism changes during focal ischemia.

**Table 1.** Physiological coupling among cerebral metabolism, EEG, and cellular response, and the consequence on neuronal injury. EEG: electroencephalography, CBF: cerebral blood flow, ATP: adenosine triphosphate.

| CBF Level (mL/100 g/min) | EEG Abnormality | Cellular Response | Degree of Neuronal Injury |
|---|---|---|---|
| 35–70 | Normal | Decreased protein synthesis | No injury |
| 25–35 | Loss of fast β frequencies and decreased amplitude of somatosensory evoked potentials | •Anaerobic metabolism<br>•Neurotransmitter release (glutamate) | Reversible |
| 18–25 | Slowing of θ rhythm and loss of fast frequencies | •Lactic acidosis<br>•Declining ATP | Reversible |
| 12–18 | Slowing of δ rhythm, increases in slow frequencies and loss of post synaptic evoked responses | •Sodium-potassium pump failure<br>•Increased intracellular water content | Reversible |
| <8–10 | Suppression of all frequencies, loss of presynaptic evoked responses | •Calcium accumulation<br>•Anoxic depolarization | Neuronal death |

4.2.3. Penumbra and Core

The ischemic territory is not homogenous in many aspects due to the variation of the hemodynamics. The core is supplied with a 20%-below-normal level of cerebral blood flow and neuronal survival is threatened by acidosis, lipolysis, proteolysis, and disaggregation of membrane microtubules after the bioenergetics failure and the ion homeostasis breakdown. Besides, because of the $K^+$ and glutamate release, the neurons depolarize but cannot repolarize. Unlike the core, neurons in the penumbra struggle to maintain function but exhibit perturbed electrical activity due to partial energy metabolism preservation. Since repolarization of neurons following depolarization consumes energy, the

succession of “peri-infarct depolarization” occurs at the expense of the valuable and scarce energy remaining in the penumbra, leading to a perpetual depletion of the energy, and hence, a further expansion of the core and penumbra [115]. To further illustrate the vulnerable and dynamic state of the peri-infarct penumbra, a recent study elegantly demonstrated that supply-demand mismatch transients triggered peri-infarct depolarizations (PIDs), a phenomenon akin to spreading depression (SD) frequently occurring in experimental and human stroke [147, 148]. SD can be detected by changes in electrical activity, ionic potential, or optical signal, and is specifically seen as propagating waves of suppressed electrocorticogram (ECoG) activity, direct coupled (DC) potential shift by two serial intracortical microelectrodes sensitive to ionic changes, or spreading pallor in time-lapsed images during intrinsic optical imaging [147, 148]. In principle, factors causing regional $pO_2$ to drop below the depolarization threshold within a penumbra hot zone can trigger PIDs, including hypoxia or hypotension. For example, sensory stimulation of the susceptible hot zone by tactile stimulation of the forelimb increased $O_2$ extraction and supply-demand mismatch, increasing the metabolic burden, triggering anoxic depolarization, and worsening tissue perfusion and ischemic outcome. Interestingly, the somatosensory stimulation-induced PIDs were prevented by normobaric hyperoxia. Induced hypotension via controlled blood withdrawal also triggered PIDs, which did not require cortical neuronal activation, nor could they be inhibited by tetrodotoxin (TTX) [147, 148].

The nature of the perturbation in brain oscillation can provide insight into the pathophysiology and evolution of the ischemic core and penumbra. For example, patients with acute unilateral ischemic stroke in the MCA territory experience an increase in δ activity (low frequency band), whereas there is a decrease in α activity (high frequency band) in the ipsilateral parieto-occipital cortex and the contralateral medial and posterior cortex [149], reflecting the state of brain metabolism as well as neural activity in the core and penumbra, respectively [150, 151]. Consistent with this concept, the power of high frequency oscillation like the β band was found to decrease proportionally with the size and proximity of the infarct in patients one day after stroke [152]. However, as an exception to the rule, penumbra could also generate slow activity like δ or θ [153].

Alternative interpretations regarding the origin of the slow frequency activity after brain ischemia have emerged since the witness of a δ variant known as the polymorphic δ activity. The core support for the alternative theory derives from the fact that a direct lesion to the cortical gray matter alone did not produce slow-wave activity due to the coincidental destruction of the neuronal generators located in the cortex; hence, a lesion in the subcortical white matter induced irregular δ activity in the cortex overlying the infarct [154]. Evidence suggests that the polymorphic δ activity is cortical and it results from a disruption of corticocortical and thalamocortical connections [155], since the deafferentation of cortical neurons with thalamal lesions led to the increase of δ-like activity in the unilateral or bilateral cortex, bilateral hypothalamus, or bilateral mesencephalon [154, 156]. Furthermore, surface positive δ waves may represent an inhibitory phenomenon such as a hyperpolarization, based on the following possibilities: (1) the presence of synaptic IPSPs at the soma or basal dendrites, and (2) an influx of the calcium mediated by the efflux of potassium after hyperpolarization. Given the fact that the administration of cholinergic antagonist atropine led to polymorphic δ activity, the apparition of the slow-wave

activity or the increase of the power of δ after stroke could result from an impairment of the cholinergic pathways [157].

To summarize, the EEG changes observed after ischemia are caused by an electrical impairment of the neurons due to the changes of the membrane potential induced by energy deprivation. This energy deprivation results from the reduction of the CBF and leads to irreversible neuronal damages if the CBF is not restored in time. However, the neuronal origin of the increase of slow or δ oscillations and the decrease of high frequency oscillations after stroke is still under debate.

## 5. EEG in Stroke Conditions

Evidence suggests that ischemic stroke, a direct consequence of CBF impairment in local cerebral areas, is associated with brain oscillation fluctuations. Due to the non-invasive and real-time nature of the technique in recording the changes in brain activity, EEG has been widely employed in both the clinical and research fields. A wealth of information regarding the modifications of the brain activity observed after stroke has been catalogued and potential electrophysiological biomarkers diagnosing stroke, monitoring treatment response as well as secondary adverse events, or predicting the post-stroke outcome have emerged.

### *5.1. Modifications of the Brain Oscillations in Experimental Stroke*

A recent comprehensive review documented the EEG changes commonly observed after focal cerebral ischemia in rodents [158]. In essence, during the acute phase of ischemia in a transient MCAO model, the distribution of the power of the EEG spectrum (0–30 Hz) after Fourier transformation in animals is as following: 85% of δ oscillations, 7% of θ oscillations, 5% of α oscillations, and 3% of β oscillations. Thus, ischemia has resulted in an increase of low frequency and a decrease of high frequency oscillations, or specifically a decrease of the α-to-δ ratio [17, 159], considering the baseline distribution as 25%–45% of δ, 40% of θ, 12%–15% of α, and 3%–20% of β oscillations [16, 17]. In particular, an increase in δ power in the ipsilateral hemisphere after transient MCA stroke was reported in both the subacute and chronic phase from 24 h to seven days or beyond [16, 17, 160-163]. Another study reported that an increase of the ipsilateral δ and θ power occurred as early as one minute following intraluminal filament occlusion of the proximal part of MCA that leads to impairment in the subcortical brain regions [164]. The increase of both δ and θ activity was also reported eight days after tMCAO in rats in the fronto-parietal, occipital, and temporal regions, whereas α and β activity were depressed [165]. Diaschisis frequently occurs after focal brain ischemia [166, 167], of which the transhemispheric diaschisis refers to changes in the contralateral hemisphere detected after unilateral stroke [168]. Some studies suggest that an increase of the δ activity in the contralateral sensorimotor cortical areas correlated with an ipsilateral increase one to seven days after MCAO in rodents [16, 159, 161, 169]. On the other hand, other studies have shown that an increase in the contralateral EEG power in the somatosensory cortex accompanied a suppression of the EEG activity in the ipsilateral side 15 minutes after tMCAO in rats. Due to the lack of consensus in the evolution of the contralateral side, an asymmetric index is often used to reflect changes of rhythms in both hemispheres over time. This asymmetry calculated by the brain symmetry index (BSI) or the global pairwise derived brain symmetry index (pdBSI) is also present in experimental studies as reported during both acute (1 h post-stroke) and chronic phases (up to 14 days post-stroke) in young and one-year-old rats, respectively [161].

The literature is less clear concerning the modifications of the power of γ, β, and α bands. In general, these three bands decrease after stroke in rodents, although contradicting results do exist. For example, a 35% reduction of the amplitude of α waves and β waves in the ipsilateral hemisphere was reported three to seven days after tMCAO [158, 160]. The α band power decreased from day one

to day 28 after pMCAO [158, 170], whereas other studies reported an increase of δ, β, and rhythmic α activity by seven days in the contralateral cortex after stroke in a rat model of tMCAO [16]. Since γ oscillations have been implicated in higher cognitive function and might depend on the mitochondrial redox state, they are highly sensitive to decreases in $pO_2$, and are thus likely to be susceptible to the reduction in blood flow [171, 172].

Some evidence seems to implicate that an increase of the infarct volume is correlated with an increase of the δ power and neurological deficits [159, 173]. The volume of infarction is also correlated with the acute δ change index [174], pdBSI [175], relative α percentage, relative α-β percentage, relative δ-θ percentage, δ/α ratio, or δ-θ/α-β ratio [150]. It is likely that the loss of the fast frequencies and the increase of slow-wave activity are caused by the pathological neural tissue, leading to an impairment of the communication in the affected network regions [154].

### *5.2. Clinical Applications of Continuous EEG Monitoring during Acute Ischemic Stroke*

In contrast to computed tomography (CT) or magnetic resonance imaging (MRI), EEG is inexpensive, less invasive, widely available, and above all, it can detect changes of brain electrical activity within minutes of stroke onset even in the conditions of sleep, sedation, or loss of consciousness [133, 176]. To attest to the sensitivity of EEG, previous studies showed the efficacy of emergency EEG to detect ischemic changes in patients with no abnormality in the initial CT scan [177, 178]. Recent advances in computer technology enable us to monitor EEG anytime and anywhere by using downsized and manageable portable EEG devices. This would be helpful for non-neurologists at the point-of-care, especially in conditions like transportation of patients by ambulance, initial assessment by paramedics, or making diagnoses in hospital facilities with no availability of CT or MRI.

Complementary to experimental findings, extensive studies in humans have been conducted to correlate EEG changes with the size of the lesion or the location of the ischemic infarct [179]. Unlike the aberrant changes commonly seen in large acute strokes, EEG often is normal or shows subtle focal θ activity in lacunar infarcts [180], further supporting the coupling between CBF and EEG patterns. Sometimes focal slow-wave activity as the δ rhythm in awake adults, which could result from deafferentation of subcortical structures, indicates a localized structural lesion [181]. Nonetheless, continuous slow-wave activity is more representative of severe brain damage, whereas intermittent slow activity is representative of smaller lesions [156]. In addition to subcortical infarct such as the lacunar stroke, EEG may also show reduced sensitivity in patients with posterior cerebral artery (PCA) infarct [177, 182, 183]. Although some recent studies suggest that EEG is useful in all types of ischemic stroke regardless of ischemic location [184], it seems still difficult to detect a transient ischemic attack (TIA) by EEG [185]. EEG also can also predict some adverse events like delayed cortical infarct in subarachnoid hemorrhage (SAH) [186, 187], or severe edema in malignant MCA infarction [188, 189]. Table 2 summarizes some major characteristics associated with subtypes of ischemic stroke including location and clinical conditions from selected literature.

**Table 2.** EEG characteristics in various locations and subtypes of ischemic stroke.

| Stroke Subtypes | Summary | Time Frame of EEG Detection Relative to Stroke Onset | EEG/qEEG Characteristics |
|---|---|---|---|
| Large (Cortical, including ACA, MCA, PCA territories) | EEG abnormalities following cortical infarction depended on infarct location | <2 weeks (<24 h (34%), <1 week (50%)) | Lateralized EEG abnormalities 80% in MCA territory, 86% in cortical watershed zone, but 50% in PCA territory [177] |
| | Strong association between EEG mapping of δ power and lesion locations by CT | <24 h | Close correlation between EEG abnormalities (increased δ power) except striatocapsular in 85% patients [182] |
| | EEG monitoring is useful in all ischemic strokes regardless of locations. Also, pdBSI predicted radiologically (CT, MRI) confirmed stroke with an accuracy higher than the National Institute of Health stroke score (NIHSS) score at admission | <7 days (<72 h (81%)) | Increased pdBSI, DTABR, even in PCS and LACS [184] |
| Small (subcortical, lacunar) | EEG has relatively low sensitivity in patients with subcortical infarcts | <2 weeks (<24 h (34%), < 1 week (50%)) | 82% normal or non-lateralized EEG changes in subcortical lesions [177] |
| | EEG has relatively low sensitivity in patients with first lacunar infarcts | <7 days | Abnormal EEG in 43% patients with first lacunar stroke [183] |
| | EEG abnormalities depend on affected lesions in subcortical regions | <24 h | Normal EEG in striatocapsular regions 70% abnormal EEG in other subcortical regions [182] |
| TIA | EEG has low sensitivity in patients with TIA | <24 h | Non-significant difference between TIA and control by using pdBSI and DTABR [185] |

**Table 2.** *Cont.*

| Stroke Subtypes | Summary | Time Frame of EEG Detection Relative to Stroke Onset | EEG/qEEG Characteristics |
|---|---|---|---|
| DCI in SAH | ADRs may allow earlier detection of DCI in patients with severe SAH | Post-operative day two to post-SAH day 14 | ADR decrease in patients with DCI [186] |
| | EEG changes preceded detection of vasospasm/DCI in standard procedures by 2.3 days | 2–12 days (median 5.2 days) | Decrease in α or θ power few days before vasospasm/DCI [187] |
| Malignant MCA infarction | Emergence of high-voltage contralateral hemisphere δ activity might represent midline shift due to substantial edema in ipsilateral hemisphere and increased intracranial pressure | <25 h | Increasing δ power in contralateral hemisphere in malignant course [188] |
| | EEG and brain stem auditory evoked potentials have prognostic value for patients who develop malignant edema | <24 h | Diffuse generalized slowing and slow δ activity in the ischemic hemisphere pointed to a malignant course [190] |

Abbreviations: CT: computed tomography; MRI: magnetic resonance imaging; qEEG: quantitative electroencephalography; ACA: anterior cerebral artery; MCA: middle cerebral artery; PCA: posterior cerebral artery; ACS: anterior circulation syndrome; POCS: posterior circulation syndrome; LACS: lacunar syndrome; DCI: delayed cerebral ischemia; SAH: subarachnoid hemorrhage; ADR: α/δ ratio; DTABR: (δ + θ)/(α + β) power ratio; pdBSI: pairwise derived brain symmetry index; TIA: transient ischemic attack.

Apart from the generalized or regional bisynchronous slow activity or generalized asynchronous slow activity, other EEG changes after stroke include focal attenuation of a specific rhythm, usually the faster activity frequencies, as well as general attenuation or suppression of one or multiple brain oscillations [179]. Besides the fact that both the repartition of the band and the power between each wave changes, there is an apparition of abnormal patterns in stroke patients [179] and in animal models of MCA stroke [158]. The abnormal patterns can be attributed to non-convulsive seizures, occasional rhythmic spike-and-wave or polyspike discharges, polymorphic slow-wave δ activity, intermittent rhythmic δ activity associated with a 4–7 Hz range large-amplitude burst, periodic lateralized epileptic discharge, rhythmic discharges with a 1–4 Hz frequency spike, recurrent sharp or slow waves every 1–8 s, and pathological high frequency oscillations.

### *5.3. Continuous EEG Monitoring during Thrombolysis*

One report using continuous EEG showed a prompt reduction of δ power before symptomatic recovery within 20 min after intravenous tissue plasminogen activator (IV tPA) administration and persisted for at least three months [191]. Another study of 16 patients with tPA treatment showed a significant correlation between changes in BSI and neurologic recovery by using National Institute of Health stroke score (NIHSS) [192]. Moreover, one case report showed that two days after treatment with tPA, there was a resolution of pre-tPA δ activity correlated with an improvement of neurological deficits and complete recanalization of occluded MCA by using MR angiography [193], though this study did not report changes of EEG soon after tPA administration. These studies may indicate indirectly that continuous EEG monitoring could provide real-time information about successful recanalization by IV tPA and this could be important information for making a decision about additional treatments such as intra-arterial thrombolysis or mechanical thrombectomy. A future EEG monitoring study combined with intra-arterial therapy may clarify more detailed EEG changes before and after recanalization and enhance the utility of continuous EEG monitoring during IV tPA therapy. Continuous EEG monitoring also may detect not only improvement but also serious secondary adverse events, such as massive hemorrhagic transformation, severe cerebral edema, restenosis or reocclusion after recanalization therapies, l in real time. Apart from the potential in early detection of secondary events, other reports indicate that continuous EEG may also provide information for early diagnosis of other stroke conditions like a TIA [153] or delayed cerebral ischemia in SAH patients [186, 187].

### *5.4. Biomarkers of Prediction after Stroke*

Real-time EEG during and after acute stroke has become not only an invaluable tool to diagnose, but also to predict the evolution and outcome of stroke as an electrophysiological biomarker. Global changes such as loss of reactivity [194] or absence of sleep-wake cycle [195] constitute a bad prognosis and may implicate the presence of brainstem impairment due

to its close relationship with the cortical layers. A unilateral prominent slow δ or a decrease of α is also a sign for poor outcomes [196]. In contrast, good outcomes are correlated with the lack of δ and presence of faster frequencies within 24 h in regional changes [189].

The severity of stroke as assessed by the NIHSS in acute and subacute periods in humans is found to correlate with some derived EEG parameters such as the brain symmetry index (BSI) [192, 197], the global pairwise derived brain symmetry index (pdBSI), the relative α percentage, the relative δ-θ percentage, the relative α-β percentage, the δ-α ratio, and the δ-θ/α-β ratio [151, 175, 198]. A positive correlation was found between an increase of δ power during acute stroke and in patients with severe stroke including those with worse NIHSS scores eight months after stroke [153, 189, 199]. High asymmetry in the BSI during the acute phase is also associated with poor outcomes [153, 197], as in the case that a post-stroke shift of scalp δ power maxima from the ipsilateral hemisphere to the contralateral hemisphere indicated substantial worsening of cerebral pathophysiology. For example, high δ power was detected during the eight-hour post-stroke period in the fronto-central and fronto-temporal electrodes in the ipsilateral side, followed by high δ in contralateral side 16 h post-stroke. This high δ remained 25 h post-stroke whereas the δ power decreased in the ipsilateral side. It is noteworthy that the patients who had an important δ shift died in the ensuing days [188], suggesting the prognostic value of δ EEG changes.

Another study reported that poor recovery was associated with increased power in δ and θ bilaterally four to ten days after unilateral acute stroke in the MCA territory, in conjunction with increased power in β and γ in the contralateral hemisphere [200]. Patients with unilateral ischemic stroke in the middle and/or anterior cerebral artery show the α band locally reduced in brain regions critical to observed behavioral deficits three months after stroke [201]. Moreover, a high δ/α power ratio [198] measured during subacute stroke is associated with high scores of NIHSS at 30 days post-stroke, indicating bad outcomes. Conversely, an absence of slow activity with minimal decrease in other background frequencies predicts good outcomes (95% of success), whereas bad outcomes are predicted by continuous polymorphic δ and a decrease of the α and β activity in the ischemic hemisphere (79% of success) [196].

Although the occurrence of slow waves after stroke was often associated with adverse consequences of stroke and even used as a predictive biomarker of post-stroke outcomes, this group of oscillations has also been considered as a marker of neuronal plasticity. Among these, axonal sprouting has been regarded as an important component of functional plasticity and recovery following central nervous system (CNS) injury including stroke [202]. Following thermal ischemic lesion in the somatosensory cortex, synchronous neuronal activities were found in the perilesion cortex with a frequency range of 0.2–2 Hz and 0.1–0.4 Hz on day one and days two to three after ischemic injury, respectively. Inactivating the latter slow-wave pattern in the perilesion area by using TTX blocked axonal sprouting, suggesting that the δ oscillations observed in the perilesion cortex can be a lesion-induced signal for

anatomical reorganization within the brain [119]. The link between slow-wave activity and post-stroke neuroplasticity is further supported from the perspective of slow-wave sleep [61]. Mice treated with γ-hydroxybutyrate, a drug used to promote slow-wave sleep in humans, showed a faster recovery in motor function after stroke [203]. In addition, sleep disruption not only negatively impacted post-stroke functional recovery, but also specifically impaired processes associated with functional recovery including axonal sprouting and neurogenesis [204, 205].

To conclude, when the rate of cerebral oxygen metabolism is reduced, there is an associated increase in the δ and θ frequency oscillations (lower frequencies) and a decrease in faster frequencies such as β and α [145], although the δ wave change appears to be the more reliable index for the reduction of CBF and brain metabolism during focal ischemia. Moreover, using global parameters such as the α-β/θ-δ power ratio in order to detect and predict early and subtle ischemic EEG changes seems to be appropriate [145, 206, 207].

## 6. EEG, Oscillations Coupling and Perspectives

Despite the variation in findings, findings in global EEG changes after stroke coalesce to an increase of slower frequency oscillations and a decrease of faster ones. However, the relationship between the contralateral hemisphere and the ipsilateral hemisphere with respect to electrical activities and their temporal evolution remains controversial. Similarly, at the cellular level, the decision for neurons to depolarize or hyperpolarize hinges on the state of resting potential even under the same condition. Apart from the biological variation to ischemia, a great deal of the variability in results can be attributed to the complex connections that propagate electrical signals, and the cerebral cortex is the very source of signals recorded in human EEG. The complexity of ipsilateral cortical connectivity is best exemplified by the barrel field somatosensory cortex that receives projections from the motor cortex, frontal cortex, and other parts of the somatosensory and parietal cortex via layers I and II/III. [208]. Cortical neurons also project to the contralateral hemisphere via the callosal neurons in layers II/III, IV, and VI. The synchronization between the homotopic areas in two hemispheres is interrupted after lesion of the corpus callosum [209]. For the subcortical inferences, we can cite the thalamus, the hypothalamus, and the basal nucleus among all the other subcortical structures projecting to the neocortex.

In light of the continuum represented by brain oscillations, using the conventional approach by treating them as individual “explicit” entities seems to reach an impasse for advancement. The shifting between oscillations under conditions of low blood flow and the detection of polymorphic δ variant are particularly insightful in this regard. Furthermore, the ability of one oscillation in modulating another across brain regions adds even more dimensions to the already complex relationship. Since low frequency waves propagate more than high frequency ones that tend to stay localized to small structures [18, 19], θ and δ waves are found to propagate through the entire brain as directional waves, whereas α, β, and γ waves are localized and

driven by θ and δ. Ample studies sought to understand the interaction between γ and θ oscillations. For example, it has been shown that neocortical neurons were modulated by the hippocampal θ rhythm, with increased firing when the phase of θ is down in the CA1. Interestingly, a greater proportion of interneurons, e.g., 32% in the parietal cortex and 46% in the prefrontal cortex were modulated by θ waves compared to that in pyramidal neurons (11% in the parietal cortex and 28% in the prefrontal cortex) [24]. Another study demonstrated that the γ oscillation was phasically modulated by the θ cycle and the amplitude of γ oscillation varied as a function of the θ cycle. Moreover, the amplitude of γ activity was larger and the hippocampal interneurons in the hilus of the dentate gyrus fired rhythmically with a higher rate during θ-associated behaviors such as exploration, sniffing, rearing, and the paradoxical phase of sleep. It should be mentioned that after entorhinal cortical lesion, the amplitude of the hippocampal θ (5–10 Hz) decreased by 50%–70% and the frequency of γ oscillations reduced in the dentate gyrus from 40–100 Hz to 40–60 Hz [89]. Additional studies further suggest that the γ oscillation in the cortex is driven by θ oscillation from the hippocampus [24, 89, 210].

Evidence showing modulation between other oscillatory bands has just begun to emerge. A recent study investigated how slow activities such as δ rhythm coordinate fast oscillations such as γ rhythm over time and space. The study recorded the local field potentials in the cortico-basal ganglia structure of freely moving, healthy rats and showed that the phase of δ waves modulates the amplitude of γ activity [211]. The complexity of the relationship between various band frequencies and how it can be modified under pathological conditions is best exemplified in the α wave in the thalamus. An increased depolarization in the thalamocortical neurons that discharge in the range of 2–13 Hz can lead to oscillation in the α frequency (8–13 Hz), while a reduced depolarization of the same neuronal subpopulation gravitates brain waves towards the θ rhythm (2–7 Hz) [212]. Modification in oscillation coupling has indeed been reported in pathological conditions including schizophrenia, Parkinson's disease, or autism [213]. Given that θ-γ coupling seems necessary for working memory [214] and that working memory is disturbed in stroke patients [215], it is surprising that there is no evidence showing an impaired θ-γ or other oscillatory couplings in human or experimental stroke. Some factors might have contributed to the paucity of data in this area; for example, θ phase calculation relies on the sinusoidal assumption, while human θ (either EEG or hippocampal θ) is not sinusoidal-like. Although rodent θ is sinusoidal and an increase in δ power does occur after experimental stroke, deciphering clear θ epochs from other frequency bands is no easy task. In addition to technical constraints, recording human hippocampal θ is rare and not favored in the clinic due to its risk. Nonetheless, using a rat model of MCA stroke with injury restricted to the parietal cortex, we found that stroke caused (1) an immediate transition to the slow-wave sleep state, (2) a decrease in low-γ power, and (3) a decrease in θ frequency in the hippocampus, a brain region remote from the ischemic site that shows no structural damage (Figure 2). It also appeared that in the ipsilateral hippocampus, the modulation index (as a measure of the strength of the θ phase modulating

the low-γ power) was reduced in the initial first hour after stroke onset. Following reperfusion of the common carotid arteries (CCAs), low-γ power remained to be reduced, suggesting a disrupted connectivity between the cortex and the hippocampus necessary for processing spatial information.

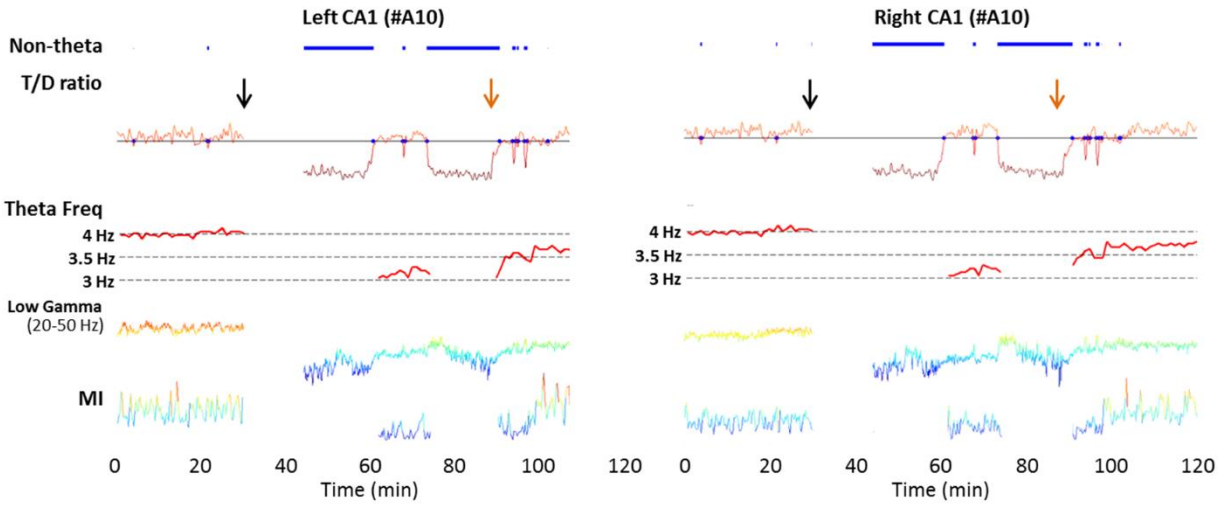


**Figure 2.** Acute cortical ischemia induces a reduction in the hippocampal θ frequency and the θ/δ ratio. Extracellular recordings were performed using multisite silicon probes (A1X16-5mm-100-703, NeuroNexus Technologies) under urethane anesthesia for 2 h. Data from the channel located at the stratum lacunosum moleculare were used for the analysis based on the high signal-to-noise ratio of θ and low-γ oscillations at the molecular layer compared to other hippocampal layers. Experimental stroke was induced by a permanent occlusion of the left, distal MCA and temporary occlusion of the bilateral common carotid arteries (CCAs) for 60 minutes. An immediate transition to slow-wave sleep from θ state occurred after MCAO, followed by the return of the θ state after reperfusion. Reductions in θ frequency, θ/δ (T/D) ratio, and modulation index between θ and low γ ($MI_{Low\ \gamma}$) and a decrease in low γ power were evident during some periods of occlusion and reperfusion. MI was computed based on Tort *et al*., (2010) with the band-pass filter set at 20–50 Hz [216], corresponding to the low-γ power modulated by the θ phase. Color: relative values of low-γ power or modulation index (warmer color reflects larger value). Black arrows: stroke onset at 30 min; orange arrows: start of the reperfusion of the bilateral common carotid arteries at 60 min after stroke. Blue line: Non-theta periods. Note: recording of the initial period after MCAO was temporarily interrupted due to ischemic surgery.

## 7. Conclusions

In summary, although the quest to understand the electrical activity in the brain commenced

more than a century ago, ever-growing endeavors in this area continue to thrive upon the improvement of technology. In light of the continuum in brain oscillations in the spectrum domain, it seems futile to attribute the behavioral states, anatomical structures, or even cellular mechanisms exclusively to a single, specific frequency band. Nonetheless, with some exceptions, a general consensus is reached that an increase in the slow band frequencies, referred to as slow oscillation and δ oscillation, is associated with not only the slow-wave sleep state but also brain ischemia. Conversely, high band frequencies, such as the α, β, and γ oscillations, are associated with awake states or cognitive task engagement, and their presence frequently reduces after stroke. To harmonize with the various physiological states such as the wakefulness phase and sleeping phase, the mammalian brain rhythms are modulated according to the degree of arousal. The oscillations in the membrane potential may underlie the coherent responses of cortical and thalamic neurons to communications from the outside world during awake states and from inside during sleep. Since all the cortical rhythms are modulated by the ascending brainstem reticular-activated system, it nominates the thalamus as a potential candidate for the supervision of the electrical activity in the brain. The immediate EEG changes observed after stroke are a direct consequence caused by the reduction of the cerebral blood flow that later results in neuronal impairment or neuronal death. This cellular impairment in turn leads to a disorganization of the electrical activity that is reflected by the global EEG changes. Individual or derived EEG parameters have been insightful in the diagnosis of ischemic stroke and prognosis of the outcomes after stroke. The utility of EEG as a potential biomarker for stroke outcome and therapeutic efficacy warrants more validation.

**Acknowledgments**

This work was supported by NIH grant R01 NS071050 (Jia-Ling Liu), VA merit award I01RX000655 (Jia-Ling Liu) and American Heart Association EIA 0940065N (Jia-Ling Liu).

**Conflicts of interest**

The authors declare no conflict of interest.

## References


1. Sanei, S.; Chambers, J. A.; Sanei, S.; Chambers, J. A., Fundamentals of EEG Signal Processing. In *EEG Signal Processing*, John Wiley & Sons Ltd: **2007**; pp 35-125.

2. Acar, E.; Aykut-Bingol, C.; Bingol, H.; Bro, R.; Yener, B., Multiway analysis of epilepsy tensors. *Bioinformatics* **2007,** 23, (13), i10-8.

3. Normann, R. A.; Maynard, E. M.; Rousche, P. J.; Warren, D. J., A neural interface for a cortical vision prosthesis. *Vision Res* **1999,** 39, (15), 2577-87.

4. Lebedev, M. A.; Nicolelis, M. A., Brain-machine interfaces: past, present and future. *Trends Neurosci* **2006,** 29, (9), 536-46.

5. Beck, A., Die Bestimmung der Localisation der Gehirn- und Rückenmarksfunctionen vermittelst der elektrischen Erscheinungen. [The determination of the localisation of the brain and spinal cord functions by way of electrical appearances]. *Centralblatt für Physiologie* **1890,** 4, 473–476.

6. Berger, H., Über das elektrenkephalogramm des menschen. *European Archives of Psychiatry and Clinical Neuroscience* **1929,** 87, (1), 527-570.

7. Buzsaki, G.; Draguhn, A., Neuronal oscillations in cortical networks. *Science (New York, N.Y.)* **2004,** 304, (5679), 1926-9.

8. Steriade, M.; Nunez, A.; Amzica, F., A novel slow (< 1 Hz) oscillation of neocortical neurons in vivo: depolarizing and hyperpolarizing components. *The Journal of neuroscience : the official journal of the Society for Neuroscience* **1993,** 13, (8), 3252-65.

9. Bragin, A.; Engel, J., Jr.; Wilson, C. L.; Fried, I.; Buzsaki, G., High-frequency oscillations in human brain. *Hippocampus* **1999,** 9, (2), 137-42.

10. Ferri, R.; Cosentino, F. I.; Elia, M.; Musumeci, S. A.; Marinig, R.; Bergonzi, P., Relationship between Delta, Sigma, Beta, and Gamma EEG bands at REM sleep onset and REM sleep end. *Clin Neurophysiol* **2001,** 112, (11), 2046-52.

11. Engel, J., Jr.; Bragin, A.; Staba, R.; Mody, I., High-frequency oscillations: what is normal and what is not? *Epilepsia* **2009,** 50, (4), 598-604.

12. Pignatelli, M.; Beyeler, A.; Leinekugel, X., Neural circuits underlying the generation of theta oscillations. *J Physiol Paris* **2012,** 106, (3-4), 81-92.

13. McCormick, D. A.; Pape, H. C., Noradrenergic and serotonergic modulation of a hyperpolarization-activated cation current in thalamic relay neurones. *The Journal of physiology* **1990,** 431, 319-42.

14. Ball, G. J.; Gloor, P.; Schaul, N., The cortical electromicrophysiology of pathological delta waves in the electroencephalogram of cats. *Electroencephalogr Clin Neurophysiol* **1977,** 43, (3), 346-61.

15. Plouin, P.; Kaminska, A.; Moutard, M. L.; Soufflet, C., Developmental aspects of normal EEG. *Handb Clin Neurol* **2013,** 111, 79-85.

16. Lu, X. C.; Williams, A. J.; Tortella, F. C., Quantitative electroencephalography spectral analysis and topographic mapping in a rat model of middle cerebral artery occlusion. *Neuropathol Appl Neurobiol* **2001,** 27, (6), 481-95.

17. Zhang, S. J.; Ke, Z.; Li, L.; Yip, S. P.; Tong, K. Y., EEG patterns from acute to chronic stroke phases in focal cerebral ischemic rats: correlations with functional recovery. *Physiol Meas* **2013,** 34, (4), 423-35.

18. Steriade, M., Impact of network activities on neuronal properties in corticothalamic systems. *Journal of neurophysiology* **2001,** 86, (1), 1-39.

19. Csicsvari, J.; Jamieson, B.; Wise, K. D.; Buzsaki, G., Mechanisms of gamma oscillations in the hippocampus of the behaving rat. *Neuron* **2003,** 37, (2), 311-22.

20. Olejniczak, P., Neurophysiologic basis of EEG. *J Clin Neurophysiol* **2006,** 23, (3), 186-9.

21. Llinas, R. R., The intrinsic electrophysiological properties of mammalian neurons: insights into central nervous system function. *Science (New York, N.Y.)* **1988,** 242, (4886), 1654-64.

22. Crunelli, V.; Hughes, S. W., The slow (<1 Hz) rhythm of non-REM sleep: a dialogue between three cardinal oscillators. *Nature neuroscience* **2010,** 13, (1), 9-17.

23. Green, J. D.; Arduini, A. A., Hippocampal electrical activity in arousal. *Journal of neurophysiology* **1954,** 17, (6), 533-57.

24. Sirota, A.; Montgomery, S.; Fujisawa, S.; Isomura, Y.; Zugaro, M.; Buzsaki, G., Entrainment of neocortical neurons and gamma oscillations by the hippocampal theta rhythm. *Neuron* **2008,** 60, (4), 683-97.

25. Monmaur, P.; Allix, M.; Schoevaert-Brossault, D.; Houcine, O.; Plotkine, M.; Willig, F., Effects of transient cerebral ischemia on the hippocampal dentate theta (theta) profile in the acute rat: a study 4-5 months following recirculation. *Brain Res* **1990,** 508, (1), 124-34.

26. Adey, W. R., EEG patterns in sleep and wakefulness in high spinal cord injuries. *Proc Annu Clin Spinal Cord Inj Conf* **1967,** 16, 2-9.

27. Mitchell, S. J.; Ranck, J. B., Jr., Generation of theta rhythm in medial entorhinal cortex of freely moving rats. *Brain research* **1980,** 189, (1), 49-66.

28. Alonso, A.; Garcia-Austt, E., Neuronal sources of theta rhythm in the entorhinal cortex of the rat. II. Phase relations between unit discharges and theta field potentials. *Experimental brain research* **1987,** 67, (3), 502-9.

29. Leung, L. W.; Borst, J. G., Electrical activity of the cingulate cortex. I. Generating mechanisms and relations to behavior. *Brain research* **1987,** 407, (1), 68-80.

30. Pare, D.; Collins, D. R., Neuronal correlates of fear in the lateral amygdala: multiple extracellular recordings in conscious cats. *The Journal of neuroscience : the official journal of the Society for Neuroscience* **2000,** 20, (7), 2701-10.

31. Hari, R.; Salmelin, R.; Makela, J. P.; Salenius, S.; Helle, M., Magnetoencephalographic cortical rhythms. *Int J Psychophysiol* **1997,** 26, (1-3), 51-62.

32. Buffalo, E. A.; Fries, P.; Landman, R.; Buschman, T. J.; Desimone, R., Laminar differences in gamma and alpha coherence in the ventral stream. *Proceedings of the National Academy of Sciences of the United States of America* **2011,** 108, (27), 11262-7.

33. Roopun, A. K.; Middleton, S. J.; Cunningham, M. O.; LeBeau, F. E.; Bibbig, A.; Whittington, M. A.; Traub, R. D., A beta2-frequency (20-30 Hz) oscillation in nonsynaptic networks of somatosensory cortex. *Proceedings of the National Academy of Sciences of the United States of America* **2006,** 103, (42), 15646-50.

34. Basar, E.; Schurmann, M.; Basar-Eroglu, C.; Karakas, S., Alpha oscillations in brain functioning: an integrative theory. *Int J Psychophysiol* **1997,** 26, (1-3), 5-29.

35. Steriade, M.; McCormick, D. A.; Sejnowski, T. J., Thalamocortical oscillations in the sleeping and aroused brain. *Science (New York, N.Y.)* **1993,** 262, (5134), 679-85.

36. Sauseng, P.; Klimesch, W.; Gruber, W. R.; Hanslmayr, S.; Freunberger, R.; Doppelmayr, M., Are event-related potential components generated by phase resetting of brain oscillations? A critical discussion. *Neuroscience* **2007,** 146, (4), 1435-44.

37. da Silva, F. H.; van Lierop, T. H.; Schrijer, C. F.; van Leeuwen, W. S., Organization of thalamic and cortical alpha rhythms: spectra and coherences. *Electroencephalogr Clin Neurophysiol* **1973,** 35, (6), 627-39.

38. Ohmoto, T.; Mimura, Y.; Baba, Y.; Miyamoto, T.; Matsumoto, Y.; Nishimoto, A.; Matsumoto, K., Thalamic control of spontaneous alpha-rhythm and evoked responses. *Appl Neurophysiol* **1978,** 41, (1-4), 188-92.

39. Terao, Y.; Sakurai, Y.; Sakuta, M.; Ishii, K.; Sugishita, M., [FDG-PET in an amnestic and hypersomnic patient with bilateral paramedian thalamic infarction]. *Rinsho Shinkeigaku* **1993,** 33, (9), 951-6.

40. Goldman, R. I.; Stern, J. M.; Engel, J., Jr.; Cohen, M. S., Simultaneous EEG and fMRI of the alpha rhythm. *Neuroreport* **2002,** 13, (18), 2487-92.

41. Feige, B.; Scheffler, K.; Esposito, F.; Di Salle, F.; Hennig, J.; Seifritz, E., Cortical and subcortical correlates of electroencephalographic alpha rhythm modulation. *Journal of neurophysiology* **2005,** 93, (5), 2864-72.

42. Sadato, N.; Nakamura, S.; Oohashi, T.; Nishina, E.; Fuwamoto, Y.; Waki, A.; Yonekura, Y., Neural networks for generation and suppression of alpha rhythm: a PET study. *Neuroreport* **1998,** 9, (5), 893-7.

43. Crone, N. E.; Miglioretti, D. L.; Gordon, B.; Lesser, R. P., Functional mapping of human sensorimotor cortex with electrocorticographic spectral analysis. II. Event-related synchronization in the gamma band. *Brain* **1998,** 121 ( Pt 12), 2301-15.

44. Tallon-Baudry, C.; Bertrand, O.; Delpuech, C.; Pernier, J., Stimulus specificity of phase-locked and non-phase-locked 40 Hz visual responses in human. *The Journal of neuroscience : the official journal of the Society for Neuroscience* **1996,** 16, (13), 4240-9.

45. Basar, E.; Basar-Eroglu, C.; Karakas, S.; Schurmann, M., Brain oscillations in perception and memory. *Int J Psychophysiol* **2000,** 35, (2-3), 95-124.

46. Basar, E.; Rahn, E.; Demiralp, T.; Schurmann, M., Spontaneous EEG theta activity controls frontal visual evoked potential amplitudes. *Electroencephalogr Clin Neurophysiol* **1998,** 108, (2), 101-9.

47. Buhl, E. H.; Tamas, G.; Fisahn, A., Cholinergic activation and tonic excitation induce persistent gamma oscillations in mouse somatosensory cortex in vitro. *The Journal of physiology* **1998,** 513 ( Pt 1), 117-26.

48. Gray, C. M.; McCormick, D. A., Chattering cells: superficial pyramidal neurons contributing to the generation of synchronous oscillations in the visual cortex. *Science (New York, N.Y.)* **1996,** 274, (5284), 109-13.

49. Whittington, M. A.; Traub, R. D.; Jefferys, J. G., Synchronized oscillations in interneuron networks driven by metabotropic glutamate receptor activation. *Nature* **1995,** 373, (6515), 612-5.

50. Macdonald, K. D.; Fifkova, E.; Jones, M. S.; Barth, D. S., Focal stimulation of the thalamic reticular nucleus induces focal gamma waves in cortex. *J Neurophysiol* **1998,** 79, (1), 474-7.

51. Bringuier, V.; Fregnac, Y.; Baranyi, A.; Debanne, D.; Shulz, D. E., Synaptic origin and stimulus dependency of neuronal oscillatory activity in the primary visual cortex of the cat. *The Journal of physiology* **1997,** 500 ( Pt 3), 751-74.

52. Cardin, J. A.; Palmer, L. A.; Contreras, D., Stimulus-dependent gamma (30-50 Hz) oscillations in simple and complex fast rhythmic bursting cells in primary visual cortex. *The Journal of neuroscience : the official journal of the Society for Neuroscience* **2005,** 25, (22), 5339-50.

53. Whittington, M. A.; Traub, R. D.; Faulkner, H. J.; Stanford, I. M.; Jefferys, J. G., Recurrent excitatory postsynaptic potentials induced by synchronized fast cortical oscillations. *Proceedings of the National Academy of Sciences of the United States of America* **1997,** 94, (22), 12198-203.

54. Traub, R. D.; Whittington, M. A.; Buhl, E. H.; Jefferys, J. G.; Faulkner, H. J., On the mechanism of the gamma --> beta frequency shift in neuronal oscillations induced in rat hippocampal slices by tetanic stimulation. *The Journal of neuroscience : the official journal of the Society for Neuroscience* **1999,** 19, (3), 1088-105.

55. Colling, S. B.; Stanford, I. M.; Traub, R. D.; Jefferys, J. G., Limbic gamma rhythms. I. Phase-locked oscillations in hippocampal CA1 and subiculum. *Journal of neurophysiology* **1998,** 80, (1), 155-61.

56. Steriade, M.; Timofeev, I., Neuronal plasticity in thalamocortical networks during sleep and waking oscillations. *Neuron* **2003,** 37, (4), 563-76.

57. Basar, E.; Basar-Eroglu, C.; Karakas, S.; Schurmann, M., Gamma, alpha, delta, and theta oscillations govern cognitive processes. *Int J Psychophysiol* **2001,** 39, (2-3), 241-8.

58. Tononi, G.; Cirelli, C., Time to be SHY? Some comments on sleep and synaptic homeostasis. *Neural Plast* **2012,** 2012, 415250.

59. Assenza, G.; Pellegrino, G.; Tombini, M.; Di Pino, G.; Di Lazzaro, V., Wakefulness delta waves increase after cortical plasticity induction. *Clin Neurophysiol* **2015,** 126, (6), 1221-7.

60. Tononi, G.; Cirelli, C., Sleep and the price of plasticity: from synaptic and cellular homeostasis to memory consolidation and integration. *Neuron* **2014,** 81, (1), 12-34.

61. Gorgoni, M.; D'Atri, A.; Lauri, G.; Rossini, P. M.; Ferlazzo, F.; De Gennaro, L., Is sleep essential for neural plasticity in humans, and how does it affect motor and cognitive recovery? *Neural Plast* **2013,** 2013, 103949.

62. Llinas, R.; Ribary, U., Coherent 40-Hz oscillation characterizes dream state in humans. *Proceedings of the National Academy of Sciences of the United States of America* **1993,** 90, (5), 2078-81.

63. Destexhe, A.; Sejnowski, T. J., Interactions between membrane conductances underlying thalamocortical slow-wave oscillations. *Physiol Rev* **2003,** 83, (4), 1401-53.

64. Singer, W., Neuronal synchrony: a versatile code for the definition of relations? *Neuron* **1999,** 24, (1), 49-65, 111-25.

65. Varela, F.; Lachaux, J. P.; Rodriguez, E.; Martinerie, J., The brainweb: phase synchronization and large-scale integration. *Nature reviews. Neuroscience* **2001,** 2, (4), 229-39.

66. Bragin, A.; Engel, J., Jr.; Staba, R. J., High-frequency oscillations in epileptic brain. *Curr Opin Neurol* **2010,** 23, (2), 151-6.

67. Engel, A. K.; Fries, P., Beta-band oscillations--signalling the status quo? *Current opinion in neurobiology* **2010,** 20, (2), 156-65.

68. Kisley, M. A.; Cornwell, Z. M., Gamma and beta neural activity evoked during a sensory gating paradigm: effects of auditory, somatosensory and cross-modal stimulation. *Clin Neurophysiol* **2006,** 117, (11), 2549-63.

69. Uhlhaas, P. J.; Haenschel, C.; Nikolic, D.; Singer, W., The role of oscillations and synchrony in cortical networks and their putative relevance for the pathophysiology of schizophrenia. *Schizophr Bull* **2008,** 34, (5), 927-43.

70. Haenschel, C.; Baldeweg, T.; Croft, R. J.; Whittington, M.; Gruzelier, J., Gamma and beta frequency oscillations in response to novel auditory stimuli: A comparison of human electroencephalogram (EEG) data with in vitro models. *Proc Natl Acad Sci U S A* **2000,** 97, (13), 7645-50.

71. Marco-Pallares, J.; Cucurell, D.; Cunillera, T.; Garcia, R.; Andres-Pueyo, A.; Munte, T. F.; Rodriguez-Fornells, A., Human oscillatory activity associated to reward processing in a gambling task. *Neuropsychologia* **2008,** 46, (1), 241-8.

72. Hasselmo, M. E., What is the function of hippocampal theta rhythm?--Linking behavioral data to phasic properties of field potential and unit recording data. *Hippocampus* **2005,** 15, (7), 936-49.

73. Kahana, M. J.; Seelig, D.; Madsen, J. R., Theta returns. *Current opinion in neurobiology* **2001,** 11, (6), 739-44.

74. Burgess, A. P.; Gruzelier, J. H., Short duration power changes in the EEG during recognition memory for words and faces. *Psychophysiology* **2000,** 37, (5), 596-606.

75. Krause, C. M.; Sillanmaki, L.; Koivisto, M.; Saarela, C.; Haggqvist, A.; Laine, M.; Hamalainen, H., The effects of memory load on event-related EEG desynchronization and synchronization. *Clin Neurophysiol* **2000,** 111, (11), 2071-8.

76. Palva, S.; Palva, J. M., New vistas for alpha-frequency band oscillations. *Trends Neurosci* **2007,** 30, (4), 150-8.

77. Steriade, M., Arousal: revisiting the reticular activating system. *Science (New York, N.Y.)* **1996,** 272, (5259), 225-6.

78. Evans, B. M., Patterns of arousal in comatose patients. *J Neurol Neurosurg Psychiatry* **1976,** 39, (4), 392-402.

79. Garcia-Rill, E.; Kezunovic, N.; Hyde, J.; Simon, C.; Beck, P.; Urbano, F. J., Coherence and frequency in the reticular activating system (RAS). *Sleep Med Rev* **2013,** 17, (3), 227-38.

80. Harris, K. D.; Thiele, A., Cortical state and attention. *Nature reviews. Neuroscience* **2011,** 12, (9), 509-23.

81. Buzsaki, G., Theta oscillations in the hippocampus. *Neuron* **2002,** 33, (3), 325-40.

82. Vanderwolf, C. H., Recovery from large medial thalamic lesions as a result of electroconvulsive therapy. *J Neurol Neurosurg Psychiatry* **1968,** 31, (1), 67-72.

83. Vertes, R. P., Hippocampal theta rhythm: a tag for short-term memory. *Hippocampus* **2005,** 15, (7), 923-35.

84. Stewart, M.; Fox, S. E., Hippocampal theta activity in monkeys. *Brain research* **1991,** 538, (1), 59-63.

85. Chrobak, J. J.; Buzsaki, G., High-frequency oscillations in the output networks of the hippocampal-entorhinal axis of the freely behaving rat. *The Journal of neuroscience : the official journal of the Society for Neuroscience* **1996,** 16, (9), 3056-66.

86. Jadhav, S. P.; Kemere, C.; German, P. W.; Frank, L. M., Awake hippocampal sharp-wave ripples support spatial memory. *Science (New York, N.Y.)* **2012,** 336, (6087), 1454-8.

87. Girardeau, G.; Benchenane, K.; Wiener, S. I.; Buzsaki, G.; Zugaro, M. B., Selective suppression of hippocampal ripples impairs spatial memory. *Nature neuroscience* **2009,** 12, (10), 1222-3.

88. Schurmann, M.; Basar-Eroglu, C.; Basar, E., Gamma responses in the EEG: elementary signals with multiple functional correlates. *Neuroreport* **1997,** 8, (7), 1793-6.

89. Bragin, A.; Jando, G.; Nadasdy, Z.; Hetke, J.; Wise, K.; Buzsaki, G., Gamma (40-100 Hz) oscillation in the hippocampus of the behaving rat. *The Journal of neuroscience : the official journal of the Society for Neuroscience* **1995,** 15, (1 Pt 1), 47-60.

90. Poulet, J. F.; Petersen, C. C., Internal brain state regulates membrane potential synchrony in barrel cortex of behaving mice. *Nature* **2008,** 454, (7206), 881-5.

91. Crochet, S.; Petersen, C. C., Correlating whisker behavior with membrane potential in barrel cortex of awake mice. *Nat Neurosci* **2006,** 9, (5), 608-10.

92. Niell, C. M.; Stryker, M. P., Modulation of visual responses by behavioral state in mouse visual cortex. *Neuron* **2010,** 65, (4), 472-9.

93. Clement, E. A.; Richard, A.; Thwaites, M.; Ailon, J.; Peters, S.; Dickson, C. T., Cyclic and sleep-like spontaneous alternations of brain state under urethane anaesthesia. *PLoS One* **2008,** 3, (4), e2004.

94. Renart, A.; de la Rocha, J.; Bartho, P.; Hollender, L.; Parga, N.; Reyes, A.; Harris, K. D., The asynchronous state in cortical circuits. *Science (New York, N.Y.)* **2010,** 327, (5965), 587-90.

95. Ribeiro, T. L.; Copelli, M.; Caixeta, F.; Belchior, H.; Chialvo, D. R.; Nicolelis, M. A.; Ribeiro, S., Spike avalanches exhibit universal dynamics across the sleep-wake cycle. *PLoS One* **2010,** 5, (11), e14129.

96. Okun, M.; Naim, A.; Lampl, I., The subthreshold relation between cortical local field potential and neuronal firing unveiled by intracellular recordings in awake rats. *The Journal of neuroscience : the official journal of the Society for Neuroscience* **2010,** 30, (12), 4440-8.

97. Poulet, J. F.; Fernandez, L. M.; Crochet, S.; Petersen, C. C., Thalamic control of cortical states. *Nature neuroscience* **2012,** 15, (3), 370-2.

98. Munk, M. H.; Roelfsema, P. R.; Konig, P.; Engel, A. K.; Singer, W., Role of reticular activation in the modulation of intracortical synchronization. *Science (New York, N.Y.)* **1996,** 272, (5259), 271-4.

99. Fries, P.; Reynolds, J. H.; Rorie, A. E.; Desimone, R., Modulation of oscillatory neuronal synchronization by selective visual attention. *Science (New York, N.Y.)* **2001,** 291, (5508), 1560-3.

100. Chalk, M.; Herrero, J. L.; Gieselmann, M. A.; Delicato, L. S.; Gotthardt, S.; Thiele, A., Attention reduces stimulus-driven gamma frequency oscillations and spike field coherence in V1. *Neuron* **2010,** 66, (1), 114-25.

101. Puig, M. V.; Watakabe, A.; Ushimaru, M.; Yamamori, T.; Kawaguchi, Y., Serotonin modulates fast-spiking interneuron and synchronous activity in the rat prefrontal cortex through 5-HT1A and 5-HT2A receptors. *The Journal of neuroscience : the official journal of the Society for Neuroscience* **2010,** 30, (6), 2211-22.

102. Gervasoni, D.; Lin, S. C.; Ribeiro, S.; Soares, E. S.; Pantoja, J.; Nicolelis, M. A., Global forebrain dynamics predict rat behavioral states and their transitions. *The Journal of neuroscience : the official journal of the Society for Neuroscience* **2004,** 24, (49), 11137-47.

103. Cantero, J. L.; Atienza, M.; Stickgold, R.; Kahana, M. J.; Madsen, J. R.; Kocsis, B., Sleep-dependent theta oscillations in the human hippocampus and neocortex. *The Journal of neuroscience : the official journal of the Society for Neuroscience* **2003,** 23, (34), 10897-903.

104. Watrous, A. J.; Lee, D. J.; Izadi, A.; Gurkoff, G. G.; Shahlaie, K.; Ekstrom, A. D., A comparative study of human and rat hippocampal low-frequency oscillations during spatial navigation. *Hippocampus* **2013,** 23, (8), 656-61.

105. Axmacher, N.; Henseler, M. M.; Jensen, O.; Weinreich, I.; Elger, C. E.; Fell, J., Cross-frequency coupling supports multi-item working memory in the human hippocampus. *Proceedings of the National Academy of Sciences of the United States of America* **2010,** 107, (7), 3228-33.

106. Canolty, R. T.; Edwards, E.; Dalal, S. S.; Soltani, M.; Nagarajan, S. S.; Kirsch, H. E.; Berger, M. S.; Barbaro, N. M.; Knight, R. T., High gamma power is phase-locked to theta oscillations in human neocortex. *Science (New York, N.Y.)* **2006,** 313, (5793), 1626-8.

107. Kahana, M. J., The cognitive correlates of human brain oscillations. *The Journal of neuroscience : the official journal of the Society for Neuroscience* **2006,** 26, (6), 1669-72.

108. Miller, K. J.; Leuthardt, E. C.; Schalk, G.; Rao, R. P.; Anderson, N. R.; Moran, D. W.; Miller, J. W.; Ojemann, J. G., Spectral changes in cortical surface potentials during motor movement. *The Journal of neuroscience : the official journal of the Society for Neuroscience* **2007,** 27, (9), 2424-32.

109. Ebersole, J. S., *Cortical generators and EEG voltage fields*. Philadelphia: Lippincott Williams & Wilkins: **2003**; p 12-31.

110. Freeman, W. J., The physiology of perception. *Sci Am* **1991,** 264, (2), 78-85.

111. Borgers, C.; Kopell, N., Effects of noisy drive on rhythms in networks of excitatory and inhibitory neurons. *Neural Comput* **2005,** 17, (3), 557-608.

112. Erdemli, G.; Crunelli, V., Response of thalamocortical neurons to hypoxia: a whole-cell patch-clamp study. *The Journal of neuroscience : the official journal of the Society for Neuroscience* **1998,** 18, (14), 5212-24.

113. Krnjevic, K., Electrophysiology of cerebral ischemia. *Neuropharmacology* **2008,** 55, (3), 319-33.

114. Gloor, P., Neuronal generators and the problem of localization in electroencephalography: application of volume conductor theory to electroencephalography. *J Clin Neurophysiol* **1985,** 2, (4), 327-54.

115. Dirnagl, U.; Iadecola, C.; Moskowitz, M. A., Pathobiology of ischaemic stroke: an integrated view. *Trends Neurosci* **1999,** 22, (9), 391-7.

116. Winship, I. R.; Murphy, T. H., In vivo calcium imaging reveals functional rewiring of single somatosensory neurons after stroke. *The Journal of neuroscience : the official journal of the Society for Neuroscience* **2008,** 28, (26), 6592-606.

117. Schiene, K.; Bruehl, C.; Zilles, K.; Qu, M.; Hagemann, G.; Kraemer, M.; Witte, O. W., Neuronal hyperexcitability and reduction of GABAA-receptor expression in the surround of cerebral photothrombosis. *Journal of cerebral blood flow and metabolism : official journal of the International Society of Cerebral Blood Flow and Metabolism* **1996,** 16, (5), 906-14.

118. Kelley, M. H.; Taguchi, N.; Ardeshiri, A.; Kuroiwa, M.; Hurn, P. D.; Traystman, R. J.; Herson, P. S., Ischemic insult to cerebellar Purkinje cells causes diminished GABA(A) receptor function and Allopregnanolone neuroprotection is associated with GABA(A) receptor stabilization. *Journal of neurochemistry* **2008,** 107, (3), 668-678.

119. Carmichael, S. T.; Chesselet, M. F., Synchronous neuronal activity is a signal for axonal sprouting after cortical lesions in the adult. *J Neurosci* **2002,** 22, (14), 6062-70.

120. Carmichael, S. T., Cellular and molecular mechanisms of neural repair after stroke: making waves. *Ann Neurol* **2006,** 59, (5), 735-42.

121. Brown, C. E.; Li, P.; Boyd, J. D.; Delaney, K. R.; Murphy, T. H., Extensive turnover of dendritic spines and vascular remodeling in cortical tissues recovering from stroke. *The Journal of neuroscience : the official journal of the Society for Neuroscience* **2007,** 27, (15), 4101-9.

122. Bender, J. E.; Vishwanath, K.; Moore, L. K.; Brown, J. Q.; Chang, V.; Palmer, G. M.; Ramanujam, N., A robust Monte Carlo model for the extraction of biological absorption and scattering in vivo. *IEEE Trans Biomed Eng* **2009,** 56, (4), 960-8.

123. Luhmann, H. J.; Heinemann, U., Hypoxia-induced functional alterations in adult rat neocortex. *Journal of neurophysiology* **1992,** 67, (4), 798-811.

124. Calabresi, P.; Pisani, A.; Mercuri, N. B.; Bernardi, G., Hypoxia-induced electrical changes in striatal neurons. *Journal of cerebral blood flow and metabolism : official journal of the International Society of Cerebral Blood Flow and Metabolism* **1995,** 15, (6), 1141-5.

125. Jiang, C.; Sigworth, F. J.; Haddad, G. G., Oxygen deprivation activates an ATP-inhibitable K+ channel in substantia nigra neurons. *The Journal of neuroscience : the official journal of the Society for Neuroscience* **1994,** 14, (9), 5590-602.

126. Spuler, A.; Grafe, P., Adenosine, 'pertussis-sensitive' G-proteins, and K+ conductance in central mammalian neurones under energy deprivation. *Neurosci Lett* **1989,** 98, (3), 280-4.

127. Knopfel, T.; Spuler, A.; Grafe, P.; Gahwiler, B. H., Cytosolic calcium during glucose deprivation in hippocampal pyramidal cells of rats. *Neurosci Lett* **1990,** 117, (3), 295-9.

128. Harata, N.; Wu, J.; Ishibashi, H.; Ono, K.; Akaike, N., Run-down of the GABAA response under experimental ischaemia in acutely dissociated CA1 pyramidal neurones of the rat. *The Journal of physiology* **1997,** 500 ( Pt 3), 673-88.

129. Tanaka, E.; Yamamoto, S.; Kudo, Y.; Mihara, S.; Higashi, H., Mechanisms underlying the rapid depolarization produced by deprivation of oxygen and glucose in rat hippocampal CA1 neurons in vitro. *Journal of neurophysiology* **1997,** 78, (2), 891-902.

130. Rosen, A. S.; Morris, M. E., Depolarizing effects of anoxia on pyramidal cells of rat neocortex. *Neurosci Lett* **1991,** 124, (2), 169-73.

131. Krnjevic, K.; Xu, Y. Z., Dantrolene suppresses the hyperpolarization or outward current observed during anoxia in hippocampal neurons. *Can J Physiol Pharmacol* **1989,** 67, (12), 1602-4.

132. Englund, M.; Hyllienmark, L.; Brismar, T., Chemical hypoxia in hippocampal pyramidal cells affects membrane potential differentially depending on resting potential. *Neuroscience* **2001,** 106, (1), 89-94.

133. Jordan, K. G., Emergency EEG and continuous EEG monitoring in acute ischemic stroke. *J Clin Neurophysiol* **2004,** 21, (5), 341-52.

134. Astrup, J.; Siesjo, B. K.; Symon, L., Thresholds in cerebral ischemia - the ischemic penumbra. *Stroke; a journal of cerebral circulation* **1981,** 12, (6), 723-5.

135. Foreman, B.; Claassen, J., Quantitative EEG for the detection of brain ischemia. *Crit Care* **2012,** 16, (2), 216.

136. O'Gorman, R. L.; Poil, S. S.; Brandeis, D.; Klaver, P.; Bollmann, S.; Ghisleni, C.; Luchinger, R.; Martin, E.; Shankaranarayanan, A.; Alsop, D. C.; Michels, L., Coupling between resting cerebral perfusion and EEG. *Brain Topogr* **2013,** 26, (3), 442-57.

137. Lennox, W. G.; Gibbs, F. A.; Gibbs, E. I., The Relationship in Man of Cerebral Activity to Blood Flow and to Blood Constituents. *J Neurol Psychiatry* **1938,** 1, (3), 211-25.

138. Faught, E., Current role of electroencephalography in cerebral ischemia. *Stroke; a journal of cerebral circulation* **1993,** 24, (4), 609-13.

139. Branston, N. M.; Symon, L.; Crockard, H. A.; Pasztor, E., Relationship between the cortical evoked potential and local cortical blood flow following acute middle cerebral artery occlusion in the baboon. *Exp Neurol* **1974,** 45, (2), 195-208.

140. Hossmann, K. A., Viability thresholds and the penumbra of focal ischemia. *Ann Neurol* **1994,** 36, (4), 557-65.

141. Sharbrough, F. W.; Messick, J. M., Jr.; Sundt, T. M., Jr., Correlation of continuous electroencephalograms with cerebral blood flow measurements during carotid endarterectomy. *Stroke* **1973,** 4, (4), 674-83.

142. Gallinat, J.; Kunz, D.; Senkowski, D.; Kienast, T.; Seifert, F.; Schubert, F.; Heinz, A., Hippocampal glutamate concentration predicts cerebral theta oscillations during cognitive processing. *Psychopharmacology (Berl)* **2006,** 187, (1), 103-11.

143. Dreier, J. P.; Major, S.; Manning, A.; Woitzik, J.; Drenckhahn, C.; Steinbrink, J.; Tolias, C.; Oliveira-Ferreira, A. I.; Fabricius, M.; Hartings, J. A.; Vajkoczy, P.; Lauritzen, M.; Dirnagl, U.; Bohner, G.; Strong, A. J.; group, C. s., Cortical spreading ischaemia is a novel process involved in ischaemic damage in patients with aneurysmal subarachnoid haemorrhage. *Brain* **2009,** 132, (Pt 7), 1866-81.

144. Guyot, L. L.; Diaz, F. G.; O'Regan, M. H.; McLeod, S.; Park, H.; Phillis, J. W., Real-time measurement of glutamate release from the ischemic penumbra of the rat cerebral cortex using a focal middle cerebral artery occlusion model. *Neurosci Lett* **2001,** 299, (1-2), 37-40.

145. Nagata, K.; Tagawa, K.; Hiroi, S.; Shishido, F.; Uemura, K., Electroencephalographic correlates of blood flow and oxygen metabolism provided by positron emission tomography in patients with cerebral infarction. *Electroencephalogr Clin Neurophysiol* **1989,** 72, (1), 16-30.

146. Powers, W. J., Cerebral hemodynamics in ischemic cerebrovascular disease. *Ann Neurol* **1991,** 29, (3), 231-40.

147. von Bornstadt, D.; Houben, T.; Seidel, J. L.; Zheng, Y.; Dilekoz, E.; Qin, T.; Sandow, N.; Kura, S.; Eikermann-Haerter, K.; Endres, M.; Boas, D. A.; Moskowitz, M. A.; Lo, E. H.; Dreier, J. P.; Woitzik, J.; Sakadzic, S.; Ayata, C., Supply-demand mismatch transients in susceptible peri-infarct hot zones explain the origins of spreading injury depolarizations. *Neuron* **2015,** 85, (5), 1117-31.

148. Ayata, C.; Lauritzen, M., Spreading Depression, Spreading Depolarizations, and the Cerebral Vasculature. *Physiol Rev* **2015,** 95, (3), 953-93.

149. Machado, C.; Cuspineda, E.; Valdes, P.; Virues, T.; Llopis, F.; Bosch, J.; Aubert, E.; Hernandez, E.; Pando, A.; Alvarez, M. A.; Barroso, E.; Galan, L.; Avila, Y., Assessing acute middle cerebral artery ischemic stroke by quantitative electric tomography. *Clin EEG Neurosci* **2004,** 35, (3), 116-24.

150. Sheorajpanday, R. V.; Nagels, G.; Weeren, A. J.; De Surgeloose, D.; De Deyn, P. P., Additional value of quantitative EEG in acute anterior circulation syndrome of presumed ischemic origin. *Clin Neurophysiol* **2010,** 121, (10), 1719-25.

151. Sheorajpanday, R. V.; Nagels, G.; Weeren, A. J.; van Putten, M. J.; De Deyn, P. P., Quantitative EEG in ischemic stroke: correlation with functional status after 6 months. *Clin Neurophysiol* **2011,** 122, (5), 874-83.

152. Wang, Y.; Zhang, X.; Huang, J.; Zhu, M.; Guan, Q.; Liu, C., Associations between EEG beta power abnormality and diagnosis in cognitive impairment post cerebral infarcts. *J Mol Neurosci* **2013,** 49, (3), 632-8.

153. Finnigan, S.; van Putten, M. J., EEG in ischaemic stroke: quantitative EEG can uniquely inform (sub-)acute prognoses and clinical management. *Clin Neurophysiol* **2013,** 124, (1), 10-9.

154. Gloor, P.; Ball, G.; Schaul, N., Brain lesions that produce delta waves in the EEG. *Neurology* **1977,** 27, (4), 326-33.

155. Ginsburg, D. A.; Pasternak, E. B.; Gurvitch, A. M., Correlation analysis of delta activity generated in cerebral hypoxia. *Electroencephalogr Clin Neurophysiol* **1977,** 42, (4), 445-55.

156. Schaul, N.; Gloor, P.; Gotman, J., The EEG in deep midline lesions. *Neurology* **1981,** 31, (2), 157-67.

157. Schaul, N.; Gloor, P.; Ball, G.; Gotman, J., The electromicrophysiology of delta waves induced by systemic atropine. *Brain research* **1978,** 143, (3), 475-86.

158. Moyanova, S. G.; Dijkhuizen, R. M., Present status and future challenges of electroencephalography- and magnetic resonance imaging-based monitoring in preclinical models of focal cerebral ischemia. *Brain Res Bull* **2014,** 102, 22-36.

159. Williams, A. J.; Lu, X. C.; Hartings, J. A.; Tortella, F. C., Neuroprotection assessment by topographic electroencephalographic analysis: effects of a sodium channel blocker to reduce polymorphic delta activity following ischaemic brain injury in rats. *Fundam Clin Pharmacol* **2003,** 17, (5), 581-93.

160. Moyanova, S.; Kortenska, L.; Kirov, R.; Iliev, I., Quantitative electroencephalographic changes due to middle cerebral artery occlusion by endothelin 1 in conscious rats. *Arch Physiol Biochem* **1998,** 106, (5), 384-91.

161. Moyanova, S. G.; Mitreva, R. G.; Kortenska, L. V.; Nicoletti, F.; Ngomba, R. T., Age-dependence of sensorimotor and cerebral electroencephalographic asymmetry in rats subjected to unilateral cerebrovascular stroke. *Exp Transl Stroke Med* **2013,** 5, (1), 13.

162. Moyanova, S. G.; Kortenska, L. V.; Mitreva, R. G.; Pashova, V. D.; Ngomba, R. T.; Nicoletti, F., Multimodal assessment of neuroprotection applied to the use of MK-801 in the endothelin-1 model of transient focal brain ischemia. *Brain research* **2007,** 1153, 58-67.

163. Moyanova, S.; Kortenska, L.; Kirov, R.; Itzev, D.; Usunoff, K., Ketanserin reduces the postischemic EEG and behavioural changes following Endothelin-1-induced occlusion of the middle cerebral artery in conscious rats. *Central European Journal of Medicine* **2008,** 3, (4), 406-416.

164. Zhang, S.; Tong, R.; Zhang, H.; Hu, X.; Zheng, X., A pilot studies in dynamic profile of multi parameters of EEG in a rat model of transient middle cerebral artery occlusion. *Conf Proc IEEE Eng Med Biol Soc* **2006,** 1, 1181-4.

165. Bhattacharya, P.; Pandey, A. K.; Paul, S.; Patnaik, R., Does Piroxicam really protect ischemic neurons and influence neuronal firing in cerebral ischemia? An exploration towards therapeutics. *Med Hypotheses* **2013,** 81, (3), 429-35.

166. Finger, S.; Koehler, P. J.; Jagella, C., The Monakow concept of diaschisis: origins and perspectives. *Archives of Neurology* **2004,** 61, (2), 283-288.

167. von Monakow, C., *Die Lokalisation im Grosshirn: und der Abbau der Funktion durch kortikale Herde*. Verlag von JF Bergmann: 1914; p 26-34.

168. Andrews, R. J., Transhemispheric diaschisis. A review and comment. *Stroke; a journal of cerebral circulation* **1991,** 22, (7), 943-9.

169. Hartings, J. A.; Williams, A. J.; Tortella, F. C., Occurrence of nonconvulsive seizures, periodic epileptiform discharges, and intermittent rhythmic delta activity in rat focal ischemia. *Exp Neurol* **2003,** 179, (2), 139-49.

170. Lammer, A. B.; Beck, A.; Grummich, B.; Forschler, A.; Krugel, T.; Kahn, T.; Schneider, D.; Illes, P.; Franke, H.; Krugel, U., The P2 receptor antagonist PPADS supports recovery from experimental stroke in vivo. *PLoS One* **2011,** 6, (5), e19983.

171. Huchzermeyer, C.; Albus, K.; Gabriel, H. J.; Otahal, J.; Taubenberger, N.; Heinemann, U.; Kovacs, R.; Kann, O., Gamma oscillations and spontaneous network activity in the hippocampus are highly sensitive to decreases in pO2 and concomitant changes in mitochondrial redox state. *The Journal of neuroscience : the official journal of the Society for Neuroscience* **2008,** 28, (5), 1153-62.

172. Kann, O.; Huchzermeyer, C.; Kovacs, R.; Wirtz, S.; Schuelke, M., Gamma oscillations in the hippocampus require high complex I gene expression and strong functional performance of mitochondria. *Brain* **2011,** 134, (Pt 2), 345-58.

173. Williams, A. J.; Tortella, F. C., Neuroprotective effects of the sodium channel blocker RS100642 and attenuation of ischemia-induced brain seizures in the rat. *Brain research* **2002,** 932, (1-2), 45-55.

174. Finnigan, S. P.; Rose, S. E.; Walsh, M.; Griffin, M.; Janke, A. L.; McMahon, K. L.; Gillies, R.; Strudwick, M. W.; Pettigrew, C. M.; Semple, J.; Brown, J.; Brown, P.; Chalk, J. B., Correlation of quantitative EEG in acute ischemic stroke with 30-day NIHSS score: comparison with diffusion and perfusion MRI. *Stroke; a journal of cerebral circulation* **2004,** 35, (4), 899-903.

175. Sheorajpanday, R. V.; Nagels, G.; Weeren, A. J.; van Putten, M. J.; De Deyn, P. P., Reproducibility and clinical relevance of quantitative EEG parameters in cerebral ischemia: a basic approach. *Clin Neurophysiol* **2009,** 120, (5), 845-55.

176. Sundt, T. M., Jr.; Sharbrough, F. W.; Piepgras, D. G.; Kearns, T. P.; Messick, J. M., Jr.; O'Fallon, W. M., Correlation of cerebral blood flow and electroencephalographic

changes during carotid endarterectomy: with results of surgery and hemodynamics of cerebral ischemia. *Mayo Clinic proceedings* **1981,** 56, (9), 533-43.

177. Macdonell, R. A.; Donnan, G. A.; Bladin, P. F.; Berkovic, S. F.; Wriedt, C. H., The electroencephalogram and acute ischemic stroke. Distinguishing cortical from lacunar infarction. *Archives of neurology* **1988,** 45, (5), 520-4.

178. Schneider, A. L.; Jordan, K. G., Regional attenuation without delta (RAWOD): a distinctive EEG pattern that can aid in the diagnosis and management of severe acute ischemic stroke. *American journal of electroneurodiagnostic technology* **2005,** 45, (2), 102-17.

179. Andraus, M. E.; Alves-Leon, S. V., Non-epileptiform EEG abnormalities: an overview. *Arq Neuropsiquiatr* **2011,** 69, (5), 829-35.

180. Alberto, P.; Elisabetta, F.; Paola, R.; Uberto, R.; Alfredo, B., The EEG in lacunar strokes. *Stroke; a journal of cerebral circulation* **1984,** 15, (3), 579-80.

181. Schaul, N., The fundamental neural mechanisms of electroencephalography. *Electroencephalogr Clin Neurophysiol* **1998,** 106, (2), 101-7.

182. Murri, L.; Gori, S.; Massetani, R.; Bonanni, E.; Marcella, F.; Milani, S., Evaluation of acute ischemic stroke using quantitative EEG: a comparison with conventional EEG and CT scan. *Neurophysiologie clinique = Clinical neurophysiology* **1998,** 28, (3), 249-57.

183. Petty, G. W.; Labar, D. R.; Fisch, B. J.; Pedley, T. A.; Mohr, J. P.; Khandji, A., Electroencephalography in lacunar infarction. *Journal of the neurological sciences* **1995,** 134, (1-2), 47-50.

184. Sheorajpanday, R. V.; Nagels, G.; Weeren, A. J.; De Deyn, P. P., Quantitative EEG in ischemic stroke: correlation with infarct volume and functional status in posterior circulation and lacunar syndromes. *Clin Neurophysiol* **2011,** 122, (5), 884-90.

185. Sheorajpanday, R. V.; Marien, P.; Weeren, A. J.; Nagels, G.; Saerens, J.; van Putten, M. J.; De Deyn, P. P., EEG in silent small vessel disease: sLORETA mapping reveals cortical sources of vascular cognitive impairment no dementia in the default mode network. *Journal of clinical neurophysiology : official publication of the American Electroencephalographic Society* **2013,** 30, (2), 178-87.

186. Claassen, J.; Hirsch, L. J.; Kreiter, K. T.; Du, E. Y.; Connolly, E. S.; Emerson, R. G.; Mayer, S. A., Quantitative continuous EEG for detecting delayed cerebral ischemia in patients with poor-grade subarachnoid hemorrhage. *Clinical neurophysiology : official journal of the International Federation of Clinical Neurophysiology* **2004,** 115, (12), 2699-710.

187. Gollwitzer, S.; Groemer, T.; Rampp, S.; Hagge, M.; Olmes, D.; Huttner, H. B.; Schwab, S.; Madzar, D.; Hopfengaertner, R.; Hamer, H. M., Early prediction of delayed cerebral ischemia in subarachnoid hemorrhage based on quantitative EEG: A prospective study in adults. *Clinical neurophysiology : official journal of the International Federation of Clinical Neurophysiology* **2015,** 126, (8), 1514-23.

188. Finnigan, S. P.; Rose, S. E.; Chalk, J. B., Contralateral hemisphere delta EEG in acute stroke precedes worsening of symptoms and death. *Clin Neurophysiol* **2008,** 119, (7), 1690-4.

189. Burghaus, L.; Hilker, R.; Dohmen, C.; Bosche, B.; Winhuisen, L.; Galldiks, N.; Szelies, B.; Heiss, W. D., Early electroencephalography in acute ischemic stroke: prediction of a malignant course? *Clin Neurol Neurosurg* **2007,** 109, (1), 45-9.

190. Burghaus, L.; Liu, W. C.; Dohmen, C.; Haupt, W. F.; Fink, G. R.; Eggers, C., Prognostic value of electroencephalography and evoked potentials in the early course of malignant middle cerebral artery infarction. *Neurological sciences : official journal of the Italian Neurological Society and of the Italian Society of Clinical Neurophysiology* **2013,** 34, (5), 671-8.

191. Finnigan, S. P.; Rose, S. E.; Chalk, J. B., Rapid EEG changes indicate reperfusion after tissue plasminogen activator injection in acute ischaemic stroke. *Clinical neurophysiology : official journal of the International Federation of Clinical Neurophysiology* **2006,** 117, (10), 2338-9.

192. de Vos, C. C.; van Maarseveen, S. M.; Brouwers, P. J.; van Putten, M. J., Continuous EEG monitoring during thrombolysis in acute hemispheric stroke patients using the brain symmetry index. *J Clin Neurophysiol* **2008,** 25, (2), 77-82.

193. Phan, T. G.; Gureyev, T.; Nesterets, Y.; Ma, H.; Thyagarajan, D., Novel application of EEG source localization in the assessment of the penumbra. *Cerebrovascular diseases* **2012,** 33, (4), 405-7.

194. Bricolo, A.; Turazzi, S.; Faccioli, F., Combined clinical and EEG examinations for assessment of severity of acute head injuries. *Acta Neurochir Suppl (Wien)* **1979,** 28, (1), 35-9.

195. Bergamasco, B.; Bergamini, L.; Doriguzzi, T.; Sacerdote, I., The sleep cycle in coma: prognostic value. *Electroencephalogr Clin Neurophysiol* **1968,** 25, (1), 87.

196. Cillessen, J. P.; van Huffelen, A. C.; Kappelle, L. J.; Algra, A.; van Gijn, J., Electroencephalography improves the prediction of functional outcome in the acute stage of cerebral ischemia. *Stroke* **1994,** 25, (10), 1968-72.

197. van Putten, M. J.; Tavy, D. L., Continuous quantitative EEG monitoring in hemispheric stroke patients using the brain symmetry index. *Stroke* **2004,** 35, (11), 2489-92.

198. Finnigan, S. P.; Walsh, M.; Rose, S. E.; Chalk, J. B., Quantitative EEG indices of sub-acute ischaemic stroke correlate with clinical outcomes. *Clin Neurophysiol* **2007,** 118, (11), 2525-32.

199. Tecchio, F.; Pasqualetti, P.; Zappasodi, F.; Tombini, M.; Lupoi, D.; Vernieri, F.; Rossini, P. M., Outcome prediction in acute monohemispheric stroke via magnetoencephalography. *J Neurol* **2007,** 254, (3), 296-305.

200. Assenza, G.; Zappasodi, F.; Pasqualetti, P.; Vernieri, F.; Tecchio, F., A contralesional EEG power increase mediated by interhemispheric disconnection provides negative prognosis in acute stroke. *Restor Neurol Neurosci* **2013,** 31, (2), 177-88.

201. Dubovik, S.; Ptak, R.; Aboulafia, T.; Magnin, C.; Gillabert, N.; Allet, L.; Pignat, J. M.; Schnider, A.; Guggisberg, A. G., EEG alpha band synchrony predicts cognitive and motor performance in patients with ischemic stroke. *Behav Neurol* **2013,** 26, (3), 187-9.

202. Carmichael, S. T.; Wei, L.; Rovainen, C. M.; Woolsey, T. A., New patterns of intracortical projections after focal cortical stroke. *Neurobiology of disease* **2001,** 8, (5), 910-22.

203. Gao, B.; Kilic, E.; Baumann, C. R.; Hermann, D. M.; Bassetti, C. L., Gamma-hydroxybutyrate accelerates functional recovery after focal cerebral ischemia. *Cerebrovascular diseases (Basel, Switzerland)* **2008,** 26, (4), 413-9.

204. Gao, B.; Cam, E.; Jaeger, H.; Zunzunegui, C.; Sarnthein, J.; Bassetti, C. L., Sleep disruption aggravates focal cerebral ischemia in the rat. *Sleep* **2010,** 33, (7), 879-87.

205. Zunzunegui, C.; Gao, B.; Cam, E.; Hodor, A.; Bassetti, C. L., Sleep disturbance impairs stroke recovery in the rat. *Sleep* **2011,** 34, (9), 1261-9.

206. Ahn, S. S.; Jordan, S. E.; Nuwer, M. R.; Marcus, D. R.; Moore, W. S., Computed electroencephalographic topographic brain mapping. A new and accurate monitor of cerebral circulation and function for patients having carotid endarterectomy. *J Vasc Surg* **1988,** 8, (3), 247-54.

207. Vespa, P. M.; Nuwer, M. R.; Juhasz, C.; Alexander, M.; Nenov, V.; Martin, N.; Becker, D. P., Early detection of vasospasm after acute subarachnoid hemorrhage using continuous EEG ICU monitoring. *Electroencephalogr Clin Neurophysiol* **1997,** 103, (6), 607-15.

208. Zhang, Z. W.; Deschenes, M., Projections to layer VI of the posteromedial barrel field in the rat: a reappraisal of the role of corticothalamic pathways. *Cerebral cortex (New York, N.Y. : 1991)* **1998,** 8, (5), 428-36.

209. Engel, A. K.; Konig, P.; Kreiter, A. K.; Singer, W., Interhemispheric synchronization of oscillatory neuronal responses in cat visual cortex. *Science (New York, N.Y.)* **1991,** 252, (5009), 1177-9.

210. Chrobak, J. J.; Buzsaki, G., Gamma oscillations in the entorhinal cortex of the freely behaving rat. *The Journal of neuroscience : the official journal of the Society for Neuroscience* **1998,** 18, (1), 388-98.

211. Lopez-Azcarate, J.; Nicolas, M. J.; Cordon, I.; Alegre, M.; Valencia, M.; Artieda, J., Delta-mediated cross-frequency coupling organizes oscillatory activity across the rat cortico-basal ganglia network. *Front Neural Circuits* **2013,** 7, 155.

212. Hughes, S. W.; Crunelli, V., Thalamic mechanisms of EEG alpha rhythms and their pathological implications. *Neuroscientist* **2005,** 11, (4), 357-72.

213. Voytek, B.; Knight, R. T., Dynamic Network Communication as a Unifying Neural Basis for Cognition, Development, Aging, and Disease. *Biol Psychiatry* **2015,** 77, (12), 1089-1097.

214. Park, J. Y.; Jhung, K.; Lee, J.; An, S. K., Theta-gamma coupling during a working memory task as compared to a simple vigilance task. *Neurosci Lett* **2013,** 532, 39-43.

215. Qureshi, A.; Hillis, A. E.; Qureshi, A.; Hillis., A. E., *Working memory dysfunction in stroke patients. The Behavioral and Cognitive Neurology of Stroke*. Cambridge University Press: **2013**; p 297-311.

216. Tort, A. B.; Komorowski, R.; Eichenbaum, H.; Kopell, N., Measuring phase-amplitude coupling between neuronal oscillations of different frequencies. *J Neurophysiol* **2010,** 104, (2), 1195-210.

In preparation

**Involvement of hippocampal diaschisis in mediating stroke-induced hippocampal hypofunction and memory deficits**

Gratianne Rabiller[4*], Yonggang Wang[1, 2, 3*], Xavier Leinekugel[4], Dezhi Hu[1, 2, 5], Zhengyan Liu[1, 2, 5], Philip R. Weinstein[1, 2], Jizong Zhao[3], Gary M. Abrams[6], Jialing Liu[1, 2 $] and Bruno Bontempi[4 $]

Departments of Neurological Surgery[1], Neurology[6], University of California, San Francisco and SFVAMC[2], San Francisco, CA 94121
Department of Neurological Surgery[3], Beijing Tiantan Hospital, Capital Medical University, Beijing, PR China, 100050.
Centre de Neurosciences Intégratives et Cognitives[4], CNRS UMR 5228, Université Bordeaux 1, Avenue des Facultés, 33405 Talence, France
Department of Neurological Surgery[5], Huashan Hospital, Fudan University, Shanghai, PR China, 200040

* These authors share first authorship.
$ These authors contributed equally to this work.

**Abstract**

While motor impairment due to ischemic damage of motor pathways is a hallmark of clinical and experimental stroke, post-stroke cognitive dysfunction can be observed without direct injury to brain regions crucial for cognitive functions such as the hippocampus. Here we examine whether hippocampal hypoactivity and spatial memory impairments in adult rats with distal middle cerebral artery occlusion (dMCAO) could result from damage to remotely connected cortical regions, a phenomenon known as diaschisis, and be reversed by environmental enrichment (EE). Rats with focal ischemia exhibited cortical damage and impaired hippocampal-dependent spatial learning in the Barnes maze while both hippocampal structural integrity and synaptic transmission were not disrupted. Imaging of the activity-dependent gene c-fos in dMCAO rats exploring a novel environment or submitted to memory testing revealed region-specific hypoactivation in the hippocampus and two other connected components of the hippocampal formation, the entorhinal and perirhinal cortices that act as the main gateway for information exchange between hippocampus and cortex. Hippocampal hypofunction and spatial memory deficits due to altered cortical inputs (i.e. decreased excitatory inputs and/or increased hippocampal inhibition) were reversed by EE, which also stimulated hippocampal neurogenesis. The present findings indicate that hippocampal hypofunction produces cognitive deficits in experimental stroke and identify hippocampal diaschisis as a crucial mechanism for mediating these effects. EE serves as a rehabilitative therapy to restore memory function by resolving hippocampal diaschisis via an array of plasticity mechanisms that include hippocampal neurogenesis.

## Introduction

Although motor impairment is often apparent and well documented in patients suffering from ischemic stroke, the cognitive consequences and the underlying mechanisms leading to cognitive impairments after cerebrovascular occlusive diseases are less understood. While the frequency of post-stroke dementia is low, post-stroke cognitive impairment is common even among the first-ever stroke patients[1, 2]. Despite our knowledge in stroke epidemiology, the neural pathways involved in post-stroke memory deficits as well as the mechanisms mediating recovery of cognition remain unclear. Evidence showing that the hippocampus plays a crucial role in memory function is compelling[3, 4]. However, this brain region is often spared in human stroke or in many rodent models of cerebral focal ischemia[5]. Consistent with this observation, a recent study shows that patients with memory impairments after stroke or transient ischemic attack do not exhibit hippocampal atrophy at early stage after the event, unlike those with Alzheimer's disease[6].

Because the brain operates as a network with multiple and intricate connections between different regions, a focal cerebral ischemic insult can potentially affect the brain circuitry in an extensive manner. In addition to the infarct zones that suffer the deadly consequence of ischemic stroke, penumbra surrounding the lesion sites and some brain regions more remote to the ischemic areas are also functionally affected to various degrees[7]. This phenomenon, known as diaschisis, has attracted considerable interest since it was first described by Von Monakow in 1914[8] due to its contributing role in functional impairment[7, 9] and in post-stroke recovery[10]. Interactions between the hippocampus and cortical areas take place through a complex array of connections in which the parahippocampal region (entorhinal, perirhinal and postrhinal cortices) plays a pivotal role[11]. In light of the importance of these functional interactions during memory processing, we hypothesized that cognitive impairment following ischemic stroke could occur in the absence of direct hippocampal insult, possibly via impaired connectivity within cortico-hippocampal networks leading to diaschisis-induced hypofunctioning in specific brain regions of the hippocampal formation. To investigate the neurobiological basis of hippocampal diaschisis following focal cerebral ischemia, we used the distal middle cerebral artery occlusion (dMCAO) in rats which induces restricted cortical infarct in the absence of

direct hippocampal injury[5, 12]. We first examined the dMCAO-induced neuronal reorganization within the hippocampal formation of rats exploring of a novel environment or confronted to hippocampal-dependent spatial memory testing using cellular imaging of the activity-dependent gene c-fos classically used as an indirect correlate of neuronal activity[13, 14]. We then determined whether dysfunctional hippocampal activity could result from reduced afferent inputs (i.e. deactivation) originating in the damaged cortex and exacerbate the memory deficits observed after dMCAO.

Environmentally-induced plasticity in the form of various stimuli including physical activity, social interaction and cognitive training has become a rapidly emerging therapeutic technique to improve the outcome of cognitive function in patients with brain injury or neurodegeneration[15]. In rodents, rehabilitative treatments have been modeled by rearing in a complex enriched environment (EE) and converging evidence show that EE is efficacious in enhancing cognitive function recovery after experimental stroke[16, 17]. However, the neural mechanisms underlying these beneficial effects remain unclear. We thus sought to explore the effects of EE on hippocampal neuronal activity and memory function as well as hippocampal plasticity via increased neurogenesis in dMCAO animals, raising the possibility that beyond their conventional role in cell replacement, newborn neurons may contribute to restoring the functional dynamics of hippocampal circuits in a damaged brain.

## Materials and methods

### *Animals and housing*

All experiments were conducted in accordance with the animal care guidelines issued by the National Institutes of Health and by the SFVAMC Institutional Animal Care and Use Committee. Adult male Sprague-Dawley rats (2.5 months of age, 230-240 g) from Charles River Laboratories (Wilmington, MA) were housed in institutional standard cages (2 rats per cage) on a 12-hr light/12-hr dark cycle with *ad libitum* access to food and water before the experimental procedures. All measurements and analyses were conducted by experimenters blinded to the experimental conditions.

### *Focal ischemia model*

Stroke was induced by the dMCAO method under isoflurane/$O_2$/$N_2O$ anesthesia as previously described[12]. Briefly, a 2 mm-diameter circular craniotomy was performed 1

mm rostral to the anterior junction of the zygoma and squamous bone. The main trunk of the left MCA was ligated just above the rhinal fissure with a 10-0 suture and the bilateral common carotid arteries (CCA) were occluded for 60 min with 4-0 sutures. The sutures were then removed to restore blood flow, and the cervical incision was closed. Sham-operated rats did not receive occlusion of either the MCA or the CCAs.

*Pharmacological challenge and spatial exploration*

To stimulate neuronal activity among various brain regions of the limbic system, dMCAO and sham animals received i.p. injections of the dopaminergic $D_2$ receptor antagonist sulpiride (100 mg/kg in 0.9% saline, Sigma, St. Louis, MO) in their home cage. Control groups were injected with vehicle. Spatial exploration (one single session of 15 min) occurred in an open field that consisted of a circular table (120 cm in diameter).

*Enriched environment*

One week after dMCAO and sham surgery, rats in each group were randomly divided into either standard housing (STD) or enriched environment (EE), resulting in 4 final experimental groups: sham-STD, sham-EE, MCAO-STD, and MCAO-EE. Rats assigned to the EE groups were transferred to special EE cages containing various objects and housed for an additional 4 weeks as previously described[12]. Rats assigned to the STD housing remained in the institutional standard home cages for the same period of time as the EE groups.

*Spatial learning*

Training was carried out in a Barnes maze (Hamilton Kinder, Poway, CA) according to methods described previously[18]. Animals had to learn the spatial position of the escape tunnel that was kept constant during the 5 days of training (2 daily blocks of 3 trials each separated by a 2 hr interval). Path length traveled, velocity and time to locate the escape tunnel were recorded using the Noldus Ethovision video tracking system (Noldus, Leesburg, VA).

*Neuronal tracing*

The anterograde tracer biotinylated dextranamine (BDA, Molecular Probes, Eugene,

OR) was injected by pressure or iontophoretically into the parietal cortex of intact rats (AP:-5.0 mm, L:-5.0 mm, D:-0.9 mm) according to previously described procedures[11, 19]. After a survival period of 10 days, animals were transcardially perfused with 4% paraformaldehyde (PFA), their brains were removed and sections were stained for BDA using Cy3 as fluorochrome.

*In vivo electrophysiological recordings*

Electrophysiological recordings were performed using multisite extracellular silicon probes (NeuroNexus Technologies) in the urethane anesthetized rat (Sigma, 15 mg/kg i.p.) as described elsewhere[20, 21]. In brief, the probe (16 sites, vertical separation 50 μm) was inserted vertically at stereotaxic coordinate AP:-3.3 mm from Bregma, L:-2.8 mm, and wide-band electrophysiological activity recorded (0.1Hz-9KHz, sampling rate 20 KHz, Neuralynx recording system, Axon Instruments) at various depth corresponding successively to neocortex and layers CA1 and CA3 of dorsal hippocampus.

*BrdU labeling and tissue preparation*

To investigate the phenotype and survival of newborn cells, BrdU (Sigma, 50 mg/kg,) was injected i.p. twice daily on days 4 to 7 after dMCAO to track divided cells. Ninety minutes after the pharmacological challenge, the spatial exploration or the last testing trial in the Barnes maze, rats were deeply anesthetized and perfused transcardially with PFA in 0.1 M phosphate buffer (PB), pH 7.4. The brains were removed, post-fixed overnight in 4% PFA-PB and placed in a 20% sucrose solution for 48 hours. Forty-μm coronal sections were cut on a microtome and collected serially.

*Immunohistochemistry staining and confocal microscopy*

Serial coronal sections (480 μm apart) were immunostained with anti-NeuN, Fos and CD11 antibodies as described previously[12, 22]. Fluorescence signals were revealed and detected by using the Zeiss LSM 510 confocal image system (Zeiss, Thornwood, NY) with a sequential scanning model for Alexa 488 and 594. Stacks of images (1024×1024 pixels) were obtained and processed with Adobe Photoshop (Adobe System, Mountain View, CA)[12].

### 4.1. *Cell counting and infarct measurement*

The number of BrdU and Fos-positive cells was determined in every twelfth coronal in the bilateral septal hippocampus manually and by an automated particle counting method using the NIH Image J software, respectively. Structures were defined according to the Franklin and Paxinos atlas (Supplementary Fig. 1). Counts in each region of interest were expressed as number of cells/mm$^2$ or as the entire region. The number of BrdU/NeuN double-labeled cells was estimated by multiplying the percentages of co-localization (determined by confocal microscopy) to the total number of BrdU-labeled cells[12]. Infarct volume was measured by subtracting the volume of intact tissue in the ipsilateral hemisphere from that in the contralateral hemisphere on NeuN-stained serial sections (480 µm apart) by unbiased stereology[22] (StereoInvestigator, MicroBrightField, VA).

*Statistical analyses*

Data were expressed as mean±sem. Statistical tests were carried out with Statview 5.0.1 software (SAS Institute Inc., Cary, NC). Group comparisons were made using analyses of variance (ANOVAs) followed by *post hoc* paired comparisons using the Fisher's PLSD test when appropriate. Values of $p<0.05$ were considered as significant.

## Results

### Focal ischemia induces hypoactivity in the hippocampus

Consistent with previous findings[5], we found that the dMCAO-induced unilateral infarct zone was restricted to cortical areas including the motor and sensorimotor cortices (**Fig. 1A**), with a mean infarct volume of 66.66±6.52 mm$^3$. No signs of hippocampal injury or cell loss were observed as revealed by ED1 and NeuN immunohistochemistry (**Fig. 1B**). To examine the possibility of altered functional activity in the hippocampus despite sparing of hippocampal integrity, we mapped the expression of the activity-dependent gene c-fos which is widely used as an indirect correlate of neuronal activation[13, 14]. Immediate early genes, including c-fos, have been reported to be transiently expressed following ischemia in response to brain injury[23]. To control for this potential confound, we waited for 4 days before examining

Fos labeling, a delay sufficient for Fos expression to return to baseline throughout the brain including the infarcted cortical areas (**Fig. 2A**), thus confirming previous findings. We first examined Fos expression in the CA1, CA3 and DG regions of the hippocampus of sham and MCAO animals that remained in their home cage (**Fig. 2B-D**). Despite a trend for a reduction in Fos expression as compared to shams, no significant difference was observed in any of the brain regions analyzed ($F<1$), most likely due to a floor effect since Fos proteins are not constitutively expressed there in resting animals.

To circumvent this issue, we stimulated Fos expression pharmacologically by injecting sham and MCAO rats systemically with the $D_2$ receptor antagonist sulpiride previously reported to enhance Fos expression throughout the limbic system[24]. As expected, sulpiride-treated sham animals exhibited increased Fos labeling in the hippocampus (**Fig. 2B-D**) compared to saline-injected animals. However, reduced levels of Fos expression throughout hippocampal regions were detected in dMCAO animals, particularly in the ipsilateral side of the cortical infarct (**Fig. 2B-D**). This lack of hippocampal activation was further confirmed when additional groups of sham and dMCAO animals were allowed to explore a novel environment. Compared to rats that remained in their home cage, spatial exploration of a circular arena 4 days after surgery in sham animals resulted in a significant increase in Fos expression in all subfields of the hippocampus (**Fig. 3A-C**). Similarly to pharmacological stimulation, dMCAO markedly reduced Fos activation in a region- and hemisphere-specific manner, thus indicating hippocampal hypofunctioning during spatial exploration. Reduced Fos activation was significant in the CA1 and DG regions (**Fig. 3A-C**) and predominantly affected the ipsilateral hemisphere (**Fig. 3D**). Not all brain regions showed decreased Fos labeling following dMCAO (Supplementary Fig. 2), indicating that the observed effects were region-specific rather than due to a generalized disruption in the regulation of c-fos resulting from ischemia.

**MCAO-induced spatial memory deficits and hippocampal hypofunction are reversed by EE**

We next examined whether hippocampal dysfunction observed following exploration in dMCAO rats could translate into memory deficits. Sham and dMCAO animals were submitted to memory testing using spatial learning in the Barnes maze that heavily

relies on hippocampal function. Over the 5 days of training, shams exposed to a standard environment (i.e. their home cage) for 4 weeks traveled progressively less distance to locate the escape box (**Fig. 4A**). Although dMCAO animals managed to learn the task, their acquisition rate was slower. This impaired memory profile was associated at the cellular level with decreased Fos expression in the hippocampus (**Fig. 4B-D**), thus confirming the hippocampal dysfunction following spatial exploration of a novel environment. In an attempt to alleviate the dMCAO-induced spatial memory impairment, animals were housed in an EE for 4 weeks. Although EE did not reduce infarct size (dMCAO Standard: 66.66±6.52 $mm^3$; dMCAO EE: 63.40±7.03 $mm^3$, $p>0.76$, NS), it improved spatial learning in both sham and dMCAO rats (**Fig. 4A**). Interestingly, EE also resulted in enhanced Fos expression in the hippocampal CA1 and DG of ischemic rats in both ipsilateral and contralateral hemispheres (**Fig. 4B, D**). Given the absence of noticeable hippocampal damage following dMCAO, we hypothesized that hippocampal hypofunction in ischemic rats could be due, at least in part, to a lack of sensorimotor inputs to the hippocampal formation originating from the cortical infarct located in the somatosensory (parietal) cortex. To examine the topographical characteristics of the parietal cortex, intact rats were microinfused with the anterograde tracer biotinylated dextranamine. In agreement with previous tracing studies[11], we could not detect any direct projections to the hippocampus. However, we found that the parietal cortex project extensively to the parahippocampal region, that include the perirhinal cortex (**Fig. 5A**). This finding further supports the concept that hippocampal hyppofunction could be the consequence of a reduced source of cortical information (i.e. deactivation) or increased inhibition through the parahippocampal region that acts as a key gateway for information exchange between cortical areas and the hippocampus. Alternatively, reduced Fos expression in the hippocampus could be due to altered transmission within this region. To examine this possibility, we performed electrophysiological recordings from ipsilateral somatosensory cortex and hippocampus during and following dMCAO in anesthetized rats. Cortical activity was severely depressed (**Fig. 5B**), a pattern that contrasted with sustained ongoing activity in the hippocampus, including sharp-wave-ripples and associated bursts of unit activity (**Fig. 5C)**, a hallmark of functional CA3 to CA1 ongoing synaptic transmission via Schaffer collaterals[21, 25]. Thus, hippocampal synaptic transmission was preserved following dMCAO, further supporting the existence of decreased excitatory inputs to the

hippocampus originating from the infarcted cortex. The topography of hippocampal innervations reported above also raised the possibility that hippocampal dysfunction and associated memory impairment could be the consequence of impaired neuronal activation in the parahippocampal region. Such a possibility was confirmed when we examined Fos expression in the entorhinal cortex (**Fig. 6A,B**), and the perirhinal cortex (**Fig. 6C**) which innervates the entorhinal cortex. Reduced levels of Fos expression in these two regions were observed in dMCAO animals compared to shams (**Fig. 6**). Exposure to EE was successful in restoring Fos expression in the entorhinal cortex ipsilateral to the infarct (**Fig. 6A,B**).

**EE-enhanced hippocampal recruitment after stroke is associated with increased neurogenesis in the DG**

Consistent with previous findings that increased environmental complexity promotes adult hippocampal neurogenesis[26], we found that the survival of newborn neurons was increased in sham rats housed for 4 weeks in an EE compared to standard housing condition (**Fig. 7**). Transient increase in progenitor cell proliferation following dMCAO has been reported during the first few fays that follows dMCAO and may result in the labeling of a larger pool of divided cells when BrdU is administered during this period[12]. In agreement with this, we detected an increase in BrdU labeling in the ipsilateral DG of rats with dMCAO compared to sham surgery (Sham-STD: 2820.00±176.22; Sham-EE: 2613.60±180.56; MCAO-STD: 4845.00±1034.47; MCAO-EE: 7594.40±901.72; $F_{1,68}$ = 31.80; $p<0.0001$), and more double-positive newborn cells 4 weeks later in both standard and EE dMCAO groups (**Fig. 7B)**. However, post-ischemic EE enhanced the survival of newborn neurons in the DG of dMCAO rats compared to dMCAO rats that remained in the standard environment (**Fig. 7A, B)**.

**Discussion**

Despite an intact hippocampus, we found that ischemic animals exhibited widespread, but region-specific, hypoactivations in anatomically connected brain regions of the hippocampal formation remote from the cortical infarct. Our data suggest that hippocampal deactivation resulting from decreased excitatory inputs

originating in the cortex, a form of focal ischemia-induced diaschisis in the hippocampus, was likely to be responsible for ischemic-induced spatial memory dysfunction.

dMCAO rats were impaired when submitted to spatial learning in the Barnes Maze. Similar to water maze, processing of spatial information in this task is dependent on the functional interaction between several brain regions among which the hippocampus and parietal cortex[27], this latter region being consistently damaged following focal ischemia[5]. Spatial memory has been shown to primarily rely on the elaboration of complex cognitive maps within hippocampal-cortical networks that support navigation though space[28]. Bilateral hippocampal or parietal cortex lesions are required to impair long-term storage and/or expression of spatial memory[29], making dMCAO-induced unilateral cortical damage unlikely to be sufficient to induce detectable cognitive impairment. Parietal cortex lesions induce hippocampal place cell firing instability suggesting that this associative cortical region actively participates in the elaboration of hippocampal spatial maps[27]. Thus, in ischemic animals with cortical damage, additional hippocampal dysfunction may exacerbate memory deficits. Consistent with this possibility, although dMCAO rats did not show any sign of hippocampal damage, we found that these animals exhibited reduced expression of the activity-dependent gene c-fos within several regions of the hippocampal formation, indicating neuronal hypofunctioning in response to experiential inputs. This observation extends previous findings showing that focal ischemia can also induce dysfunction in remotely connected brain regions such as the cerebellum[30]. These remote regions often exhibit reduced metabolic rates routinely detected by PET clinically[31] which has led to the proposal that diaschisis is presumably caused by a disruption of afferent excitatory input originating from distant infarcted areas[7, 30]. Here, we identify hippocampal diaschisis as a crucial mechanism underlying, at least in part, memory deficits following focal cerebral ischemia. In agreement with previous tracing studies[19], we found direct projections from somatosensory cortex to perirhinal cortex, a main component of the parahippocampal region which constitutes the major source of processed cortical information entering the hippocampus[11]. Electrophysiological recordings of hippocampal activity during and following dMCAO showed that neuronal discharge and synaptic transmission were still active within the hippocampal circuit, thus supporting the concept of a diaschisis-like hippocampal deactivation due to reduced efferent excitatory activity

from cortical areas to relay neurons in the perirhinal and entorhinal cortices of the parahippocampal region. In line with our findings, hippocampal dysfunction and memory impairments resulting from injury to remote brain regions has been demonstrated in animals with thalamic or fornix lesions[14, 32]. At the cellular level, freezing-induced damage limited to the cortex induces changes in GABA subunit receptors not only in the cortex, but also in remote brains regions including the hippocampus[33].

Maximizing neurological recovery remains a major goal after a stroke episode. While natural recovery mechanisms have been reported following ischemia, active treatments in the form of occupational rehabilitative therapies have proven to be beneficial for patients with stroke[15]. In an attempt to restore the memory deficit observed after focal ischemia, we examined the outcome of post-ischemic housing in an EE, a rehabilitative treatment that has been shown to dramatically reduce impairment in many experimental models of brain injury and neurodegeneration[17]. In agreement with previous studies[16], we found that one month of EE was sufficient to induce learning and memory recovery after experimental stroke. Importantly, this treatment also reinstated neuronal activation within the hippocampal circuitry, indicating that rescuing hippocampal activity was sufficient to alleviate the observed spatial memory deficits despite permanent cortical damage. EE has been shown to induce neurogenesis in the adult hippocampus[12, 26], raising the possibility that new neurons continuously produced in the hippocampal DG throughout adulthood and preferentially recruited into spatial memory network[34], may represent valuable therapeutic targets. In this study, we also found that post-ischemic EE increased neurogenesis in the DG of dMCAO rats. However, studies using invasive approaches such as cranial irradiation have failed to establish that newborn cells directly mediate the beneficial effects of EE[35], possibly because the findings were obtained from intact animals wherein different mechanisms underlying the effects of EE coexist and enable compensatory phenomena. Concomitant mechanisms may involve upregulation of neurotrophic factors leading to dendritic sprouting and synaptogenesis as well as chromatin remodeling[36]. In the case of a damaged brain however, these mechanisms may be insufficient, thus conferring to new adult-generated granule cells a privileged role in mediating the beneficial effects of EE on spatial memory.

Navigation through space has been shown to rely on integrated spatial maps

that enable the formation of relevant spatial representations of the environment. Two forms of spatial maps are thought to act in concert to enable successful spatial navigation[28]. The sketch map is constructed from distal landmarks in the CA1 regions of the hippocampus while the bearing map is primarily constructed in the DG from directional landmarks. By adding new highly-plastic structural elements to neuronal networks in the DG that may act as place cells (neurons that encode the animal's specific position in space[37]), neurogenesis may thus constitute a relevant plasticity mechanism enhancing the functioning of pre-existing bearing maps. In addition, neurogenesis-induced remodelling of these maps, via expanded storage and computational capacity, could compensate for the loss of extrahippocampal maps initially located at the cortical level and damaged following focal ischemia. The new neurons in the DG could also influence, via their axonal projections to the hippocampal CA3 relay region, the activity within the CA1 region and thereby the elaboration of relevant sketch maps. Despite a very low number of newly born cells being recruited into functional networks[34, 38], computational models suggest that even a few neurons are capable of modulating the activity within an extended network area and lead to restored function[39]. Thus, contrasting to their conventional role in cell replacement, newly born cells could play an important role in restoring the dynamics of hippocampal circuits and possibly of connected remote regions which normally receive excitatory drives from the cortical areas damaged after ischemic stroke.

Other neurogenesis-independent plasticity mechanisms are also likely to contribute to the beneficial effects of EE since this treatment upregulates the expression of a variety of genes involved in neuronal structure, synaptic formation and cell signaling[40]. One possible host for such mechanisms is the entorhinal cortex whose neuronal activity was restored after EE. The grid cells recently identified in the entorhinal cortex are thought to provide a spatial metric framework enabling the hippocampus to maintain stable CA1 place cell spatial representations[41], therefore suggesting a close interaction between this region and the hippocampus[42]. Thus, restoring activity in the entorhinal cortex could contribute to a diaschisis-induced recovery of neuronal activity in the hippocampus and alleviate the dMCAO-induced spatial memory.

Taken together, our data provide novel insights into the neurobiological basis of memory impairments associated with focal cerebral ischemia. They point to hippocampal diaschisis as a crucial mechanism responsible for the observed deficits

and to the beneficial effects of EE in promoting the resolution of diaschisis. Additional studies are warranted to further investigate the nature of the dynamics of cortical-hippocampal interactions in response to focal cerebral ischemia. Of interest would be to record neuronal activity of individual neurons simultaneously in hippocampus and cortex using extracellular multisite probes in freely-moving animals engaged in memory tasks. In this context, the dMCAO model of focal ischemic stroke appears as a valuable experimental tool to study diaschisis-related cognitive impairment.

## References


1. Patel M, Coshall C, Rudd AG, Wolfe CD. Natural history of cognitive impairment after stroke and factors associated with its recovery. Clin Rehabil. 2003;17:158-166
2. Srikanth VK, Thrift AG, Saling MM et al. Increased risk of cognitive impairment 3 months after mild to moderate first-ever stroke: a Community-Based Prospective Study of Nonaphasic English-Speaking Survivors. Stroke. 2003;34:1136-1143
3. Martin SJ, Clark RE. The rodent hippocampus and spatial memory: from synapses to systems. Cell Mol Life Sci. 2007;64:401-431
4. Eichenbaum H. A cortical-hippocampal system for declarative memory. Nat Rev Neurosci. 2000;1:41-50
5. Carmichael ST. Rodent models of focal stroke: size, mechanism, and purpose. NeuroRx. 2005;2:396-409
6. Sachdev PS, Chen X, Joscelyne A et al. Hippocampal size and dementia in stroke patients: the Sydney stroke study. J Neurol Sci. 2007;260:71-77
7. Witte OW, Bidmon HJ, Schiene K et al. Functional differentiation of multiple perilesional zones after focal cerebral ischemia. J Cereb Blood Flow Metab. 2000;20:1149-1165
8. von Monakow C. Die Lokalisation im Grosshirn un der Abbau der Funktion durch Kortikale Herde. Bergman, JF, ed ed: Germany: Wiesbaden, 1914:26-34
9. Mountz JM. Nuclear medicine in the rehabilitative treatment evaluation in stroke recovery. Role of diaschisis resolution and cerebral reorganization. Eura Medicophys. 2007;43:221-239
10. Seitz RJ, Azari NP, Knorr U et al. The role of diaschisis in stroke recovery. Stroke. 1999;30:1844-1850
11. Burwell RD. The parahippocampal region: corticocortical connectivity. Ann N Y Acad Sci. 2000;911:25-42
12. Matsumori Y, Hong SM, Fan Y et al. Enriched environment and spatial learning enhance hippocampal neurogenesis and salvages ischemic penumbra after focal cerebral ischemia. Neurobiol Dis. 2006;22:187-198
13. Maviel T, Durkin TP, Menzaghi F, Bontempi B. Sites of neocortical reorganization critical for remote spatial memory. Science. 2004;305:96-99
14. Vann SD, Brown MW, Aggleton JP. Fos expression in the rostral thalamic nuclei and associated cortical regions in response to different spatial memory tests. Neuroscience. 2000;101:983-991
15. Cicerone KD, Dahlberg C, Malec JF et al. Evidence-based cognitive rehabilitation: updated review of the literature from 1998 through 2002. Arch Phys Med Rehabil.

2005;86:1681-1692
16. Johansson BB. Environmental influence on outcome after experiment brain infarction. Acta Neurochir Suppl (Wien). 1996;66:63-67
17. Nithianantharajah J, Hannan AJ. Enriched environments, experience-dependent plasticity and disorders of the nervous system. Nat Rev Neurosci. 2006;7:697-709
18. Rapp JH, Pan XM, Neumann M et al. Microemboli composed of cholesterol crystals disrupt the blood-brain barrier and reduce cognition. Stroke. 2008;39:2354-2361
19. Lavenex P, Amaral DG. Hippocampal-neocortical interaction: a hierarchy of associativity. Hippocampus. 2000;10:420-430
20. Leinekugel X, Khazipov R, Cannon R et al. Correlated bursts of activity in the neonatal hippocampus in vivo. Science. 2002;296:2049-2052
21. Ylinen A, Bragin A, Nadasdy Z et al. Sharp wave-associated high-frequency oscillation (200 Hz) in the intact hippocampus: network and intracellular mechanisms. J Neurosci. 1995;15:30-46
22. Liu Z, Fan Y, Won SJ et al. Chronic treatment with minocycline preserves adult new neurons and reduces functional impairment after focal cerebral ischemia. Stroke. 2007;38:146-152
23. Honkaniemi J, States BA, Weinstein PR et al. Expression of zinc finger immediate early genes in rat brain after permanent middle cerebral artery occlusion. J Cereb Blood Flow Metab. 1997;17:636-646
24. Ozaki T, Katsumoto E, Mui K et al. Distribution of Fos- and Jun-related proteins and activator protein-1 composite factors in mouse brain induced by neuroleptics. Neuroscience. 1998;84:1187-1196
25. Csicsvari J, Hirase H, Mamiya A, Buzsaki G. Ensemble patterns of hippocampal CA3-CA1 neurons during sharp wave-associated population events. Neuron. 2000;28:585-594
26. Kempermann G, Kuhn HG, Gage FH. More hippocampal neurons in adult mice living in an enriched environment. Nature. 1997;386:493-495
27. Save E, Paz-Villagran V, Alexinsky T, Poucet B. Functional interaction between the associative parietal cortex and hippocampal place cell firing in the rat. Eur J Neurosci. 2005;21:522-530
28. Jacobs LF, Schenk F. Unpacking the cognitive map: the parallel map theory of hippocampal function. Psychol Rev. 2003;110:285-315
29. Kesner RP, Farnsworth G, Kametani H. Role of parietal cortex and hippocampus in representing spatial information. Cereb Cortex. 1991;1:367-373
30. Gold L, Lauritzen M. Neuronal deactivation explains decreased cerebellar blood flow in response to focal cerebral ischemia or suppressed neocortical function. Proc Natl Acad Sci U S A. 2002;99:7699-7704
31. Fiorelli M, Blin J, Bakchine S et al. PET studies of cortical diaschisis in patients with motor hemi-neglect. J Neurol Sci. 1991;104:135-142
32. Vann SD, Brown MW, Erichsen JT, Aggleton JP. Using fos imaging in the rat to reveal the anatomical extent of the disruptive effects of fornix lesions. J Neurosci. 2000;20:8144-8152
33. Redecker C, Luhmann HJ, Hagemann G et al. Differential downregulation of GABAA receptor subunits in widespread brain regions in the freeze-lesion model of focal cortical malformations. J Neurosci. 2000;20:5045-5053
34. Kee N, Teixeira CM, Wang AH, Frankland PW. Preferential incorporation of adult-generated granule cells into spatial memory networks in the dentate gyrus. Nat Neurosci. 2007;10:355-362
35. Meshi D, Drew MR, Saxe M et al. Hippocampal neurogenesis is not required for behavioral effects of environmental enrichment. Nat Neurosci. 2006;9:729-731

36. Fischer A, Sananbenesi F, Wang X et al. Recovery of learning and memory is associated with chromatin remodelling. Nature. 2007;447:178-182
37. O'Keefe J, Dostrovsky J. The hippocampus as a spatial map. Preliminary evidence from unit activity in the freely-moving rat. Brain Res. 1971;34:171-175
38. Ramirez-Amaya V, Marrone DF, Gage FH et al. Integration of new neurons into functional neural networks. J Neurosci. 2006;26:12237-12241
39. Airan RD, Meltzer LA, Roy M et al. High-speed imaging reveals neurophysiological links to behavior in an animal model of depression. Science. 2007;317:819-823
40. Rampon C, Jiang CH, Dong H et al. Effects of environmental enrichment on gene expression in the brain. Proc Natl Acad Sci U S A. 2000;97:12880-12884
41. Moser EI, Kropff E, Moser MB. Place cells, grid cells, and the brain's spatial representation system. Annu Rev Neurosci. 2008;31:69-89
42. Van Cauter T, Poucet B, Save E. Unstable CA1 place cell representation in rats with entorhinal cortex lesions. Eur J Neurosci. 2008;27:1933-1946

## Figure legends

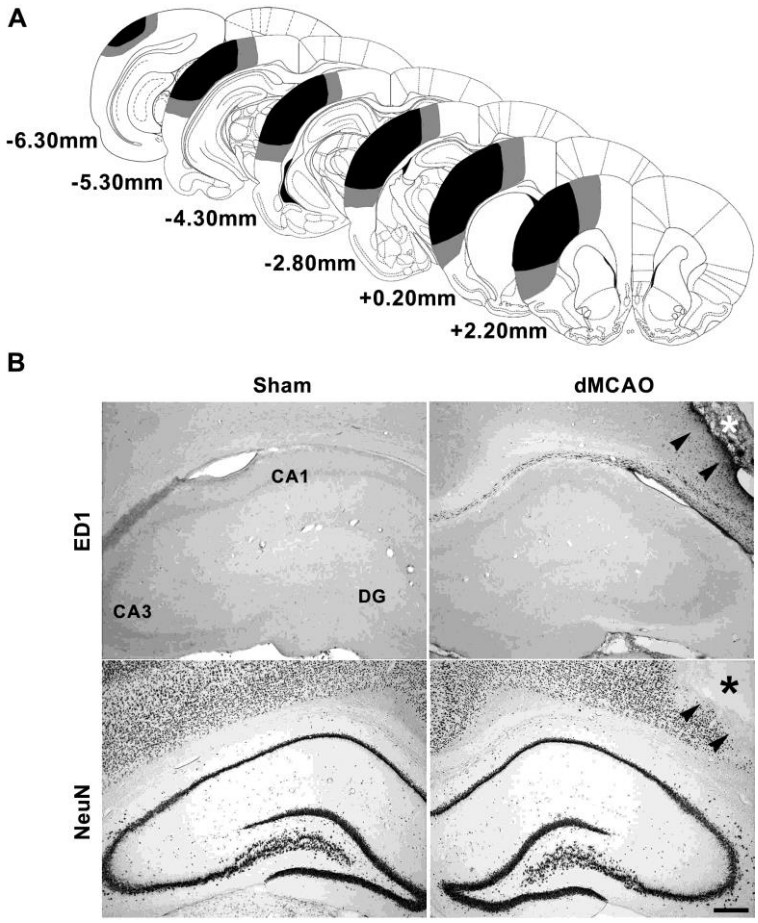


**Figure 1. Damage following focal ischemia produced by left dMCAO is restricted to the ipsilateral cortex**. **(A)** Reconstructions of coronal sections showing the extent of ischemic infarct in rats with dMCAO. Smallest and largest damaged areas appear in black and gray, respectively. Numbers indicate the section distance in millimeters from Bregma. **(B**) The expression of ED1, a marker for activated microglia was absent throughout the hippocampus (left CA1, CA3 and DG areas are shown), indicating no sign of injury. However, ED1 was robustly expressed in the infarcted and peri-infarcted somatosensory cortex ipsilateral to ischemic stroke (arrowheads). Similar expression of the neuronal marker NeuN throughout the hippocampus of shams and dMCAO rats confirmed the lack of hippocampal damage. Note in contrast the absence of NeuN staining indicating complete cell loss in the left peri-infarcted cortex (arrowheads). Star indicates the core of the infarct. Scale bar, 100 μm.

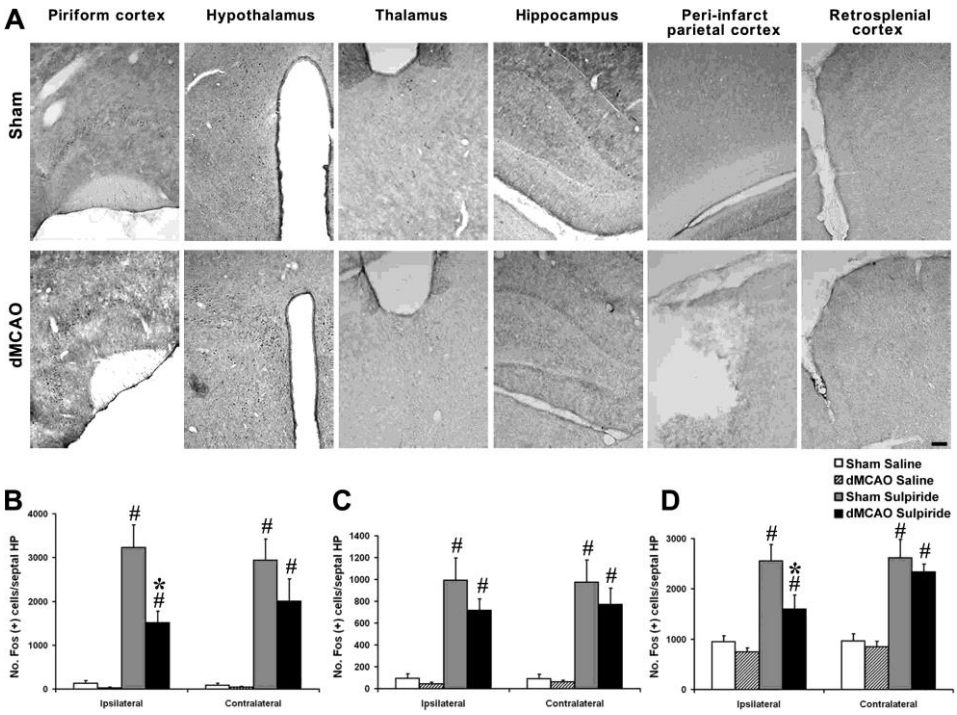


**Figure 2. Reduced hippocampal activation following pharmacological challenge. (A)** Photomicrographs of coronally-cut sections showing minimal Fos expression throughout various brain regions 4 days after induction of focal ischemia in shams and dMCAO animals that remained in their home cage. Scale bar, 100 μm. **(B)** Counts of Fos-positive nuclei in the hippocampal CA1 region of shams and dMCAO rats injected in their home cage with saline or sulpiride (100 mg/kg, i.p.). Fos expression was increased by sulpiride treatment ($F_{1,56}$ = 268.39; $p < 0.0001$), but this effect was less pronounced in ischemic rats (interaction treatment x surgery: $F_{1,56}$ = 18.94; $p < 0.0001$) **(C)** Sulpiride increased Fos expression in the CA3 region of the hippocampus compared to home cage controls ($F_{1,56}$ = 188.04; $p < 0.0001$) but the treatment x surgery effect failed to reach significance ($F_{1,56}$ = 2.99; $p < 0.08$). **(D)** In the hippocampal DG, sulpiride stimulated Fos expression ($F_{1,56}$ = 89.26; $p < 0.0001$). Hypoactivation occurred in dMCAO rats and predominantly affected the ipsilateral infarcted hemisphere (interaction treatment x surgery x side: $F_{1,56}$ = 8.65; $p < 0.01$). #p<0.05 versus saline; *p<0.05 versus Sham-sulpiride; n = 4-15 rats/group.

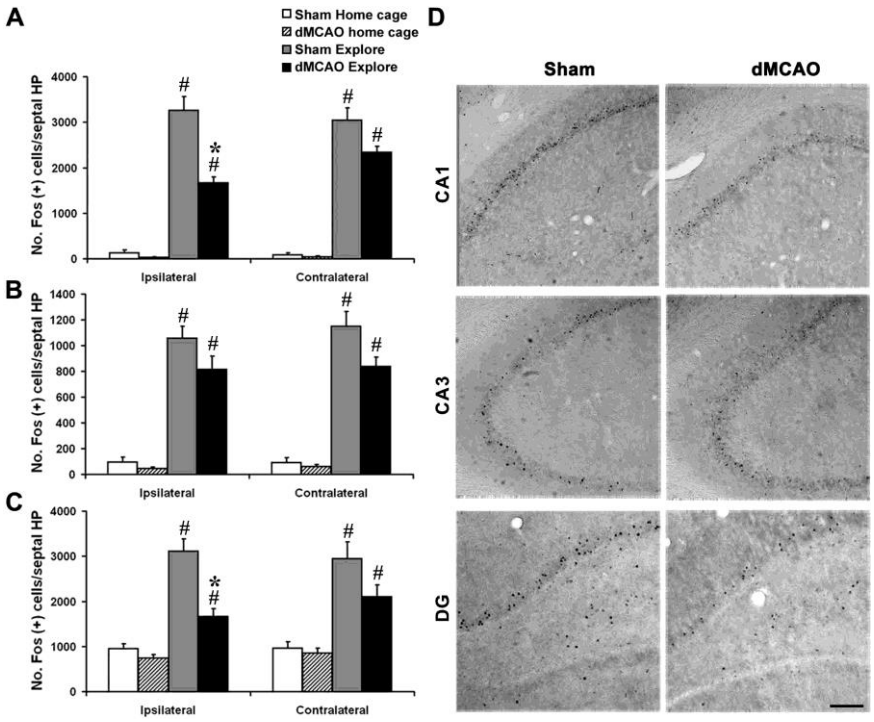


**Figure 3. Reduced hippocampal activation following exploration of a novel environment. (A)** Counts of Fos-positive nuclei in the hippocampal CA1 region of shams and dMCAO rats remaining in their home cage or exploring a circular arena. Spatial exploration increased Fos expression ($F_{1,74}$ = 695.71; $p < 0.0001$) but this effect was reduced in ischemic rats. Although affecting both hemispheres, it was predominant in the ipsilateral infarcted hemisphere (interaction treatment x surgery x side: $F_{1,74}$ = 4.87; $p < 0.03$) **(B)** A similar pattern of effect was observed in the CA3 region of the hippocampus. Spatial exploration increased Fos expression compared to home cage controls ($F_{1,74}$ = 379.22; $p < 0.0001$). This effect was diminished in ischemic rats (interaction treatment x surgery: $F_{1,74}$ = 6.60; $p < 0.05$). **(C)** In the DG of the hippocampus, spatial exploration enhanced Fos expression ($F_{1,74}$ = 134.57; $p < 0.0001$) and revealed hypoactivation in dMCAO rats (interaction treatment x surgery: $F_{1,74}$ = 13.11; $p < 0.0005$). **(D)** Representative photomicrographs showing reduced Fos expression in the ipsilateral CA1, CA3 and DG of dMCAO-Exploring rats (right panel) compared to sham-Exploring controls (left panel). Scale bar, 100 μm. #p<0.05 versus home cage; *p<0.05 versus Sham-explore; n = 8-15 rats/group.

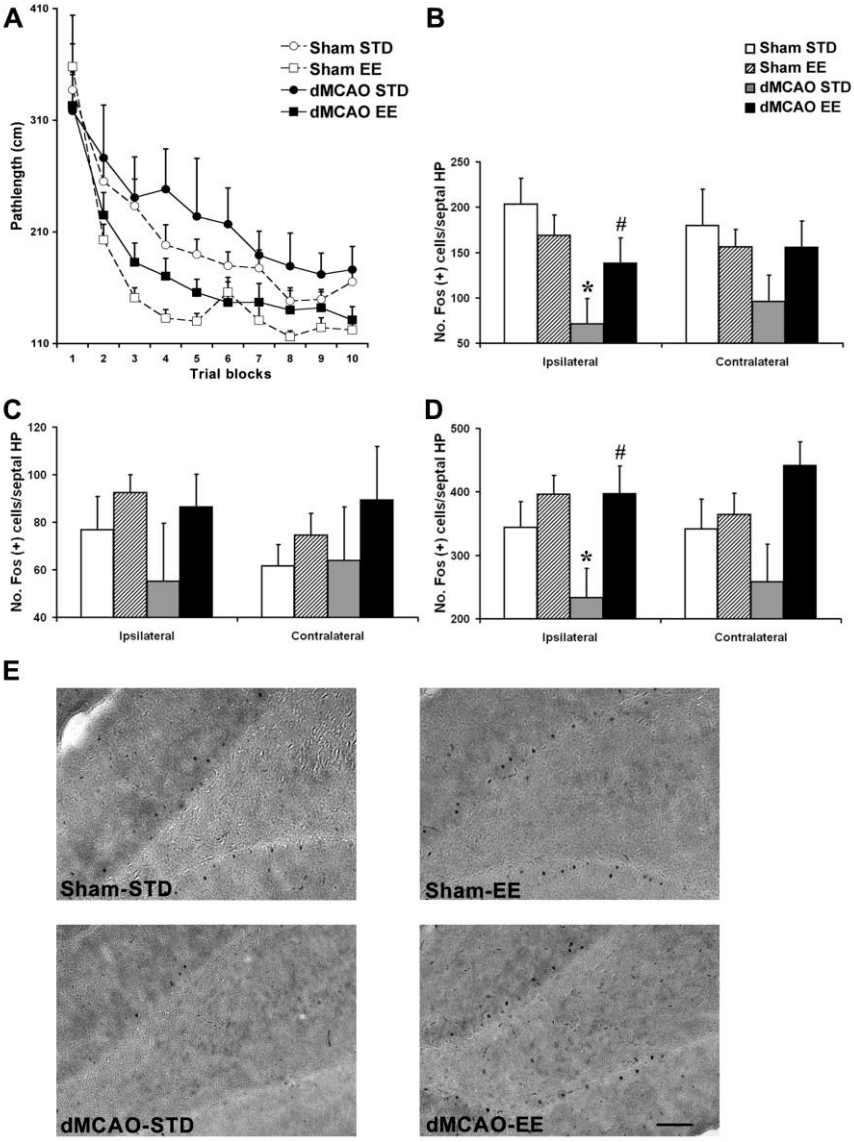


**Figure 4. Focal ischemia-induced spatial memory impairment and associated hippocampal dysfunction are restored by EE. (A)** dMCAO rats housed in a standard environment (STD) performed more poorly than sham controls during spatial learning in the Barnes maze ($F_{1,459} = 6.88$; $p < 0.02$). However, path length to locate the escape box in the Barnes maze decreased for both groups over trial blocks ($F_{9,459} = 35.17$; $p < 0.0001$). There was a main effect of housing ($F_{1,459} = 26.22$; $p < 0.0001$), EE being beneficial for both shams and dMCAO rats (interaction surgery x housing x trials: $F < 1$, NS). **(B)** Counts of Fos-positive nuclei in the hippocampal CA1 region of shams and dMCAO rats exposed to STD or EE and tested for spatial memory. Fos expression was reduced in MCAO-STD rats compared to Sham-STD ($F_{1,30} = 8.02$ ; $p<0.01$). This effect was observed on both ipsilateral and contralateral hemispheres. While without effect in shams, EE enhanced neuronal activity in dMCAO animals (interaction surgery x housing: $F_{1,30} = 4.50$ ; $p < 0.05$). **(C)** dMCAO

did not affect neuronal activity in the CA3 ($F < 1$, NS). **(D)** In the DG, dMCAO-STD rats showed reduced Fos counts compared to Sham-STD rats. ($F_{1,30} = 4.59$ ; $p<0.05$). This effect was predominant in the ipsilateral side and was reversed by EE (interaction: surgery x housing: $F_{1,30} = 4.64$ ; $p < 0.04$). **(E)** Photomicrographs of Fos staining in the ipsilateral DG from animals of all four groups. Scale bar, 100 μm. *p<0.05 versus Sham-STD; #p<0.05 versus dMCAO-STD; n = 7-11 rats/group.

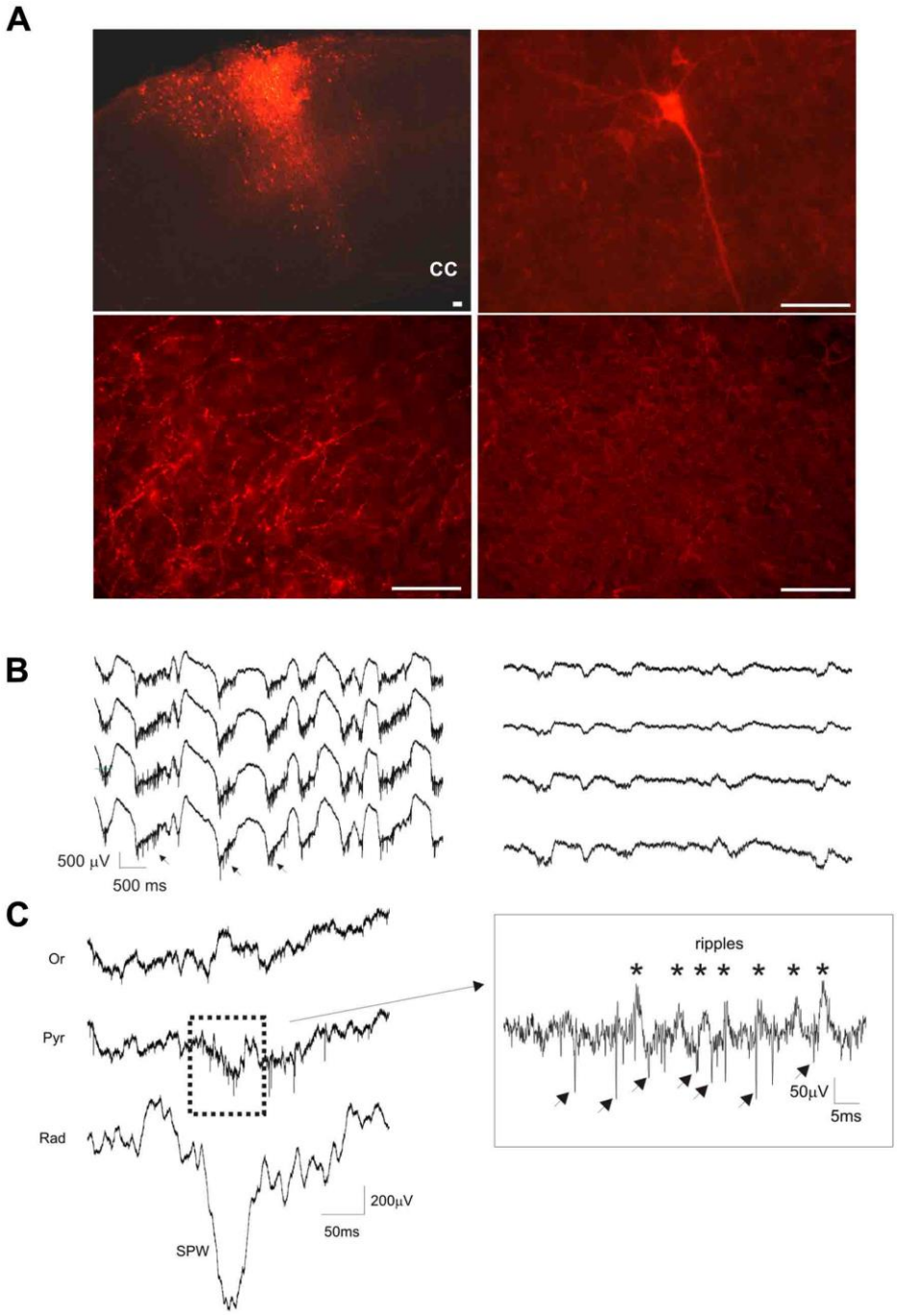


**Figure 5. Demonstration of parahippocampal connectivity and preserved synaptic transmission in the hippocampus following dMCAO. (A)** Unilateral injection of the anterograde tracer BDA into the parietal cortex of intact rats resulted

in labeled fibers in the ipsilateral perirhinal cortex. Coronal sections were stained using Cy3-red immunofluorescence. The injection site (upper left) and an example of fluorescent neuron in the cortex (upper right) are shown. Fibers in the perirhinal cortex were apparent in the side ipsilateral to the cortical injection (lower left) with no trace of staining contralaterally. Scale bars, 50 μm. **(B)** Example of electrophysiological recordings made during dMCAO of an anesthetized rat. Prior to the ischemic episode (left), neocortical activity was characterized by slow (1Hz) oscillations, driving recurrent multi-unit bursting activity (arrows) separated by almost complete silence. Upon ischemia, neocortical activity was severely depressed and neurons became silent, as shown by the absence of unit activity. **(C)** Hippocampal network activity in the same animal was not abolished by dMCAO. Simultaneous recording made from CA1 Strata Oriens (Or), Pyramidale (Pyr) and Radiatum (Rad) showed spontaneous downward deflection (lower trace, Sharp-Wave: SPW) in which polarity reverses in Stratum Pyramidale, and associated with fast oscillations (ripples: stars) and multi-unit burst of activity (arrows), displayed at higher time scale in the right insert.

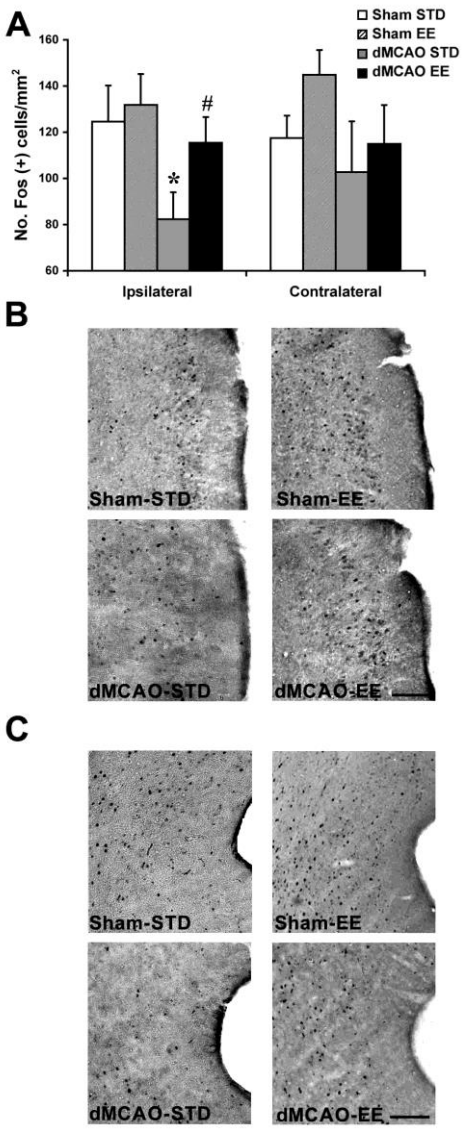


**Figure 6. Hypoactivation in the parahippocampal region occurs following dMCAO and is restored by EE. (A)** Counts of Fos-positive nuclei in the entorhinal cortex of shams and dMCAO rats exposed to STD or EE housing condition and tested for spatial memory in the Barnes maze. There were less Fos-positive cells in MCAO-STD rats compared to Sham-STD ($F_{1,27} = 9.04$; $p<0.01$). EE was efficacious in restoring neuronal activity in dMCAO rats but not in shams. However, the surgery x housing interaction failed to reach significance ($F_{1,27} = 3.44$ ; $p < 0.07$) **(B)** Corresponding photomicrographs showing Fos labelling in the ipsilateral entorhinal cortex of shams and dMCAO animals exposed to standard or EE conditions. **(C)** Photomicrographs showing that similar to the entorhinal cortex, Fos labelling was reduced in the ispilatera perirhinal cortex of dMCAO-STD rats. This hypoactivation was reversed by EE. Scale bars, 100 μm. *p<0.05 versus Sham-STD; #p<0.05 versus dMCAO-STD; n = 5-10 rats/group.

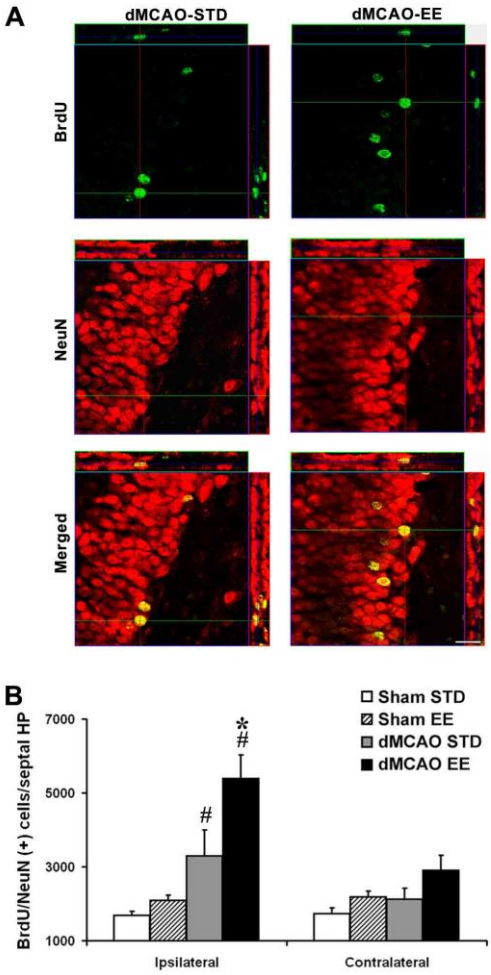


**Figure 7. EE enhances newborn cells survival in dMCAO rats. (A)** Representative orthogonal reconstructions of confocal microscopic images with BrdU as green, NeuN as red, and merged images as viewed in the x-z (top) and y-z (right) planes. The majority of newly divided cells assumed neuronal identity in the gcl of the DG at 4 weeks following BrdU labeling. More new neurons survived in dMCAO rats reared in the EE compared to those remained in the STD environment. Scale bar, 50 μm **(B)** dMCAO elicited an increase in progenitor cell proliferation during the time of BrdU administration, resulting in increased BrdU/NeuN double-positive cells in the ipsilateral DG of dMCAO-STD and dMCAO-EE groups compared to sham surgery ($F_{1,68}$ = 32.00 ; p<0.0001). There was a main housing effect ($F_{1,68}$ = 12.65 ; p<0.0008). EE enhanced the survival of newborn neurons predominantly in the ipsilateral DG of dMCAO rats compared to dMCAO rats reared in the STD environment. *p<0.05 versus dMCAO-STD; #p<0.05 versus shams; n = 8-10 rats/group.

## Supplementary materials

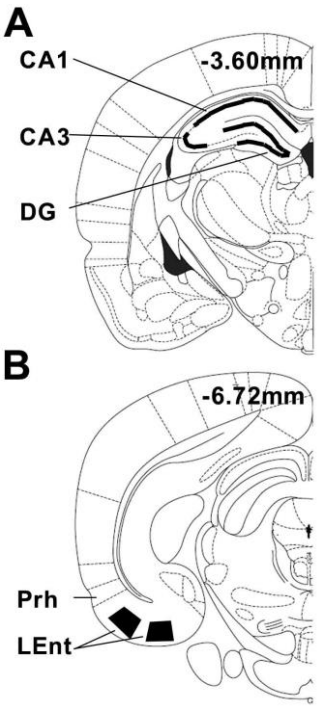


**Supplementary Figure 1. Schematic drawings of rat brain coronal sections showing the regions of interest (filled areas) selected for measurements of Fos labelling.** Numbers indicate the distance in millimeters of the sections from Bregma. CA1: CA1 field of dorsal hippocampus; CA3: CA3 field of dorsal hippocampus; DG: dentate gyrus; Prh: perirhinal cortex. LEnt: lateral entorhinal cortex (averaged Fos labelling from the two areas shown).

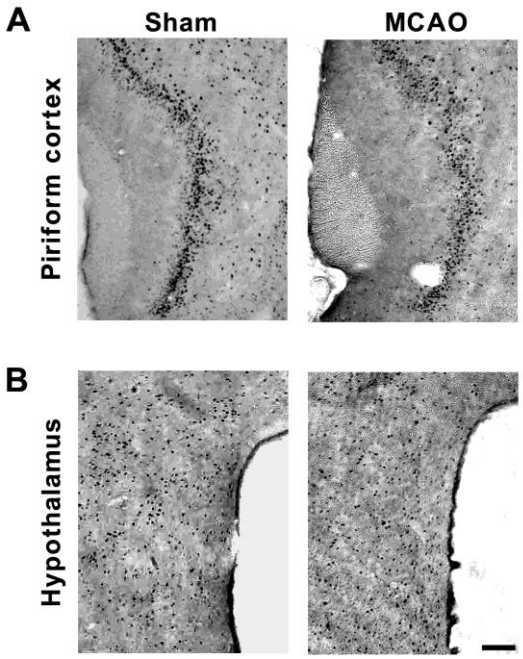


**Supplementary Figure 2. Photomicrographs taken at the level of the pririform cortex and hypothalamus of sham and dMCAO animals exploring a novel environment.** Fos labelling was not affected in these two regions following focal ischemia. Scale bars, 100 μm.

# References


Abel T, Nguyen PV (2008) Regulation of hippocampus-dependent memory by cyclic AMP-dependent protein kinase. Prog Brain Res 169:97-115.

Acar E, Aykut-Bingol C, Bingol H, Bro R, Yener B (2007) Multiway analysis of epilepsy tensors. Bioinformatics 23:i10-18.

Adey WR (1967) EEG patterns in sleep and wakefulness in high spinal cord injuries. Proc Annu Clin Spinal Cord Inj Conf 16:2-9.

Aggleton JP, Vann SD, Oswald CJ, Good M (2000) Identifying cortical inputs to the rat hippocampus that subserve allocentric spatial processes: a simple problem with a complex answer. Hippocampus 10:466-474.

Al-Qazzaz NK, Ali SH, Ahmad SA, Islam S, Mohamad K (2014) Cognitive impairment and memory dysfunction after a stroke diagnosis: a post-stroke memory assessment. Neuropsychiatr Dis Treat 10:1677-1691.

Alonso A, Garcia-Austt E (1987) Neuronal sources of theta rhythm in the entorhinal cortex of the rat. II. Phase relations between unit discharges and theta field potentials. Experimental brain research 67:502-509.

Alvarez P, Lipton PA, Melrose R, Eichenbaum H (2001) Differential effects of damage within the hippocampal region on memory for a natural, nonspatial Odor-Odor Association. Learning & memory (Cold Spring Harbor, NY) 8:79-86.

Amaral DG (1999) Introduction: What is where in the medial temporal lobe? Hippocampus 9:1-6.

Amaral DG, Witter MP (1989) The three-dimensional organization of the hippocampal formation: a review of anatomical data. Neuroscience 31:571-591.

Amaral DG, Dolorfo C, Alvarez-Royo P (1991) Organization of CA1 projections to the subiculum: a PHA-L analysis in the rat. Hippocampus 1:415-435.

Andrews RJ (1991) Transhemispheric diaschisis. A review and comment. Stroke; a journal of cerebral circulation 22:943-949.

Ang CW, Carlson GC, Coulter DA (2005) Hippocampal CA1 circuitry dynamically gates direct cortical inputs preferentially at theta frequencies. The Journal of neuroscience : the official journal of the Society for Neuroscience 25:9567-9580.

Asano T, Ikegaki I, Suzuki Y, Satoh S, Shibuya M (1989) Endothelin and the production of cerebral vasospasm in dogs. Biochem Biophys Res Commun 159:1345-1351.

Aspey BS, Cohen S, Patel Y, Terruli M, Harrison MJ (1998) Middle cerebral artery occlusion in the rat: consistent protocol for a model of stroke. Neuropathol Appl Neurobiol 24:487-497.

Astrup J, Siesjo BK, Symon L (1981) Thresholds in cerebral ischemia - the ischemic

penumbra. Stroke; a journal of cerebral circulation 12:723-725.

Atherton LA, Dupret D, Mellor JR (2015) Memory trace replay: the shaping of memory consolidation by neuromodulation. Trends Neurosci 38:560-570.

Attwell PJ, Rahman S, Ivarsson M, Yeo CH (1999) Cerebellar cortical AMPA-kainate receptor blockade prevents performance of classically conditioned nictitating membrane responses. The Journal of neuroscience : the official journal of the Society for Neuroscience 19:RC45.

Axmacher N, Elger CE, Fell J (2008) Ripples in the medial temporal lobe are relevant for human memory consolidation. Brain 131:1806-1817.

Baddeley A (2001) The concept of episodic memory. Philosophical transactions of the Royal Society of London Series B, Biological sciences 356:1345-1350.

Ball GJ, Gloor P, Schaul N (1977) The cortical electromicrophysiology of pathological delta waves in the electroencephalogram of cats. Electroencephalogr Clin Neurophysiol 43:346-361.

Bandera E, Botteri M, Minelli C, Sutton A, Abrams KR, Latronico N (2006) Cerebral blood flow threshold of ischemic penumbra and infarct core in acute ischemic stroke: a systematic review. Stroke; a journal of cerebral circulation 37:1334-1339.

Barba R, Martinez-Espinosa S, Rodriguez-Garcia E, Pondal M, Vivancos J, Del Ser T (2000) Poststroke dementia : clinical features and risk factors. Stroke; a journal of cerebral circulation 31:1494-1501.

Barker-Collo S, Starkey N, Lawes CM, Feigin V, Senior H, Parag V (2012) Neuropsychological profiles of 5-year ischemic stroke survivors by Oxfordshire stroke classification and hemisphere of lesion. Stroke; a journal of cerebral circulation 43:50-55.

Baron JC (2001) Perfusion thresholds in human cerebral ischemia: historical perspective and therapeutic implications. Cerebrovasc Dis 11 Suppl 1:2-8.

Barth AM, Mody I (2011) Changes in hippocampal neuronal activity during and after unilateral selective hippocampal ischemia in vivo. The Journal of neuroscience : the official journal of the Society for Neuroscience 31:851-860.

Basar E, Schurmann M, Basar-Eroglu C, Karakas S (1997) Alpha oscillations in brain functioning: an integrative theory. Int J Psychophysiol 26:5-29.

Basar E, Rahn E, Demiralp T, Schurmann M (1998) Spontaneous EEG theta activity controls frontal visual evoked potential amplitudes. Electroencephalogr Clin Neurophysiol 108:101-109.

Basar E, Basar-Eroglu C, Karakas S, Schurmann M (2000) Brain oscillations in perception and memory. Int J Psychophysiol 35:95-124.

Basar E, Basar-Eroglu C, Karakas S, Schurmann M (2001) Gamma, alpha, delta, and theta oscillations govern cognitive processes. Int J Psychophysiol 39:241-248.

Başar E (1998) Brain Function and Oscillations: Springer-Verlag Berlin Heidelberg.

Başar E (1999) Brain Function and Oscillations. : Springer-Verlag Berlin Heidelberg.

Battaglia FP, Sutherland GR, McNaughton BL (2004) Hippocampal sharp wave bursts coincide with neocortical "up-state" transitions. Learning & memory (Cold Spring Harbor, NY) 11:697-704.

Battaglia FP, Benchenane K, Sirota A, Pennartz CM, Wiener SI (2011) The hippocampus: hub of brain network communication for memory. Trends in cognitive sciences 15:310-318.

Beattie EC, Carroll RC, Yu X, Morishita W, Yasuda H, von Zastrow M, Malenka RC (2000) Regulation of AMPA receptor endocytosis by a signaling mechanism shared with LTD. Nature neuroscience 3:1291-1300.

Benchenane K, Peyrache A, Khamassi M, Tierney PL, Gioanni Y, Battaglia FP, Wiener SI (2010) Coherent theta oscillations and reorganization of spike timing in the hippocampal- prefrontal network upon learning. Neuron 66:921-936.

Bender JE, Vishwanath K, Moore LK, Brown JQ, Chang V, Palmer GM, Ramanujam N (2009) A robust Monte Carlo model for the extraction of biological absorption and scattering in vivo. IEEE Trans Biomed Eng 56:960-968.

Bennett MR (2000) The concept of long term potentiation of transmission at synapses. Prog Neurobiol 60:109-137.

Bhattacharya P, Pandey AK, Paul S, Patnaik R (2013) Does Piroxicam really protect ischemic neurons and influence neuronal firing in cerebral ischemia? An exploration towards therapeutics. Med Hypotheses 81:429-435.

Bitzenhofer SH, Sieben K, Siebert KD, Spehr M, Hanganu-Opatz IL (2015) Oscillatory activity in developing prefrontal networks results from theta-gamma-modulated synaptic inputs. Cell reports 11:486-497.

Bliss TV, Lomo T (1973) Long-lasting potentiation of synaptic transmission in the dentate area of the anaesthetized rabbit following stimulation of the perforant path. The Journal of physiology 232:331-356.

Bliss TV, Gardner-Medwin AR (1973) Long-lasting potentiation of synaptic transmission in the dentate area of the unanaestetized rabbit following stimulation of the perforant path. The Journal of physiology 232:357-374.

Bliss TV, Collingridge GL (1993) A synaptic model of memory: long-term potentiation in the hippocampus. Nature 361:31-39.

Borgers C, Kopell N (2005) Effects of noisy drive on rhythms in networks of excitatory and inhibitory neurons. Neural Comput 17:557-608.

Boveris A, Costa LE, Poderoso JJ, Carreras MC, Cadenas E (2000) Regulation of mitochondrial respiration by oxygen and nitric oxide. Annals of the New York Academy of Sciences 899:121-135.

Bragin A, Engel J, Jr., Staba RJ (2010) High-frequency oscillations in epileptic brain. Curr Opin Neurol 23:151-156.

Bragin A, Jando G, Nadasdy Z, van Landeghem M, Buzsaki G (1995a) Dentate EEG spikes and associated interneuronal population bursts in the hippocampal hilar region of the rat. Journal of neurophysiology 73:1691-1705.

Bragin A, Engel J, Jr., Wilson CL, Fried I, Buzsaki G (1999) High-frequency oscillations in human brain. Hippocampus 9:137-142.

Bragin A, Jando G, Nadasdy Z, Hetke J, Wise K, Buzsaki G (1995b) Gamma (40-100 Hz) oscillation in the hippocampus of the behaving rat. The Journal of neuroscience : the official journal of the Society for Neuroscience 15:47-60.

Branston NM, Symon L, Crockard HA, Pasztor E (1974) Relationship between the cortical evoked potential and local cortical blood flow following acute middle cerebral artery occlusion in the baboon. Exp Neurol 45:195-208.

Bringuier V, Fregnac Y, Baranyi A, Debanne D, Shulz DE (1997) Synaptic origin and stimulus dependency of neuronal oscillatory activity in the primary visual cortex of the cat. The Journal of physiology 500 ( Pt 3):751-774.

Brinker G, Franke C, Hoehn M, Uhlenkuken U, Hossmann KA (1999) Thrombolysis of cerebral clot embolism in rat: effect of treatment delay. Neuroreport 10:3269-3272.

Brookes PS, Bolanos JP, Heales SJ (1999) The assumption that nitric oxide inhibits mitochondrial ATP synthesis is correct. FEBS Lett 446:261-263.

Brown CE, Li P, Boyd JD, Delaney KR, Murphy TH (2007) Extensive turnover of dendritic spines and vascular remodeling in cortical tissues recovering from stroke. The Journal of neuroscience : the official journal of the Society for Neuroscience 27:4101-4109.

Brunel N, Wang XJ (2003) What determines the frequency of fast network oscillations with irregular neural discharges? I. Synaptic dynamics and excitation-inhibition balance. Journal of neurophysiology 90:415-430.

Buffalo EA, Fries P, Landman R, Buschman TJ, Desimone R (2011) Laminar differences in gamma and alpha coherence in the ventral stream. Proceedings of the National Academy of Sciences of the United States of America 108:11262-11267.

Buhl EH, Tamas G, Fisahn A (1998) Cholinergic activation and tonic excitation induce persistent gamma oscillations in mouse somatosensory cortex in vitro. The Journal of physiology 513 ( Pt 1):117-126.

Bullock R, Zauner A, Woodward JJ, Myseros J, Choi SC, Ward JD, Marmarou A, Young HF (1998) Factors affecting excitatory amino acid release following severe human head injury. Journal of neurosurgery 89:507-518.

Burette F, Jay TM, Laroche S (1997) Reversal of LTP in the hippocampal afferent fiber system to the prefrontal cortex in vivo with low-frequency patterns of stimulation that do not produce LTD. Journal of neurophysiology 78:1155-1160.

Burgess AP, Gruzelier JH (2000) Short duration power changes in the EEG during recognition

memory for words and faces. Psychophysiology 37:596-606.

Burwell RD (2000) The parahippocampal region: corticocortical connectivity. Annals of the New York Academy of Sciences 911:25-42.

Burwell RD, Amaral DG (1998) Cortical afferents of the perirhinal, postrhinal, and entorhinal cortices of the rat. J Comp Neurol 398:179-205.

Burwell RD, Witter MP, Amaral DG (1995) Perirhinal and postrhinal cortices of the rat: a review of the neuroanatomical literature and comparison with findings from the monkey brain. Hippocampus 5:390-408.

Buzsaki G (1986) Hippocampal sharp waves: their origin and significance. Brain research 398:242-252.

Buzsaki G (1996) The hippocampo-neocortical dialogue. Cerebral cortex (New York, NY : 1991) 6:81-92.

Buzsaki G (2002) Theta oscillations in the hippocampus. Neuron 33:325-340.

Buzsaki G (2015) Hippocampal sharp wave-ripple: A cognitive biomarker for episodic memory and planning. Hippocampus 25:1073-1188.

Buzsaki G, Draguhn A (2004) Neuronal oscillations in cortical networks. Science (New York, NY) 304:1926-1929.

Buzsaki G, Chrobak JJ (2005) Synaptic plasticity and self-organization in the hippocampus. Nature neuroscience 8:1418-1420.

Buzsaki G, Leung LW, Vanderwolf CH (1983) Cellular bases of hippocampal EEG in the behaving rat. Brain research 287:139-171.

Buzsaki G, Horvath Z, Urioste R, Hetke J, Wise K (1992) High-frequency network oscillation in the hippocampus. Science (New York, NY) 256:1025-1027.

Calabresi P, Pisani A, Mercuri NB, Bernardi G (1995) Hypoxia-induced electrical changes in striatal neurons. Journal of cerebral blood flow and metabolism : official journal of the International Society of Cerebral Blood Flow and Metabolism 15:1141-1145.

Canazza A, Minati L, Boffano C, Parati E, Binks S (2014) Experimental models of brain ischemia: a review of techniques, magnetic resonance imaging, and investigational cell-based therapies. Front Neurol 5:19.

Canto CB, Wouterlood FG, Witter MP (2008) What does the anatomical organization of the entorhinal cortex tell us? Neural Plast 2008:381243.

Cardin JA, Palmer LA, Contreras D (2005) Stimulus-dependent gamma (30-50 Hz) oscillations in simple and complex fast rhythmic bursting cells in primary visual cortex. The Journal of neuroscience : the official journal of the Society for Neuroscience 25:5339-5350.

Carmichael ST (2005) Rodent models of focal stroke: size, mechanism, and purpose. NeuroRx 2:396-409.

Carmichael ST (2006) Cellular and molecular mechanisms of neural repair after stroke: making waves. Ann Neurol 59:735-742.

Carmichael ST, Chesselet MF (2002) Synchronous neuronal activity is a signal for axonal sprouting after cortical lesions in the adult. The Journal of neuroscience : the official journal of the Society for Neuroscience 22:6062-6070.

Carr MF, Jadhav SP, Frank LM (2011) Hippocampal replay in the awake state: a potential substrate for memory consolidation and retrieval. Nature neuroscience 14:147-153.

Carrera E, Tononi G (2014) Diaschisis: past, present, future. Brain 137:2408-2422.

Carroll RC, Beattie EC, Xia H, Luscher C, Altschuler Y, Nicoll RA, Malenka RC, von Zastrow M (1999) Dynamin-dependent endocytosis of ionotropic glutamate receptors. Proceedings of the National Academy of Sciences of the United States of America 96:14112-14117.

Castillo J, Davalos A, Naveiro J, Noya M (1996) Neuroexcitatory amino acids and their relation to infarct size and neurological deficit in ischemic stroke. Stroke; a journal of cerebral circulation 27:1060-1065.

Chalk M, Herrero JL, Gieselmann MA, Delicato LS, Gotthardt S, Thiele A (2010) Attention reduces stimulus-driven gamma frequency oscillations and spike field coherence in V1. Neuron 66:114-125.

Chan PH (2001) Reactive oxygen radicals in signaling and damage in the ischemic brain. Journal of cerebral blood flow and metabolism : official journal of the International Society of Cerebral Blood Flow and Metabolism 21:2-14.

Charpak S, Pare D, Llinas R (1995) The entorhinal cortex entrains fast CA1 hippocampal oscillations in the anaesthetized guinea-pig: role of the monosynaptic component of the perforant path. The European journal of neuroscience 7:1548-1557.

Chen ST, Hsu CY, Hogan EL, Maricq H, Balentine JD (1986) A model of focal ischemic stroke in the rat: reproducible extensive cortical infarction. Stroke; a journal of cerebral circulation 17:738-743.

Choi DW, Koh JY, Peters S (1988) Pharmacology of glutamate neurotoxicity in cortical cell culture: attenuation by NMDA antagonists. The Journal of neuroscience : the official journal of the Society for Neuroscience 8:185-196.

Chrobak JJ, Buzsaki G (1994) Selective activation of deep layer (V-VI) retrohippocampal cortical neurons during hippocampal sharp waves in the behaving rat. The Journal of neuroscience : the official journal of the Society for Neuroscience 14:6160-6170.

Chrobak JJ, Buzsaki G (1996) High-frequency oscillations in the output networks of the hippocampal-entorhinal axis of the freely behaving rat. The Journal of neuroscience : the official journal of the Society for Neuroscience 16:3056-3066.

Chrobak JJ, Buzsaki G (1998) Gamma oscillations in the entorhinal cortex of the freely behaving rat. The Journal of neuroscience : the official journal of the Society for Neuroscience 18:388-398.

Cimadevilla JM, Mendez M, Mendez-Lopez M, Arias JL (2007) Unilateral hippocampal blockade reveals that one hippocampus is sufficient for learning a passive avoidance task. J Neurosci Res 85:1138-1142.

Cipolotti L, Shallice T, Chan D, Fox N, Scahill R, Harrison G, Stevens J, Rudge P (2001) Long-term retrograde amnesia...the crucial role of the hippocampus. Neuropsychologia 39:151-172.

Citri A, Malenka RC (2008) Synaptic plasticity: multiple forms, functions, and mechanisms. Neuropsychopharmacology 33:18-41.

Clark RE, Broadbent NJ, Zola SM, Squire LR (2002) Anterograde amnesia and temporally graded retrograde amnesia for a nonspatial memory task after lesions of hippocampus and subiculum. The Journal of neuroscience : the official journal of the Society for Neuroscience 22:4663-4669.

Clement EA, Richard A, Thwaites M, Ailon J, Peters S, Dickson CT (2008) Cyclic and sleep-like spontaneous alternations of brain state under urethane anaesthesia. PLoS One 3:e2004.

Colgin LL (2011) Oscillations and hippocampal-prefrontal synchrony. Current opinion in neurobiology 21:467-474.

Colling SB, Stanford IM, Traub RD, Jefferys JG (1998) Limbic gamma rhythms. I. Phase-locked oscillations in hippocampal CA1 and subiculum. Journal of neurophysiology 80:155-161.

Cooper S, Greene JD (2005) The clinical assessment of the patient with early dementia. J Neurol Neurosurg Psychiatry 76 Suppl 5:v15-24.

Cordonnier C, Leys D (2008) Stroke: the bare essentials. Pract Neurol 8:263-272.

Coutureau E, Di Scala G (2009) Entorhinal cortex and cognition. Prog Neuropsychopharmacol Biol Psychiatry 33:753-761.

Crack PJ, Taylor JM (2005) Reactive oxygen species and the modulation of stroke. Free Radic Biol Med 38:1433-1444.

Crochet S, Petersen CC (2006) Correlating whisker behavior with membrane potential in barrel cortex of awake mice. Nat Neurosci 9:608-610.

Crone NE, Miglioretti DL, Gordon B, Lesser RP (1998) Functional mapping of human sensorimotor cortex with electrocorticographic spectral analysis. II. Event-related synchronization in the gamma band. Brain 121 ( Pt 12):2301-2315.

Crumrine RC, Marder VJ, Taylor GM, Lamanna JC, Tsipis CP, Scuderi P, Petteway SR, Jr., Arora V (2011) Intra-arterial administration of recombinant tissue-type plasminogen activator (rt-PA) causes more intracranial bleeding than does intravenous rt-PA in a transient rat middle cerebral artery occlusion model. Exp Transl Stroke Med 3:10.

Crunelli V, Hughes SW (2010) The slow (<1 Hz) rhythm of non-REM sleep: a dialogue between three cardinal oscillators. Nature neuroscience 13:9-17.

Csicsvari J, Hirase H, Mamiya A, Buzsaki G (2000) Ensemble patterns of hippocampal CA3-CA1 neurons during sharp wave-associated population events. Neuron 28:585-594.

Csicsvari J, Jamieson B, Wise KD, Buzsaki G (2003) Mechanisms of gamma oscillations in the hippocampus of the behaving rat. Neuron 37:311-322.

Csicsvari J, Hirase H, Czurkó A, Mamiya A, Buzsáki G (1999a) Oscillatory Coupling of Hippocampal Pyramidal Cells and Interneurons in the Behaving Rat. The Journal of Neuroscience 19:274-287.

Csicsvari J, Hirase H, Czurko A, Mamiya A, Buzsaki G (1999b) Oscillatory coupling of hippocampal pyramidal cells and interneurons in the behaving Rat. The Journal of neuroscience : the official journal of the Society for Neuroscience 19:274-287.

Csicsvari J, Hirase H, Czurko A, Mamiya A, Buzsaki G (1999c) Fast network oscillations in the hippocampal CA1 region of the behaving rat. The Journal of neuroscience : the official journal of the Society for Neuroscience 19:RC20.

Cullen B, O'Neill B, Evans JJ, Coen RF, Lawlor BA (2007) A review of screening tests for cognitive impairment. J Neurol Neurosurg Psychiatry 78:790-799.

Cumming TB, Marshall RS, Lazar RM (2013) Stroke, cognitive deficits, and rehabilitation: still an incomplete picture. Int J Stroke 8:38-45.

da Silva FH, van Lierop TH, Schrijer CF, van Leeuwen WS (1973) Organization of thalamic and cortical alpha rhythms: spectra and coherences. Electroencephalogr Clin Neurophysiol 35:627-639.

Dahlqvist P, Ronnback A, Bergstrom SA, Soderstrom I, Olsson T (2004) Environmental enrichment reverses learning impairment in the Morris water maze after focal cerebral ischemia in rats. The European journal of neuroscience 19:2288-2298.

de Haan EH, Nys GM, Van Zandvoort MJ (2006) Cognitive function following stroke and vascular cognitive impairment. Curr Opin Neurol 19:559-564.

Del Pino I, Garcia-Frigola C, Dehorter N, Brotons-Mas JR, Alvarez-Salvado E, Martinez de Lagran M, Ciceri G, Gabaldon MV, Moratal D, Dierssen M, Canals S, Marin O, Rico B (2013) Erbb4 deletion from fast-spiking interneurons causes schizophrenia-like phenotypes. Neuron 79:1152-1168.

del Zoppo GJ, Poeck K, Pessin MS, Wolpert SM, Furlan AJ, Ferbert A, Alberts MJ, Zivin JA, Wechsler L, Busse O, et al. (1992) Recombinant tissue plasminogen activator in acute thrombotic and embolic stroke. Ann Neurol 32:78-86.

Dennis M, O'Rourke S, Lewis S, Sharpe M, Warlow C (2000) Emotional outcomes after stroke: factors associated with poor outcome. J Neurol Neurosurg Psychiatry 68:47-52.

Deshmukh SS, Yoganarasimha D, Voicu H, Knierim JJ (2010) Theta modulation in the medial and the lateral entorhinal cortices. Journal of neurophysiology 104:994-1006.

Desmond DW, Moroney JT, Paik MC, Sano M, Mohr JP, Aboumatar S, Tseng CL, Chan S, Williams JB, Remien RH, Hauser WA, Stern Y (2000) Frequency and clinical

determinants of dementia after ischemic stroke. Neurology 54:1124-1131.

Destexhe A, Sejnowski TJ (2003) Interactions between membrane conductances underlying thalamocortical slow-wave oscillations. Physiol Rev 83:1401-1453.

Dewar MT, Cowan N, Sala SD (2007) Forgetting due to retroactive interference: a fusion of Muller and Pilzecker's (1900) early insights into everyday forgetting and recent research on anterograde amnesia. Cortex 43:616-634.

Dickson CT, Magistretti J, Shalinsky M, Hamam B, Alonso A (2000) Oscillatory activity in entorhinal neurons and circuits. Mechanisms and function. Annals of the New York Academy of Sciences 911:127-150.

Dirnagl U, Iadecola C, Moskowitz MA (1999) Pathobiology of ischaemic stroke: an integrated view. Trends Neurosci 22:391-397.

Doeppner TR, Pehlke JR, Kaltwasser B, Schlechter J, Kilic E, Bahr M, Hermann DM (2015) The indirect NMDAR antagonist acamprosate induces postischemic neurologic recovery associated with sustained neuroprotection and neuroregeneration. Journal of cerebral blood flow and metabolism : official journal of the International Society of Cerebral Blood Flow and Metabolism.

Dolorfo CL, Amaral DG (1998) Entorhinal cortex of the rat: topographic organization of the cells of origin of the perforant path projection to the dentate gyrus. J Comp Neurol 398:25-48.

Donnan GA, Fisher M, Macleod M, Davis SM (2008) Stroke. Lancet 371:1612-1623.

Douglas RJ, Martin KA (2004) Neuronal circuits of the neocortex. Annu Rev Neurosci 27:419-451.

Doyle KP, Simon RP, Stenzel-Poore MP (2008) Mechanisms of ischemic brain damage. Neuropharmacology 55:310-318.

Dreier JP, Major S, Manning A, Woitzik J, Drenckhahn C, Steinbrink J, Tolias C, Oliveira-Ferreira AI, Fabricius M, Hartings JA, Vajkoczy P, Lauritzen M, Dirnagl U, Bohner G, Strong AJ, group Cs (2009) Cortical spreading ischaemia is a novel process involved in ischaemic damage in patients with aneurysmal subarachnoid haemorrhage. Brain 132:1866-1881.

Dudai Y (2004) The neurobiology of consolidations, or, how stable is the engram? Annu Rev Psychol 55:51-86.

Dudek SM, Bear MF (1992) Homosynaptic long-term depression in area CA1 of hippocampus and effects of N-methyl-D-aspartate receptor blockade. Proceedings of the National Academy of Sciences of the United States of America 89:4363-4367.

Durukan A, Tatlisumak T (2007) Acute ischemic stroke: overview of major experimental rodent models, pathophysiology, and therapy of focal cerebral ischemia. Pharmacol Biochem Behav 87:179-197.

Easton JD, Saver JL, Albers GW, Alberts MJ, Chaturvedi S, Feldmann E, Hatsukami TS, Higashida RT, Johnston SC, Kidwell CS, Lutsep HL, Miller E, Sacco RL (2009)

Definition and evaluation of transient ischemic attack: a scientific statement for healthcare professionals from the American Heart Association/American Stroke Association Stroke Council; Council on Cardiovascular Surgery and Anesthesia; Council on Cardiovascular Radiology and Intervention; Council on Cardiovascular Nursing; and the Interdisciplinary Council on Peripheral Vascular Disease. The American Academy of Neurology affirms the value of this statement as an educational tool for neurologists. Stroke; a journal of cerebral circulation 40:2276-2293.

Ebersole JS (**2003**) Cortical generators and EEG voltage fields: Philadelphia: Lippincott Williams & Wilkins.

Ebrahim S, Nouri F, Barer D (1985) Cognitive impairment after stroke. Age Ageing 14:345-348.

Ego-Stengel V, Wilson MA (2010) Disruption of ripple-associated hippocampal activity during rest impairs spatial learning in the rat. Hippocampus 20:1-10.

Eichenbaum H, Lipton PA (2008) Towards a functional organization of the medial temporal lobe memory system: role of the parahippocampal and medial entorhinal cortical areas. Hippocampus 18:1314-1324.

Eichenbaum H, Yonelinas AP, Ranganath C (2007) The medial temporal lobe and recognition memory. Annu Rev Neurosci 30:123-152.

Elfant D, Pal BZ, Emptage N, Capogna M (2008) Specific inhibitory synapses shift the balance from feedforward to feedback inhibition of hippocampal CA1 pyramidal cells. The European journal of neuroscience 27:104-113.

Endres M, Dirnagl U (2002) Ischemia and stroke. Adv Exp Med Biol 513:455-473.

Engel AK, Fries P (2010) Beta-band oscillations--signalling the status quo? Current opinion in neurobiology 20:156-165.

Engel AK, Fries P, Singer W (2001) Dynamic predictions: oscillations and synchrony in top-down processing. Nature reviews Neuroscience 2:704-716.

Engel J, Jr., Bragin A, Staba R, Mody I (2009) High-frequency oscillations: what is normal and what is not? Epilepsia 50:598-604.

Englund M, Hyllienmark L, Brismar T (2001) Chemical hypoxia in hippocampal pyramidal cells affects membrane potential differentially depending on resting potential. Neuroscience 106:89-94.

Erdemli G, Crunelli V (1998) Response of thalamocortical neurons to hypoxia: a whole-cell patch-clamp study. The Journal of neuroscience : the official journal of the Society for Neuroscience 18:5212-5224.

Erkinjuntti T (2007) Vascular cognitive deterioration and stroke. Cerebrovasc Dis 24 Suppl 1:189-194.

Eschenko O, Ramadan W, Molle M, Born J, Sara SJ (2008) Sustained increase in hippocampal sharp-wave ripple activity during slow-wave sleep after learning. Learning & memory (Cold Spring Harbor, NY) 15:222-228.

Evans BM (1976) Patterns of arousal in comatose patients. J Neurol Neurosurg Psychiatry 39:392-402.

Faught E (1993) Current role of electroencephalography in cerebral ischemia. Stroke; a journal of cerebral circulation 24:609-613.

Feige B, Scheffler K, Esposito F, Di Salle F, Hennig J, Seifritz E (2005) Cortical and subcortical correlates of electroencephalographic alpha rhythm modulation. Journal of neurophysiology 93:2864-2872.

Fenton AA, Bures J (1993) Place navigation in rats with unilateral tetrodotoxin inactivation of the dorsal hippocampus: place but not procedural learning can be lateralized to one hippocampus. Behav Neurosci 107:552-564.

Ferri R, Cosentino FI, Elia M, Musumeci SA, Marinig R, Bergonzi P (2001) Relationship between Delta, Sigma, Beta, and Gamma EEG bands at REM sleep onset and REM sleep end. Clin Neurophysiol 112:2046-2052.

Ferro JM (2001) Hyperacute cognitive stroke syndromes. J Neurol 248:841-849.

Finger S, Koehler PJ, Jagella C (2004) The Monakow concept of diaschisis: origins and perspectives. Archives of Neurology 61:283-288.

Finnigan S, van Putten MJ (2013) EEG in ischaemic stroke: quantitative EEG can uniquely inform (sub-)acute prognoses and clinical management. Clin Neurophysiol 124:10-19.

Finnigan SP, Rose SE, Walsh M, Griffin M, Janke AL, McMahon KL, Gillies R, Strudwick MW, Pettigrew CM, Semple J, Brown J, Brown P, Chalk JB (2004) Correlation of quantitative EEG in acute ischemic stroke with 30-day NIHSS score: comparison with diffusion and perfusion MRI. Stroke; a journal of cerebral circulation 35:899-903.

Fiorelli M, Blin J, Bakchine S, Laplane D, Baron JC (1991) PET studies of cortical diaschisis in patients with motor hemi-neglect. Journal of the neurological sciences 104:135-142.

Foreman B, Claassen J (2012) Quantitative EEG for the detection of brain ischemia. Crit Care 16:216.

Frankland PW, Bontempi B (2005) The organization of recent and remote memories. Nature reviews Neuroscience 6:119-130.

Freeman WJ (1991) The physiology of perception. Sci Am 264:78-85.

Frey U, Morris RG (1997) Synaptic tagging and long-term potentiation. Nature 385:533-536.

Fries P, Reynolds JH, Rorie AE, Desimone R (2001) Modulation of oscillatory neuronal synchronization by selective visual attention. Science (New York, NY) 291:1560-1563.

Gallinat J, Kunz D, Senkowski D, Kienast T, Seifert F, Schubert F, Heinz A (2006) Hippocampal glutamate concentration predicts cerebral theta oscillations during cognitive processing. Psychopharmacology (Berl) 187:103-111.

Garcia-Rill E, Kezunovic N, Hyde J, Simon C, Beck P, Urbano FJ (2013) Coherence and

frequency in the reticular activating system (RAS). Sleep Med Rev 17:227-238.

Gilboa A, Winocur G, Grady CL, Hevenor SJ, Moscovitch M (2004) Remembering our past: functional neuroanatomy of recollection of recent and very remote personal events. Cerebral cortex (New York, NY : 1991) 14:1214-1225.

Gillies MJ, Traub RD, LeBeau FE, Davies CH, Gloveli T, Buhl EH, Whittington MA (2002) A model of atropine-resistant theta oscillations in rat hippocampal area CA1. The Journal of physiology 543:779-793.

Ginsberg MD, Busto R (1989) Rodent models of cerebral ischemia. Stroke; a journal of cerebral circulation 20:1627-1642.

Ginsburg DA, Pasternak EB, Gurvitch AM (1977) Correlation analysis of delta activity generated in cerebral hypoxia. Electroencephalogr Clin Neurophysiol 42:445-455.

Girardeau G, Zugaro M (2011) Hippocampal ripples and memory consolidation. Current opinion in neurobiology 21:452-459.

Girardeau G, Cei A, Zugaro M (2014) Learning-induced plasticity regulates hippocampal sharp wave-ripple drive. The Journal of neuroscience : the official journal of the Society for Neuroscience 34:5176-5183.

Girardeau G, Benchenane K, Wiener SI, Buzsaki G, Zugaro MB (2009) Selective suppression of hippocampal ripples impairs spatial memory. Nature neuroscience 12:1222-1223.

Givens BS, Olton DS (1990) Cholinergic and GABAergic modulation of medial septal area: effect on working memory. Behav Neurosci 104:849-855.

Gloor P (1985) Neuronal generators and the problem of localization in electroencephalography: application of volume conductor theory to electroencephalography. J Clin Neurophysiol 2:327-354.

Gloor P, Ball G, Schaul N (1977) Brain lesions that produce delta waves in the EEG. Neurology 27:326-333.

Gold L, Lauritzen M (2002) Neuronal deactivation explains decreased cerebellar blood flow in response to focal cerebral ischemia or suppressed neocortical function. Proceedings of the National Academy of Sciences of the United States of America 99:7699-7704.

Goldman RI, Stern JM, Engel J, Jr., Cohen MS (2002) Simultaneous EEG and fMRI of the alpha rhythm. Neuroreport 13:2487-2492.

Gonzalez Delgado M, Bogousslavsky J (2012) Superficial middle cerebral artery territory infarction. Front Neurol Neurosci 30:111-114.

Gonzalez RG (2006) Imaging-guided acute ischemic stroke therapy: From "time is brain" to "physiology is brain". AJNR Am J Neuroradiol 27:728-735.

Gorgoni M, D'Atri A, Lauri G, Rossini PM, Ferlazzo F, De Gennaro L (2013) Is sleep essential for neural plasticity in humans, and how does it affect motor and cognitive recovery? Neural Plast 2013:103949.

Gray CM, McCormick DA (1996) Chattering cells: superficial pyramidal neurons contributing to the generation of synchronous oscillations in the visual cortex. Science (New York, NY) 274:109-113.

Green JD, Arduini AA (1954) Hippocampal electrical activity in arousal. Journal of neurophysiology 17:533-557.

Gursoy-Ozdemir Y, Can A, Dalkara T (2004) Reperfusion-induced oxidative/nitrative injury to neurovascular unit after focal cerebral ischemia. Stroke; a journal of cerebral circulation 35:1449-1453.

Guyot LL, Diaz FG, O'Regan MH, McLeod S, Park H, Phillis JW (2001) Real-time measurement of glutamate release from the ischemic penumbra of the rat cerebral cortex using a focal middle cerebral artery occlusion model. Neurosci Lett 299:37-40.

Haenschel C, Baldeweg T, Croft RJ, Whittington M, Gruzelier J (2000) Gamma and beta frequency oscillations in response to novel auditory stimuli: A comparison of human electroencephalogram (EEG) data with in vitro models. Proc Natl Acad Sci U S A 97:7645-7650.

Hahn TT, Sakmann B, Mehta MR (2007) Differential responses of hippocampal subfields to cortical up-down states. Proceedings of the National Academy of Sciences of the United States of America 104:5169-5174.

Hallenbeck JM, Dutka AJ (1990) Background review and current concepts of reperfusion injury. Arch Neurol 47:1245-1254.

Hamilton BB, Granger CV (1994) Disability outcomes following inpatient rehabilitation for stroke. Phys Ther 74:494-503.

Hamm RJ, Temple MD, O'Dell DM, Pike BR, Lyeth BG (1996) Exposure to environmental complexity promotes recovery of cognitive function after traumatic brain injury. Journal of neurotrauma 13:41-47.

Hammerman C, Kaplan M (1998) Ischemia and reperfusion injury. The ultimate pathophysiologic paradox. Clin Perinatol 25:757-777.

Harata N, Wu J, Ishibashi H, Ono K, Akaike N (1997) Run-down of the GABAA response under experimental ischaemia in acutely dissociated CA1 pyramidal neurones of the rat. The Journal of physiology 500 ( Pt 3):673-688.

Hari R, Salmelin R, Makela JP, Salenius S, Helle M (1997) Magnetoencephalographic cortical rhythms. Int J Psychophysiol 26:51-62.

Harris KD, Thiele A (2011) Cortical state and attention. Nature reviews Neuroscience 12:509-523.

Harris KD, Csicsvari J, Hirase H, Dragoi G, Buzsaki G (2003) Organization of cell assemblies in the hippocampus. Nature 424:552-556.

Hartings JA, Williams AJ, Tortella FC (2003) Occurrence of nonconvulsive seizures, periodic epileptiform discharges, and intermittent rhythmic delta activity in rat focal ischemia. Exp Neurol 179:139-149.

Hartkamp MJ, van Der Grond J, van Everdingen KJ, Hillen B, Mali WP (1999) Circle of Willis collateral flow investigated by magnetic resonance angiography. Stroke; a journal of cerebral circulation 30:2671-2678.

Hasselmo ME (2005) What is the function of hippocampal theta rhythm?--Linking behavioral data to phasic properties of field potential and unit recording data. Hippocampus 15:936-949.

Hochstenbach J, Mulder T, van Limbeek J, Donders R, Schoonderwaldt H (1998) Cognitive decline following stroke: a comprehensive study of cognitive decline following stroke. J Clin Exp Neuropsychol 20:503-517.

Hoffman RE, Cavus I (2002) Slow transcranial magnetic stimulation, long-term depotentiation, and brain hyperexcitability disorders. The American journal of psychiatry 159:1093-1102.

Holscher C, Anwyl R, Rowan MJ (1997) Stimulation on the positive phase of hippocampal theta rhythm induces long-term potentiation that can Be depotentiated by stimulation on the negative phase in area CA1 in vivo. The Journal of neuroscience : the official journal of the Society for Neuroscience 17:6470-6477.

Honkaniemi J, States BA, Weinstein PR, Espinoza J, Sharp FR (1997) Expression of zinc finger immediate early genes in rat brain after permanent middle cerebral artery occlusion. Journal of cerebral blood flow and metabolism : official journal of the International Society of Cerebral Blood Flow and Metabolism 17:636-646.

Hossmann KA (1994) Viability thresholds and the penumbra of focal ischemia. Ann Neurol 36:557-565.

Hossmann KA (1996) Periinfarct depolarizations. Cerebrovasc Brain Metab Rev 8:195-208.

Hossmann KA (1998) Experimental models for the investigation of brain ischemia. Cardiovasc Res 39:106-120.

Hossmann KA (2006) Pathophysiology and therapy of experimental stroke. Cell Mol Neurobiol 26:1057-1083.

Hou Q, Gilbert J, Man HY (2011) Homeostatic regulation of AMPA receptor trafficking and degradation by light-controlled single-synaptic activation. Neuron 72:806-818.

Howells DW, Porritt MJ, Rewell SS, O'Collins V, Sena ES, van der Worp HB, Traystman RJ, Macleod MR (2010) Different strokes for different folks: the rich diversity of animal models of focal cerebral ischemia. Journal of cerebral blood flow and metabolism : official journal of the International Society of Cerebral Blood Flow and Metabolism 30:1412-1431.

Hoyte L, Kaur J, Buchan AM (2004) Lost in translation: taking neuroprotection from animal models to clinical trials. Exp Neurol 188:200-204.

Huchzermeyer C, Albus K, Gabriel HJ, Otahal J, Taubenberger N, Heinemann U, Kovacs R, Kann O (2008) Gamma oscillations and spontaneous network activity in the hippocampus are highly sensitive to decreases in pO2 and concomitant changes in

mitochondrial redox state. The Journal of neuroscience : the official journal of the Society for Neuroscience 28:1153-1162.

Hughes SW, Crunelli V (2005) Thalamic mechanisms of EEG alpha rhythms and their pathological implications. Neuroscientist 11:357-372.

Hunsaker MR, Mooy GG, Swift JS, Kesner RP (2007) Dissociations of the medial and lateral perforant path projections into dorsal DG, CA3, and CA1 for spatial and nonspatial (visual object) information processing. Behav Neurosci 121:742-750.

Hyndman D, Pickering RM, Ashburn A (2008) The influence of attention deficits on functional recovery post stroke during the first 12 months after discharge from hospital. J Neurol Neurosurg Psychiatry 79:656-663.

Insausti R, Amaral DG, Cowan WM (1987) The entorhinal cortex of the monkey: II. Cortical afferents. J Comp Neurol 264:356-395.

Isomura Y, Sirota A, Ozen S, Montgomery S, Mizuseki K, Henze DA, Buzsaki G (2006) Integration and segregation of activity in entorhinal-hippocampal subregions by neocortical slow oscillations. Neuron 52:871-882.

Izquierdo I, Bevilaqua LR, Rossato JI, Bonini JS, Medina JH, Cammarota M (2006) Different molecular cascades in different sites of the brain control memory consolidation. Trends Neurosci 29:496-505.

Jadhav SP, Kemere C, German PW, Frank LM (2012) Awake hippocampal sharp-wave ripples support spatial memory. Science (New York, NY) 336:1454-1458.

Jaeger HM, Pehlke JR, Kaltwasser B, Kilic E, Bahr M, Hermann DM, Doeppner TR (2015) The indirect NMDAR inhibitor flupirtine induces sustained post-ischemic recovery, neuroprotection and angioneurogenesis. Oncotarget 6:14033-14044.

Jaillard A, Grand S, Le Bas JF, Hommel M (2010) Predicting cognitive dysfunctioning in nondemented patients early after stroke. Cerebrovasc Dis 29:415-423.

Jay TM, Burette F, Laroche S (1996) Plasticity of the hippocampal-prefrontal cortex synapses. J Physiol Paris 90:361-366.

Jeewajee A, Lever C, Burton S, O'Keefe J, Burgess N (2008) Environmental novelty is signaled by reduction of the hippocampal theta frequency. Hippocampus 18:340-348.

Jenkins TA, Dias R, Amin E, Brown MW, Aggleton JP (2002) Fos imaging reveals that lesions of the anterior thalamic nuclei produce widespread limbic hypoactivity in rats. The Journal of neuroscience : the official journal of the Society for Neuroscience 22:5230-5238.

Jiang C, Sigworth FJ, Haddad GG (1994) Oxygen deprivation activates an ATP-inhibitable K+ channel in substantia nigra neurons. The Journal of neuroscience : the official journal of the Society for Neuroscience 14:5590-5602.

Johansson BB (1996) Functional outcome in rats transferred to an enriched environment 15 days after focal brain ischemia. Stroke; a journal of cerebral circulation 27:324-326.

Jones RS (1994) Synaptic and intrinsic properties of neurons of origin of the perforant path in layer II of the rat entorhinal cortex in vitro. Hippocampus 4:335-353.

Jordan KG (2004) Emergency EEG and continuous EEG monitoring in acute ischemic stroke. J Clin Neurophysiol 21:341-352.

Kahana MJ, Seelig D, Madsen JR (2001) Theta returns. Current opinion in neurobiology 11:739-744.

Kajiwara R, Wouterlood FG, Sah A, Boekel AJ, Baks-te Bulte LT, Witter MP (2008) Convergence of entorhinal and CA3 inputs onto pyramidal neurons and interneurons in hippocampal area CA1--an anatomical study in the rat. Hippocampus 18:266-280.

Kamondi A, Acsady L, Wang XJ, Buzsaki G (1998) Theta oscillations in somata and dendrites of hippocampal pyramidal cells in vivo: activity-dependent phase-precession of action potentials. Hippocampus 8:244-261.

Kandel ER (2001) The molecular biology of memory storage: a dialog between genes and synapses. Biosci Rep 21:565-611.

Kann O, Huchzermeyer C, Kovacs R, Wirtz S, Schuelke M (2011) Gamma oscillations in the hippocampus require high complex I gene expression and strong functional performance of mitochondria. Brain 134:345-358.

Kelley MH, Taguchi N, Ardeshiri A, Kuroiwa M, Hurn PD, Traystman RJ, Herson PS (2008) Ischemic insult to cerebellar Purkinje cells causes diminished GABA(A) receptor function and Allopregnanolone neuroprotection is associated with GABA(A) receptor stabilization. Journal of neurochemistry 107:668-678.

Kemp A, Manahan-Vaughan D (2004) Hippocampal long-term depression and long-term potentiation encode different aspects of novelty acquisition. Proceedings of the National Academy of Sciences of the United States of America 101:8192-8197.

Kerr KM, Agster KL, Furtak SC, Burwell RD (2007) Functional neuroanatomy of the parahippocampal region: the lateral and medial entorhinal areas. Hippocampus 17:697-708.

Kesner RP, Farnsworth G, Kametani H (1991) Role of parietal cortex and hippocampus in representing spatial information. Cerebral cortex (New York, NY : 1991) 1:367-373.

Kim JJ, Baxter MG (2001) Multiple brain-memory systems: the whole does not equal the sum of its parts. Trends in neurosciences 24:324-330.

Kinouchi H, Huang H, Arai S, Mizoi K, Yoshimoto T (1999) Induction of cyclooxygenase-2 messenger RNA after transient and permanent middle cerebral artery occlusion in rats: comparison with c-fos messenger RNA by using in situ hybridization. Journal of neurosurgery 91:1005-1012.

Kinouchi H, Sharp FR, Chan PH, Koistinaho J, Sagar SM, Yoshimoto T (1994) Induction of c-fos, junB, c-jun, and hsp70 mRNA in cortex, thalamus, basal ganglia, and hippocampus following middle cerebral artery occlusion. Journal of cerebral blood flow and metabolism : official journal of the International Society of Cerebral Blood

Flow and Metabolism 14:808-817.

Kisley MA, Cornwell ZM (2006) Gamma and beta neural activity evoked during a sensory gating paradigm: effects of auditory, somatosensory and cross-modal stimulation. Clin Neurophysiol 117:2549-2563.

Klausberger T, Somogyi P (2008) Neuronal diversity and temporal dynamics: the unity of hippocampal circuit operations. Science (New York, NY) 321:53-57.

Knopfel T, Spuler A, Grafe P, Gahwiler BH (1990) Cytosolic calcium during glucose deprivation in hippocampal pyramidal cells of rats. Neurosci Lett 117:295-299.

Kohler C (1985) Intrinsic projections of the retrohippocampal region in the rat brain. I. The subicular complex. J Comp Neurol 236:504-522.

Kopniczky Z, Dobo E, Borbely S, Vilagi I, Detari L, Krisztin-Peva B, Bagosi A, Molnar E, Mihaly A (2005) Lateral entorhinal cortex lesions rearrange afferents, glutamate receptors, increase seizure latency and suppress seizure-induced c-fos expression in the hippocampus of adult rat. Journal of neurochemistry 95:111-124.

Koralek KA, Olavarria J, Killackey HP (1990) Areal and laminar organization of corticocortical projections in the rat somatosensory cortex. J Comp Neurol 299:133-150.

Kovacs KR, Czuriga D, Bereczki D, Bornstein NM, Csiba L (2013) Silent brain infarction--a review of recent observations. Int J Stroke 8:334-347.

Krause CM, Sillanmaki L, Koivisto M, Saarela C, Haggqvist A, Laine M, Hamalainen H (2000) The effects of memory load on event-related EEG desynchronization and synchronization. Clin Neurophysiol 111:2071-2078.

Krnjevic K (2008) Electrophysiology of cerebral ischemia. Neuropharmacology 55:319-333.

Krnjevic K, Xu YZ (1989) Dantrolene suppresses the hyperpolarization or outward current observed during anoxia in hippocampal neurons. Can J Physiol Pharmacol 67:1602-1604.

Lakatos P, Shah AS, Knuth KH, Ulbert I, Karmos G, Schroeder CE (2005) An oscillatory hierarchy controlling neuronal excitability and stimulus processing in the auditory cortex. Journal of neurophysiology 94:1904-1911.

Lammer AB, Beck A, Grummich B, Forschler A, Krugel T, Kahn T, Schneider D, Illes P, Franke H, Krugel U (2011) The P2 receptor antagonist PPADS supports recovery from experimental stroke in vivo. PLoS One 6:e19983.

Lansink CS, Goltstein PM, Lankelma JV, McNaughton BL, Pennartz CM (2009) Hippocampus leads ventral striatum in replay of place-reward information. PLoS Biol 7:e1000173.

Lavenex P, Amaral DG (2000) Hippocampal-neocortical interaction: a hierarchy of associativity. Hippocampus 10:420-430.

Le Van Quyen M, Bragin A, Staba R, Crépon B, Wilson CL, Engel J (2008) Cell Type-

Specific Firing during Ripple Oscillations in the Hippocampal Formation of Humans. The Journal of Neuroscience 28:6104-6110.

Lebedev MA, Nicolelis MA (2006) Brain-machine interfaces: past, present and future. Trends Neurosci 29:536-546.

Lennox WG, Gibbs FA, Gibbs EI (1938) The Relationship in Man of Cerebral Activity to Blood Flow and to Blood Constituents. J Neurol Psychiatry 1:211-225.

Leranth C, Hajszan T (2007) Extrinsic afferent systems to the dentate gyrus. Prog Brain Res 163:63-84.

Lesburgueres E, Gobbo OL, Alaux-Cantin S, Hambucken A, Trifilieff P, Bontempi B (2011) Early tagging of cortical networks is required for the formation of enduring associative memory. Science (New York, NY) 331:924-928.

Lesniak M, Bak T, Czepiel W, Seniow J, Czlonkowska A (2008) Frequency and prognostic value of cognitive disorders in stroke patients. Dement Geriatr Cogn Disord 26:356-363.

Leung LW, Borst JG (1987) Electrical activity of the cingulate cortex. I. Generating mechanisms and relations to behavior. Brain research 407:68-80.

Levine S, Payan H (1966) Effects of ischemia and other procedures on the brain and retina of the gerbil (Meriones unguiculatus). Exp Neurol 16:255-262.

Lewandowski CA, Rao CP, Silver B (2008) Transient ischemic attack: definitions and clinical presentations. Ann Emerg Med 52:S7-16.

Leys D, Deplanque D, Mounier-Vehier C, Mackowiak-Cordoliani MA, Lucas C, Bordet R (2002) Stroke prevention: management of modifiable vascular risk factors. J Neurol 249:507-517.

Li W, Huang R, Shetty RA, Thangthaeng N, Liu R, Chen Z, Sumien N, Rutledge M, Dillon GH, Yuan F, Forster MJ, Simpkins JW, Yang SH (2013) Transient focal cerebral ischemia induces long-term cognitive function deficit in an experimental ischemic stroke model. Neurobiology of disease 59:18-25.

Liebeskind DS (2003) Collateral circulation. Stroke; a journal of cerebral circulation 34:2279-2284.

Lim C, Alexander MP (2009) Stroke and episodic memory disorders. Neuropsychologia 47:3045-3058.

Lisman J, Schulman H, Cline H (2002) The molecular basis of CaMKII function in synaptic and behavioural memory. Nature reviews Neuroscience 3:175-190.

Liu PK (2003) Ischemia-reperfusion-related repair deficit after oxidative stress: implications of faulty transcripts in neuronal sensitivity after brain injury. J Biomed Sci 10:4-13.

Llinas R, Ribary U (1993) Coherent 40-Hz oscillation characterizes dream state in humans. Proceedings of the National Academy of Sciences of the United States of America 90:2078-2081.

Llinas RR (1988) The intrinsic electrophysiological properties of mammalian neurons: insights into central nervous system function. Science (New York, NY) 242:1654-1664.

Logothetis NK, Eschenko O, Murayama Y, Augath M, Steudel T, Evrard HC, Besserve M, Oeltermann A (2012) Hippocampal-cortical interaction during periods of subcortical silence. Nature 491:547-553.

Longa EZ, Weinstein PR, Carlson S, Cummins R (1989) Reversible middle cerebral artery occlusion without craniectomy in rats. Stroke; a journal of cerebral circulation 20:84-91.

Lopes MW, Soares FM, de Mello N, Nunes JC, Cajado AG, de Brito D, de Cordova FM, da Cunha RM, Walz R, Leal RB (2013) Time-dependent modulation of AMPA receptor phosphorylation and mRNA expression of NMDA receptors and glial glutamate transporters in the rat hippocampus and cerebral cortex in a pilocarpine model of epilepsy. Experimental brain research 226:153-163.

Lopez-Azcarate J, Nicolas MJ, Cordon I, Alegre M, Valencia M, Artieda J (2013) Delta-mediated cross-frequency coupling organizes oscillatory activity across the rat cortico-basal ganglia network. Front Neural Circuits 7:155.

Lu XC, Williams AJ, Tortella FC (2001) Quantitative electroencephalography spectral analysis and topographic mapping in a rat model of middle cerebral artery occlusion. Neuropathol Appl Neurobiol 27:481-495.

Lubenov EV, Siapas AG (2009) Hippocampal theta oscillations are travelling waves. Nature 459:534-539.

Luhmann HJ, Heinemann U (1992) Hypoxia-induced functional alterations in adult rat neocortex. Journal of neurophysiology 67:798-811.

Luxenberg JS, Feigenbaum LZ (1986) Cognitive impairment on a rehabilitation service. Arch Phys Med Rehabil 67:796-798.

Lynch MA (2004) Long-term potentiation and memory. Physiol Rev 84:87-136.

Maccaferri G, McBain CJ (1995) Passive propagation of LTD to stratum oriens-alveus inhibitory neurons modulates the temporoammonic input to the hippocampal CA1 region. Neuron 15:137-145.

Macdonald KD, Fifkova E, Jones MS, Barth DS (1998) Focal stimulation of the thalamic reticular nucleus induces focal gamma waves in cortex. Journal of neurophysiology 79:474-477.

Machado C, Cuspineda E, Valdes P, Virues T, Llopis F, Bosch J, Aubert E, Hernandez E, Pando A, Alvarez MA, Barroso E, Galan L, Avila Y (2004) Assessing acute middle cerebral artery ischemic stroke by quantitative electric tomography. Clin EEG Neurosci 35:116-124.

Macrae IM (2011) Preclinical stroke research--advantages and disadvantages of the most common rodent models of focal ischaemia. Br J Pharmacol 164:1062-1078.

Macrae IM, Robinson MJ, Graham DI, Reid JL, McCulloch J (1993) Endothelin-1-induced reductions in cerebral blood flow: dose dependency, time course, and neuropathological consequences. Journal of cerebral blood flow and metabolism : official journal of the International Society of Cerebral Blood Flow and Metabolism 13:276-284.

Macrides F, Eichenbaum HB, Forbes WB (1982) Temporal relationship between sniffing and the limbic theta rhythm during odor discrimination reversal learning. The Journal of neuroscience : the official journal of the Society for Neuroscience 2:1705-1717.

Maguire EA, Frith CD (2003) Lateral asymmetry in the hippocampal response to the remoteness of autobiographical memories. The Journal of neuroscience : the official journal of the Society for Neuroscience 23:5302-5307.

Malenka RC, Bear MF (2004) LTP and LTD: an embarrassment of riches. Neuron 44:5-21.

Malik R, Chattarji S (2012) Enhanced intrinsic excitability and EPSP-spike coupling accompany enriched environment-induced facilitation of LTP in hippocampal CA1 pyramidal neurons. Journal of neurophysiology 107:1366-1378.

Malinow R, Malenka RC (2002) AMPA receptor trafficking and synaptic plasticity. Annu Rev Neurosci 25:103-126.

Malinow R, Schulman H, Tsien RW (1989) Inhibition of postsynaptic PKC or CaMKII blocks induction but not expression of LTP. Science (New York, NY) 245:862-866.

Manahan-Vaughan D, Braunewell KH (1999) Novelty acquisition is associated with induction of hippocampal long-term depression. Proceedings of the National Academy of Sciences of the United States of America 96:8739-8744.

Marco-Pallares J, Cucurell D, Cunillera T, Garcia R, Andres-Pueyo A, Munte TF, Rodriguez-Fornells A (2008) Human oscillatory activity associated to reward processing in a gambling task. Neuropsychologia 46:241-248.

Mariucci G, Stasi MA, Taurelli R, Nardo P, Tantucci M, Pacifici L, Carminati P, Ambrosini MV (2003) EEG power spectra changes and forebrain ischemia in rats. Can J Neurol Sci 30:54-60.

Marr D (1970) A theory for cerebral neocortex. Proceedings of the Royal Society of London Series B, Biological sciences 176:161-234.

Marr D (1971) Simple memory: a theory for archicortex. Philosophical transactions of the Royal Society of London Series B, Biological sciences 262:23-81.

Martin JH (1991) Autoradiographic estimation of the extent of reversible inactivation produced by microinjection of lidocaine and muscimol in the rat. Neurosci Lett 127:160-164.

Martin SJ, Clark RE (2007) The rodent hippocampus and spatial memory: from synapses to systems. Cell Mol Life Sci 64:401-431.

Martin SJ, de Hoz L, Morris RG (2005) Retrograde amnesia: neither partial nor complete hippocampal lesions in rats result in preferential sparing of remote spatial memory,

even after reminding. Neuropsychologia 43:609-624.

Massey PV, Bashir ZI (2007) Long-term depression: multiple forms and implications for brain function. Trends Neurosci 30:176-184.

Matsumori Y, Hong SM, Fan Y, Kayama T, Hsu CY, Weinstein PR, Liu J (2006) Enriched environment and spatial learning enhance hippocampal neurogenesis and salvages ischemic penumbra after focal cerebral ischemia. Neurobiology of disease 22:187-198.

Mattson MP, Culmsee C, Yu ZF (2000) Apoptotic and antiapoptotic mechanisms in stroke. Cell Tissue Res 301:173-187.

Maviel T, Durkin TP, Menzaghi F, Bontempi B (2004) Sites of neocortical reorganization critical for remote spatial memory. Science (New York, NY) 305:96-99.

Mayford M, Wang J, Kandel ER, O'Dell TJ (1995) CaMKII regulates the frequency-response function of hippocampal synapses for the production of both LTD and LTP. Cell 81:891-904.

McBride SM, Giuliani G, Choi C, Krause P, Correale D, Watson K, Baker G, Siwicki KK (1999) Mushroom body ablation impairs short-term memory and long-term memory of courtship conditioning in Drosophila melanogaster. Neuron 24:967-977.

McClelland JL, McNaughton BL, O'Reilly RC (1995) Why there are complementary learning systems in the hippocampus and neocortex: insights from the successes and failures of connectionist models of learning and memory. Psychological review 102:419-457.

McCormick DA, Pape HC (1990) Noradrenergic and serotonergic modulation of a hyperpolarization-activated cation current in thalamic relay neurones. The Journal of physiology 431:319-342.

McGaugh JL (2000) Memory--a century of consolidation. Science (New York, NY) 287:248-251.

McVeigh C, Passmore P (2006) Vascular dementia: prevention and treatment. Clin Interv Aging 1:229-235.

Mendoza J (2011) Unimodal Cortex. In: Encyclopedia of Clinical Neuropsychology (Kreutzer J, DeLuca J, Caplan B, eds), pp 2578-2578: Springer New York.

Menzel R (2001) Searching for the memory trace in a mini-brain, the honeybee. Learning & memory (Cold Spring Harbor, NY) 8:53-62.

Mhairi Macrae I (1992) New models of focal cerebral ischaemia. Br J Clin Pharmacol 34:302-308.

Mitchell SJ, Ranck JB, Jr. (1980) Generation of theta rhythm in medial entorhinal cortex of freely moving rats. Brain research 189:49-66.

Miwa K, Hoshi T, Hougaku H, Tanaka M, Furukado S, Abe Y, Okazaki S, Sakaguchi M, Sakoda S, Kitagawa K (2010) Silent cerebral infarction is associated with incident stroke and TIA independent of carotid intima-media thickness. Intern Med 49:817-822.

Mollajew R, Toloe J, Mironov SL (2013) Single KATP channel opening in response to stimulation of AMPA/kainate receptors is mediated by Na(+) accumulation and submembrane ATP and ADP changes. The Journal of physiology 591:2593-2609.

Molle M, Yeshenko O, Marshall L, Sara SJ, Born J (2006) Hippocampal sharp wave-ripples linked to slow oscillations in rat slow-wave sleep. Journal of neurophysiology 96:62-70.

Monmaur P, Allix M, Schoevaert-Brossault D, Houcine O, Plotkine M, Willig F (1990) Effects of transient cerebral ischemia on the hippocampal dentate theta (theta) profile in the acute rat: a study 4-5 months following recirculation. Brain research 508:124-134.

Montoya CP, Sainsbury RS (1985) The effects of entorhinal cortex lesions on type 1 and type 2 theta. Physiology & behavior 35:121-126.

Morishita W, Marie H, Malenka RC (2005) Distinct triggering and expression mechanisms underlie LTD of AMPA and NMDA synaptic responses. Nature neuroscience 8:1043-1050.

Morris RG, Anderson E, Lynch GS, Baudry M (1986) Selective impairment of learning and blockade of long-term potentiation by an N-methyl-D-aspartate receptor antagonist, AP5. Nature 319:774-776.

Moscovitch M, Rosenbaum RS, Gilboa A, Addis DR, Westmacott R, Grady C, McAndrews MP, Levine B, Black S, Winocur G, Nadel L (2005) Functional neuroanatomy of remote episodic, semantic and spatial memory: a unified account based on multiple trace theory. J Anat 207:35-66.

Moustafa RR, Baron JC (2007) Clinical review: Imaging in ischaemic stroke--implications for acute management. Crit Care 11:227.

Moyanova S, Kortenska L, Kirov R, Iliev I (1998) Quantitative electroencephalographic changes due to middle cerebral artery occlusion by endothelin 1 in conscious rats. Arch Physiol Biochem 106:384-391.

Moyanova S, Kortenska L, Kirov R, Itzev D, Usunoff K (2008) Ketanserin reduces the postischemic EEG and behavioural changes following Endothelin-1-induced occlusion of the middle cerebral artery in conscious rats. Central European Journal of Medicine 3:406-416.

Moyanova SG, Dijkhuizen RM (2014) Present status and future challenges of electroencephalography- and magnetic resonance imaging-based monitoring in preclinical models of focal cerebral ischemia. Brain Res Bull 102:22-36.

Moyanova SG, Mitreva RG, Kortenska LV, Nicoletti F, Ngomba RT (2013) Age-dependence of sensorimotor and cerebral electroencephalographic asymmetry in rats subjected to unilateral cerebrovascular stroke. Exp Transl Stroke Med 5:13.

Moyanova SG, Kortenska LV, Mitreva RG, Pashova VD, Ngomba RT, Nicoletti F (2007) Multimodal assessment of neuroprotection applied to the use of MK-801 in the endothelin-1 model of transient focal brain ischemia. Brain research 1153:58-67.

Mozaffarian D et al. (2015) Heart disease and stroke statistics--2015 update: a report from the American Heart Association. Circulation 131:e29-322.

Mulkey RM, Endo S, Shenolikar S, Malenka RC (1994) Involvement of a calcineurin/inhibitor-1 phosphatase cascade in hippocampal long-term depression. Nature 369:486-488.

Munk MH, Roelfsema PR, Konig P, Engel AK, Singer W (1996) Role of reticular activation in the modulation of intracortical synchronization. Science (New York, NY) 272:271-274.

Nadel L, Moscovitch M (1997) Memory consolidation, retrograde amnesia and the hippocampal complex. Current opinion in neurobiology 7:217-227.

Nagata K, Tagawa K, Hiroi S, Shishido F, Uemura K (1989) Electroencephalographic correlates of blood flow and oxygen metabolism provided by positron emission tomography in patients with cerebral infarction. Electroencephalogr Clin Neurophysiol 72:16-30.

Nakka VP, Gusain A, Mehta SL, Raghubir R (2008) Molecular mechanisms of apoptosis in cerebral ischemia: multiple neuroprotective opportunities. Mol Neurobiol 37:7-38.

Nguyen PV, Woo NH (2003) Regulation of hippocampal synaptic plasticity by cyclic AMP-dependent protein kinases. Prog Neurobiol 71:401-437.

Nicoll RA, Malenka RC (1999) Expression mechanisms underlying NMDA receptor-dependent long-term potentiation. Annals of the New York Academy of Sciences 868:515-525.

Nieber K (1999) Hypoxia and neuronal function under in vitro conditions. Pharmacol Ther 82:71-86.

Niell CM, Stryker MP (2010) Modulation of visual responses by behavioral state in mouse visual cortex. Neuron 65:472-479.

Nikolova S, Moyanova S, Hughes S, Bellyou-Camilleri M, Lee TY, Bartha R (2009) Endothelin-1 induced MCAO: dose dependency of cerebral blood flow. J Neurosci Methods 179:22-28.

Normann RA, Maynard EM, Rousche PJ, Warren DJ (1999) A neural interface for a cortical vision prosthesis. Vision Res 39:2577-2587.

O'Brien MD, Waltz AG (1973) Transorbital approach for occluding the middle cerebral artery without craniectomy. Stroke; a journal of cerebral circulation 4:201-206.

O'Gorman RL, Poil SS, Brandeis D, Klaver P, Bollmann S, Ghisleni C, Luchinger R, Martin E, Shankaranarayanan A, Alsop DC, Michels L (2013) Coupling between resting cerebral perfusion and EEG. Brain Topogr 26:442-457.

O'Neill J, Pleydell-Bouverie B, Dupret D, Csicsvari J (2010) Play it again: reactivation of waking experience and memory. Trends Neurosci 33:220-229.

Ohmoto T, Mimura Y, Baba Y, Miyamoto T, Matsumoto Y, Nishimoto A, Matsumoto K

(1978) Thalamic control of spontaneous alpha-rhythm and evoked responses. Appl Neurophysiol 41:188-192.

Okun M, Naim A, Lampl I (2010) The subthreshold relation between cortical local field potential and neuronal firing unveiled by intracellular recordings in awake rats. The Journal of neuroscience : the official journal of the Society for Neuroscience 30:4440-4448.

Olejniczak P (2006) Neurophysiologic basis of EEG. J Clin Neurophysiol 23:186-189.

Onizuka S, Kasaba T, Takasaki M (2008) The effect of lidocaine on cholinergic neurotransmission in an identified reconstructed synapse. Anesth Analg 107:1236-1242.

Orset C, Macrez R, Young AR, Panthou D, Angles-Cano E, Maubert E, Agin V, Vivien D (2007) Mouse model of in situ thromboembolic stroke and reperfusion. Stroke; a journal of cerebral circulation 38:2771-2778.

Ovbiagele B, Nguyen-Huynh MN (2011) Stroke epidemiology: advancing our understanding of disease mechanism and therapy. Neurotherapeutics 8:319-329.

Ozaki T, Katsumoto E, Mui K, Furutsuka D, Yamagami S (1998) Distribution of Fos- and Jun-related proteins and activator protein-1 composite factors in mouse brain induced by neuroleptics. Neuroscience 84:1187-1196.

Paciaroni M, Caso V, Agnelli G (2009) The concept of ischemic penumbra in acute stroke and therapeutic opportunities. Eur Neurol 61:321-330.

Palva S, Palva JM (2007) New vistas for alpha-frequency band oscillations. Trends Neurosci 30:150-158.

Pare D, Collins DR (2000) Neuronal correlates of fear in the lateral amygdala: multiple extracellular recordings in conscious cats. The Journal of neuroscience : the official journal of the Society for Neuroscience 20:2701-2710.

Park JY, Jhung K, Lee J, An SK (2013) Theta-gamma coupling during a working memory task as compared to a simple vigilance task. Neurosci Lett 532:39-43.

Parron C, Save E (2004) Evidence for entorhinal and parietal cortices involvement in path integration in the rat. Experimental brain research 159:349-359.

Parron C, Poucet B, Save E (2004) Entorhinal cortex lesions impair the use of distal but not proximal landmarks during place navigation in the rat. Behavioural brain research 154:345-352.

Pastalkova E, Serrano P, Pinkhasova D, Wallace E, Fenton AA, Sacktor TC (2006) Storage of spatial information by the maintenance mechanism of LTP. Science (New York, NY) 313:1141-1144.

Patel J, Fujisawa S, Berenyi A, Royer S, Buzsaki G (2012) Traveling theta waves along the entire septotemporal axis of the hippocampus. Neuron 75:410-417.

Patel J, Schomburg EW, Berenyi A, Fujisawa S, Buzsaki G (2013) Local generation and

propagation of ripples along the septotemporal axis of the hippocampus. The Journal of neuroscience : the official journal of the Society for Neuroscience 33:17029-17041.

Patel M, Coshall C, Rudd AG, Wolfe CD (2003) Natural history of cognitive impairment after stroke and factors associated with its recovery. Clin Rehabil 17:158-166.

Pelisek J, Eckstein HH, Zernecke A (2012) Pathophysiological mechanisms of carotid plaque vulnerability: impact on ischemic stroke. Arch Immunol Ther Exp (Warsz) 60:431-442.

Penfield W (1950) Observations on the anatomy of memory. Folia Psychiatr Neurol Neurochir Neerl 53:349-351.

Pennartz CM, Lee E, Verheul J, Lipa P, Barnes CA, McNaughton BL (2004) The ventral striatum in off-line processing: ensemble reactivation during sleep and modulation by hippocampal ripples. The Journal of neuroscience : the official journal of the Society for Neuroscience 24:6446-6456.

Pereira de Vasconcelos A, Klur S, Muller C, Cosquer B, Lopez J, Certa U, Cassel JC (2006) Reversible inactivation of the dorsal hippocampus by tetrodotoxin or lidocaine: a comparative study on cerebral functional activity and motor coordination in the rat. Neuroscience 141:1649-1663.

Peyrache A, Battaglia FP, Destexhe A (2011) Inhibition recruitment in prefrontal cortex during sleep spindles and gating of hippocampal inputs. Proceedings of the National Academy of Sciences of the United States of America 108:17207-17212.

Pignatelli M, Beyeler A, Leinekugel X (2012) Neural circuits underlying the generation of theta oscillations. J Physiol Paris 106:81-92.

Plouin P, Kaminska A, Moutard ML, Soufflet C (2013) Developmental aspects of normal EEG. Handb Clin Neurol 111:79-85.

Pohjasvaara T, Erkinjuntti T, Vataja R, Kaste M (1997) Dementia three months after stroke. Baseline frequency and effect of different definitions of dementia in the Helsinki Stroke Aging Memory Study (SAM) cohort. Stroke; a journal of cerebral circulation 28:785-792.

Poulet JF, Petersen CC (2008) Internal brain state regulates membrane potential synchrony in barrel cortex of behaving mice. Nature 454:881-885.

Poulet JF, Fernandez LM, Crochet S, Petersen CC (2012) Thalamic control of cortical states. Nature neuroscience 15:370-372.

Powers WJ (1991) Cerebral hemodynamics in ischemic cerebrovascular disease. Ann Neurol 29:231-240.

Puig MV, Watakabe A, Ushimaru M, Yamamori T, Kawaguchi Y (2010) Serotonin modulates fast-spiking interneuron and synchronous activity in the rat prefrontal cortex through 5-HT1A and 5-HT2A receptors. The Journal of neuroscience : the official journal of the Society for Neuroscience 30:2211-2222.

Pulsinelli WA, Brierley JB (1979) A new model of bilateral hemispheric ischemia in the

unanesthetized rat. Stroke; a journal of cerebral circulation 10:267-272.

Purves D AG, Fitzpatrick D, et al (2001) Mechanisms of Short-Term Synaptic Plasticity in the Mammalian Nervous System. In: Neuroscience. 2nd edition. (Associates SMS, ed).

Qureshi A, Hillis AE, Qureshi A, Hillis. AE (**2013**) Working memory dysfunction in stroke patients. The Behavioral and Cognitive Neurology of Stroke: Cambridge University Press.

Qutub AA, Hunt CA (2005) Glucose transport to the brain: a systems model. Brain Res Brain Res Rev 49:595-617.

Ramadan W, Eschenko O, Sara SJ (2009) Hippocampal sharp wave/ripples during sleep for consolidation of associative memory. PLoS One 4:e6697.

Rampon C, Tsien JZ (2000) Genetic analysis of learning behavior-induced structural plasticity. Hippocampus 10:605-609.

Ranganath C (2010) A unified framework for the functional organization of the medial temporal lobes and the phenomenology of episodic memory. Hippocampus 20:1263-1290.

Rasmussen RS, Overgaard K, Pakola S, Boysen G (2008) Effects of microplasmin on recovery in a rat embolic stroke model. Neurol Res 30:75-81.

Rasquin SM, Verhey FR, Lousberg R, Winkens I, Lodder J (2002) Vascular cognitive disorders: memory, mental speed and cognitive flexibility after stroke. Journal of the neurological sciences 203-204:115-119.

Rasquin SM, Lodder J, Ponds RW, Winkens I, Jolles J, Verhey FR (2004) Cognitive functioning after stroke: a one-year follow-up study. Dement Geriatr Cogn Disord 18:138-144.

Redecker C, Luhmann HJ, Hagemann G, Fritschy JM, Witte OW (2000) Differential downregulation of GABAA receptor subunits in widespread brain regions in the freeze-lesion model of focal cortical malformations. The Journal of neuroscience : the official journal of the Society for Neuroscience 20:5045-5053.

Renart A, de la Rocha J, Bartho P, Hollender L, Parga N, Reyes A, Harris KD (2010) The asynchronous state in cortical circuits. Science (New York, NY) 327:587-590.

Ribeiro TL, Copelli M, Caixeta F, Belchior H, Chialvo DR, Nicolelis MA, Ribeiro S (2010) Spike avalanches exhibit universal dynamics across the sleep-wake cycle. PLoS One 5:e14129.

Rizzuto DS, Madsen JR, Bromfield EB, Schulze-Bonhage A, Kahana MJ (2006) Human neocortical oscillations exhibit theta phase differences between encoding and retrieval. Neuroimage 31:1352-1358.

Robinson MJ, McCulloch J (1990) Contractile responses to endothelin in feline cortical vessels in situ. Journal of cerebral blood flow and metabolism : official journal of the International Society of Cerebral Blood Flow and Metabolism 10:285-289.

Roof RL, Schielke GP, Ren X, Hall ED (2001) A comparison of long-term functional outcome after 2 middle cerebral artery occlusion models in rats. Stroke; a journal of cerebral circulation 32:2648-2657.

Roopun AK, Middleton SJ, Cunningham MO, LeBeau FE, Bibbig A, Whittington MA, Traub RD (2006) A beta2-frequency (20-30 Hz) oscillation in nonsynaptic networks of somatosensory cortex. Proceedings of the National Academy of Sciences of the United States of America 103:15646-15650.

Rosen AS, Morris ME (1991) Depolarizing effects of anoxia on pyramidal cells of rat neocortex. Neurosci Lett 124:169-173.

Rosenbaum RS, Priselac S, Kohler S, Black SE, Gao F, Nadel L, Moscovitch M (2000) Remote spatial memory in an amnesic person with extensive bilateral hippocampal lesions. Nature neuroscience 3:1044-1048.

Ross RS, Eichenbaum H (2006) Dynamics of hippocampal and cortical activation during consolidation of a nonspatial memory. The Journal of neuroscience : the official journal of the Society for Neuroscience 26:4852-4859.

Rossi DJ, Brady JD, Mohr C (2007) Astrocyte metabolism and signaling during brain ischemia. Nature neuroscience 10:1377-1386.

Rotstein HG, Pervouchine DD, Acker CD, Gillies MJ, White JA, Buhl EH, Whittington MA, Kopell N (2005) Slow and fast inhibition and an H-current interact to create a theta rhythm in a model of CA1 interneuron network. Journal of neurophysiology 94:1509-1518.

Ruitenberg A, Ott A, van Swieten JC, Hofman A, Breteler MM (2001) Incidence of dementia: does gender make a difference? Neurobiol Aging 22:575-580.

Ryan L, Nadel L, Keil K, Putnam K, Schnyer D, Trouard T, Moscovitch M (2001) Hippocampal complex and retrieval of recent and very remote autobiographical memories: evidence from functional magnetic resonance imaging in neurologically intact people. Hippocampus 11:707-714.

Sadato N, Nakamura S, Oohashi T, Nishina E, Fuwamoto Y, Waki A, Yonekura Y (1998) Neural networks for generation and suppression of alpha rhythm: a PET study. Neuroreport 9:893-897.

Sakai N, Yanai K, Ryu JH, Nagasawa H, Hasegawa T, Sasaki T, Kogure K, Watanabe T (1996) Behavioral studies on rats with transient cerebral ischemia induced by occlusion of the middle cerebral artery. Behavioural brain research 77:181-188.

Sanei S, Chambers JA (2013) EEG signal processing: John Wiley & Sons.

Sauseng P, Klimesch W, Gruber WR, Hanslmayr S, Freunberger R, Doppelmayr M (2007) Are event-related potential components generated by phase resetting of brain oscillations? A critical discussion. Neuroscience 146:1435-1444.

Save E, Paz-Villagran V, Alexinsky T, Poucet B (2005) Functional interaction between the associative parietal cortex and hippocampal place cell firing in the rat. The European

journal of neuroscience 21:522-530.

Schaul N, Gloor P, Gotman J (1981) The EEG in deep midline lesions. Neurology 31:157-167.

Schaul N, Gloor P, Ball G, Gotman J (1978) The electromicrophysiology of delta waves induced by systemic atropine. Brain research 143:475-486.

Scheffer-Teixeira R, Belchior H, Caixeta FV, Souza BC, Ribeiro S, Tort ABL (2012) Theta Phase Modulates Multiple Layer-Specific Oscillations in the CA1 Region. Cerebral Cortex 22:2404-2414.

Schiene K, Bruehl C, Zilles K, Qu M, Hagemann G, Kraemer M, Witte OW (1996) Neuronal hyperexcitability and reduction of GABAA-receptor expression in the surround of cerebral photothrombosis. Journal of cerebral blood flow and metabolism : official journal of the International Society of Cerebral Blood Flow and Metabolism 16:906-914.

Scholler K, Zausinger S, Baethmann A, Schmid-Elsaesser R (2004) Neuroprotection in ischemic stroke--combination drug therapy and mild hypothermia in a rat model of permanent focal cerebral ischemia. Brain research 1023:272-278.

Schultz C, Engelhardt M (2014) Anatomy of the hippocampal formation. Front Neurol Neurosci 34:6-17.

Schurmann M, Basar-Eroglu C, Basar E (1997) Gamma responses in the EEG: elementary signals with multiple functional correlates. Neuroreport 8:1793-1796.

Scoville WB, Milner B (1957) Loss of recent memory after bilateral hippocampal lesions. J Neurol Neurosurg Psychiatry 20:11-21.

Seta KA, Yuan Y, Spicer Z, Lu G, Bedard J, Ferguson TK, Pathrose P, Cole-Strauss A, Kaufhold A, Millhorn DE (2004) The role of calcium in hypoxia-induced signal transduction and gene expression. Cell Calcium 36:331-340.

Shadmehr R, Holcomb HH (1997) Neural correlates of motor memory consolidation. Science (New York, NY) 277:821-825.

Sharbrough FW, Messick JM, Jr., Sundt TM, Jr. (1973) Correlation of continuous electroencephalograms with cerebral blood flow measurements during carotid endarterectomy. Stroke 4:674-683.

Sharkey J, Ritchie IM, Kelly PA (1993) Perivascular microapplication of endothelin-1: a new model of focal cerebral ischaemia in the rat. Journal of cerebral blood flow and metabolism : official journal of the International Society of Cerebral Blood Flow and Metabolism 13:865-871.

Sheorajpanday RV, Nagels G, Weeren AJ, van Putten MJ, De Deyn PP (2009) Reproducibility and clinical relevance of quantitative EEG parameters in cerebral ischemia: a basic approach. Clin Neurophysiol 120:845-855.

Sheorajpanday RV, Nagels G, Weeren AJ, De Surgeloose D, De Deyn PP (2010) Additional value of quantitative EEG in acute anterior circulation syndrome of presumed

ischemic origin. Clin Neurophysiol 121:1719-1725.

Sheorajpanday RV, Nagels G, Weeren AJ, van Putten MJ, De Deyn PP (2011) Quantitative EEG in ischemic stroke: correlation with functional status after 6 months. Clin Neurophysiol 122:874-883.

Shinohara Y, Hosoya A, Hirase H (2013) Experience enhances gamma oscillations and interhemispheric asymmetry in the hippocampus. Nat Commun 4:1652.

Siapas AG, Lubenov EV, Wilson MA (2005) Prefrontal phase locking to hippocampal theta oscillations. Neuron 46:141-151.

Simpson IA, Carruthers A, Vannucci SJ (2007) Supply and demand in cerebral energy metabolism: the role of nutrient transporters. Journal of cerebral blood flow and metabolism : official journal of the International Society of Cerebral Blood Flow and Metabolism 27:1766-1791.

Singer W (1999) Neuronal synchrony: a versatile code for the definition of relations? Neuron 24:49-65, 111-125.

Sirota A, Csicsvari J, Buhl D, Buzsaki G (2003) Communication between neocortex and hippocampus during sleep in rodents. Proceedings of the National Academy of Sciences of the United States of America 100:2065-2069.

Sirota A, Montgomery S, Fujisawa S, Isomura Y, Zugaro M, Buzsaki G (2008) Entrainment of neocortical neurons and gamma oscillations by the hippocampal theta rhythm. Neuron 60:683-697.

Skaggs WE, McNaughton BL, Permenter M, Archibeque M, Vogt J, Amaral DG, Barnes CA (2007) EEG sharp waves and sparse ensemble unit activity in the macaque hippocampus. Journal of neurophysiology 98:898-910.

Slawinska U, Kasicki S (1998) The frequency of rat's hippocampal theta rhythm is related to the speed of locomotion. Brain research 796:327-331.

Smith CA, Countryman RA, Sahuque LL, Colombo PJ (2007) Time-courses of Fos expression in rat hippocampus and neocortex following acquisition and recall of a socially transmitted food preference. Neurobiol Learn Mem 88:65-74.

Snaphaan L, de Leeuw FE (2007) Poststroke memory function in nondemented patients: a systematic review on frequency and neuroimaging correlates. Stroke; a journal of cerebral circulation 38:198-203.

Snaphaan L, Rijpkema M, van Uden I, Fernandez G, de Leeuw FE (2009) Reduced medial temporal lobe functionality in stroke patients: a functional magnetic resonance imaging study. Brain 132:1882-1888.

Sorensen KE (1985) The connections of the hippocampal region. New observations on efferent connections in the guinea pig, and their functional implications. Acta Neurol Scand 72:550-560.

Sporns O, Tononi G, Edelman GM (2000) Connectivity and complexity: the relationship between neuroanatomy and brain dynamics. Neural networks : the official journal of

the International Neural Network Society 13:909-922.

Spuler A, Grafe P (1989) Adenosine, 'pertussis-sensitive' G-proteins, and K+ conductance in central mammalian neurones under energy deprivation. Neurosci Lett 98:280-284.

Squire LR (1992) Declarative and nondeclarative memory: multiple brain systems supporting learning and memory. J Cogn Neurosci 4:232-243.

Squire LR (2004) Memory systems of the brain: a brief history and current perspective. Neurobiol Learn Mem 82:171-177.

Squire LR, Alvarez P (1995) Retrograde amnesia and memory consolidation: a neurobiological perspective. Current opinion in neurobiology 5:169-177.

Squire LR, Bayley PJ (2007) The neuroscience of remote memory. Current opinion in neurobiology 17:185-196.

Squire LR, Stark CE, Clark RE (2004) The medial temporal lobe. Annu Rev Neurosci 27:279-306.

Srikanth VK, Thrift AG, Saling MM, Anderson JF, Dewey HM, Macdonell RA, Donnan GA (2003) Increased risk of cognitive impairment 3 months after mild to moderate first-ever stroke: a Community-Based Prospective Study of Nonaphasic English-Speaking Survivors. Stroke; a journal of cerebral circulation 34:1136-1143.

Srikanth VK, Anderson JF, Donnan GA, Saling MM, Didus E, Alpitsis R, Dewey HM, Macdonell RA, Thrift AG (2004) Progressive dementia after first-ever stroke: a community-based follow-up study. Neurology 63:785-792.

Staba RJ, Worrell GA (2014) What is the importance of abnormal "background" activity in seizure generation? Adv Exp Med Biol 813:43-54.

Stark E, Roux L, Eichler R, Senzai Y, Royer S, Buzsaki G (2014) Pyramidal cell-interneuron interactions underlie hippocampal ripple oscillations. Neuron 83:467-480.

Staubli U, Thibault O, DiLorenzo M, Lynch G (1989) Antagonism of NMDA receptors impairs acquisition but not retention of olfactory memory. Behav Neurosci 103:54-60.

Steiner TJ, Rail DL, Rose FC (1980) Cholesterol crystal embolization in rat brain: a model for atheroembolic cerebral infarction. Stroke; a journal of cerebral circulation 11:184-189.

Steriade M (1996) Arousal: revisiting the reticular activating system. Science (New York, NY) 272:225-226.

Steriade M (2001) Impact of network activities on neuronal properties in corticothalamic systems. Journal of neurophysiology 86:1-39.

Steriade M, Timofeev I (2003) Neuronal plasticity in thalamocortical networks during sleep and waking oscillations. Neuron 37:563-576.

Steriade M, McCormick DA, Sejnowski TJ (1993a) Thalamocortical oscillations in the sleeping and aroused brain. Science (New York, NY) 262:679-685.

Steriade M, Nunez A, Amzica F (1993b) A novel slow (< 1 Hz) oscillation of neocortical neurons in vivo: depolarizing and hyperpolarizing components. The Journal of neuroscience : the official journal of the Society for Neuroscience 13:3252-3265.

Steward O (1976) Topographic organization of the projections from the entorhinal area to the hippocampal formation of the rat. J Comp Neurol 167:285-314.

Stewart M, Fox SE (1991) Hippocampal theta activity in monkeys. Brain research 538:59-63.

Sugimori H, Yao H, Ooboshi H, Ibayashi S, Iida M (2004) Krypton laser-induced photothrombotic distal middle cerebral artery occlusion without craniectomy in mice. Brain Res Brain Res Protoc 13:189-196.

Sullivan D, Csicsvari J, Mizuseki K, Montgomery S, Diba K, Buzsaki G (2011) Relationships between hippocampal sharp waves, ripples, and fast gamma oscillation: influence of dentate and entorhinal cortical activity. The Journal of neuroscience : the official journal of the Society for Neuroscience 31:8605-8616.

Sun J-H, Tan L, Yu J-T (2014) Post-stroke cognitive impairment: epidemiology, mechanisms and management. Annals of Translational Medicine 2:80.

Sundar U, Adwani S (2010) Post-stroke cognitive impairment at 3 months. Annals of Indian Academy of Neurology 13:42-46.

Sunyer B, Patil S, Höger H, Lubec G (2007) Barnes maze, a useful task to assess spatial reference memory in the mice.

Sweatt JD (1999) Toward a molecular explanation for long-term potentiation. Learning & memory (Cold Spring Harbor, NY) 6:399-416.

Sweatt JD (2001) The neuronal MAP kinase cascade: a biochemical signal integration system subserving synaptic plasticity and memory. Journal of neurochemistry 76:1-10.

Tallon-Baudry C, Bertrand O, Delpuech C, Pernier J (1996) Stimulus specificity of phase-locked and non-phase-locked 40 Hz visual responses in human. The Journal of neuroscience : the official journal of the Society for Neuroscience 16:4240-4249.

Tamura A, Graham DI, McCulloch J, Teasdale GM (1981) Focal cerebral ischaemia in the rat: 1. Description of technique and early neuropathological consequences following middle cerebral artery occlusion. Journal of cerebral blood flow and metabolism : official journal of the International Society of Cerebral Blood Flow and Metabolism 1:53-60.

Tanaka E, Yamamoto S, Kudo Y, Mihara S, Higashi H (1997) Mechanisms underlying the rapid depolarization produced by deprivation of oxygen and glucose in rat hippocampal CA1 neurons in vitro. Journal of neurophysiology 78:891-902.

Tatemichi TK, Desmond DW, Stern Y, Paik M, Sano M, Bagiella E (1994) Cognitive impairment after stroke: frequency, patterns, and relationship to functional abilities. J Neurol Neurosurg Psychiatry 57:202-207.

Tatemichi TK, Foulkes MA, Mohr JP, Hewitt JR, Hier DB, Price TR, Wolf PA (1990) Dementia in stroke survivors in the Stroke Data Bank cohort. Prevalence, incidence,

risk factors, and computed tomographic findings. Stroke; a journal of cerebral circulation 21:858-866.

Teng E, Squire LR (1999) Memory for places learned long ago is intact after hippocampal damage. Nature 400:675-677.

Terao Y, Sakurai Y, Sakuta M, Ishii K, Sugishita M (1993) [FDG-PET in an amnestic and hypersomnic patient with bilateral paramedian thalamic infarction]. Rinsho Shinkeigaku 33:951-956.

Tomida S, Nowak TS, Jr., Vass K, Lohr JM, Klatzo I (1987) Experimental model for repetitive ischemic attacks in the gerbil: the cumulative effect of repeated ischemic insults. Journal of cerebral blood flow and metabolism : official journal of the International Society of Cerebral Blood Flow and Metabolism 7:773-782.

Tononi G, Cirelli C (2012) Time to be SHY? Some comments on sleep and synaptic homeostasis. Neural Plast 2012:415250.

Tononi G, Cirelli C (2014) Sleep and the price of plasticity: from synaptic and cellular homeostasis to memory consolidation and integration. Neuron 81:12-34.

Traub RD, Whittington MA, Buhl EH, Jefferys JG, Faulkner HJ (1999) On the mechanism of the gamma --> beta frequency shift in neuronal oscillations induced in rat hippocampal slices by tetanic stimulation. The Journal of neuroscience : the official journal of the Society for Neuroscience 19:1088-1105.

Tsien JZ, Huerta PT, Tonegawa S (1996) The essential role of hippocampal CA1 NMDA receptor-dependent synaptic plasticity in spatial memory. Cell 87:1327-1338.

Tsumoto T (1993) Long-term depression in cerebral cortex: a possible substrate of "forgetting" that should not be forgotten. Neurosci Res 16:263-270.

Tulving E, Schacter DL (1990) Priming and human memory systems. Science (New York, NY) 247:301-306.

Uhlhaas PJ, Haenschel C, Nikolic D, Singer W (2008) The role of oscillations and synchrony in cortical networks and their putative relevance for the pathophysiology of schizophrenia. Schizophr Bull 34:927-943.

van Bruggen N, Thibodeaux H, Palmer JT, Lee WP, Fu L, Cairns B, Tumas D, Gerlai R, Williams SP, van Lookeren Campagne M, Ferrara N (1999) VEGF antagonism reduces edema formation and tissue damage after ischemia/reperfusion injury in the mouse brain. J Clin Invest 104:1613-1620.

Van Cauter T, Camon J, Alvernhe A, Elduayen C, Sargolini F, Save E (2013) Distinct roles of medial and lateral entorhinal cortex in spatial cognition. Cerebral cortex (New York, NY : 1991) 23:451-459.

van Groen T, Miettinen P, Kadish I (2003) The entorhinal cortex of the mouse: organization of the projection to the hippocampal formation. Hippocampus 13:133-149.

van Haeften T, Wouterlood FG, Witter MP (2000) Presubicular input to the dendrites of layer-V entorhinal neurons in the rat. Annals of the New York Academy of Sciences

911:471-473.

Vanderwolf CH (1968) Recovery from large medial thalamic lesions as a result of electroconvulsive therapy. J Neurol Neurosurg Psychiatry 31:67-72.

Vann SD, Brown MW, Erichsen JT, Aggleton JP (2000a) Using fos imaging in the rat to reveal the anatomical extent of the disruptive effects of fornix lesions. The Journal of neuroscience : the official journal of the Society for Neuroscience 20:8144-8152.

Vann SD, Brown MW, Erichsen JT, Aggleton JP (2000b) Fos imaging reveals differential patterns of hippocampal and parahippocampal subfield activation in rats in response to different spatial memory tests. The Journal of neuroscience : the official journal of the Society for Neuroscience 20:2711-2718.

Varela F, Lachaux JP, Rodriguez E, Martinerie J (2001) The brainweb: phase synchronization and large-scale integration. Nature reviews Neuroscience 2:229-239.

Vermeer SE, Longstreth WT, Jr., Koudstaal PJ (2007) Silent brain infarcts: a systematic review. Lancet Neurol 6:611-619.

Vertes RP (2005) Hippocampal theta rhythm: a tag for short-term memory. Hippocampus 15:923-935.

Virley D, Hadingham SJ, Roberts JC, Farnfield B, Elliott H, Whelan G, Golder J, David C, Parsons AA, Hunter AJ (2004) A new primate model of focal stroke: endothelin-1-induced middle cerebral artery occlusion and reperfusion in the common marmoset. Journal of cerebral blood flow and metabolism : official journal of the International Society of Cerebral Blood Flow and Metabolism 24:24-41.

Viskontas IV, McAndrews MP, Moscovitch M (2002) Memory for famous people in patients with unilateral temporal lobe epilepsy and excisions. Neuropsychology 16:472-480.

von Monakow C (1914) Die Lokalisation im Grosshirn: und der Abbau der Funktion durch kortikale Herde: Verlag von JF Bergmann.

Voytek B, Knight RT (2015) Dynamic Network Communication as a Unifying Neural Basis for Cognition, Development, Aging, and Disease. Biol Psychiatry 77:1089-1097.

Wang DV, Yau HJ, Broker CJ, Tsou JH, Bonci A, Ikemoto S (2015) Mesopontine median raphe regulates hippocampal ripple oscillation and memory consolidation. Nature neuroscience 18:728-735.

Wang H, Hu Y, Tsien JZ (2006) Molecular and systems mechanisms of memory consolidation and storage. Prog Neurobiol 79:123-135.

Wang RY, Wang PS, Yang YR (2003) Effect of age in rats following middle cerebral artery occlusion. Gerontology 49:27-32.

Wang SH, Morris RG (2010) Hippocampal-neocortical interactions in memory formation, consolidation, and reconsolidation. Annu Rev Psychol 61:49-79, C41-44.

Wang Y, Zhang X, Huang J, Zhu M, Guan Q, Liu C (2013) Associations between EEG beta power abnormality and diagnosis in cognitive impairment post cerebral infarcts. J Mol

Neurosci 49:632-638.

Wang Y, Bontempi B, Hong SM, Mehta K, Weinstein PR, Abrams GM, Liu J (2008) A comprehensive analysis of gait impairment after experimental stroke and the therapeutic effect of environmental enrichment in rats. Journal of cerebral blood flow and metabolism : official journal of the International Society of Cerebral Blood Flow and Metabolism 28:1936-1950.

Watson BD, Dietrich WD, Busto R, Wachtel MS, Ginsberg MD (1985) Induction of reproducible brain infarction by photochemically initiated thrombosis. Ann Neurol 17:497-504.

Whishaw IQ, Vanderwolf CH (1973) Hippocampal EEG and behavior: changes in amplitude and frequency of RSA (theta rhythm) associated with spontaneous and learned movement patterns in rats and cats. Behav Biol 8:461-484.

Whitlock JR, Heynen AJ, Shuler MG, Bear MF (2006) Learning induces long-term potentiation in the hippocampus. Science (New York, NY) 313:1093-1097.

Whittington MA, Traub RD, Jefferys JG (1995) Synchronized oscillations in interneuron networks driven by metabotropic glutamate receptor activation. Nature 373:612-615.

Whittington MA, Traub RD, Faulkner HJ, Stanford IM, Jefferys JG (1997) Recurrent excitatory postsynaptic potentials induced by synchronized fast cortical oscillations. Proceedings of the National Academy of Sciences of the United States of America 94:12198-12203.

Williams AJ, Tortella FC (2002) Neuroprotective effects of the sodium channel blocker RS100642 and attenuation of ischemia-induced brain seizures in the rat. Brain research 932:45-55.

Williams AJ, Lu XC, Hartings JA, Tortella FC (2003) Neuroprotection assessment by topographic electroencephalographic analysis: effects of a sodium channel blocker to reduce polymorphic delta activity following ischaemic brain injury in rats. Fundam Clin Pharmacol 17:581-593.

Winocur G (1990) Anterograde and retrograde amnesia in rats with dorsal hippocampal or dorsomedial thalamic lesions. Behavioural brain research 38:145-154.

Winocur G, McDonald RM, Moscovitch M (2001) Anterograde and retrograde amnesia in rats with large hippocampal lesions. Hippocampus 11:18-26.

Winship IR, Murphy TH (2008) In vivo calcium imaging reveals functional rewiring of single somatosensory neurons after stroke. The Journal of neuroscience : the official journal of the Society for Neuroscience 28:6592-6606.

Winson J (1978) Loss of hippocampal theta rhythm results in spatial memory deficit in the rat. Science (New York, NY) 201:160-163.

Witte OW, Bidmon HJ, Schiene K, Redecker C, Hagemann G (2000) Functional differentiation of multiple perilesional zones after focal cerebral ischemia. Journal of cerebral blood flow and metabolism : official journal of the International Society of

Cerebral Blood Flow and Metabolism 20:1149-1165.

Witter MP, Naber PA, van Haeften T, Machielsen WC, Rombouts SA, Barkhof F, Scheltens P, Lopes da Silva FH (2000) Cortico-hippocampal communication by way of parallel parahippocampal-subicular pathways. Hippocampus 10:398-410.

Wolansky T, Clement EA, Peters SR, Palczak MA, Dickson CT (2006) Hippocampal slow oscillation: a novel EEG state and its coordination with ongoing neocortical activity. The Journal of neuroscience : the official journal of the Society for Neuroscience 26:6213-6229.

Woolsey TA, Van der Loos H (1970) The structural organization of layer IV in the somatosensory region (SI) of mouse cerebral cortex. The description of a cortical field composed of discrete cytoarchitectonic units. Brain research 17:205-242.

Yanovsky Y, Ciatipis M, Draguhn A, Tort AB, Brankack J (2014) Slow oscillations in the mouse hippocampus entrained by nasal respiration. The Journal of neuroscience : the official journal of the Society for Neuroscience 34:5949-5964.

Ylinen A, Bragin A, Nadasdy Z, Jando G, Szabo I, Sik A, Buzsaki G (1995) Sharp wave-associated high-frequency oscillation (200 Hz) in the intact hippocampus: network and intracellular mechanisms. The Journal of neuroscience : the official journal of the Society for Neuroscience 15:30-46.

Yonemori F, Yamaguchi T, Yamada H, Tamura A (1999) Spatial cognitive performance after chronic focal cerebral ischemia in rats. Journal of cerebral blood flow and metabolism : official journal of the International Society of Cerebral Blood Flow and Metabolism 19:483-494.

Yonemori F, Yamada H, Yamaguchi T, Uemura A, Tamura A (1996) Spatial memory disturbance after focal cerebral ischemia in rats. Journal of cerebral blood flow and metabolism : official journal of the International Society of Cerebral Blood Flow and Metabolism 16:973-980.

Yu G, Wu F, Wang ES (2015) BQ-869, a novel NMDA receptor antagonist, protects against excitotoxicity and attenuates cerebral ischemic injury in stroke. International journal of clinical and experimental pathology 8:1213-1225.

Yu K, Wu Y, Zhang Q, Xie H, Liu G, Guo Z, Li F, Jia J, Kuang S, Hu R (2014) Enriched environment induces angiogenesis and improves neural function outcomes in rat stroke model. Journal of the neurological sciences 347:275-280.

Zhang H, Jacobs J (2015) Traveling Theta Waves in the Human Hippocampus. The Journal of neuroscience : the official journal of the Society for Neuroscience 35:12477-12487.

Zhang L, Zhang ZG, Zhang C, Zhang RL, Chopp M (2004) Intravenous administration of a GPIIb/IIIa receptor antagonist extends the therapeutic window of intra-arterial tenecteplase-tissue plasminogen activator in a rat stroke model. Stroke; a journal of cerebral circulation 35:2890-2895.

Zhang S, Tong R, Zhang H, Hu X, Zheng X (2006) A pilot studies in dynamic profile of multi parameters of EEG in a rat model of transient middle cerebral artery occlusion. Conf

Proc IEEE Eng Med Biol Soc 1:1181-1184.

Zhang SJ, Ke Z, Li L, Yip SP, Tong KY (2013) EEG patterns from acute to chronic stroke phases in focal cerebral ischemic rats: correlations with functional recovery. Physiol Meas 34:423-435.

Zhang W, Linden DJ (2003) The other side of the engram: experience-driven changes in neuronal intrinsic excitability. Nature reviews Neuroscience 4:885-900.

Zhang W, Huguenard JR, Buckmaster PS (2012) Increased excitatory synaptic input to granule cells from hilar and CA3 regions in a rat model of temporal lobe epilepsy. The Journal of neuroscience : the official journal of the Society for Neuroscience 32:1183-1196.

Zhang Y, Bhavnani BR (2006) Glutamate-induced apoptosis in neuronal cells is mediated via caspase-dependent and independent mechanisms involving calpain and caspase-3 proteases as well as apoptosis inducing factor (AIF) and this process is inhibited by equine estrogens. BMC Neurosci 7:49.

Zhou Q, Homma KJ, Poo MM (2004) Shrinkage of dendritic spines associated with long-term depression of hippocampal synapses. Neuron 44:749-757.

Zimmermann PK, Wagner U, Krauth J, Huston JP (1997) Unilateral lesion of dorsal hippocampus enhances reinforcing lateral hypothalamic stimulation in the contralateral hemisphere. Brain Res Bull 44:265-271.

Zvejniece L, Svalbe B, Liepinsh E, Pulks E, Dambrova M (2012) The sensorimotor and cognitive deficits in rats following 90- and 120-min transient occlusion of the middle cerebral artery. J Neurosci Methods 208:197-204.